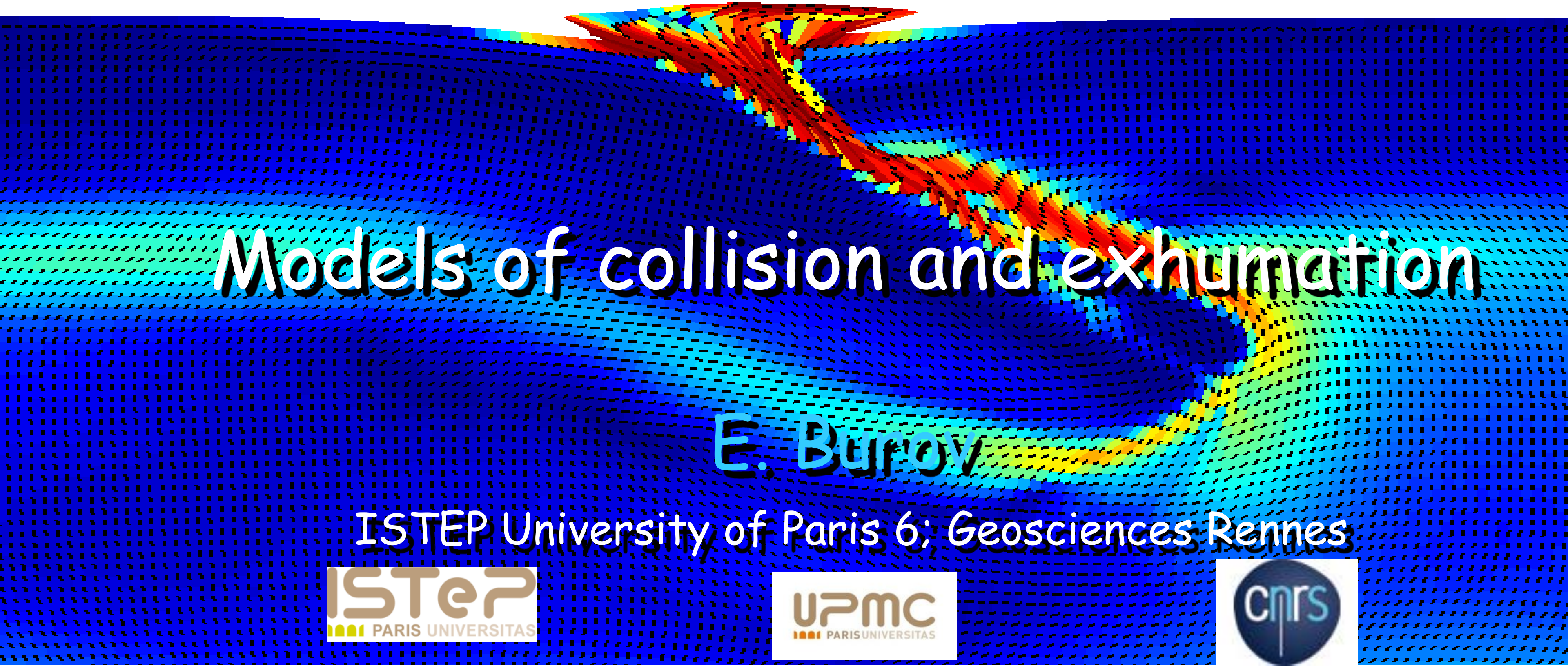

Models of collision and exhumation

E. Burov

ISTEP University of Paris 6; Geosciences Rennes

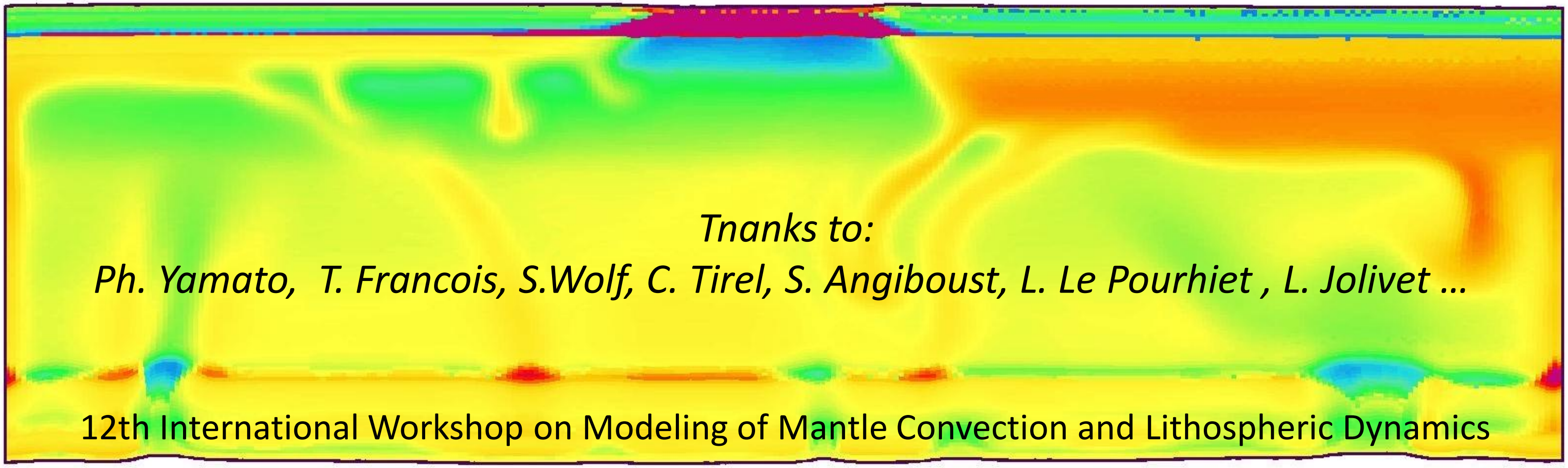

Tnanks to:

Ph. Yamato, T. Francois, S.Wolf, C. Tirel, S. Angiboust, L. Le Pourhiet , L. Jolivet …

12th International Workshop on Modeling of Mantle Convection and Lithospheric Dynamics

possible collision modes

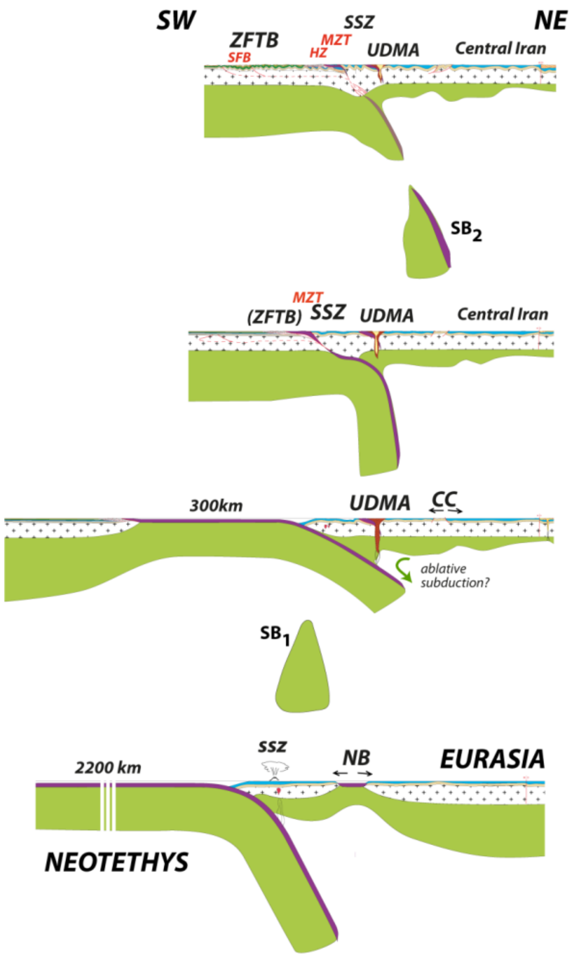

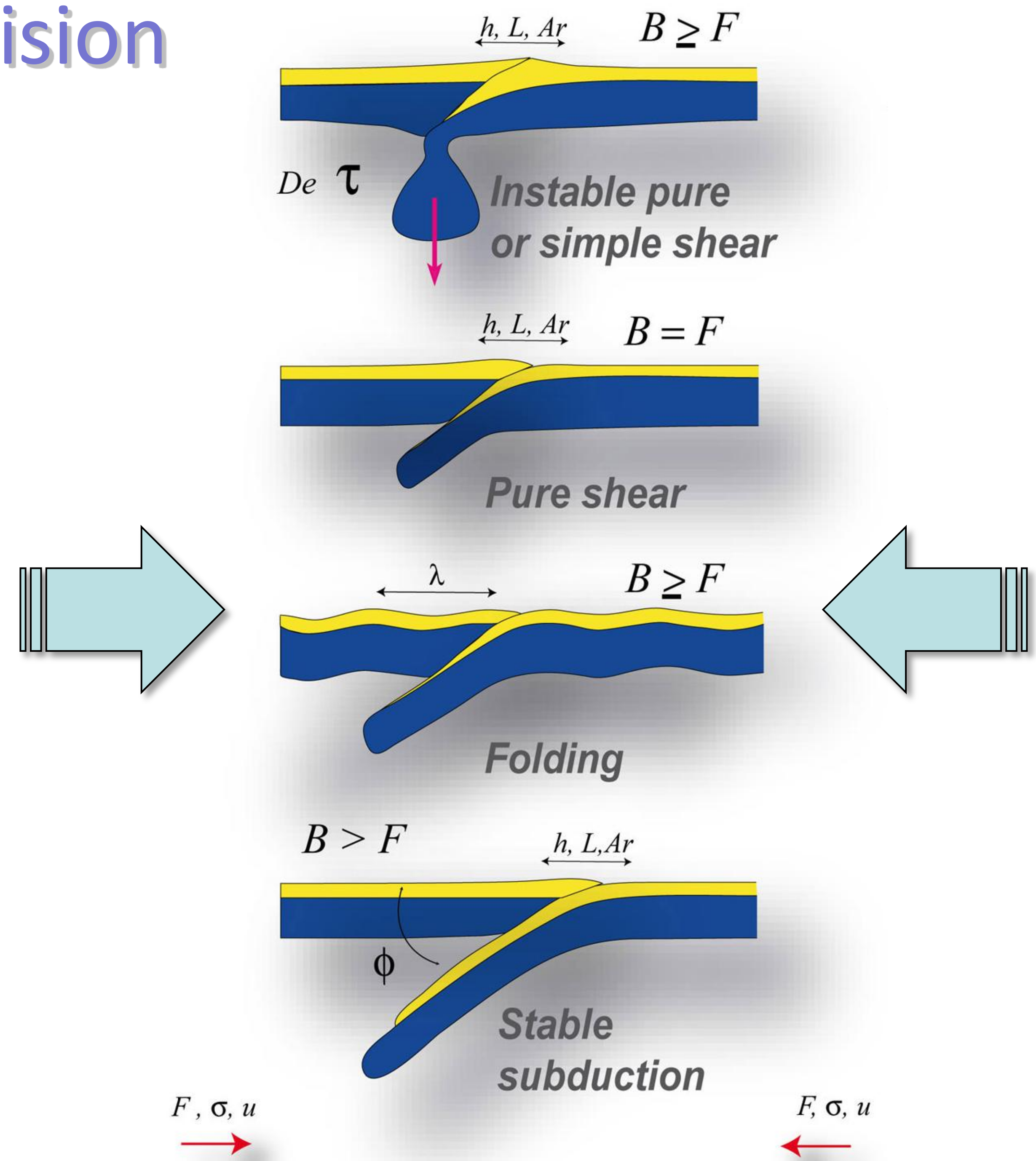

Petrologic P-T-(t) paths: indicators of rock burial and exhumation

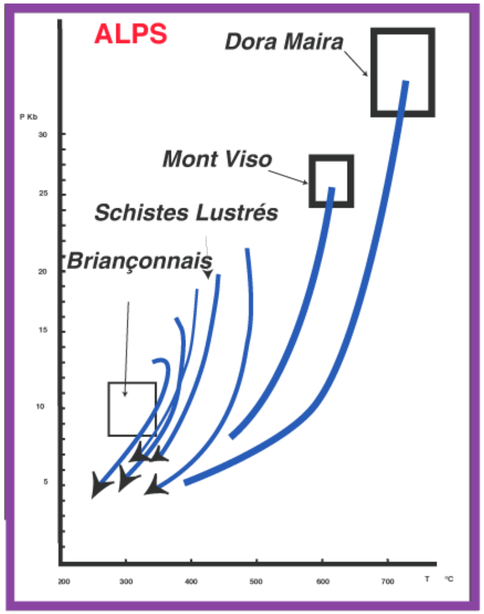

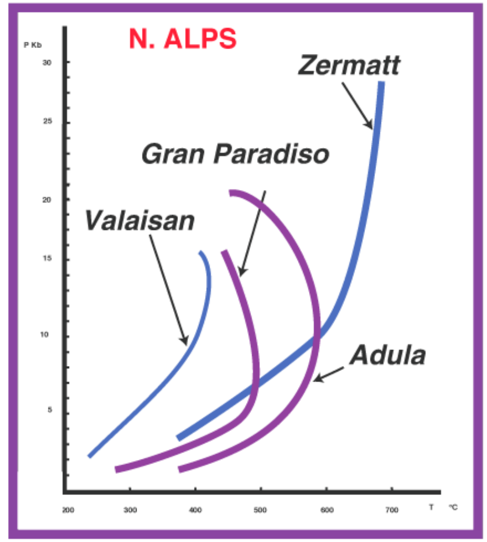

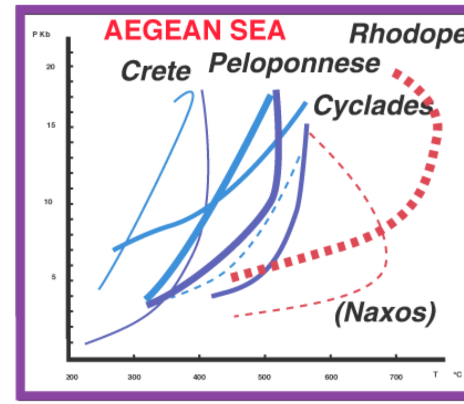

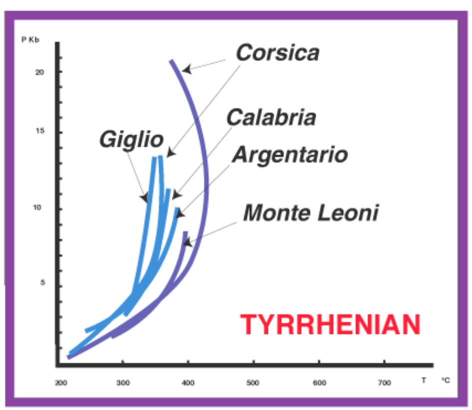

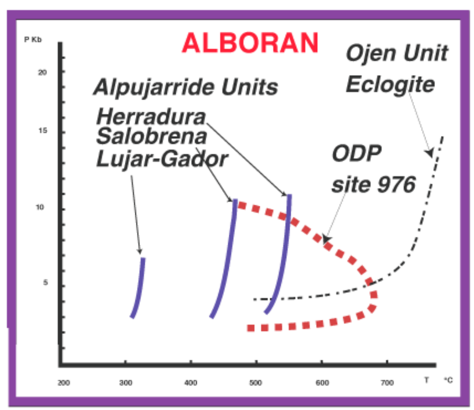

Retrograde Pressure-Temperature paths

tectonic denudation (Platt)

frontal accretion

no

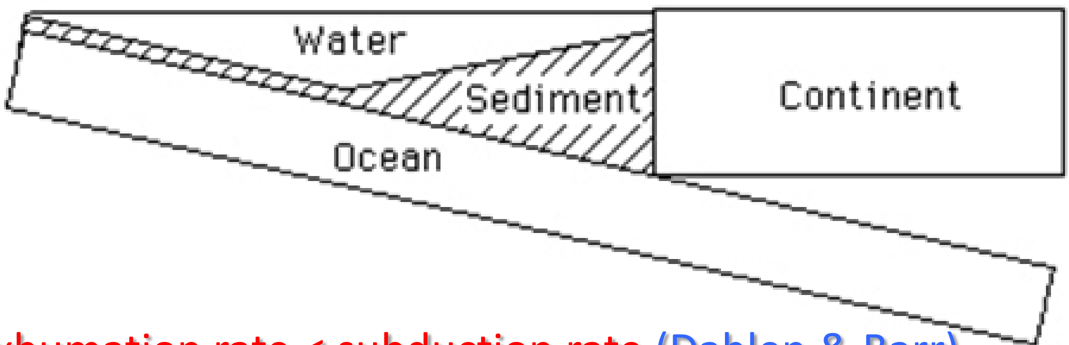

exhumation rate < subduction rate (Dahlen & Barr)

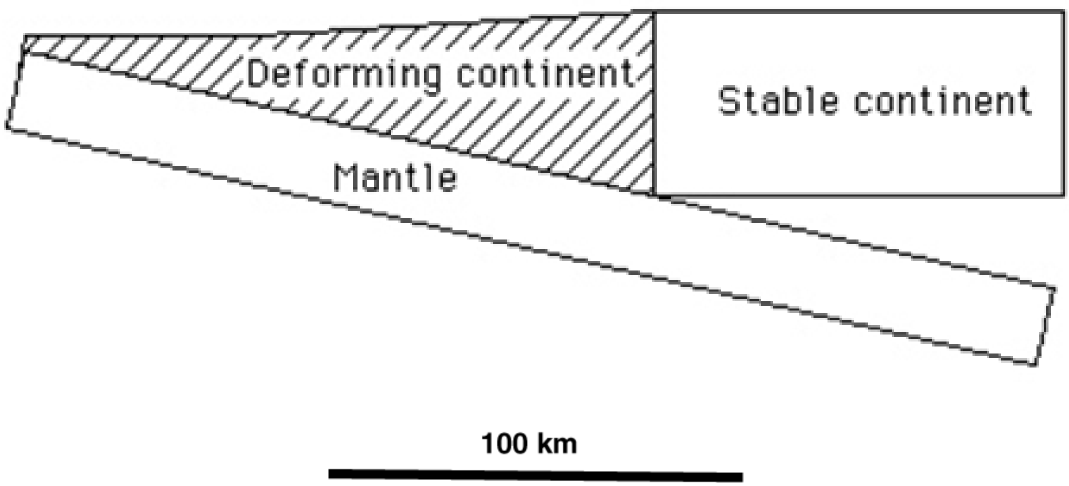

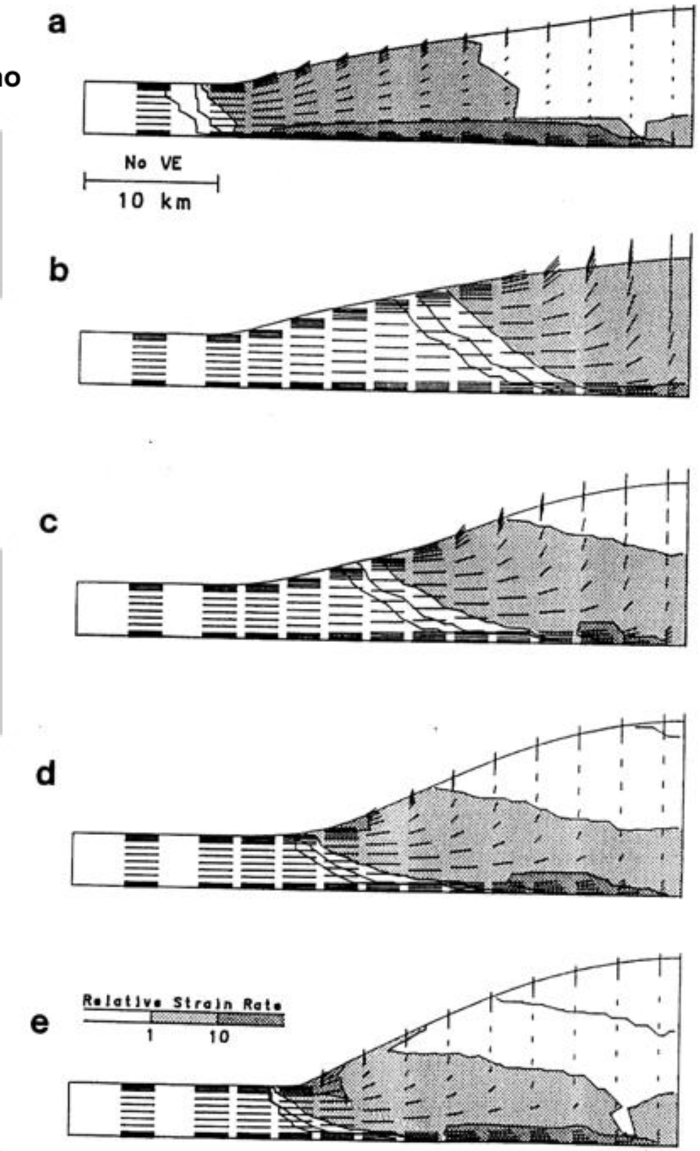

Classical exhumation concepts

… and their numerical implementation:

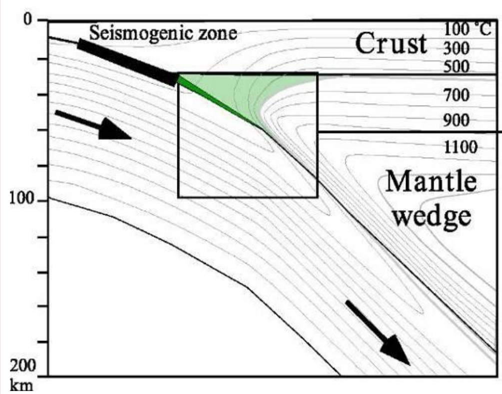

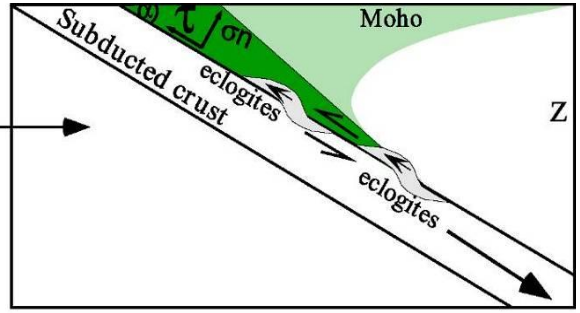

(Guillot et al., 2001)

semi-kinematic (oceanic) …

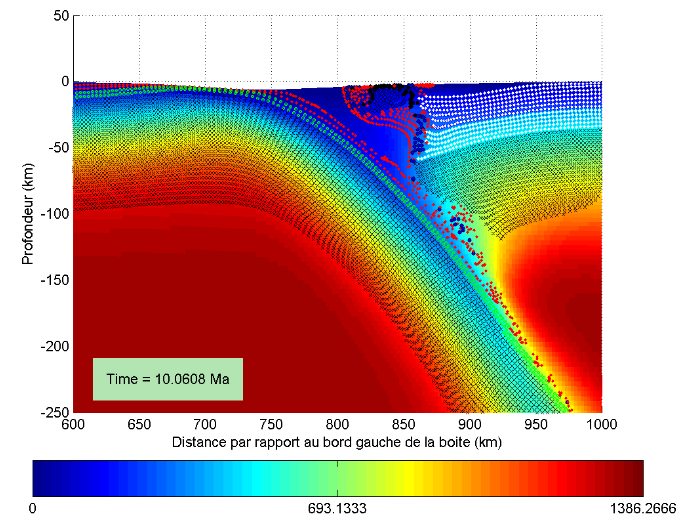

(Yamato et al., 2007)

unconstrained (oceanic)…

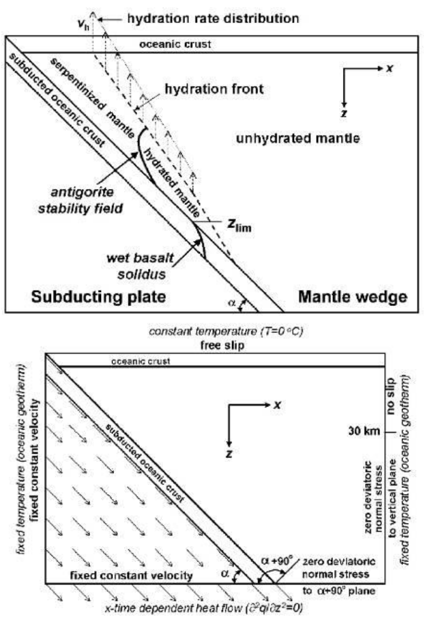

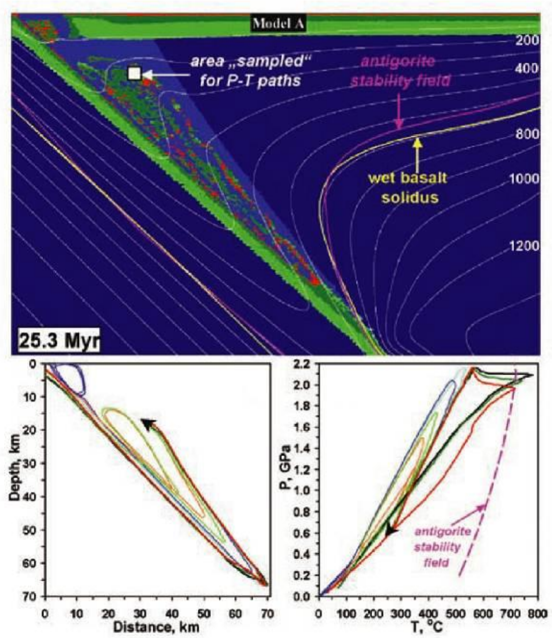

(Gerya et al., 2002)

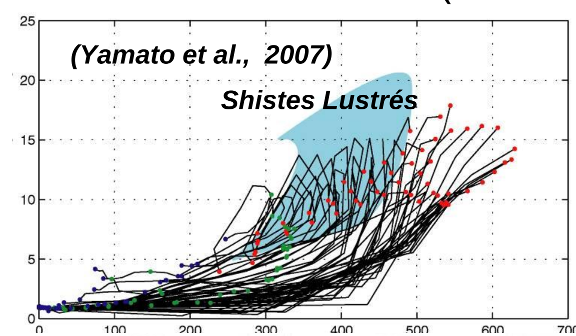

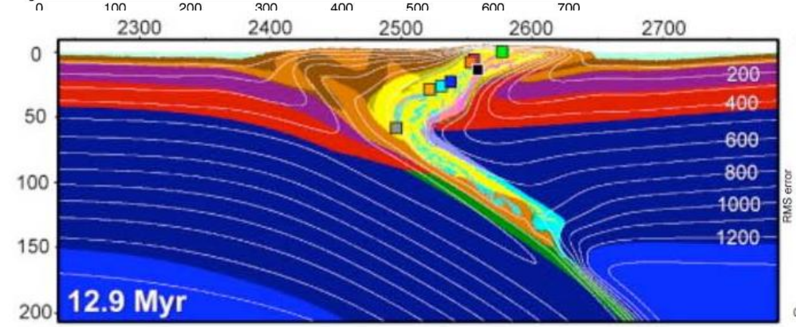

Gerya et al., Lithos, 2008

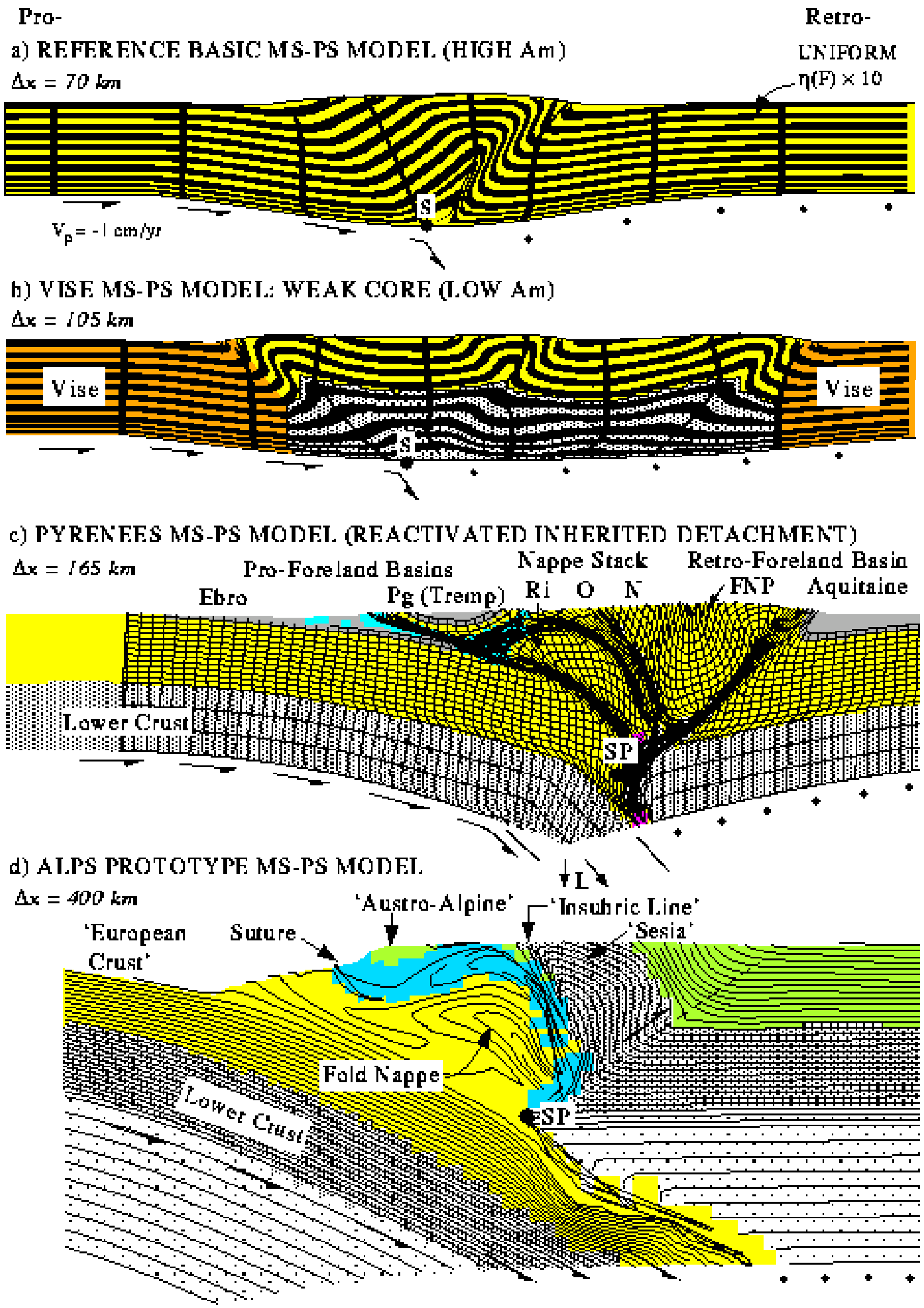

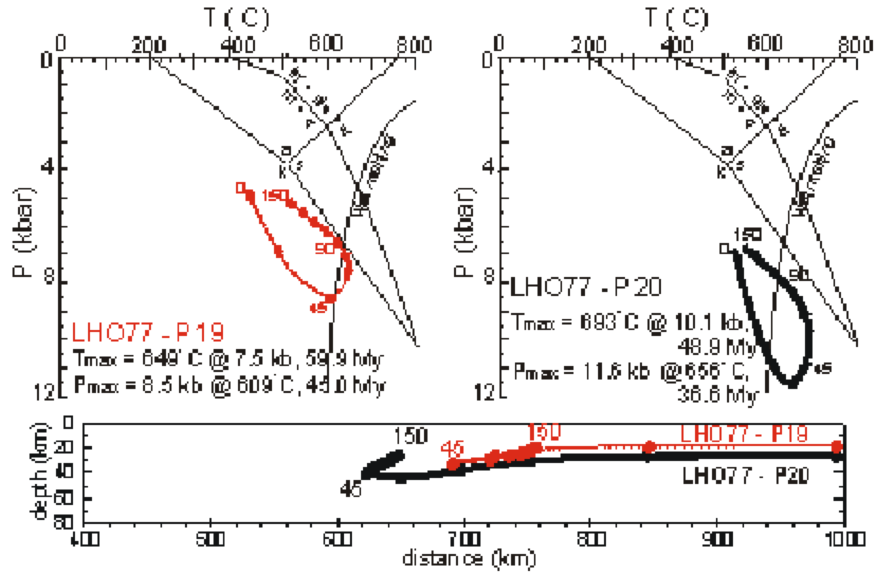

Beaumont et al., 2001

Rocks-indicators of HP-LT

after ***Yamato, PhD 2007***

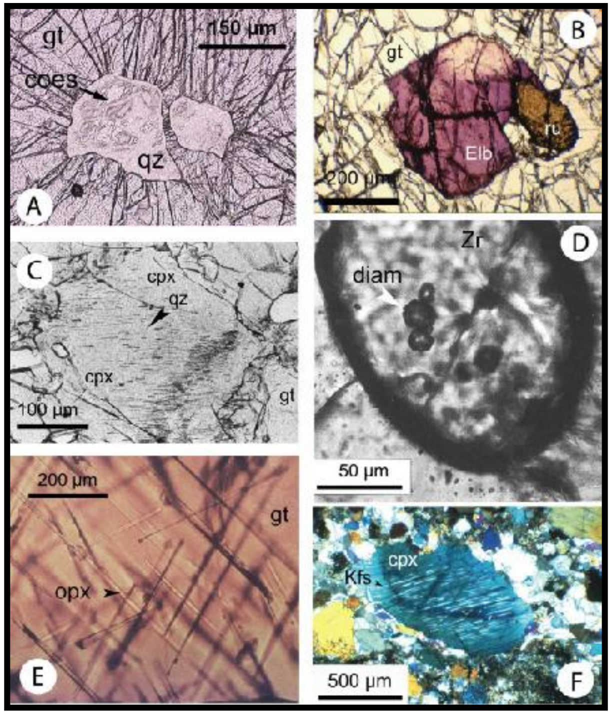

(Chopin, 2003)

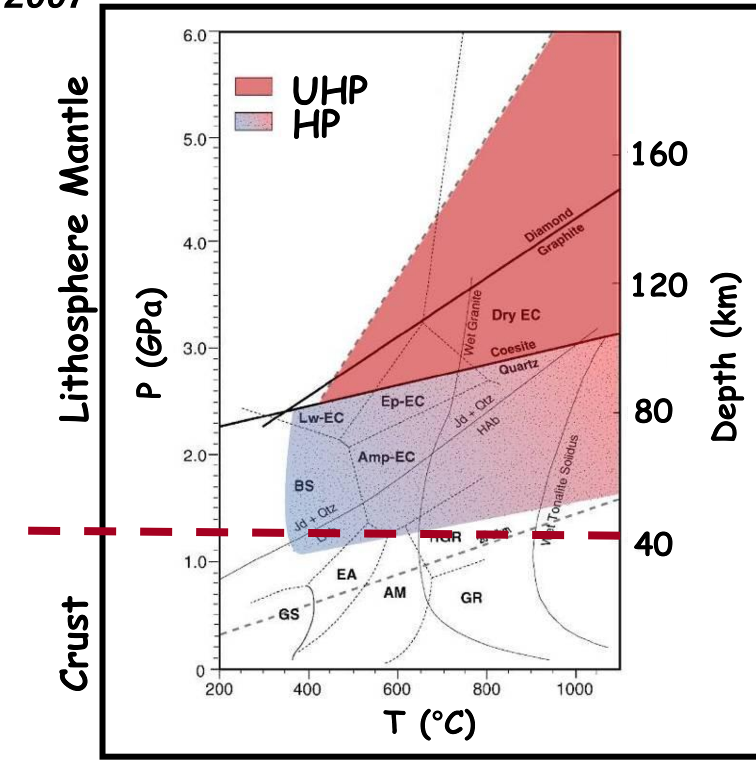

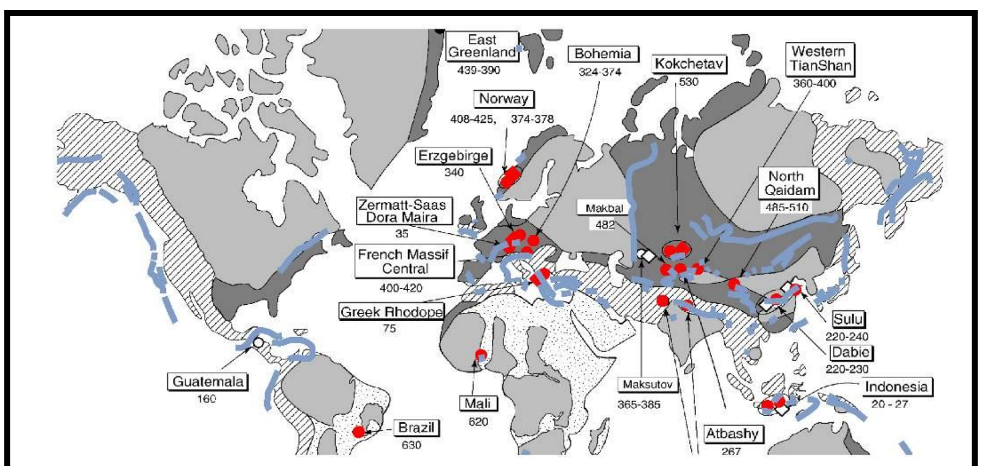

(Liou et al., 2004; Maruyama et al., 1996)

Geodynamic contexts

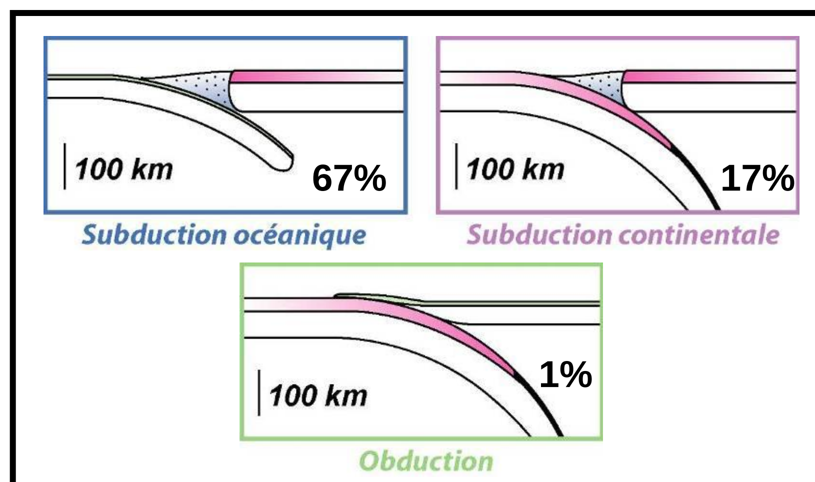

Alpine Collision

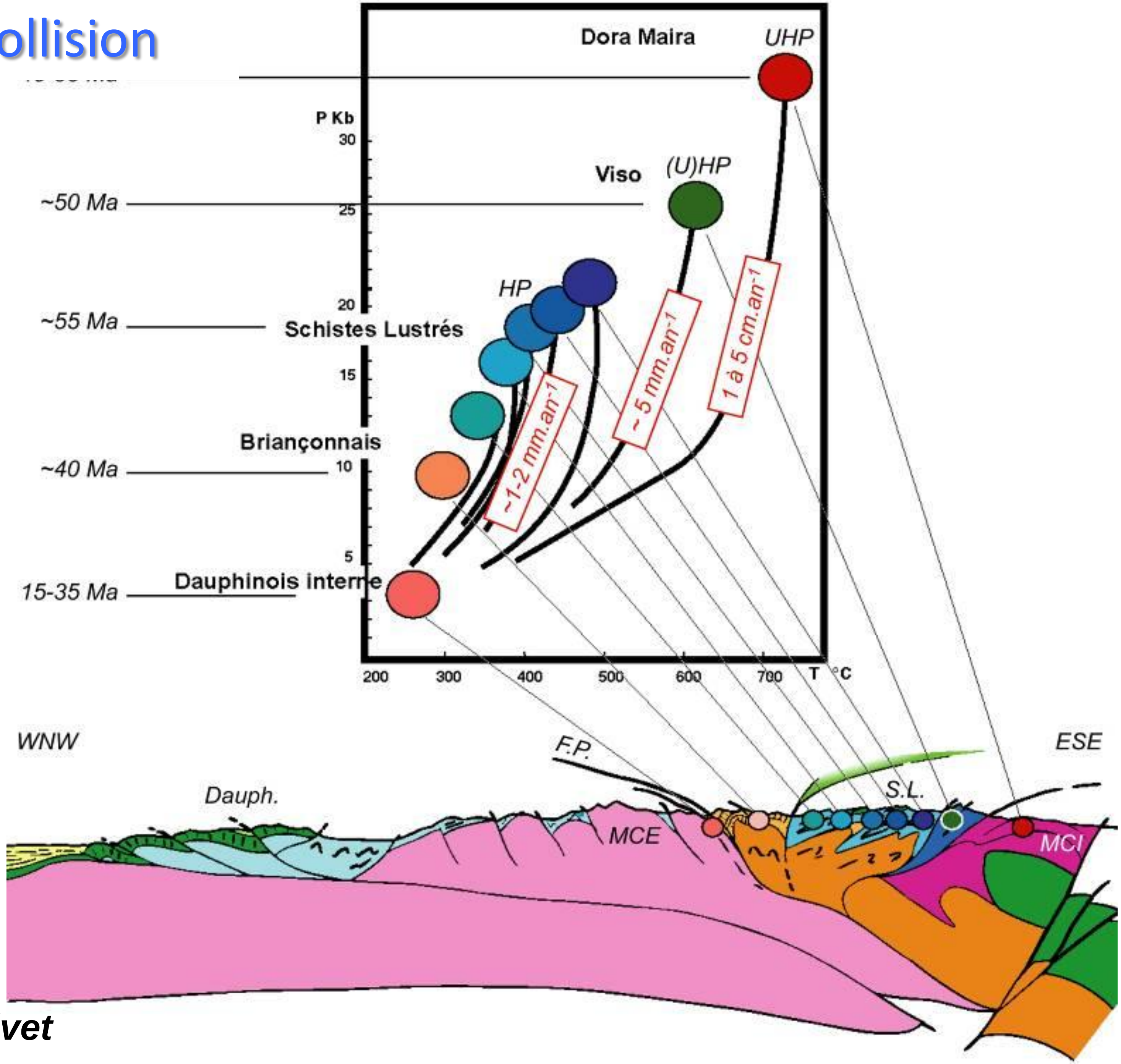

Source: ***L. Jolivet***

Continental UHP exhumation rates may exceed 10x the convergence rate !

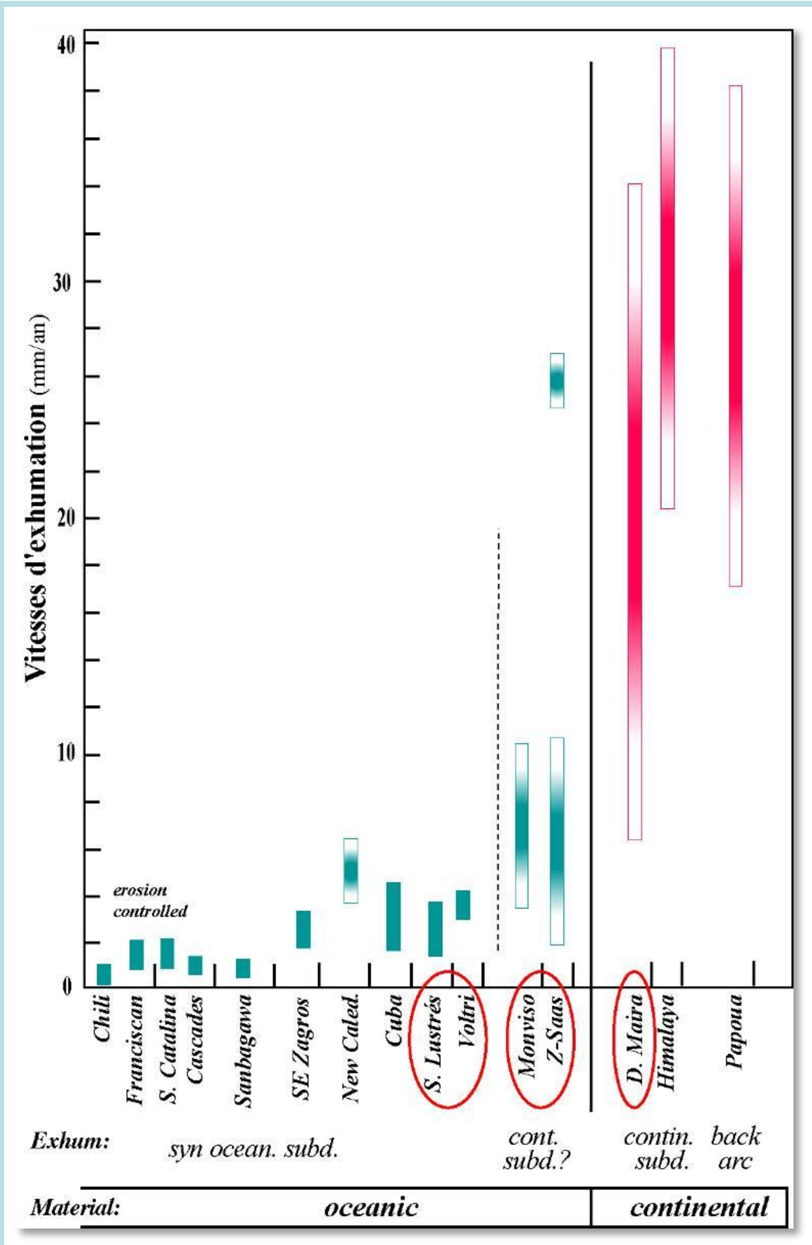

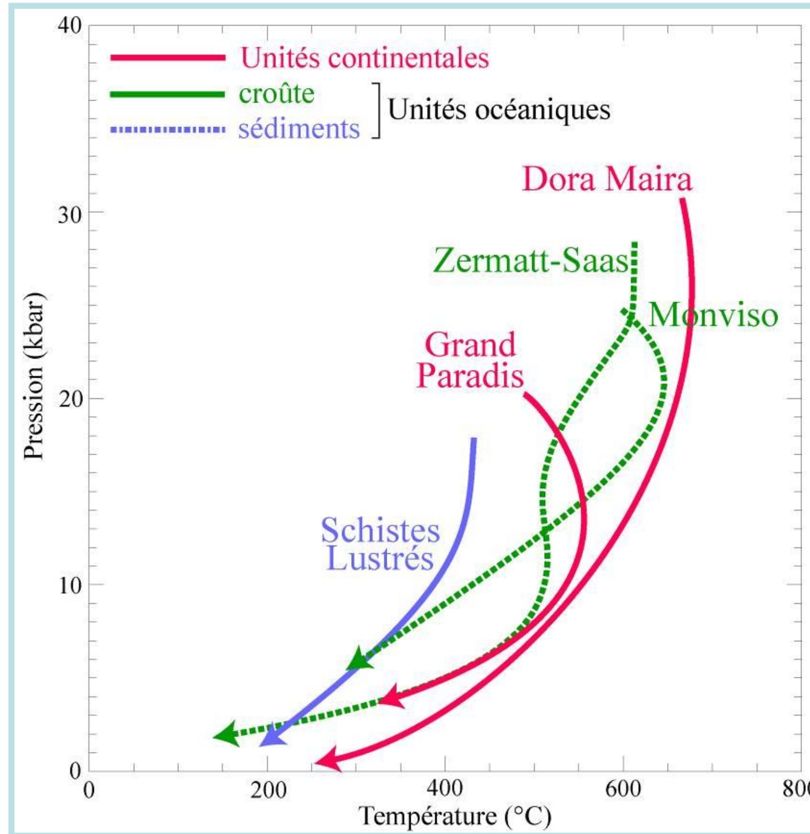

(Yamato et al., 2007)

Accretionary complex: LP and HP rocks, brittle material,
Slow exhumation
Overburden removal by the accretional mechanism and erosion

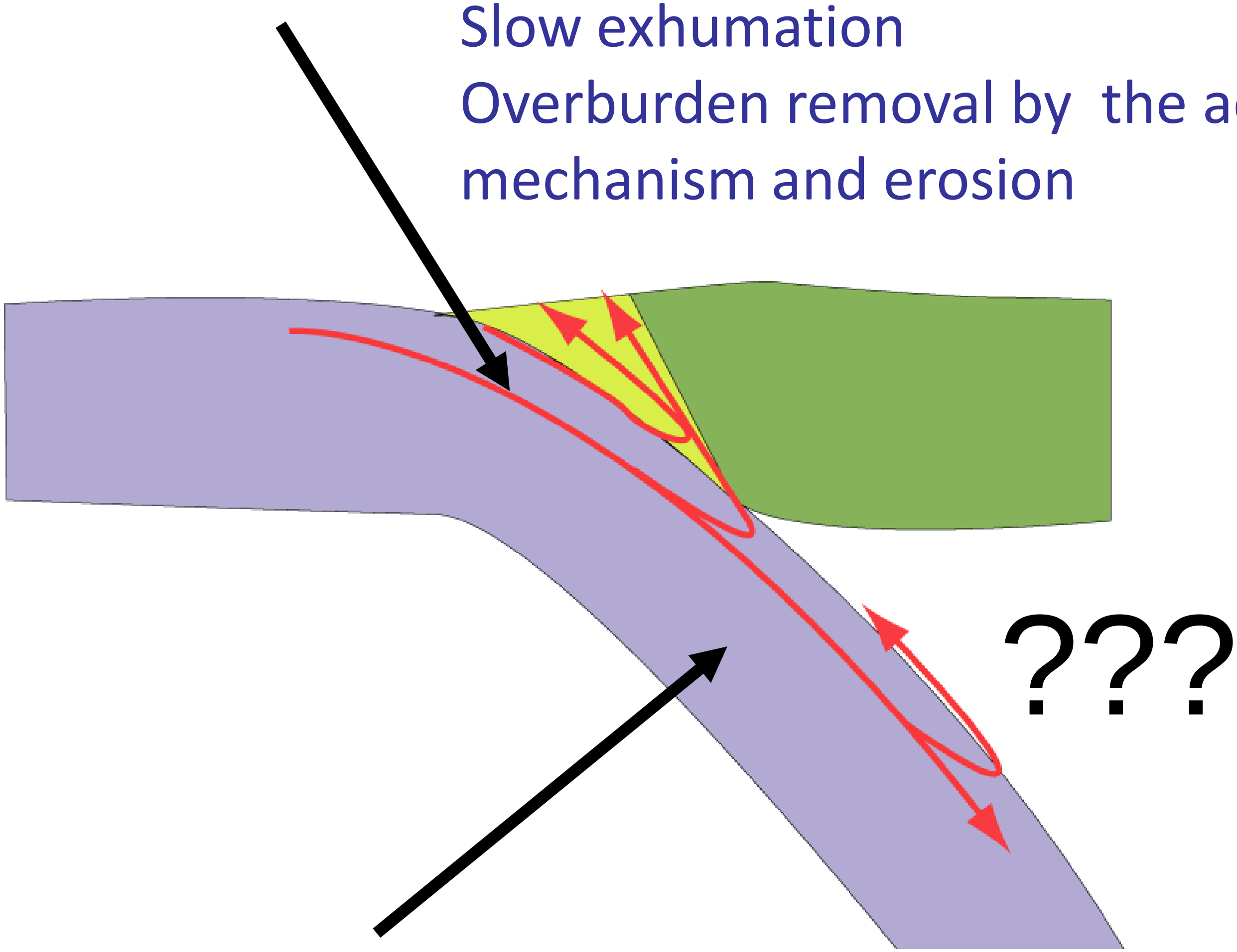

Subduction channel: HP and UHP rocks
Fast exhumation, Ductile material,
Special Mechanisms

« CHEMENDA MODEL »

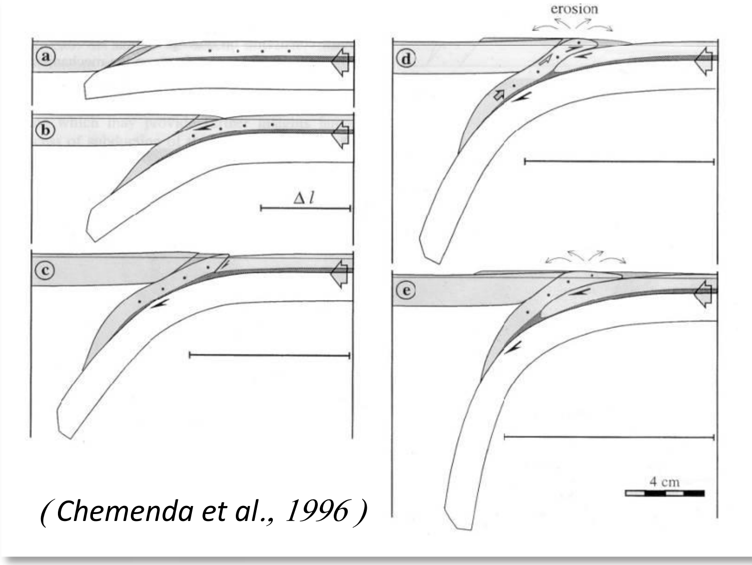

(Chemenda et al., 1996)

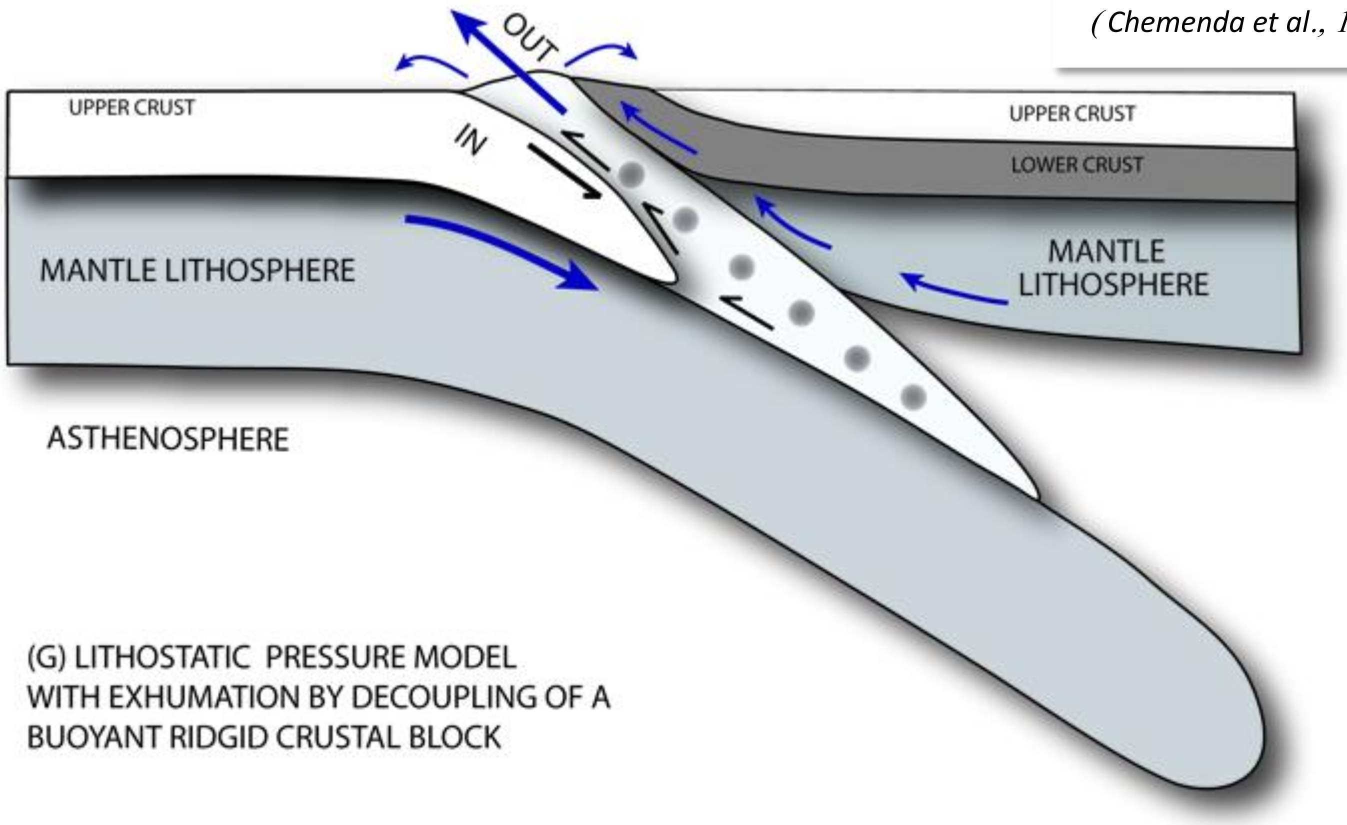

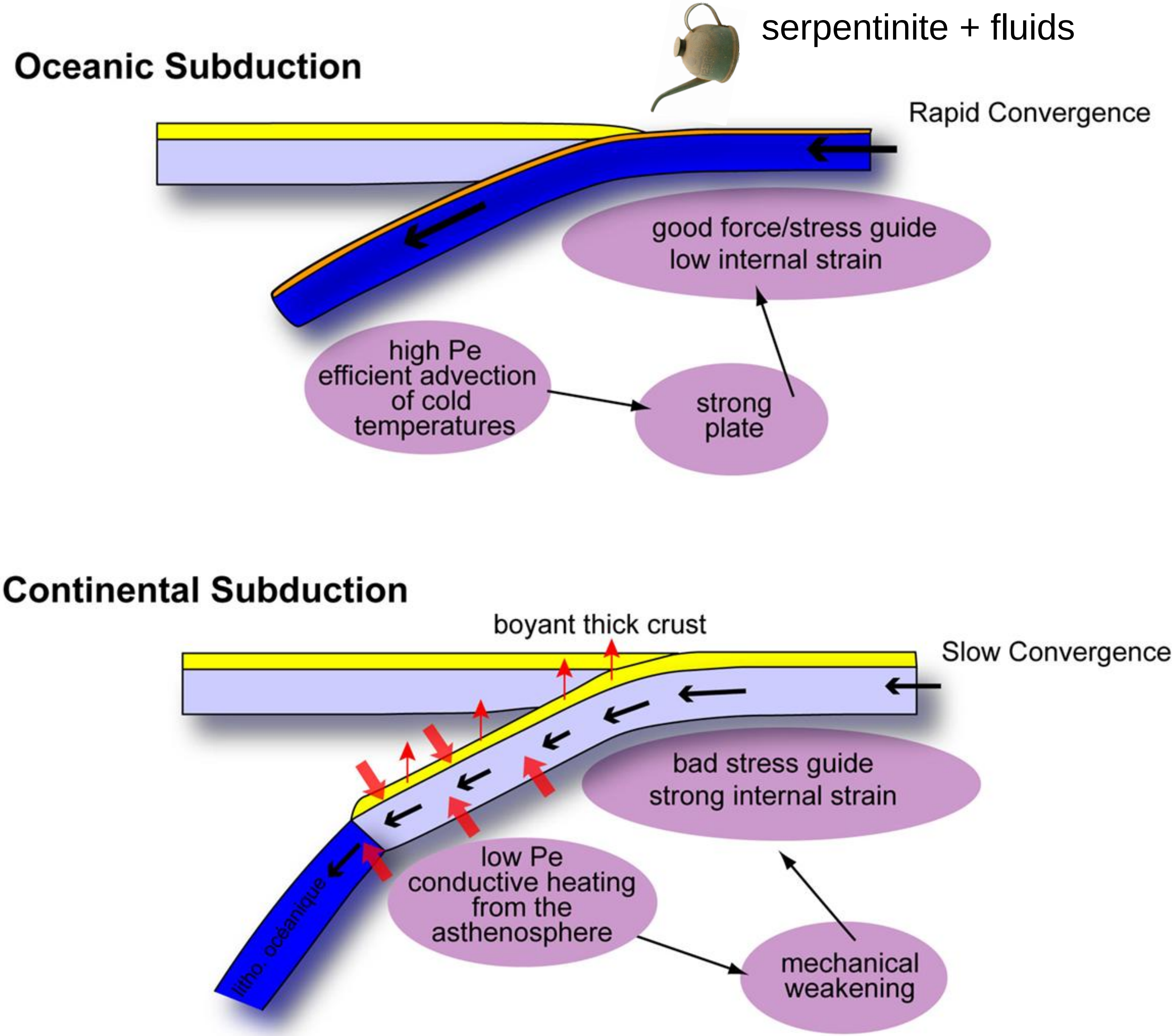
serpentinite + fluids
Oceanic Subduction
Rapid Convergence
good force/stress guide
low internal strain
high Pe
efficient advection
of cold
temperatures
strong
plate
Continental Subduction
boyant thick crust
Slow Convergence
bad stress guide
strong internal strain
low Pe
conductive heating
from the
asthenosphere
mechanical
weakening
litho. océanique

UHP exhumation: dynamic flow overpressure $P=\rho gz+P_d$ (rocket-nozzle model by N. Manctelow) ?

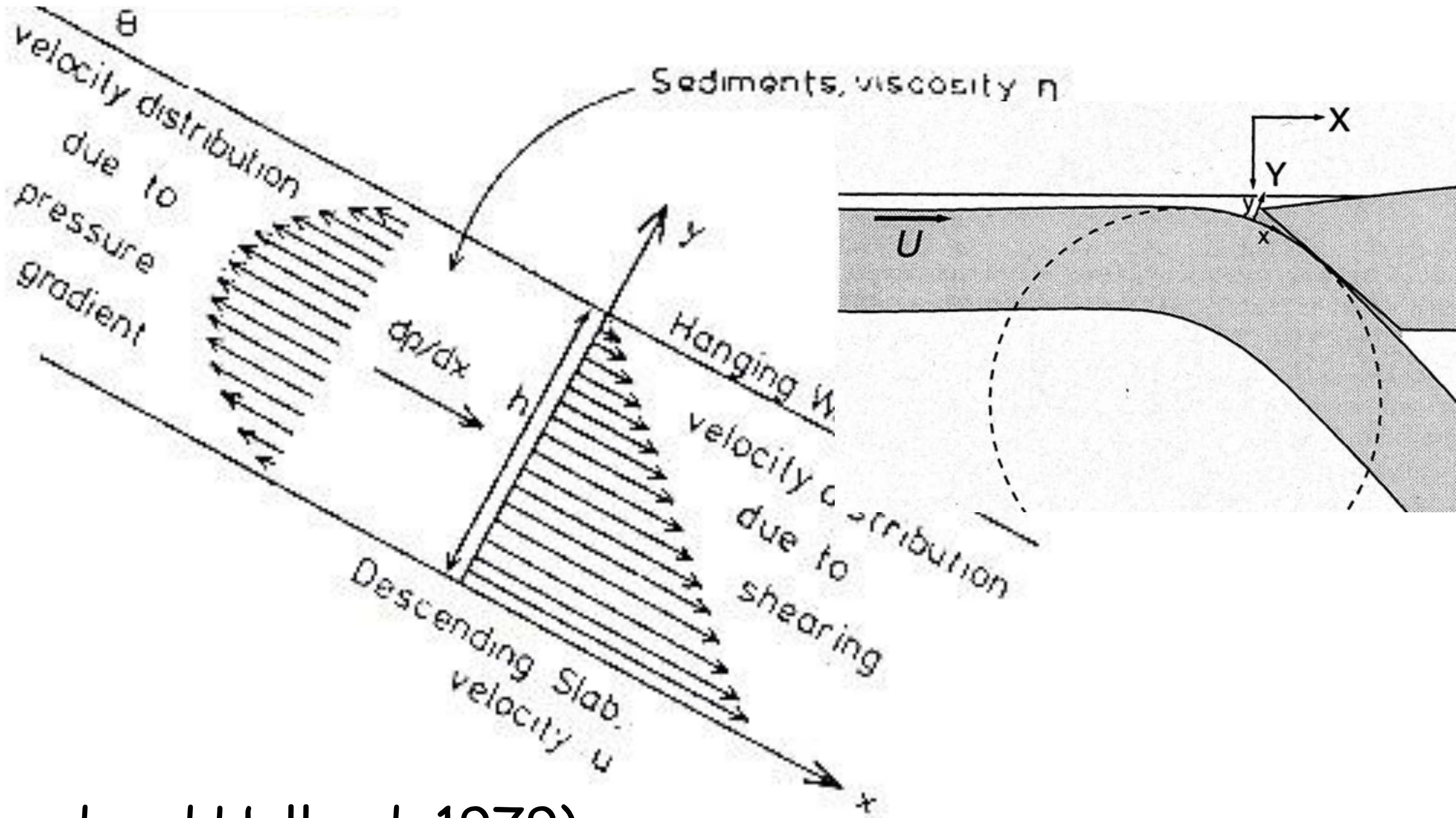

(England and Holland, 1979)

Static overpressure ?

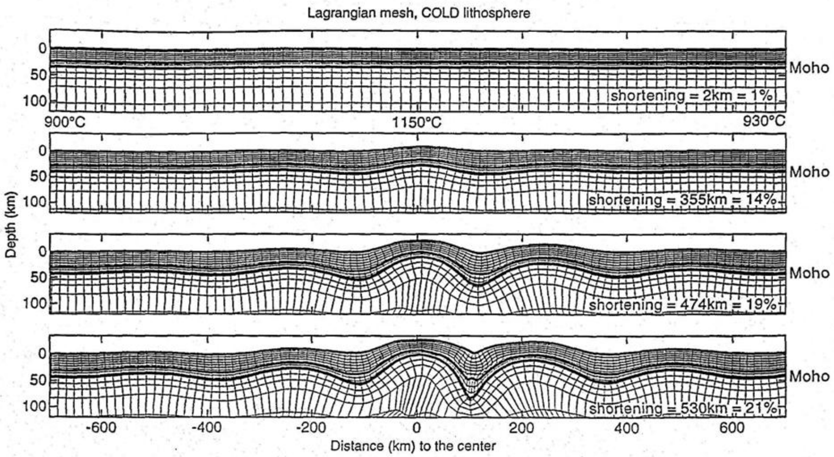

(Burg and Podladchikov, 2000)

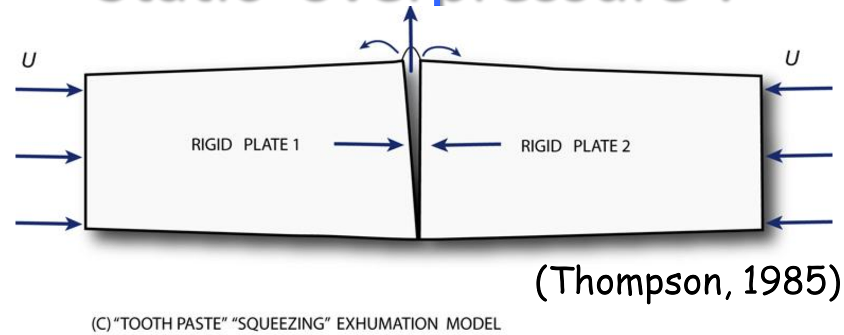

(Thompson, 1985)

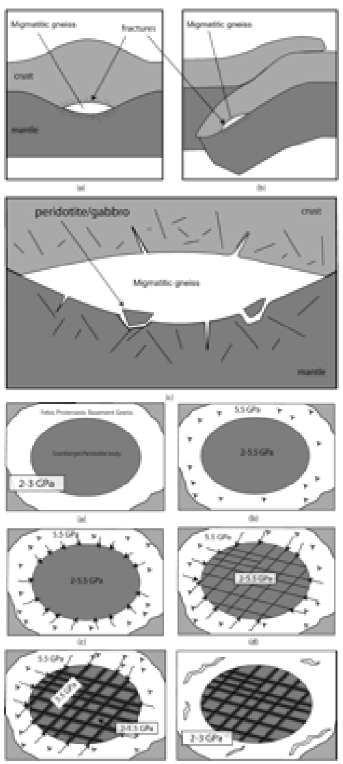

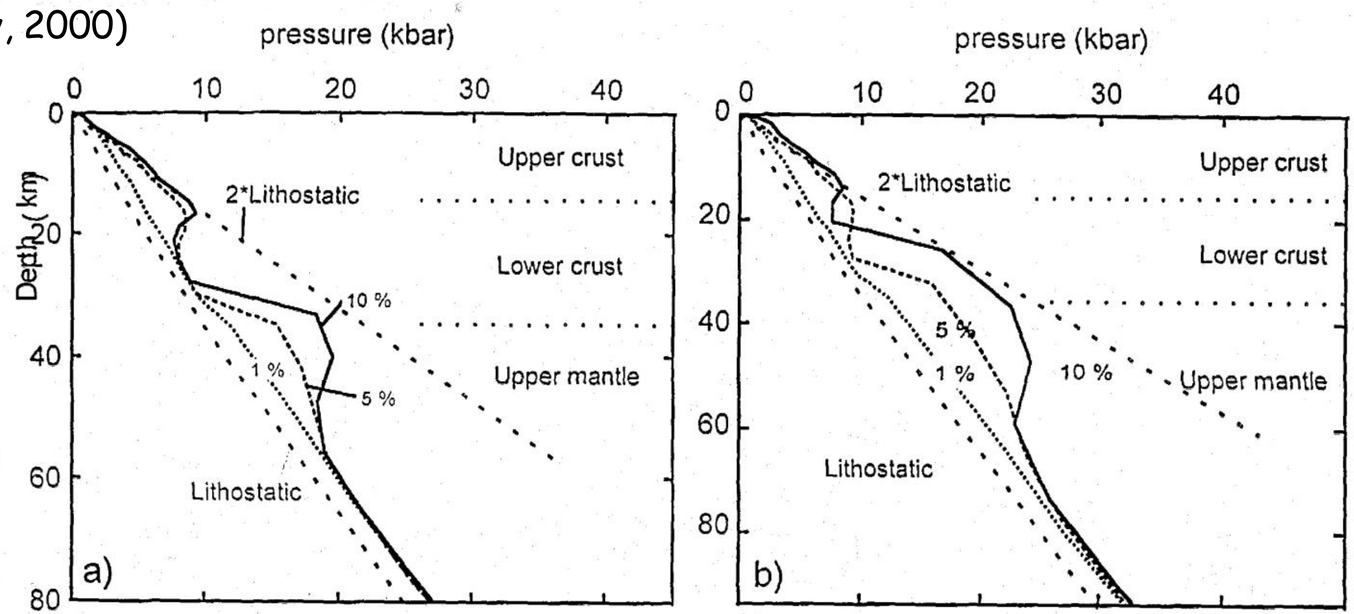

Fig. 7: Pressure distribution with depth at different % shortening for (a) 120 km thick lithosphere, and (b) 160 km thick lithosphere. The line indicated with 'lithostatic' corresponds to a lithostatic pressure gradient ($P=1\rho gz$); the other lines correspond to the pressure resulting from the model at different stages of shortening.

(Vrijmoed et al, 2009)

(Petrini and Podlachikov, 2000)

Continental Lithosphere:
THICK MULTI-LAYER with EVP rheology

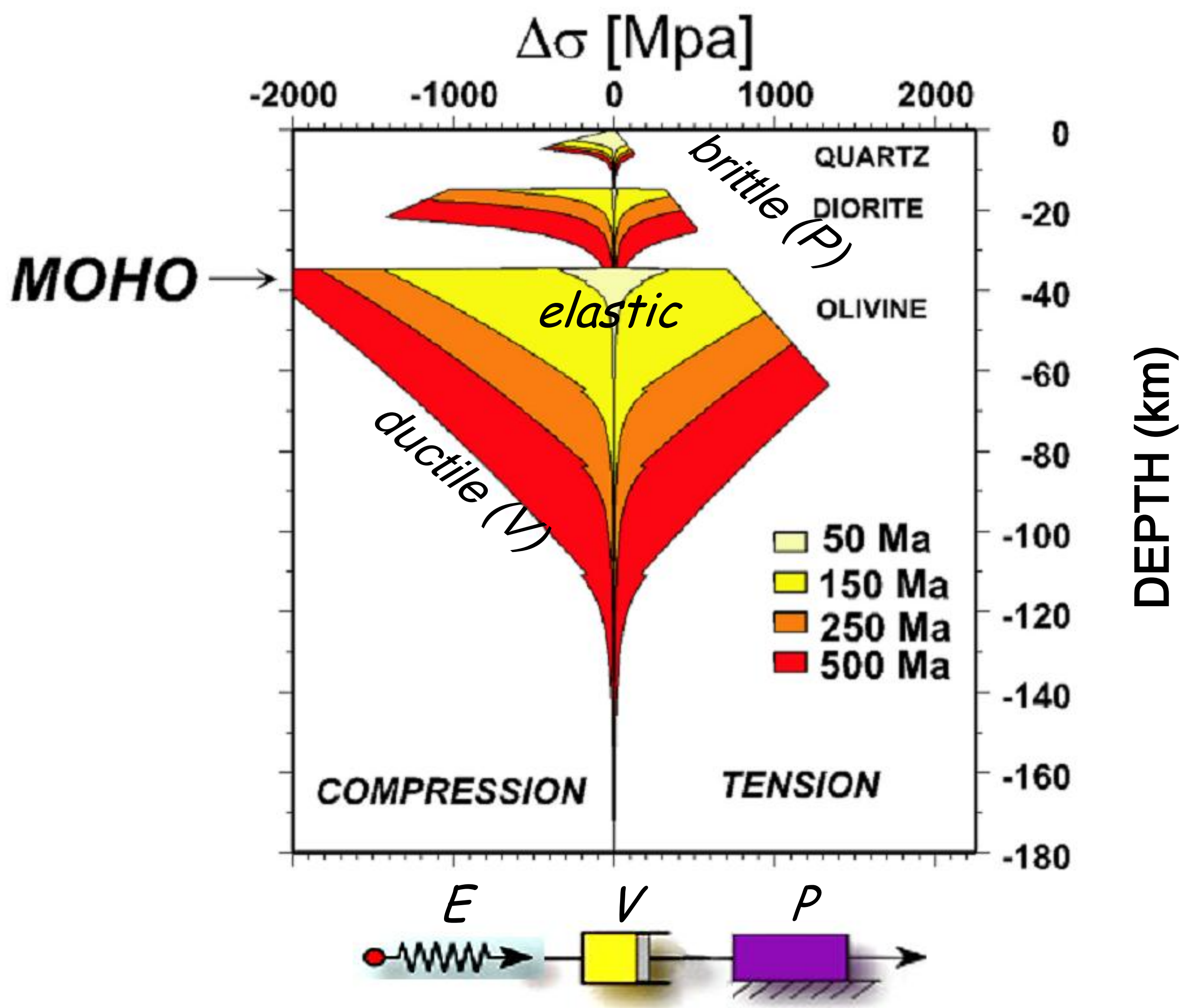

UHP exhumation: continental subduction ?

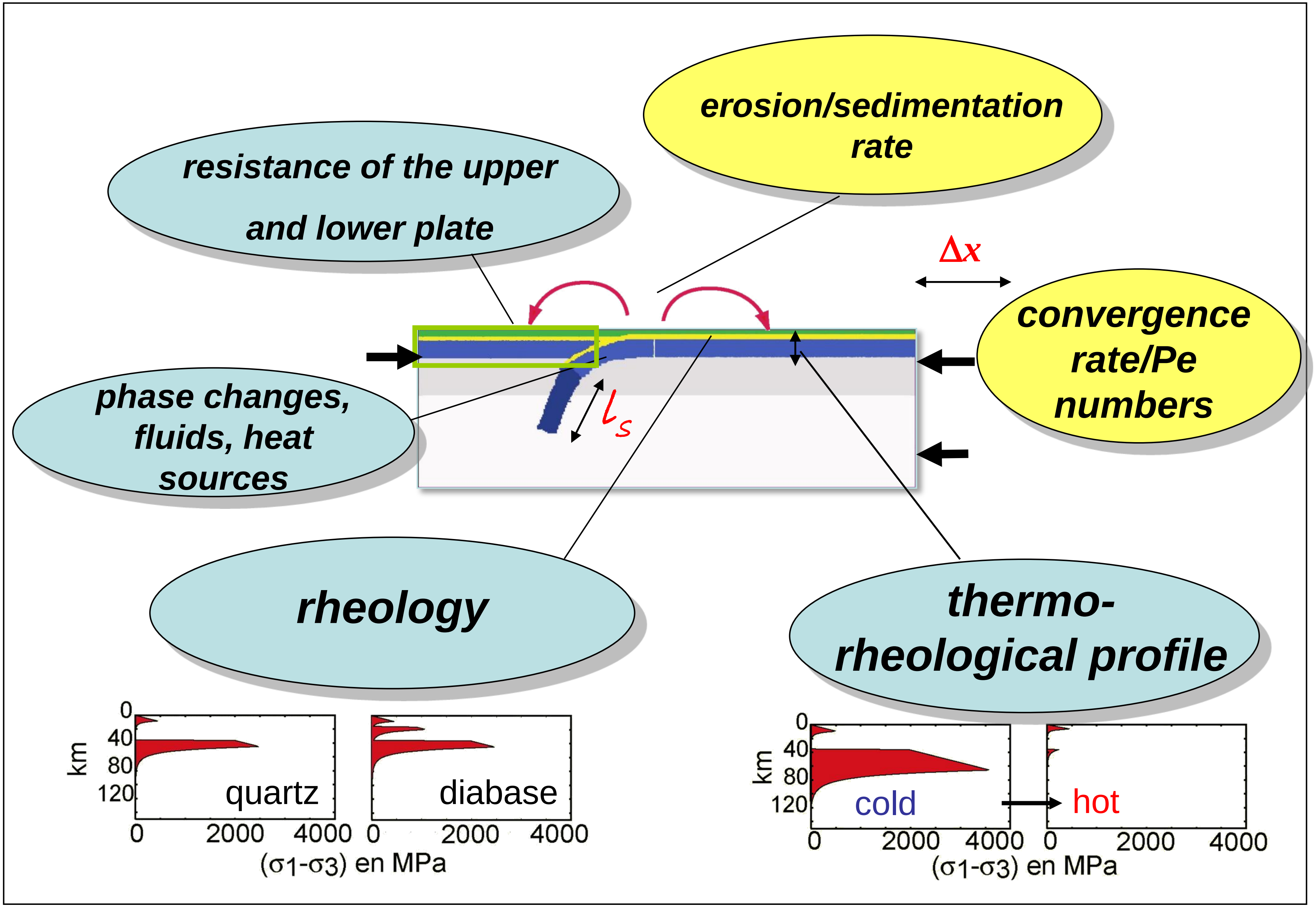

SUBDUCTION NUMBER:

$$1 < \boldsymbol{S} = \frac{l_s}{\Delta x}$$

l_s *(subduction length)*

Δx *(amount of shortening)*

MINIMAL CONDITION via Peclet number :

$$Pe / \; u_x h_k / \kappa > 1; \quad Pe \gg 1$$

$$\boldsymbol{Pe} = \frac{\text{heat advection rate}}{\text{heat diffusion rate}}$$

Collision/Subduction models

After B. Kaus

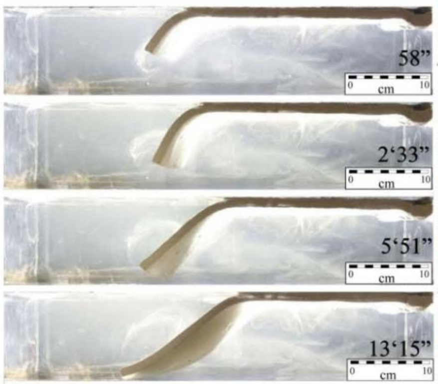

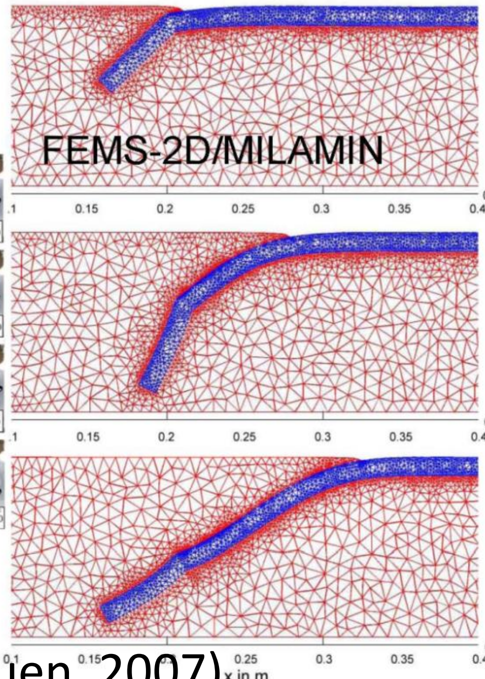

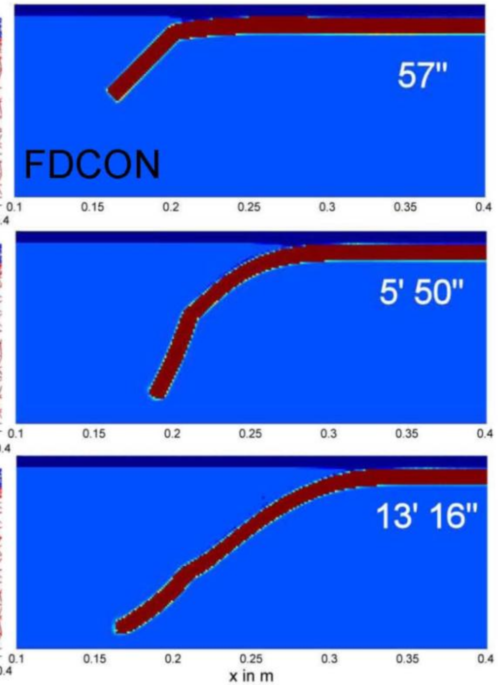

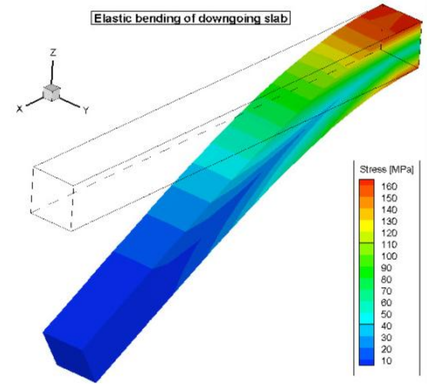

Popov & Sobolev, 2007

I3ELVIS (Gerya & Yuen, 2007)

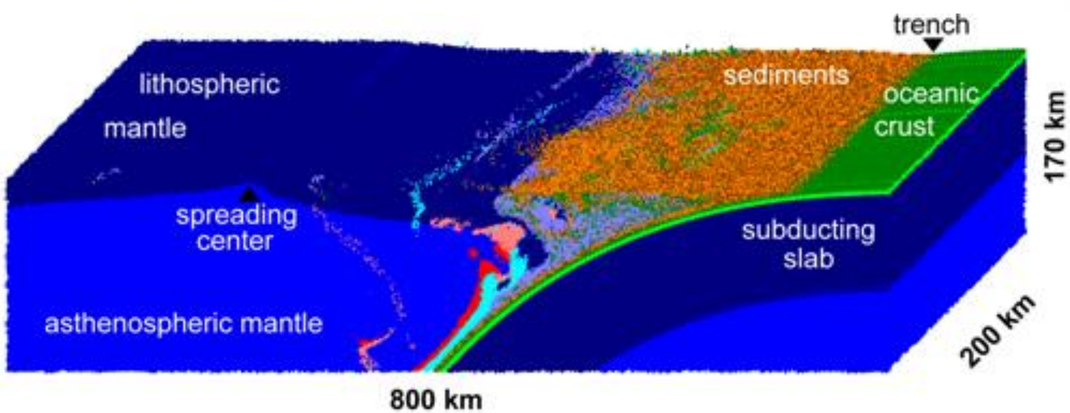

FLAMAR (Burov & Yamato, 2007)

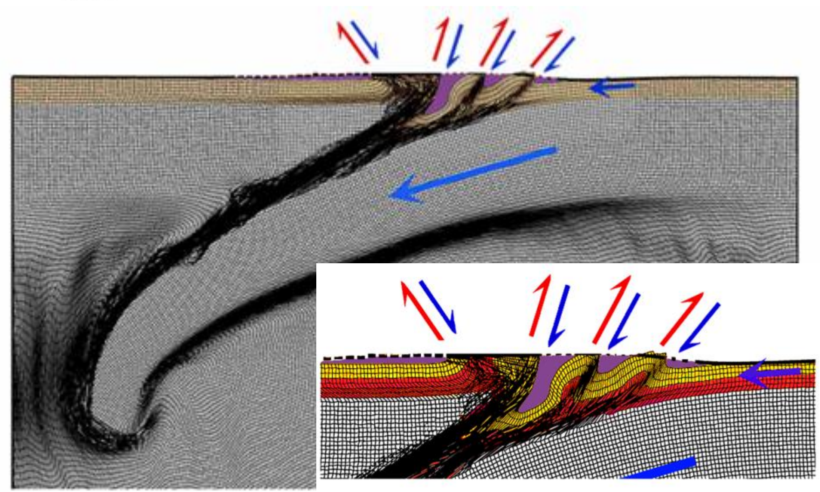

Continental collision and UHP exhumation

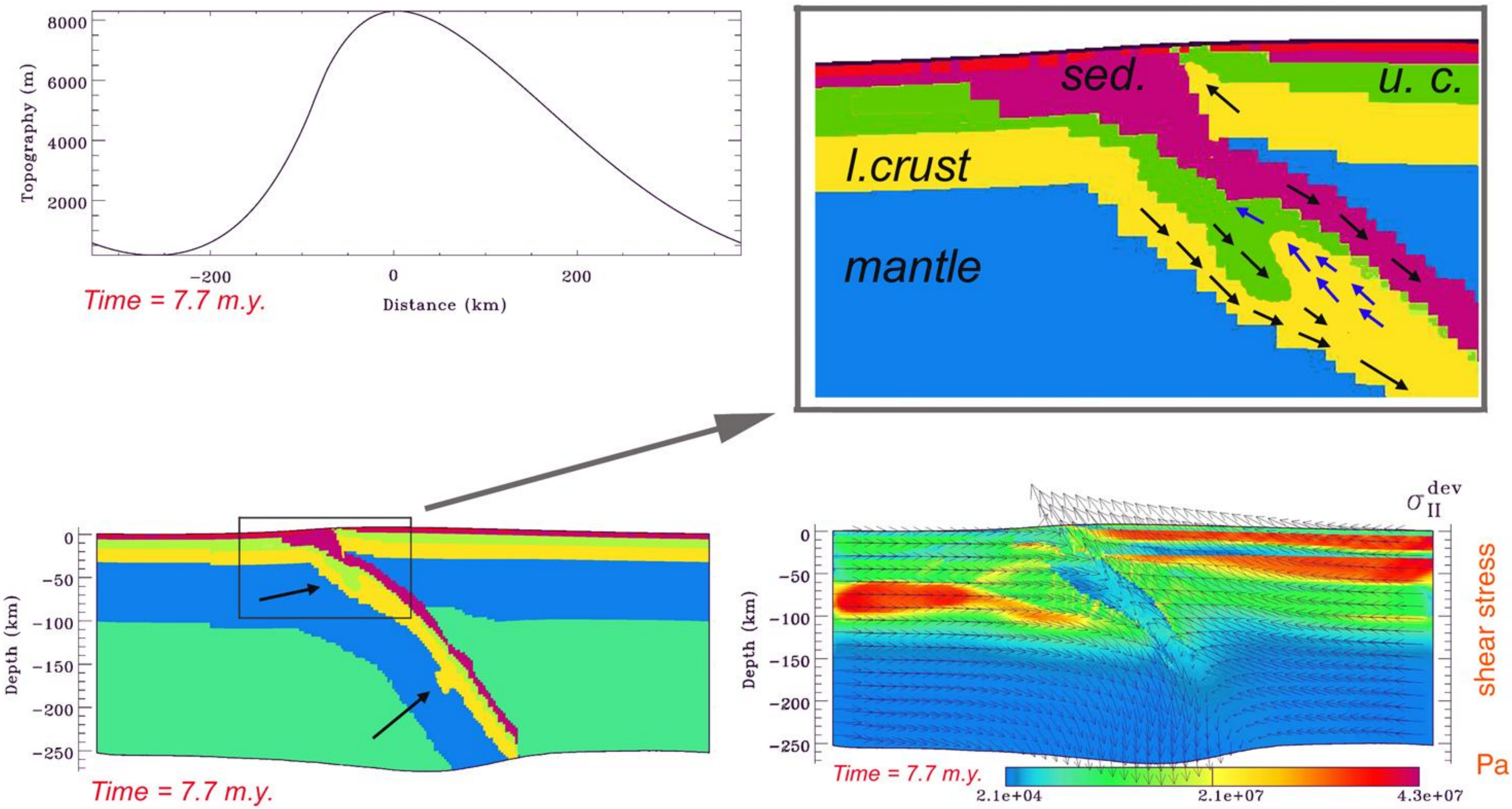

Multi-level exhumation, Stokes mechanism for UHP part

Burov et al., 2001

Summary of requirements to numerical code

- *Large strain/transformations*
- *viscous-elastic-plastic rheology:*
- *Thermo-mechanical coupling*
- *Thermodynamic coupling*
- *Coupling with surface processes*
- *Free surface as upper boundary condition*

Mohr-Coulomb and Peierls plasticity

Softening-hardening

Non-linear ductile creep

Latent heat sources
Radiogenic sources
Shear heating

fluids, melting
chemestry

(RED: specific requirements compared to convection codes)

Hybrid FEM-FDM FLAC-*like* codes (e.g., Paravoz, Flamar)

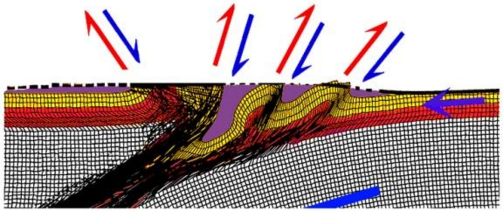

Equilibrium Equation
(Equation of Motion)

new
velocities and
displacements

Heat transport equations,
Surface transport (erosion/sedim.),
Thermodynamic and
other processes equations

new
stresses
or forces

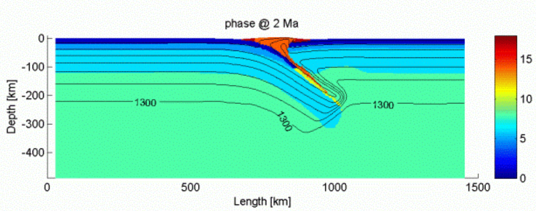

Stress / Strain Relation
(Constitutive Equation)

visco-plastic (+elastic) Stokes FDM
(P. Tackley, T. Gerya …)

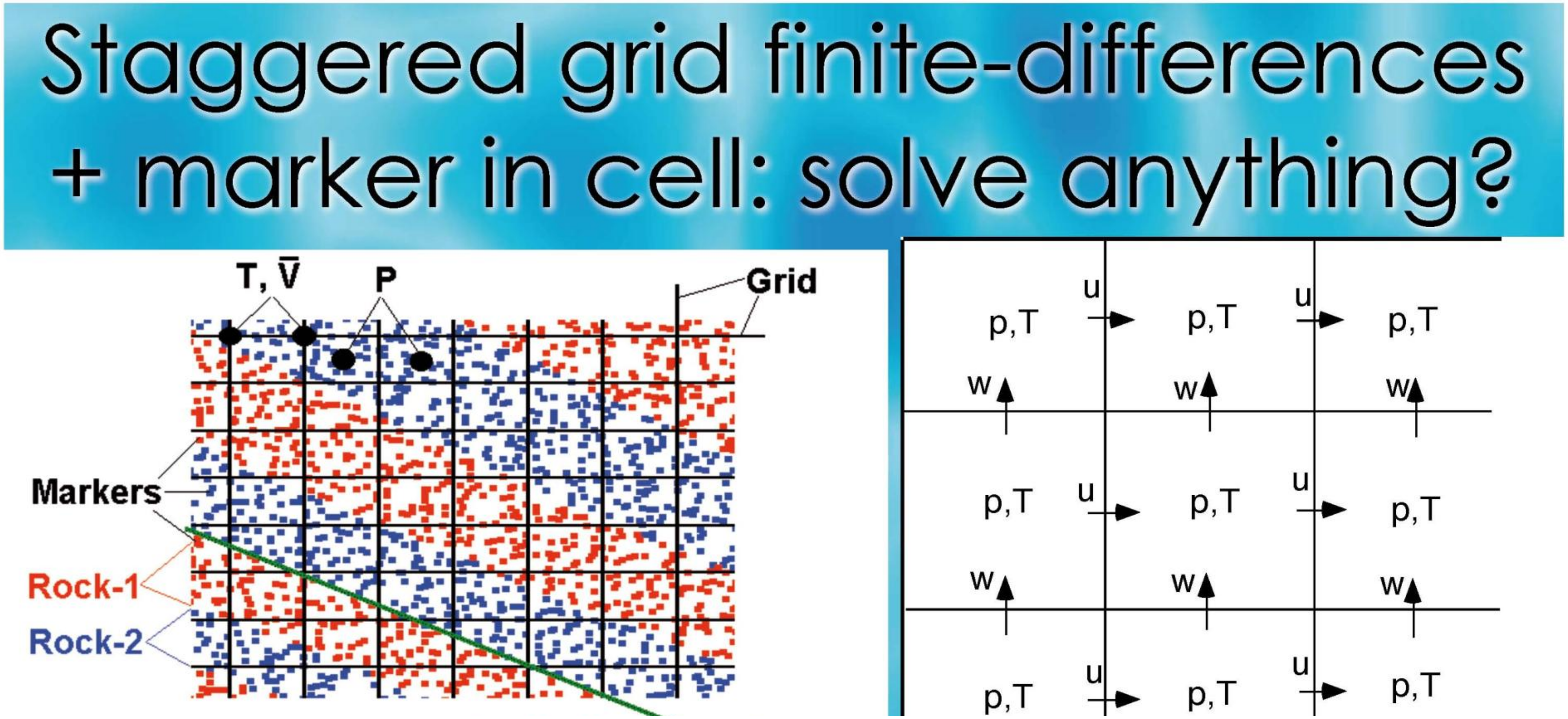

Newton's 2nd law of motion

$$\rho g_i + \frac{\partial \sigma_{ij}}{\partial x_j} = \rho \frac{\partial V_i}{\partial t}$$

Heat Diffusion, Production, Advection

$$\frac{DT}{Dt} = \frac{\partial}{\partial x_i}\left(\chi \frac{\partial T}{\partial x_i}\right) + \frac{\sum H_i}{\rho\, C_p} - V_i \frac{\partial T}{\partial x_i}$$

$$H_a = \alpha T v_i \frac{\partial P}{\partial x_i},$$

$$H_s = \sigma_{ij}\dot{\varepsilon}_{ij(\text{non-elastic})},$$

$$H_r = H_s e^{-z/h}$$

Constitutive laws

$$\frac{D\sigma}{Dt} = F\left(\sigma, \mathbf{u}, \mathbf{V}, \nabla\mathbf{V}, \ldots, T, \ldots\right)$$

Additional laws

$$\rho = f(P,T); \quad G = \sum_{i=1}^{n} \mu_i N_i$$

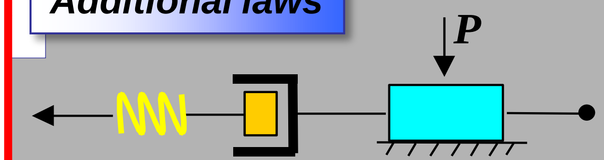

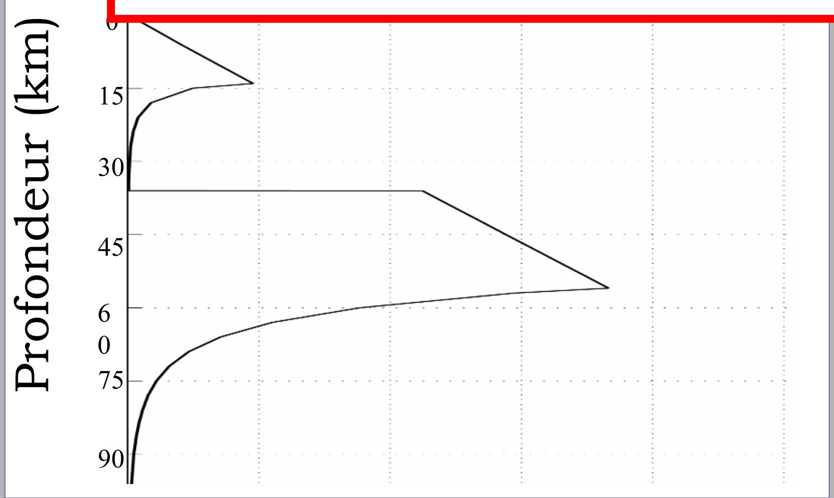

Viscous $$\dot{\varepsilon} = A\ \exp\left(-\frac{E}{RT}\right)\sigma^n$$

Elastic $$\sigma_{ij} = \lambda\ \delta_{ij}\sum_k \varepsilon_{kk} + 2\mu\varepsilon_{ij}$$

Plastic $$\tau = (\tan\varphi)\,\sigma_n + C_0$$

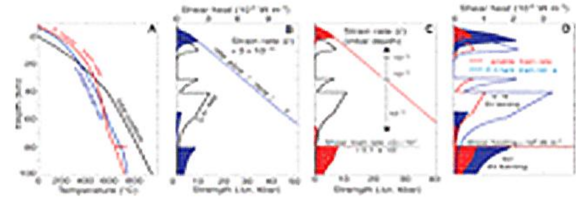

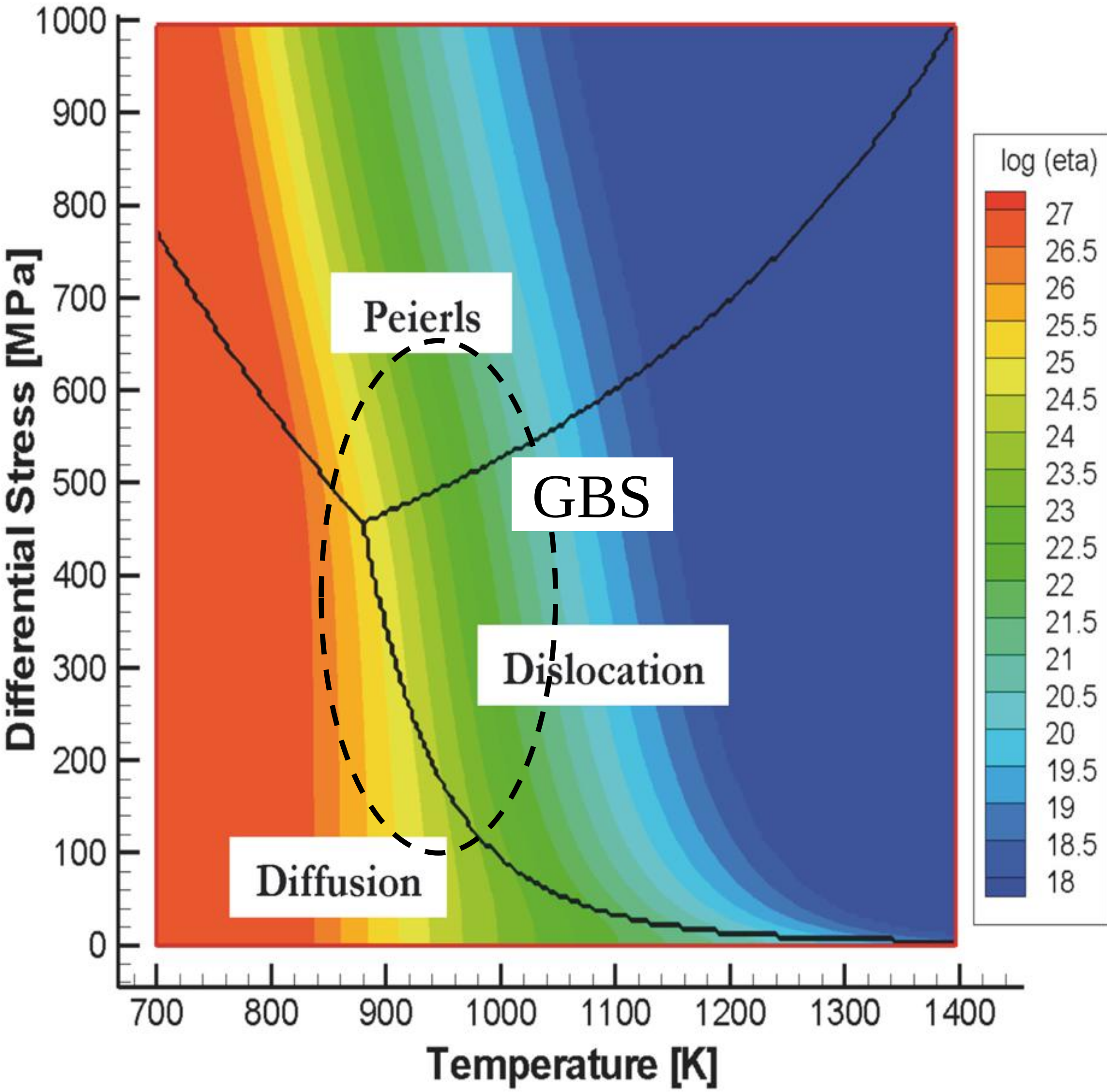

$$\dot{\varepsilon} = A_{DF} a^{-m} C_{H_2O} \tau_{II}^{n} \exp(-\frac{E_{DF}+PV}{RT})$$

diffusion creep

$$\dot{\varepsilon} = A_{DS} C_{H_2O} \tau_{II}^{n} \exp(-\frac{E_{ds}+PV}{RT})$$

dislocation creep

$$\dot{\varepsilon} = A_{P} \exp(-\frac{E_p}{RT}(1-\frac{\tau_{II}}{\tau_p}))$$

Peierls creep

$$\dot{\varepsilon} = A_{GBS} a^{-m} C_{H_2O} \tau_{II}^{n} \exp(-\frac{E_{GBS}+PV}{RT})$$

GBS creep

***Popov and Sobolev,* 2008**

Mechanical properties:

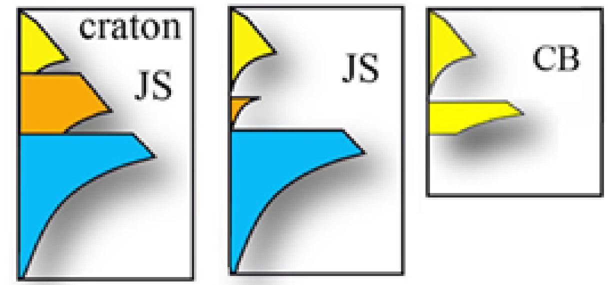

- Lithology : thicknesses of different layers and their composition
- Geotherm and thermal thickness $z(1330°C)$
- Rheology → Ductile flow
- Fluids → Rheology
- Background strain rate

Ductile flow

- Elastic properties
- Brittle properties

- more than 30-50 variants for certain mineral/rock types
- more than 4 major flow types
- Grain size dependence
- etc.

Possible combinations:

> SEVERAL HUNDRED

Example: density - P-T for mantle

- ⇨ Erosion – sedimentation

- ⇨ Progressive phase changes
  Thermodynamic processes
  (via Perple-X and Theriak)

$$\rho = f(P,T) \leftarrow G = \sum_{i=1}^{n} \mu_i N_i$$

λ, G k, f_p, σ, H

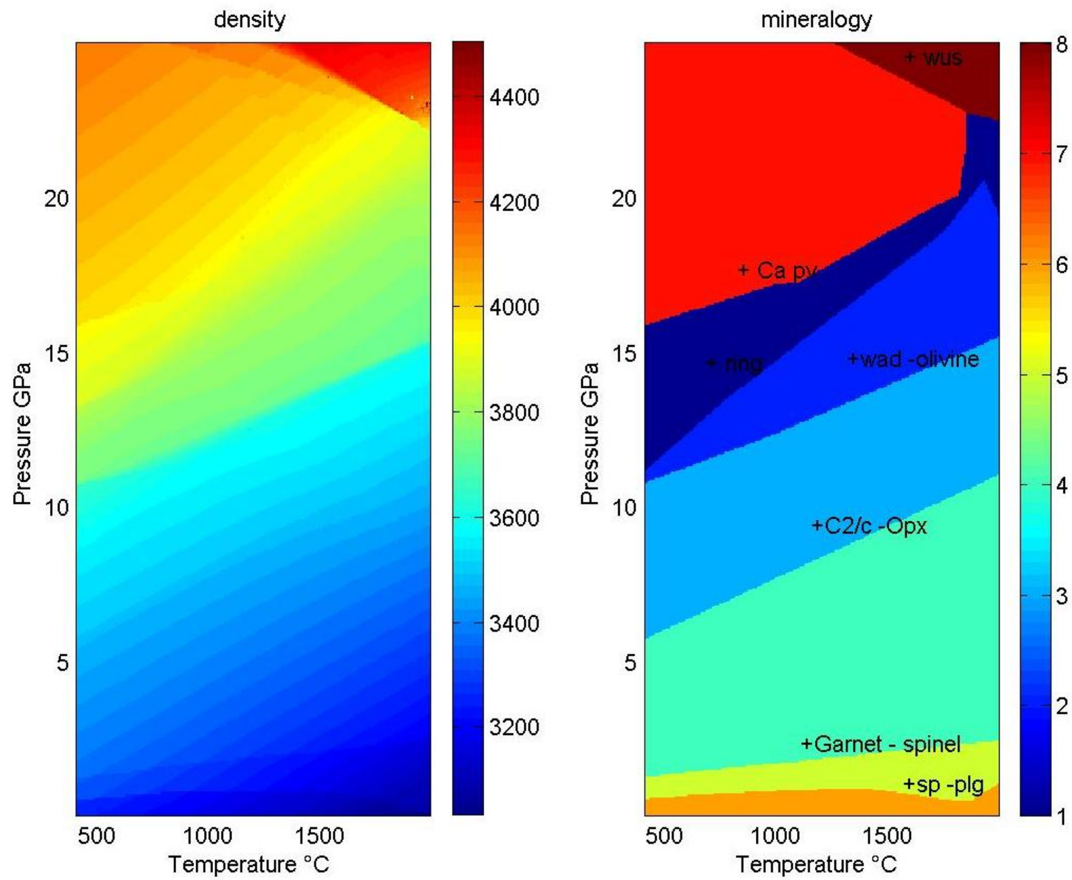

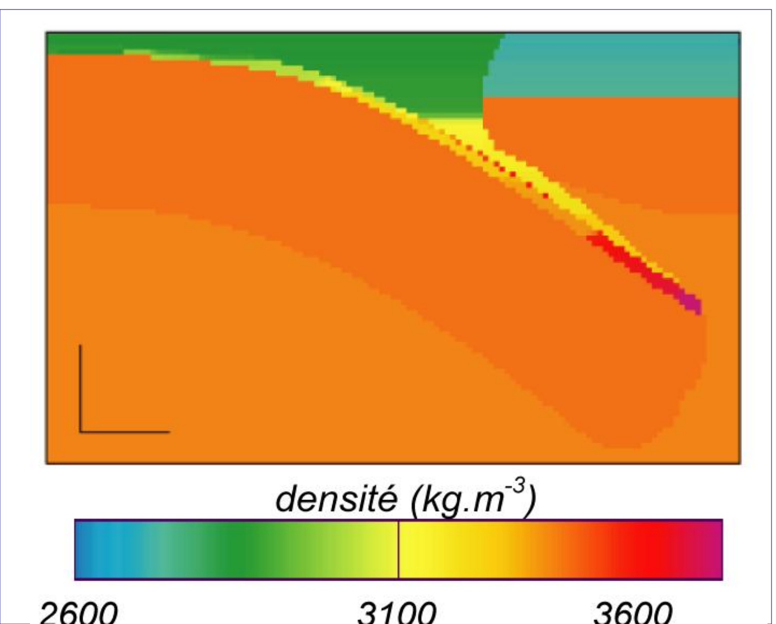

$$\partial h_s/\partial t - \nabla(k_e (\nabla h)^m \nabla h_s) = 0$$

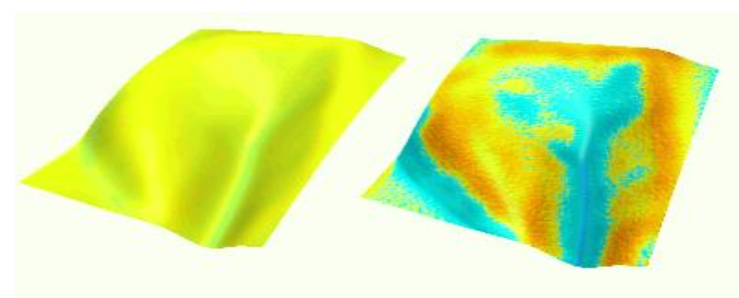

primitive mantle

PerpleX (J. Connolly)

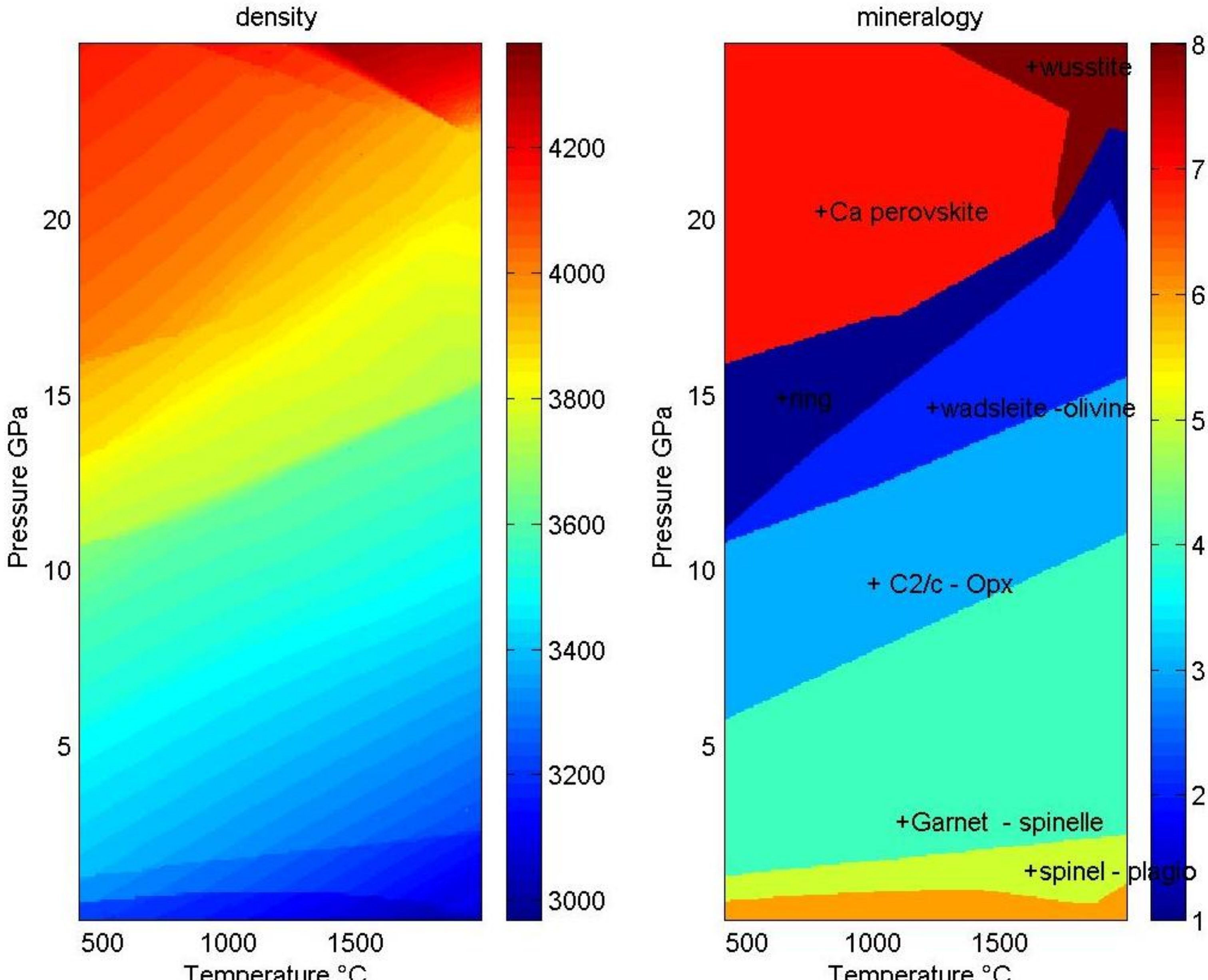

Predicted seismic velocities (m/s)

Vp

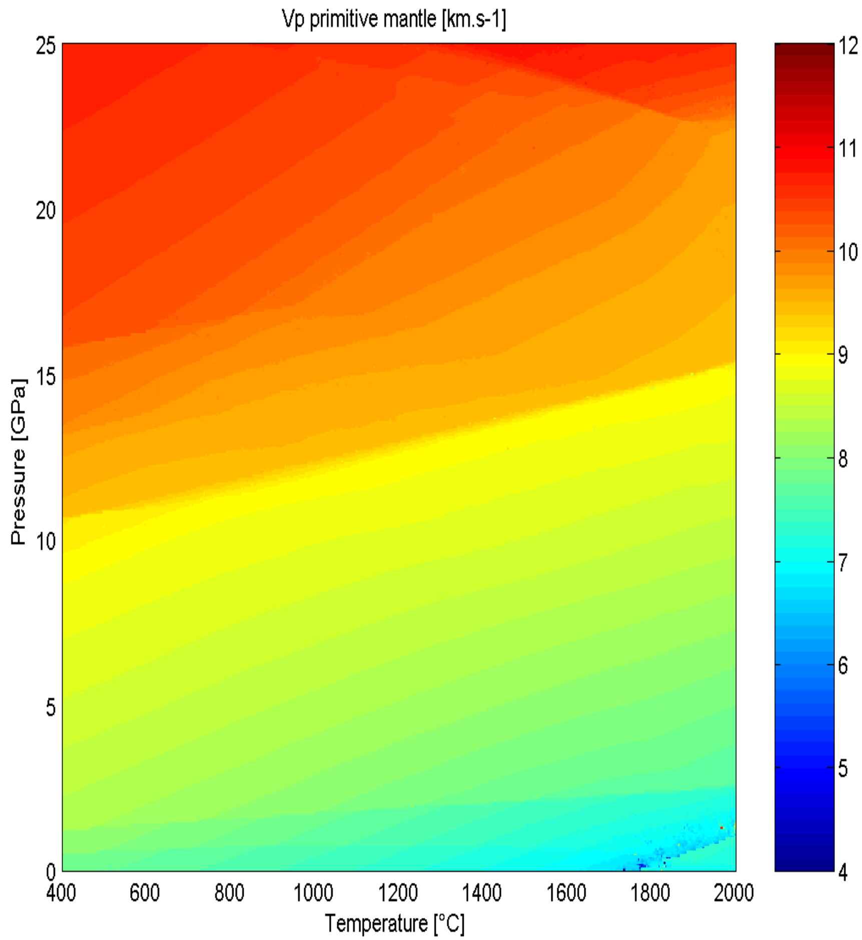

Vs

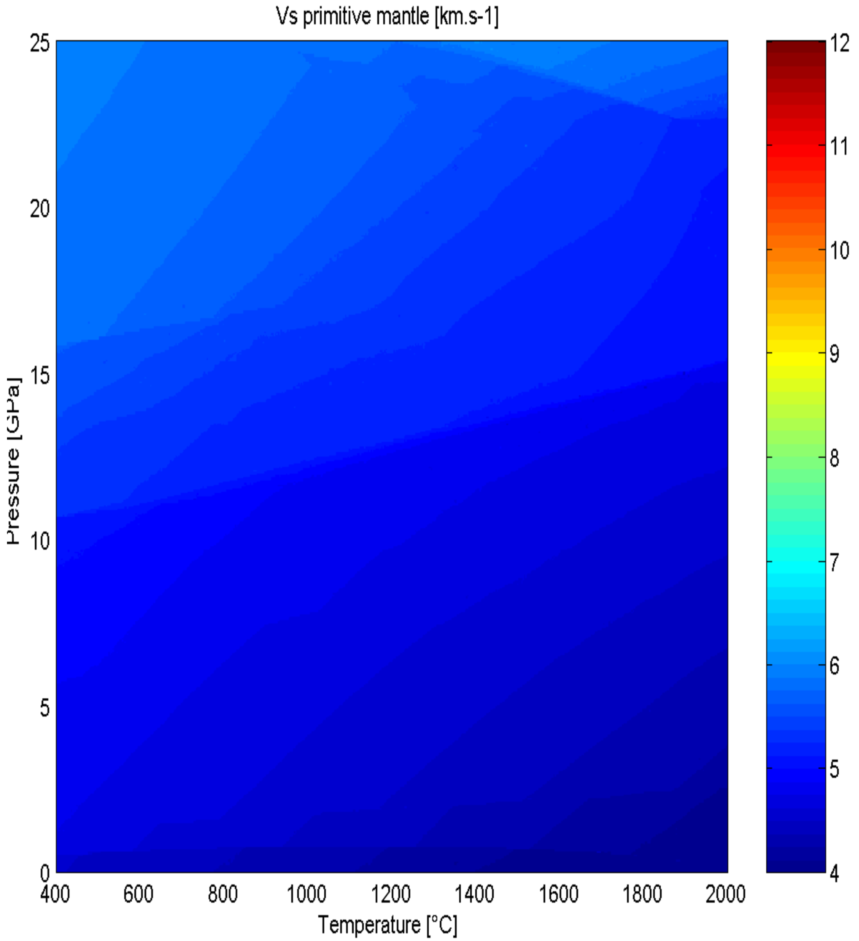

Predicted density anomaly

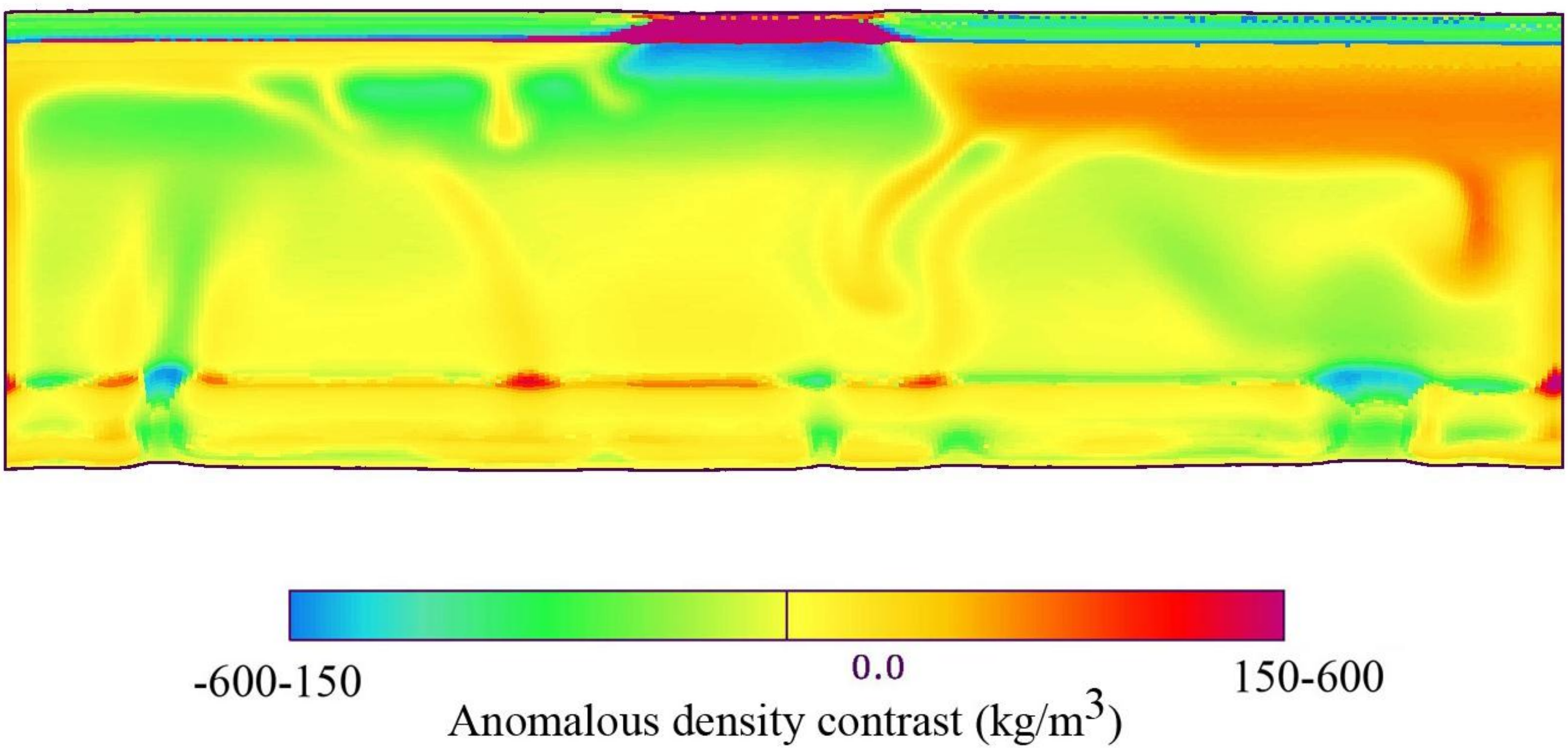

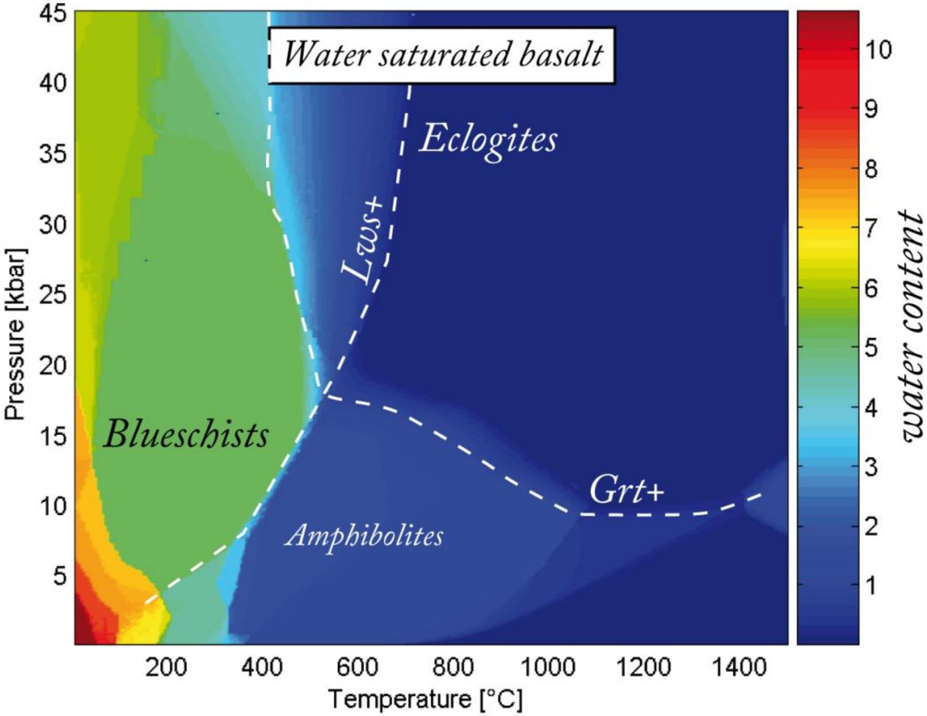

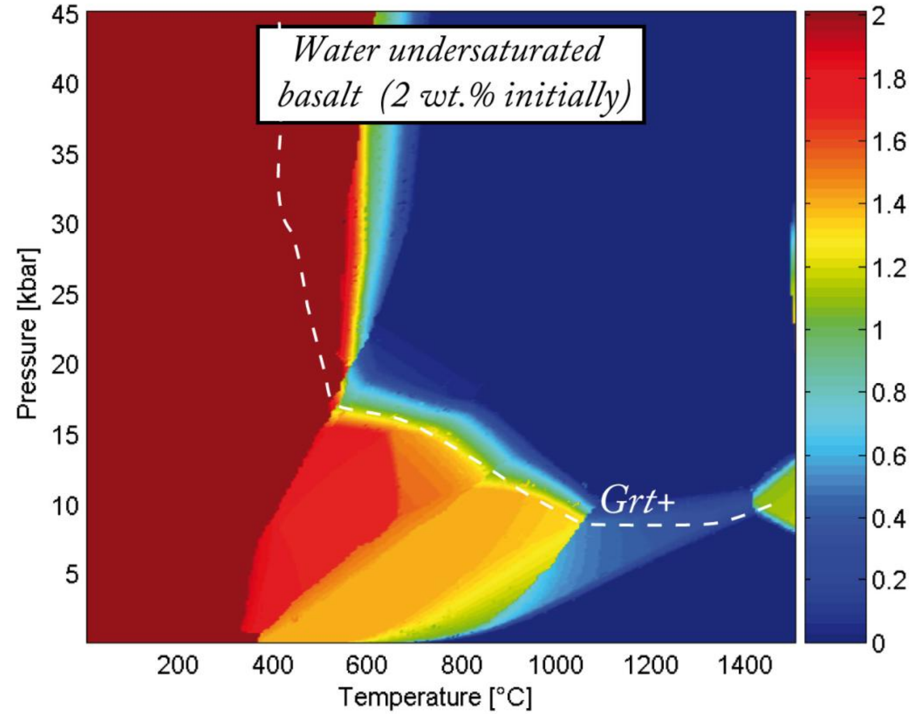

Calculated grids of basalt water content for both undersaturated and saturated cases (PerpleX)

Angiboust et al., in prep.

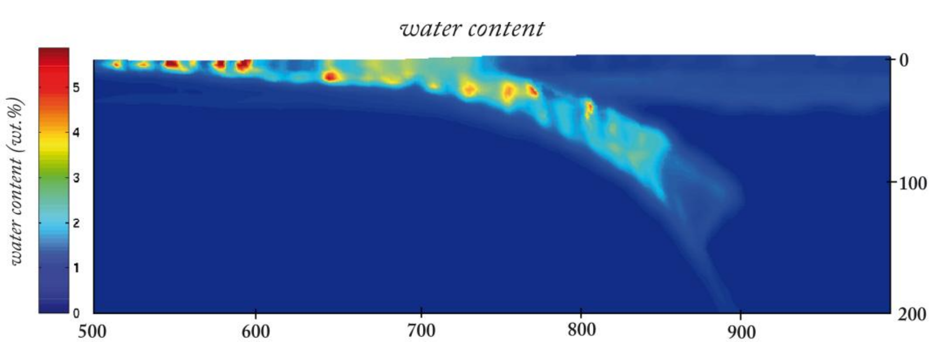

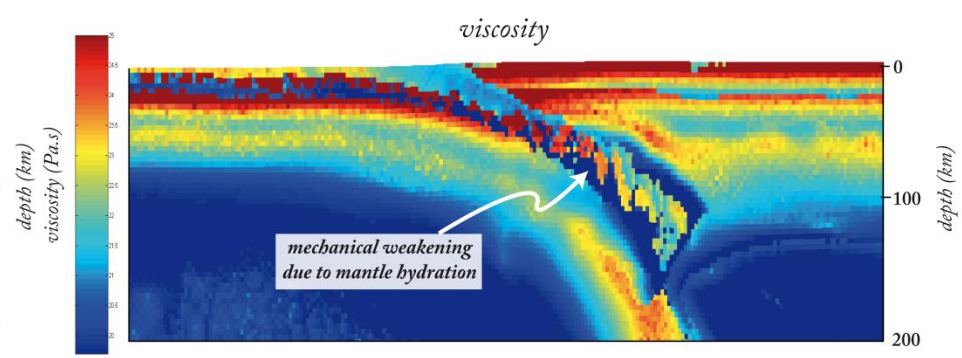

$$\vec{q} = -K \nabla P_{fl}^{*}$$: fluid diffusion equation, with $$P_{fl}^{*} = (P_{total} - P_{litho}) \times \frac{P_{usat}}{P_{sat}}$$

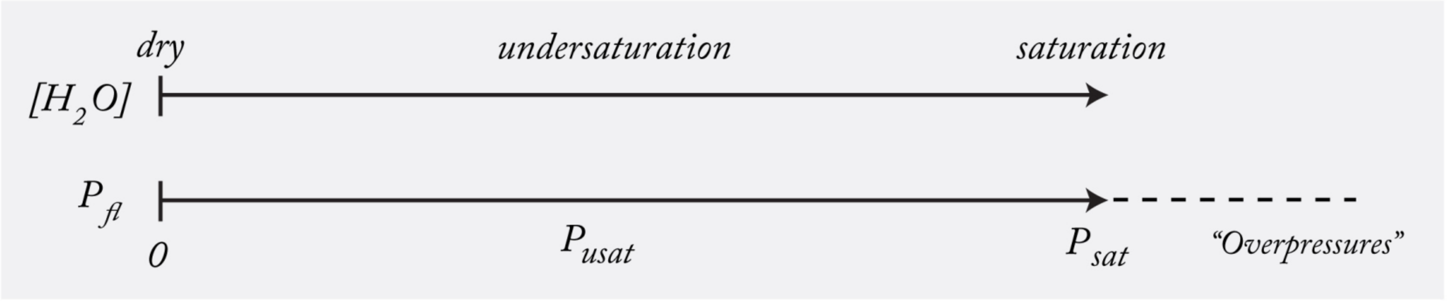

$$K = \frac{k}{\mu} \times \varepsilon^{*}$$: calculated diffusion coefficient

k : intrinsic permeability (m^2) as a function of depth (Manning & Ingebritsen, 1999)
μ : dynamic viscosity of the fluid (Pa.s) as a function of T (Seeton, 2006)

$$\varepsilon^{*} = \frac{\dot{\varepsilon}}{\bar{\varepsilon}}$$

$\dot{\varepsilon}$ ← instaneous strain rate
$\bar{\varepsilon}$ ← average model strain rate

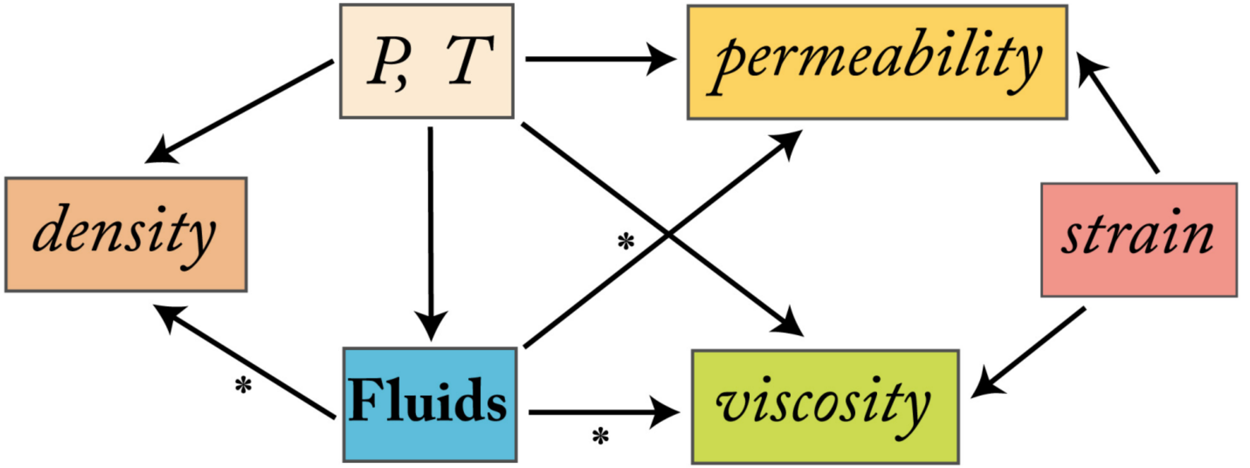

*: only for mantle phases

Angiboust et al., in prep.

Initial water content distribution (PerpleX) as a function of the lithology and PT conditions

High resolution experiment

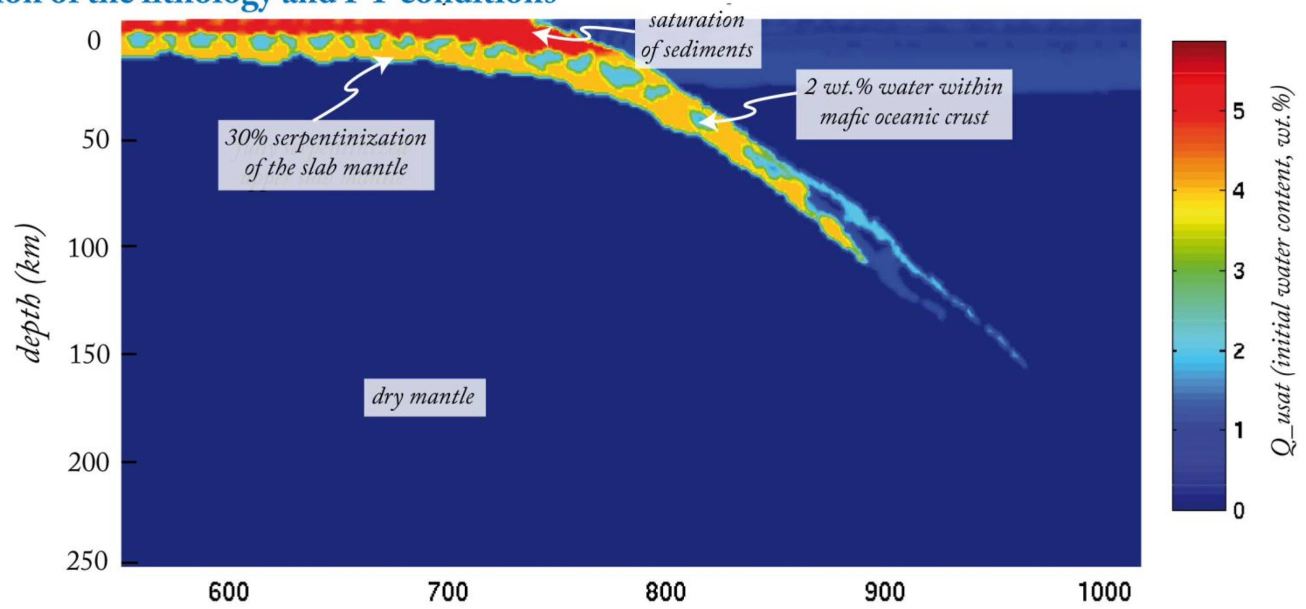

Maximum water content allowed as a function of the lithological distribution of the model and PT conditions

High resolution experiment

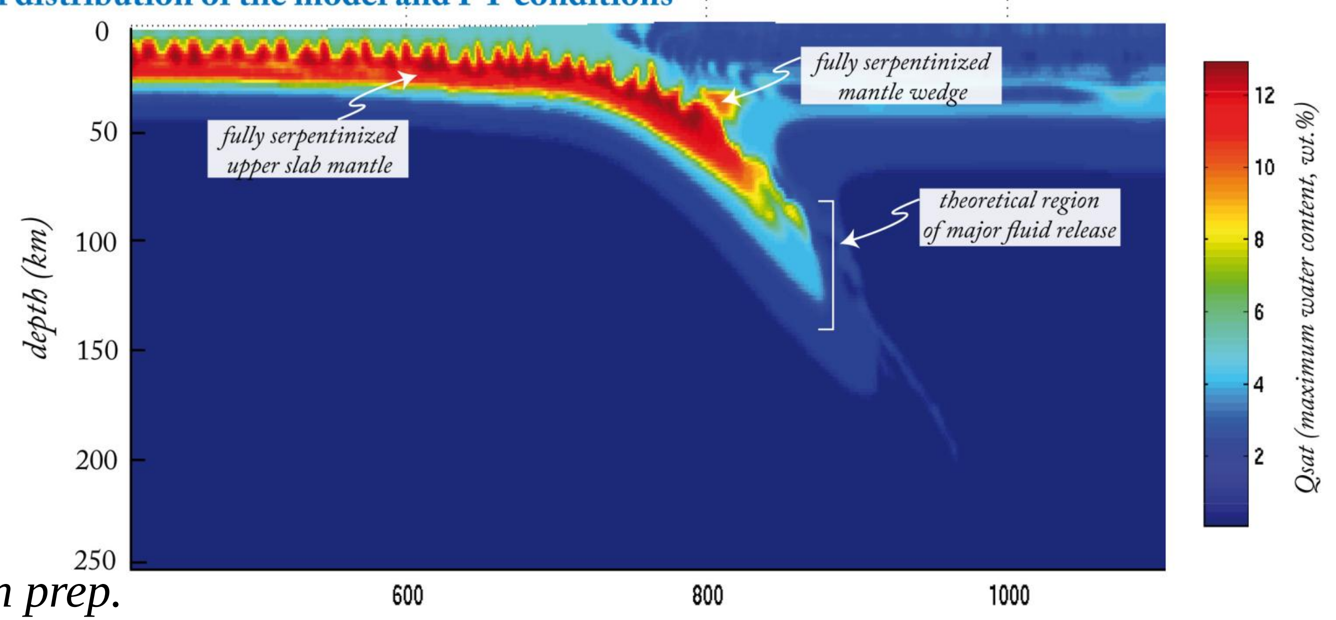

Angiboust et al., in prep.

Typical initial setup

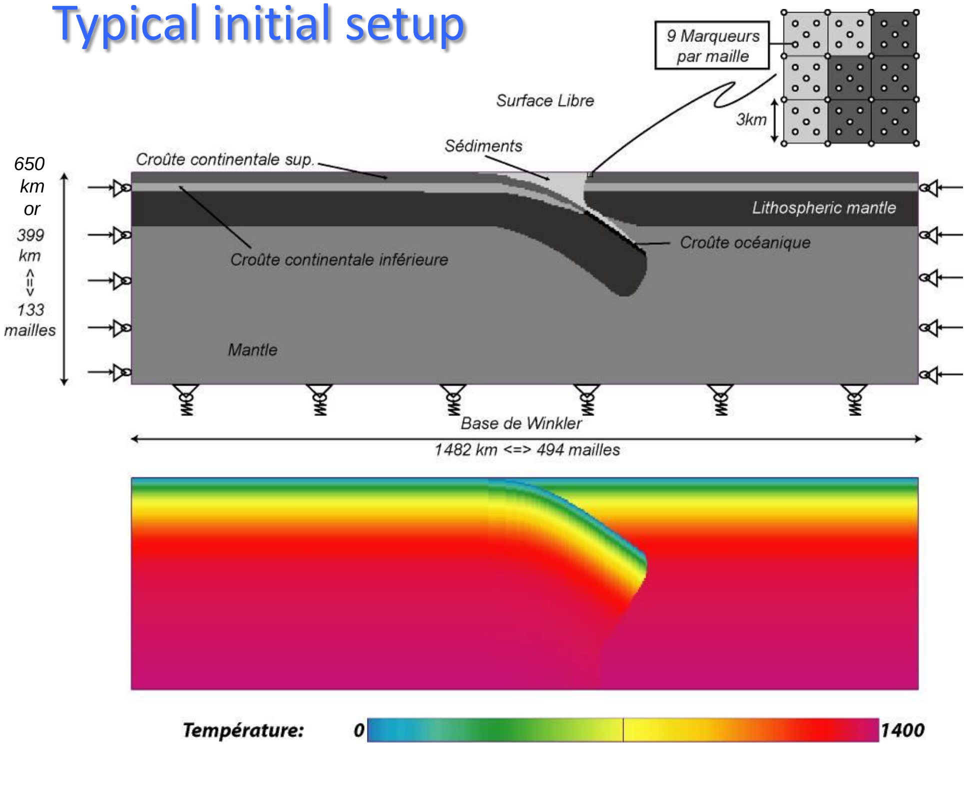

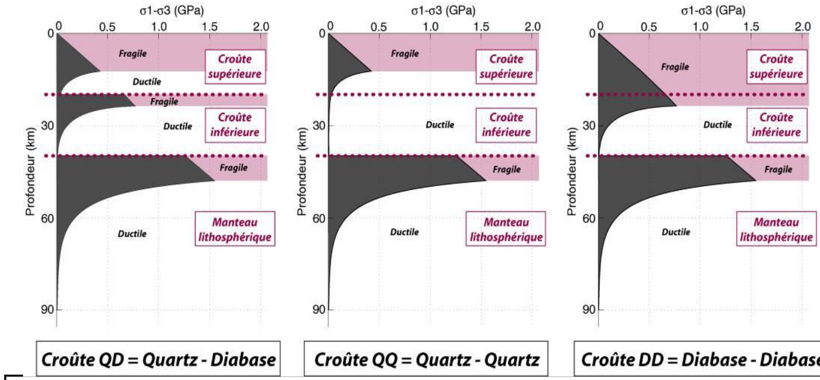

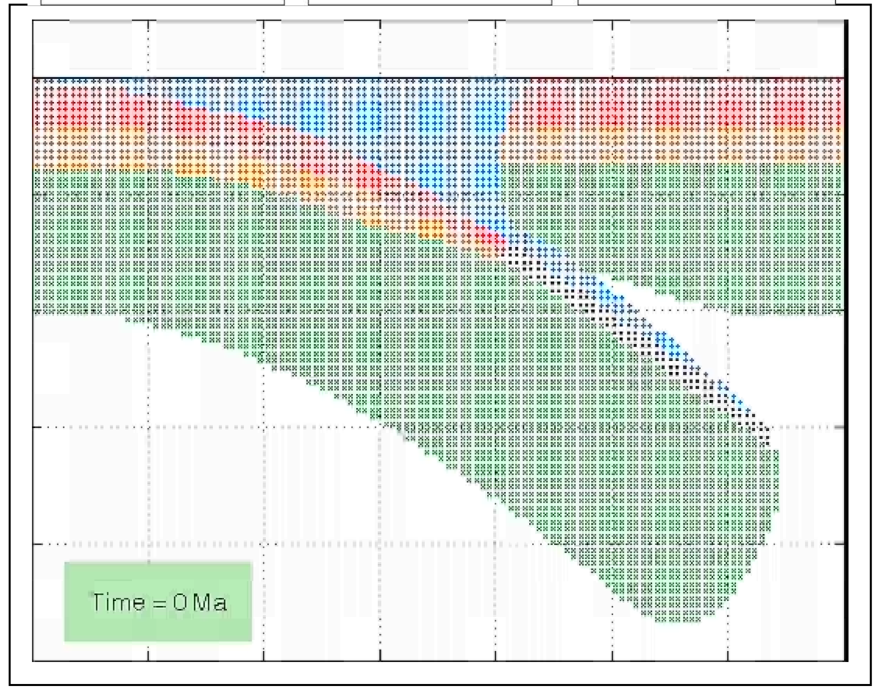

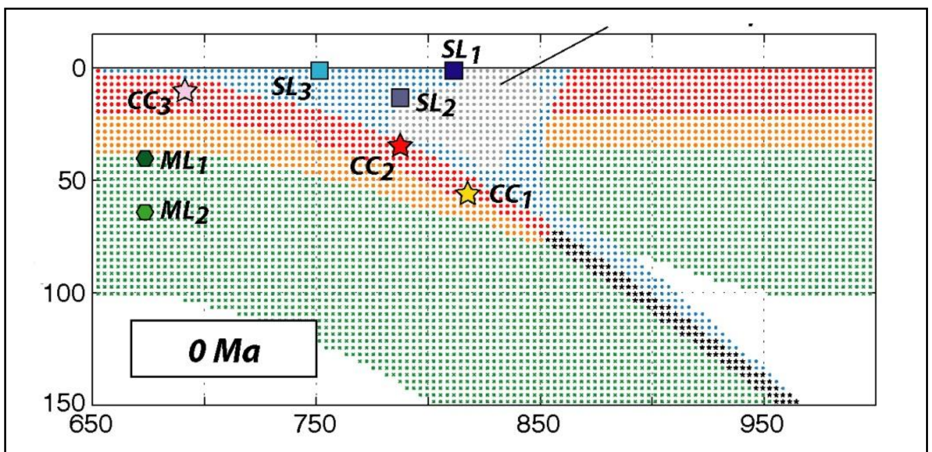

Yamato et al., 2007

TYPICAL SETUP INCLUDING OCEANIC SUBDUCTION PHASE

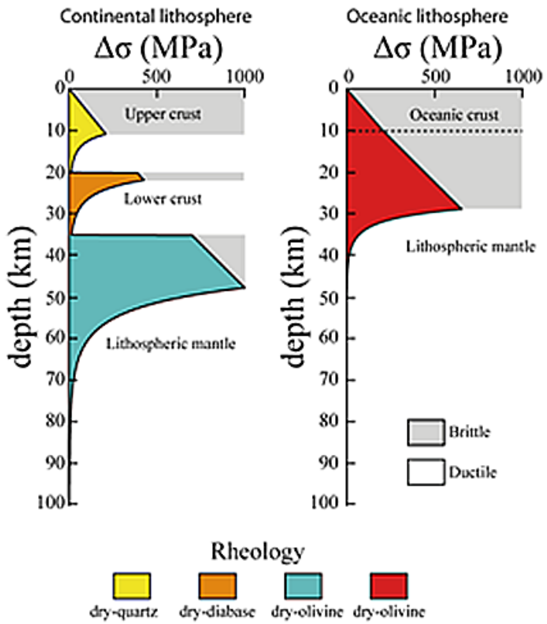

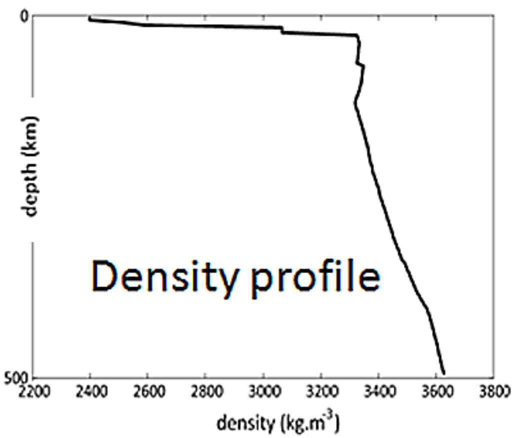

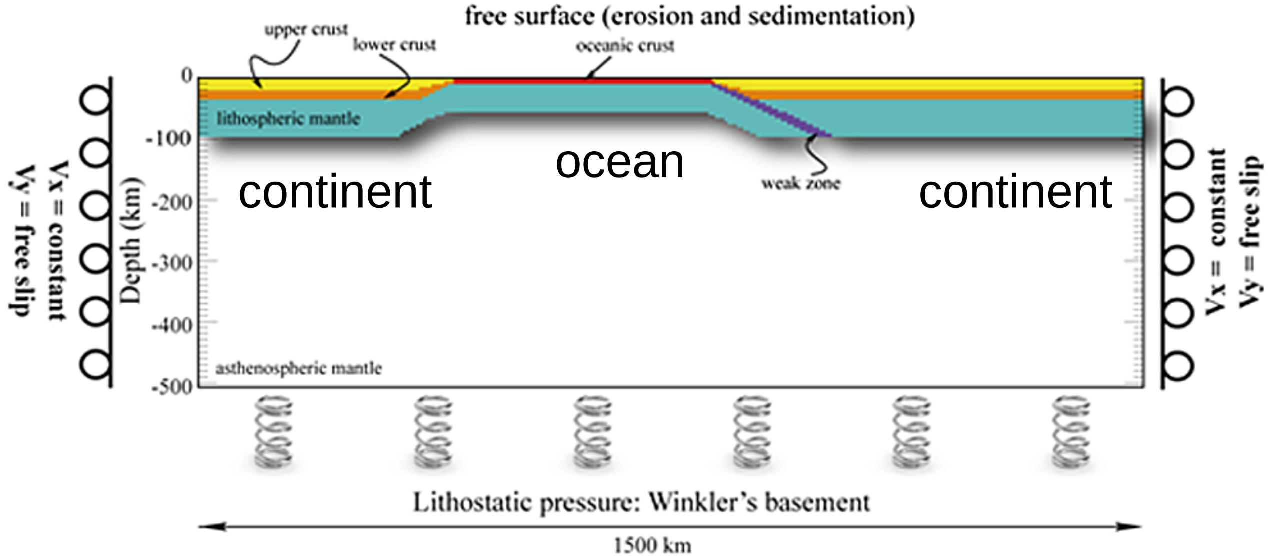

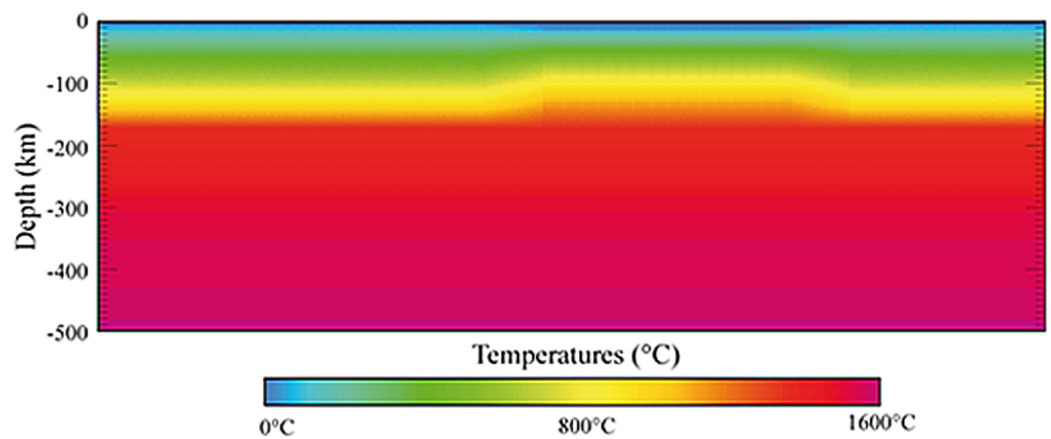

Francois et al., 2010

1. Influence of the convergence rate

Dependence on shortening rate. Snapshot at Δx = 180 km

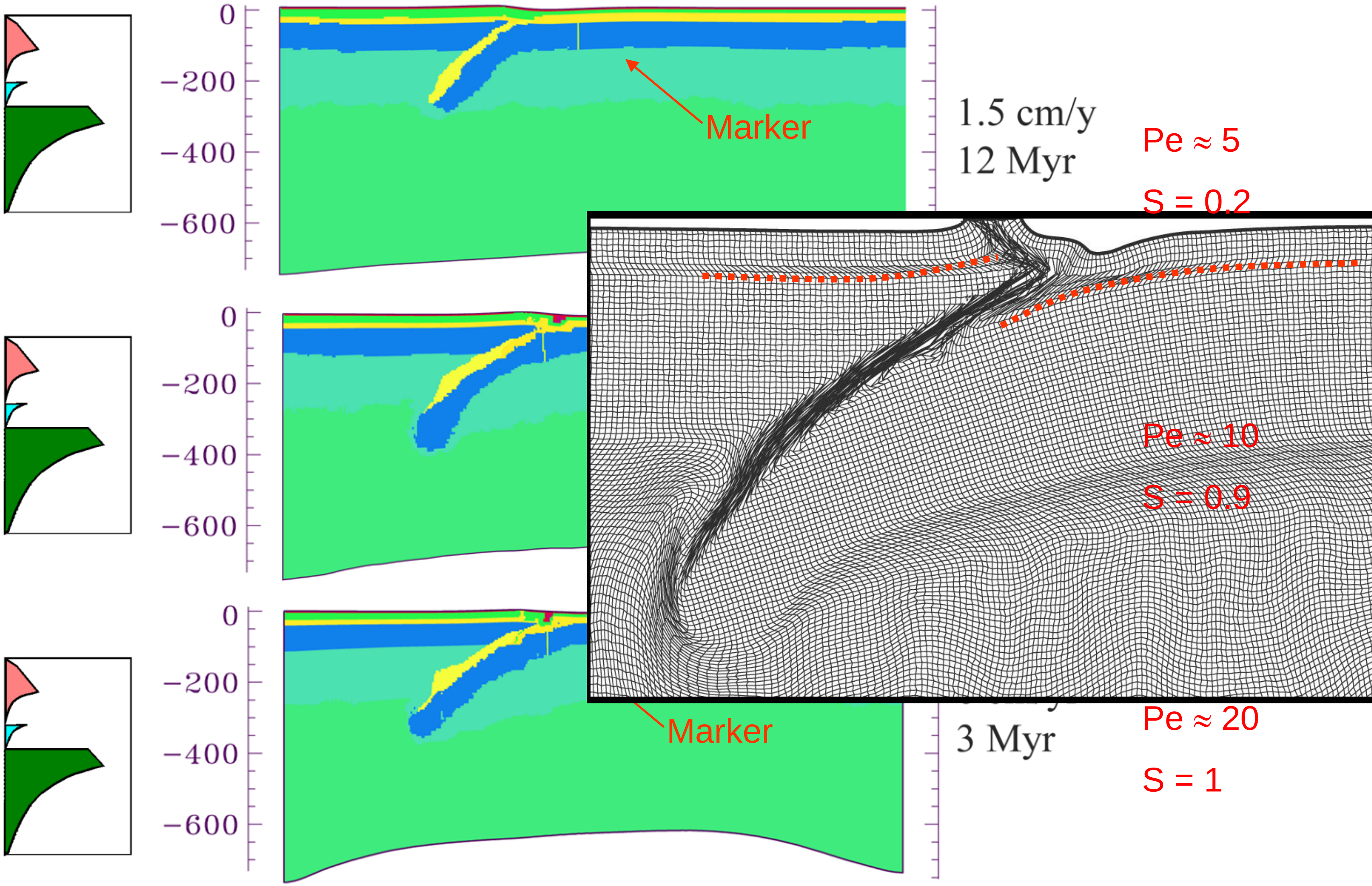

Influence of absolute velocity

influence de l'orientation de la convergence

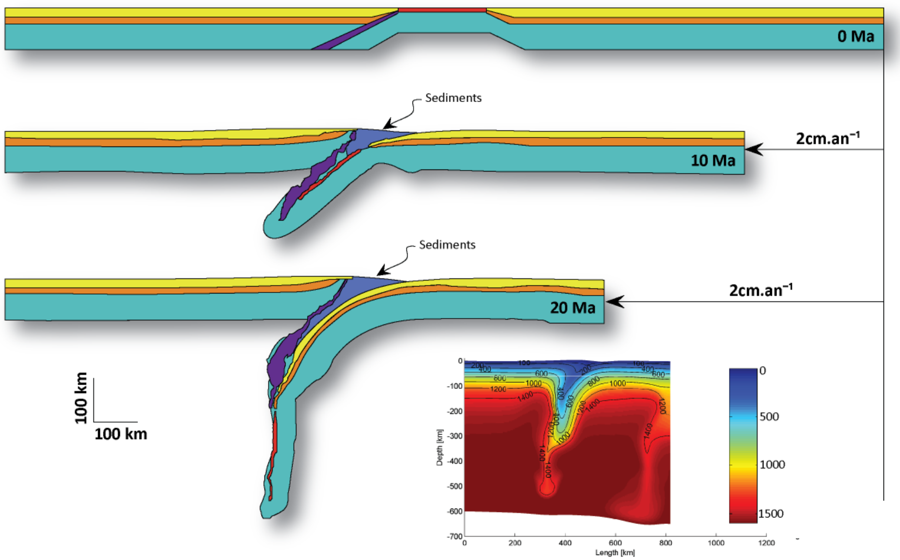

influence de la vitesse de convergence

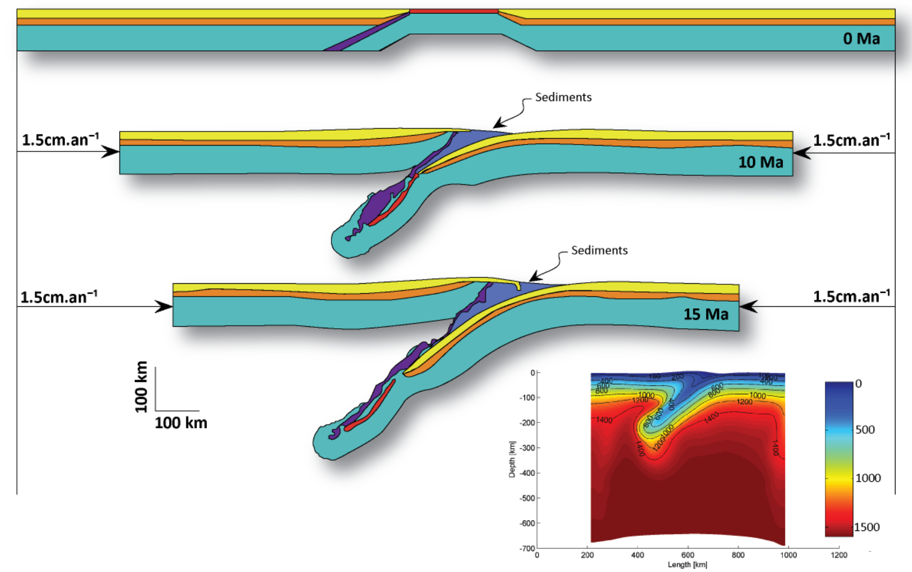

Evolution de la topographie du modèle en fonction du temps

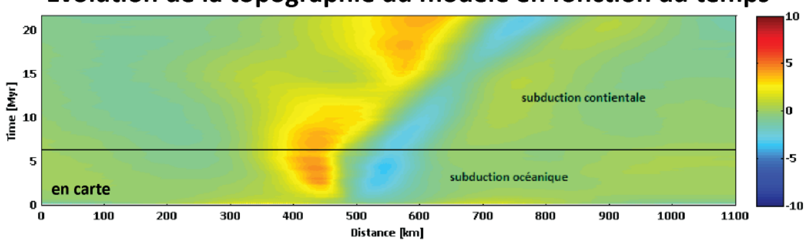

Evolution de la topographie du modèle en fonction du temps

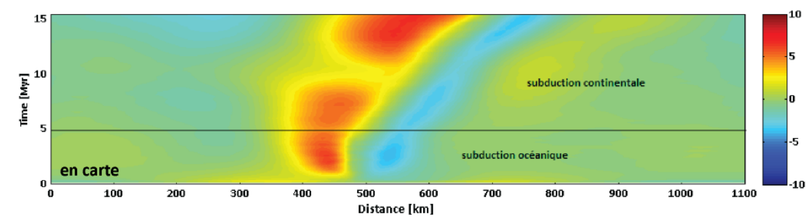

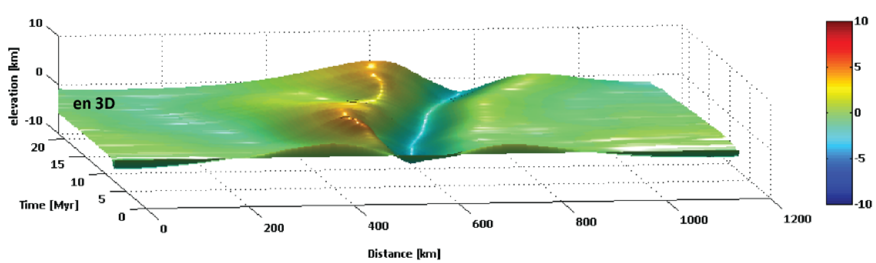

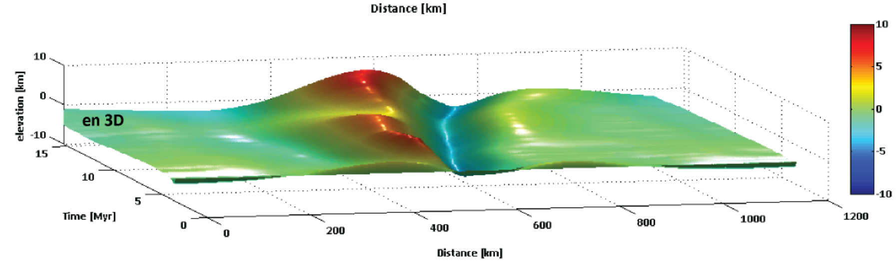

Francois et al., 2010

2. Influence of thermo-rheological profile

The *jelly sandwich* versus *crème-brûlée*

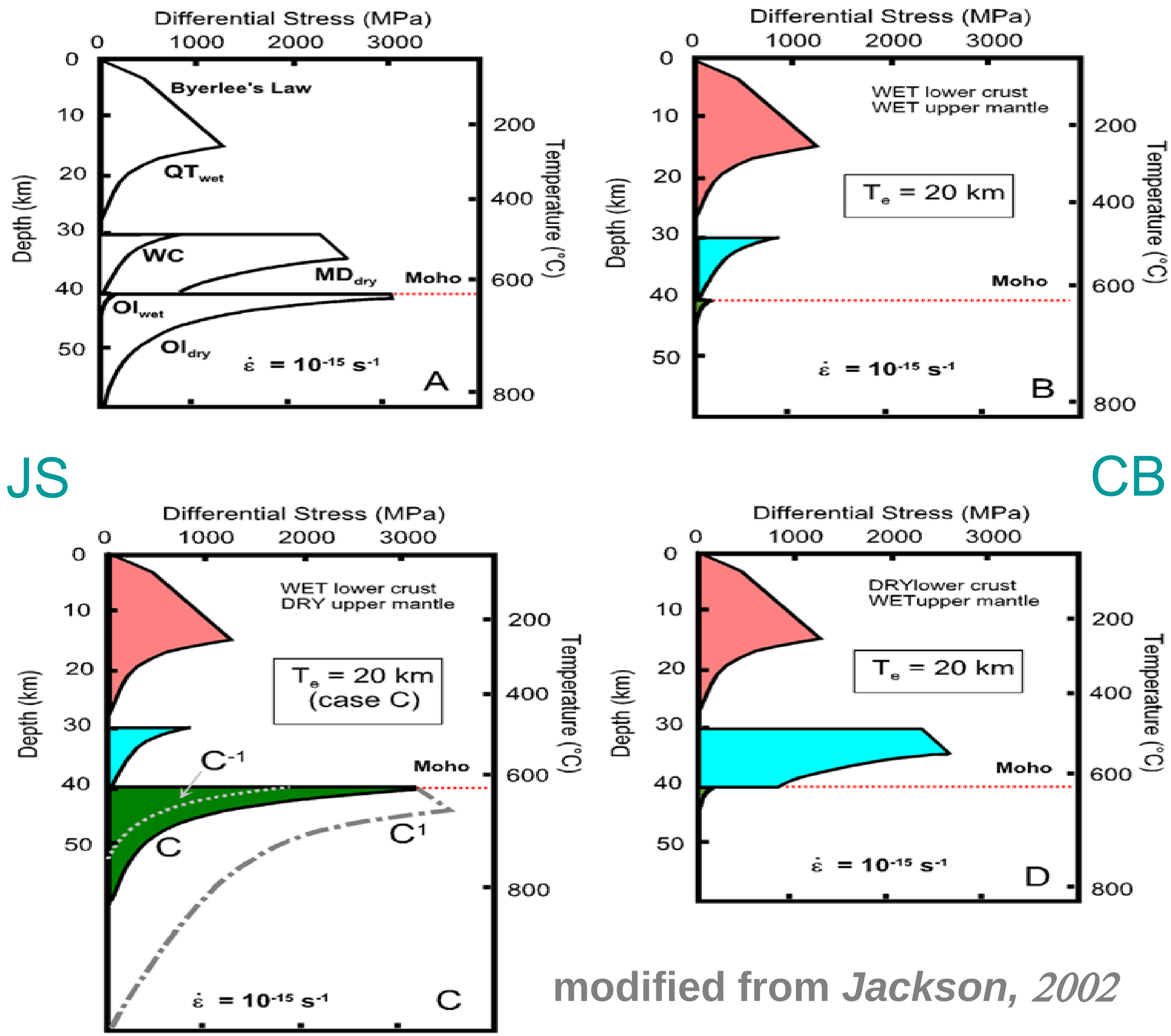

modified from *Jackson*, *2002*

Influence of thermo-rheological age – A1: CREME – BRULEE RHEOLOGY (SOFT)

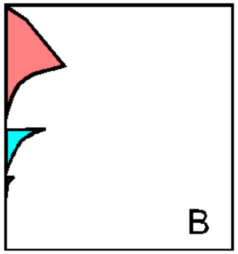

S < 0.1

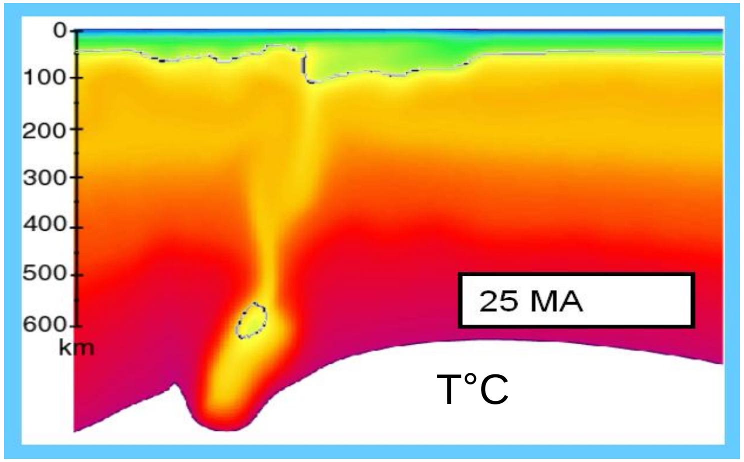

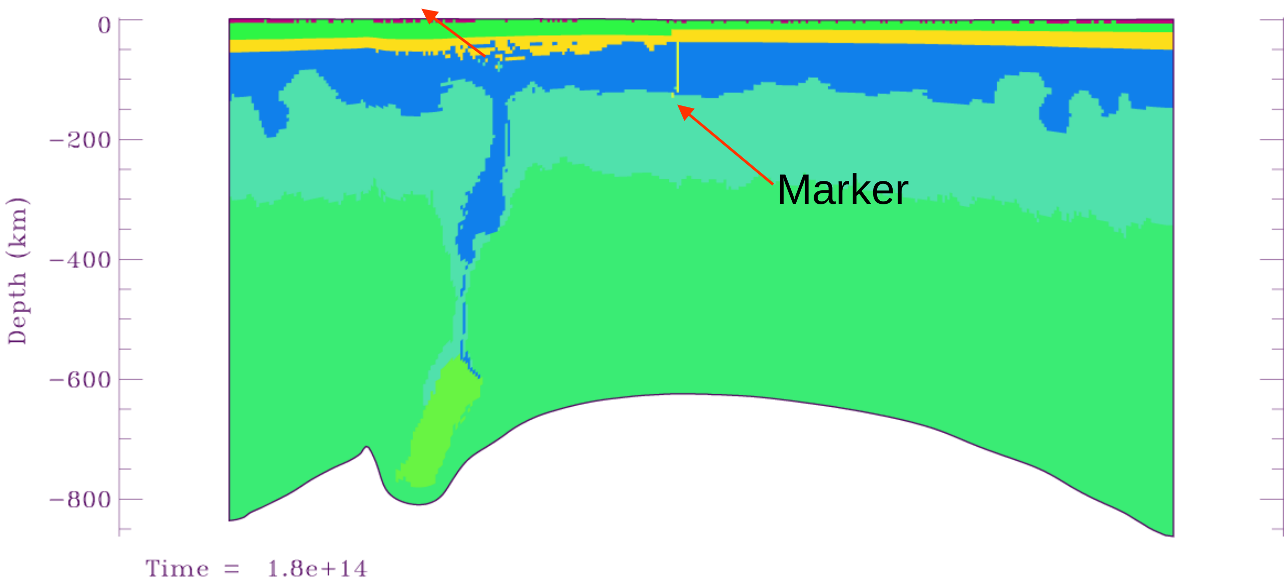

Thermal age of 25 Ma Tm = 850°C, Δx = 330 km, t = 5,5 Ma, 2x3 cm/yr

wait …

Example: Pannonian Basin / Carpathians

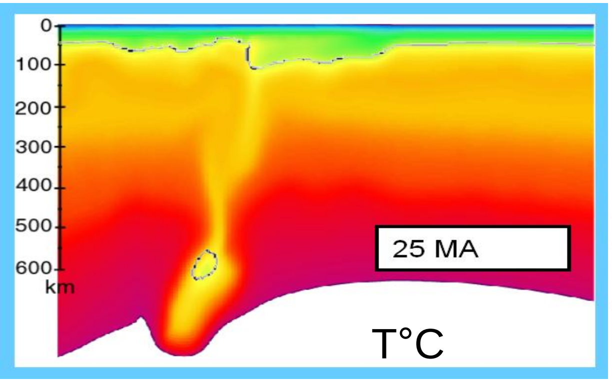

S < 0.1

Burov et al, 2007

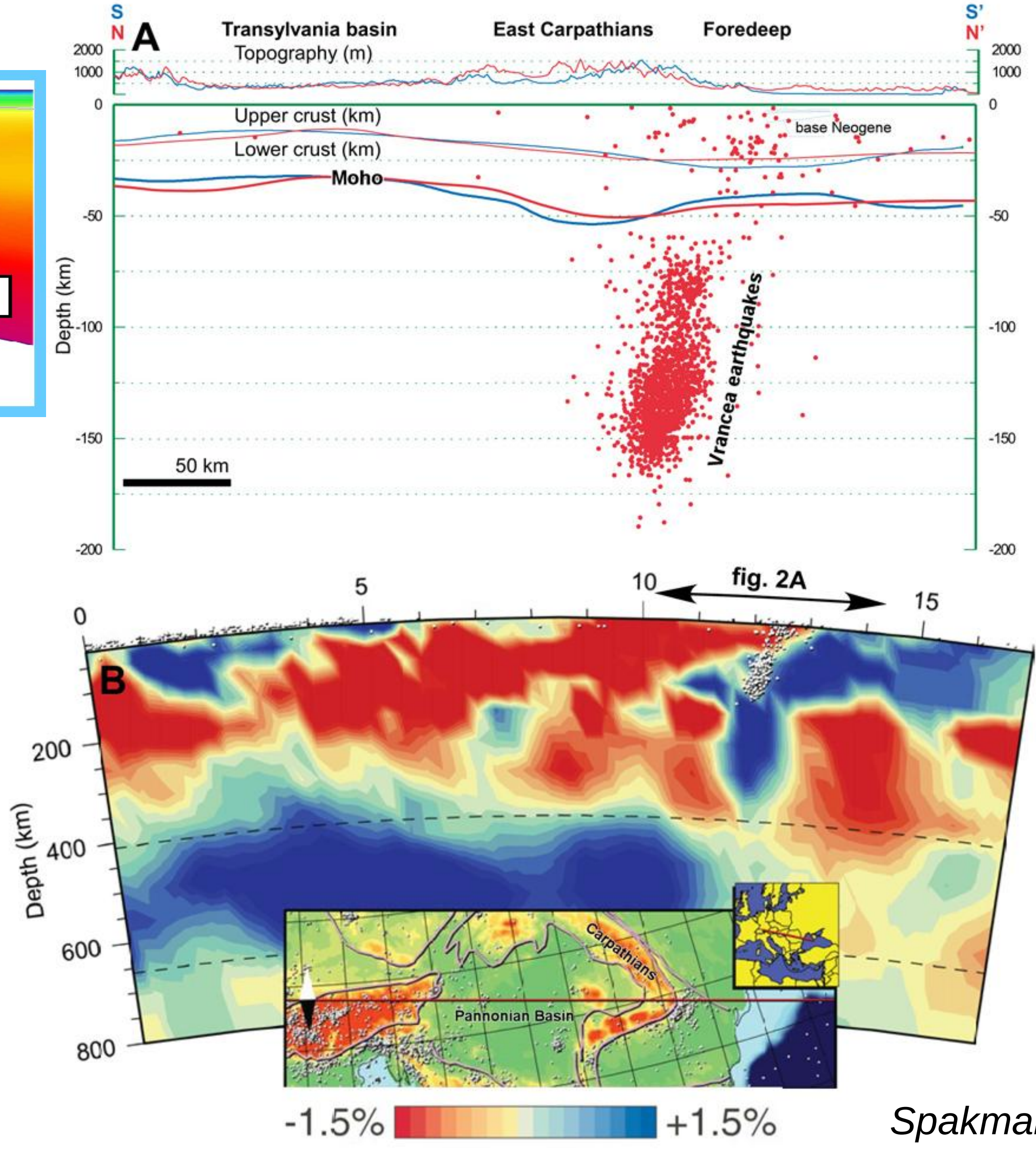

Spakman

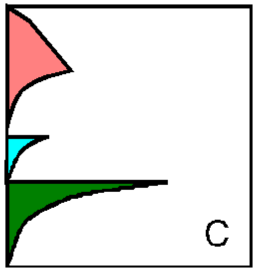

S < 0.3

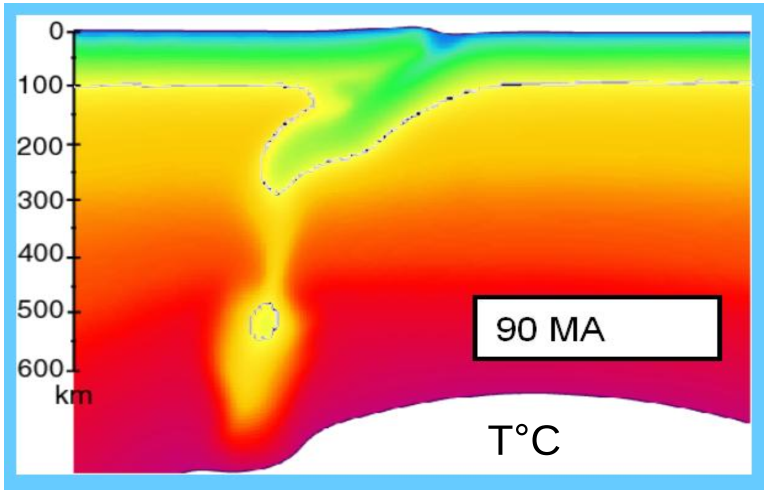

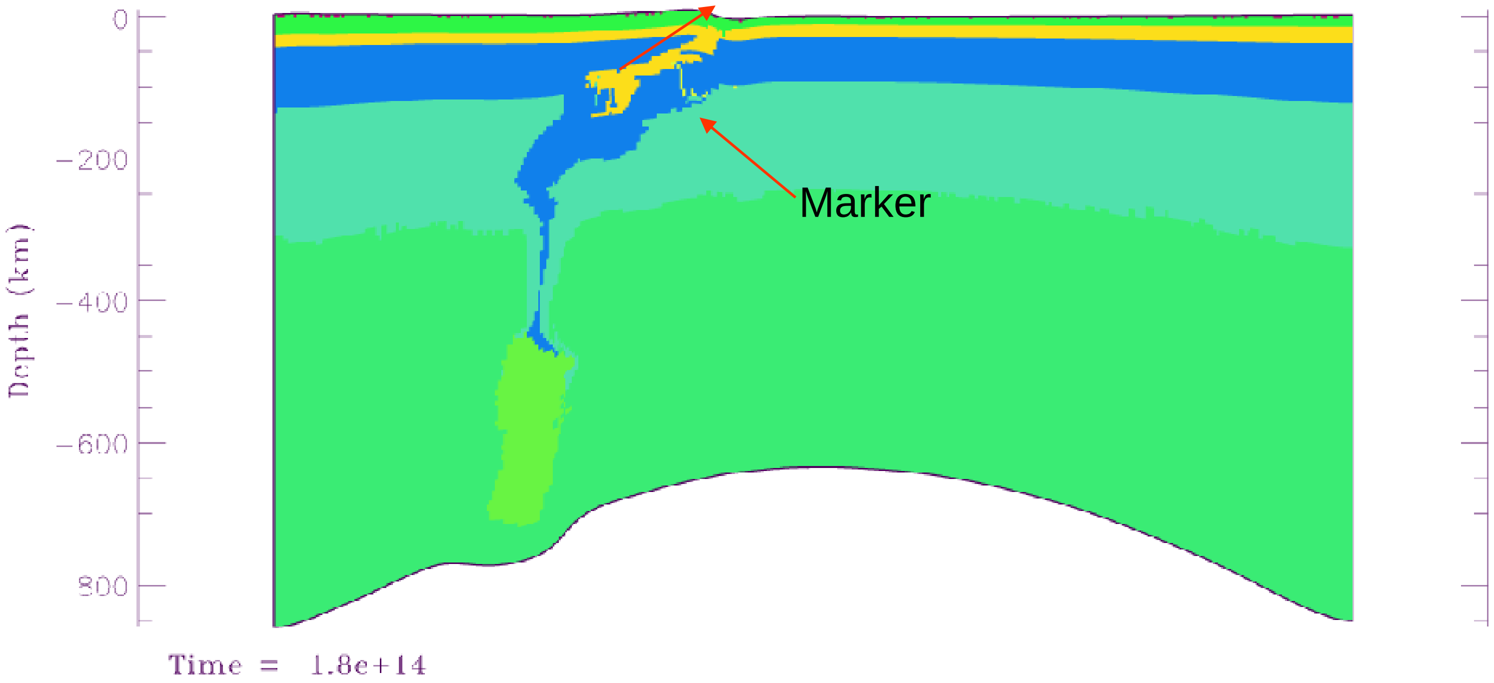

Thermal age of 90 MA, Tm =600°C, Δx = 330 km, t = 5,5 Ma, 2x3 cm/yr

wait …

Influence of thermo-rheological age - B1 JELLY SANDWICH RHEOLOGY

S ~ 0.7

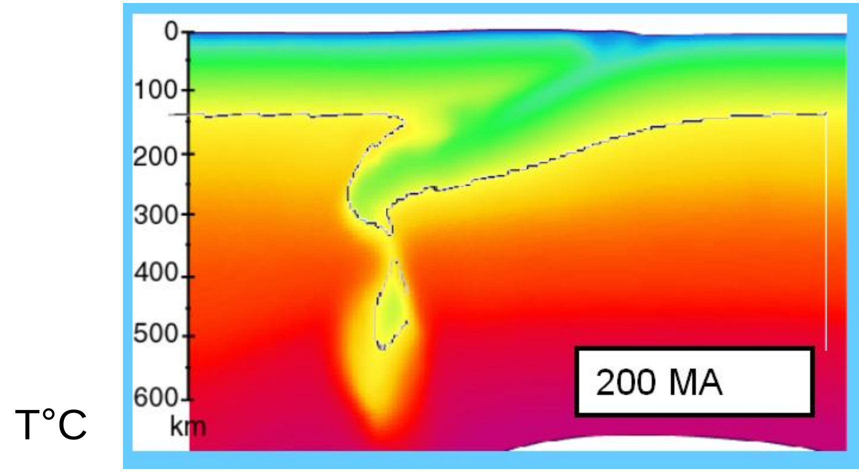

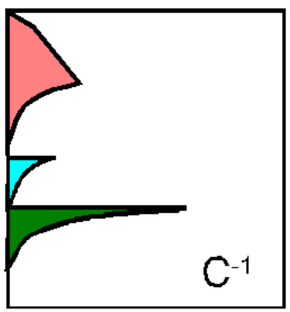

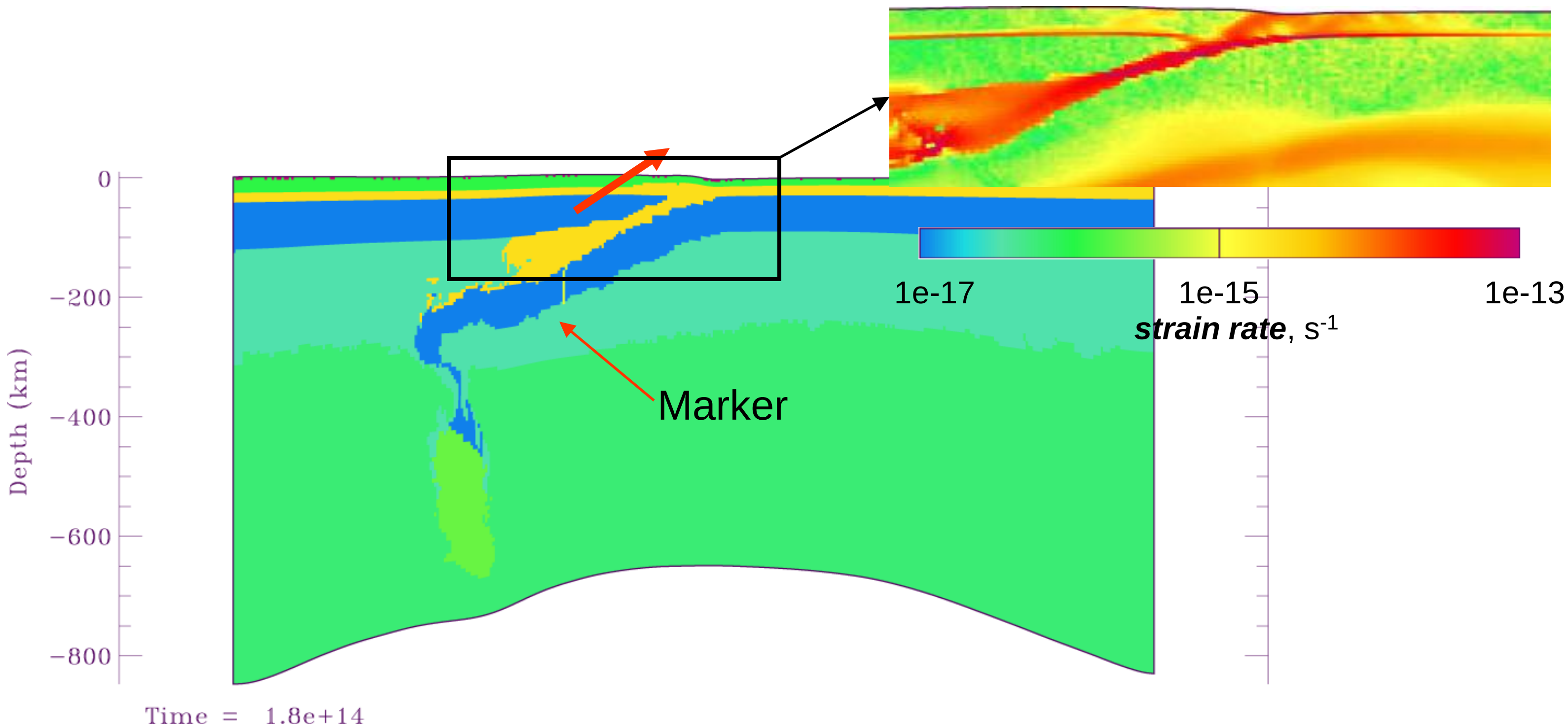

Thermal age of 200MA, Tm =500°C, Δx = 330 km, t = 5,5 Ma, 2x3 cm/yr ***wait …***

Influence of thermo-rheological age – C1 JELLY – SANDWICH RHEOLOGY

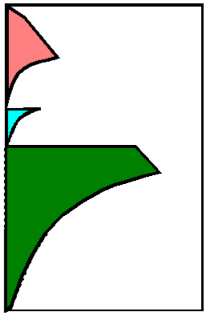

S ~ 1.

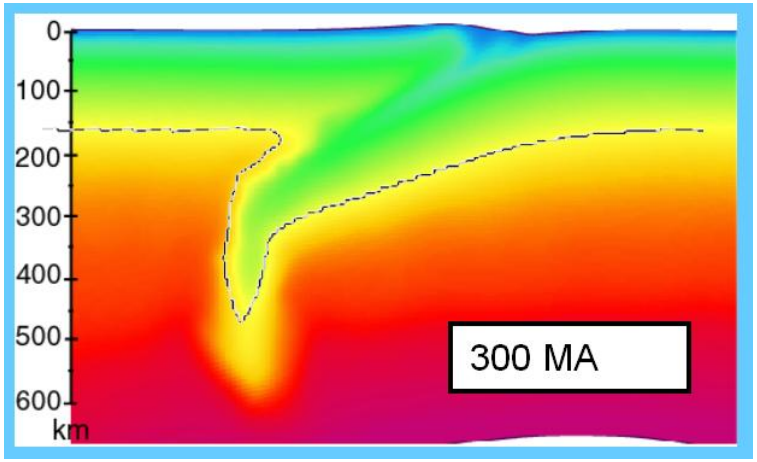

T°C

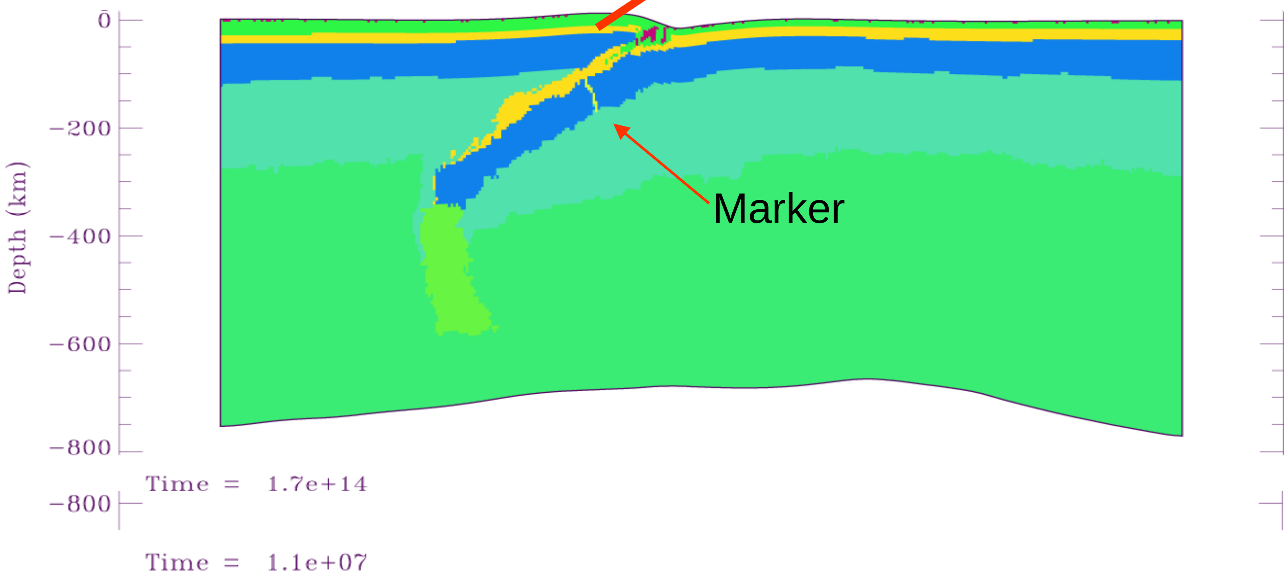

Thermal age of 300MA, Tm =450°C, Δx = 330 km, t = 5,5 Ma, 2x3 cm/yr

wait …

Dependence on rheology: summary

$$S = \frac{l_s \text{ (subduction length)}}{\Delta x}$$

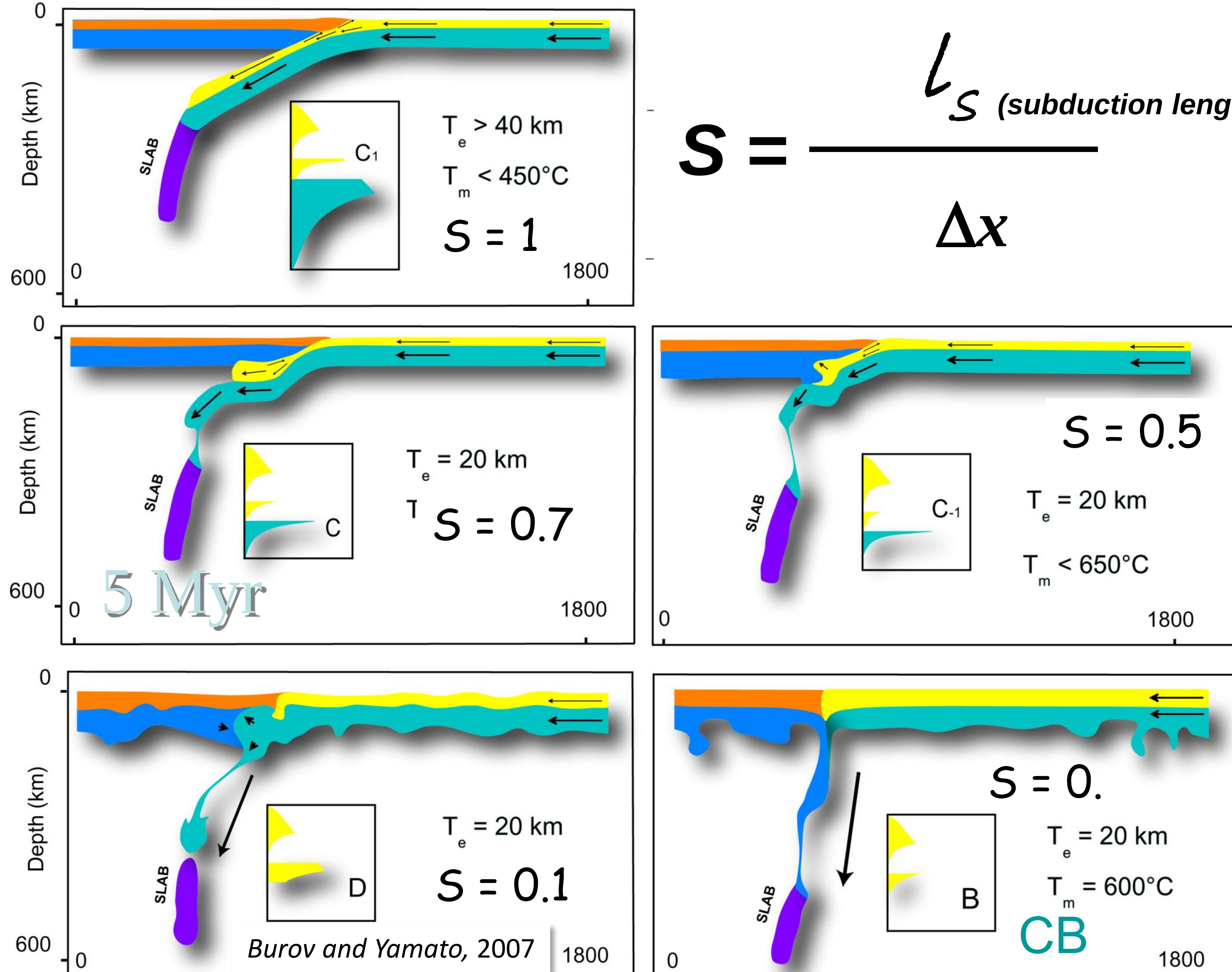

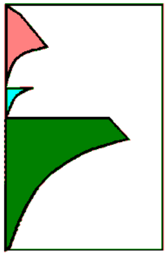

COTRIBUTION TO THE COLLISION STYLE

FROM DIFFERENT DEFORMATION MODES

amount of shortening Δx

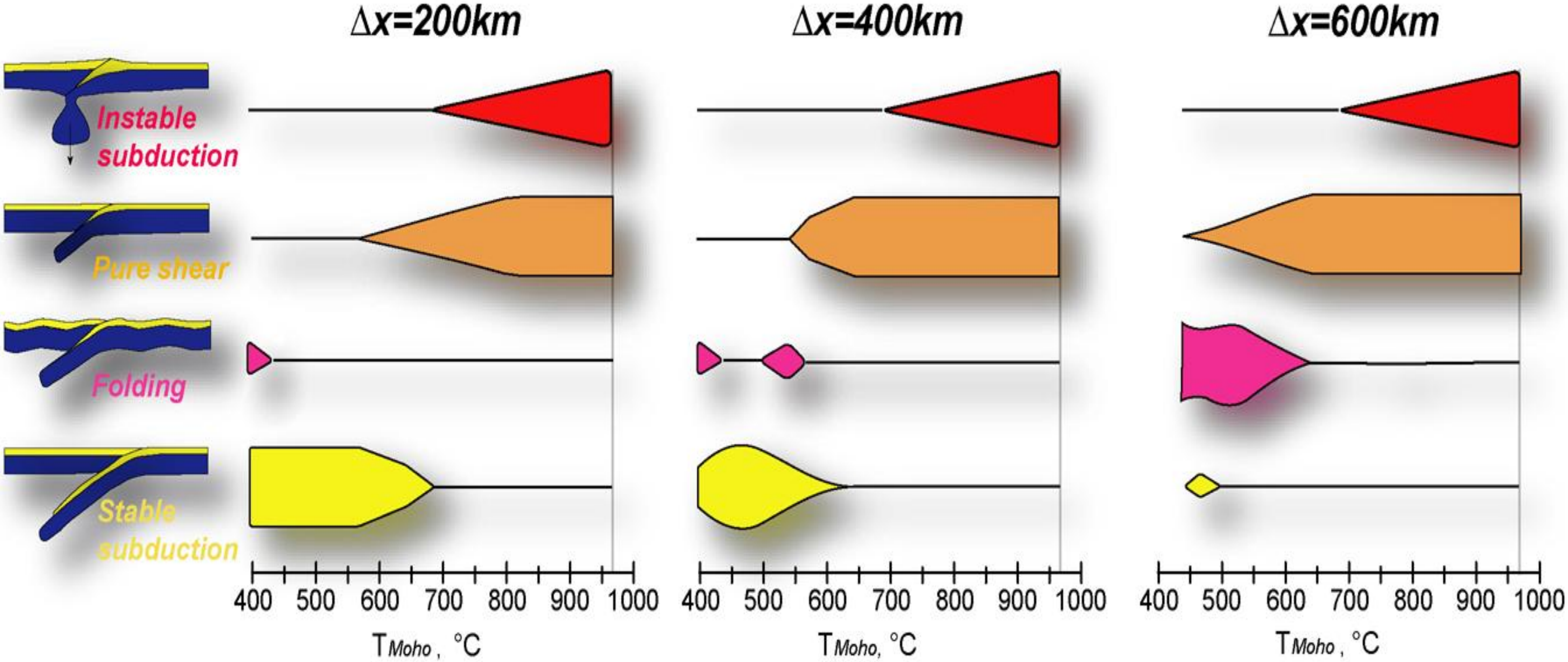

Moho temperature = Thermotectonic Age = thermo-rheological profile

Toussaint et al., 2004

Zagros-type collision: oceanic-to contient phase, 3 cm/y

Francois et al., 2011

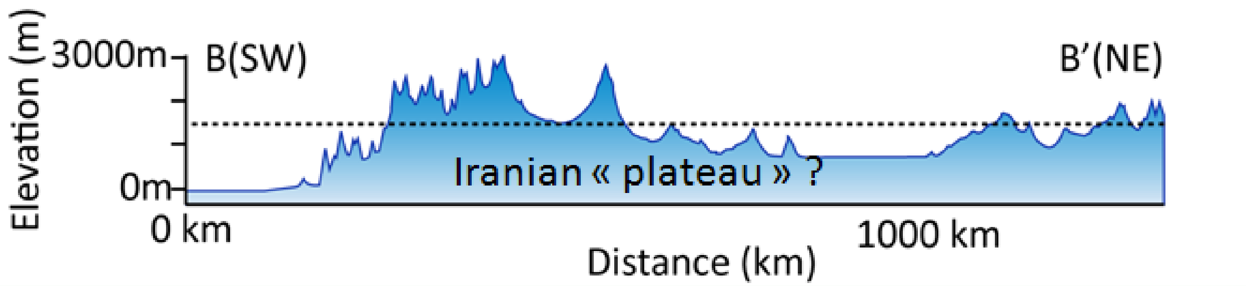

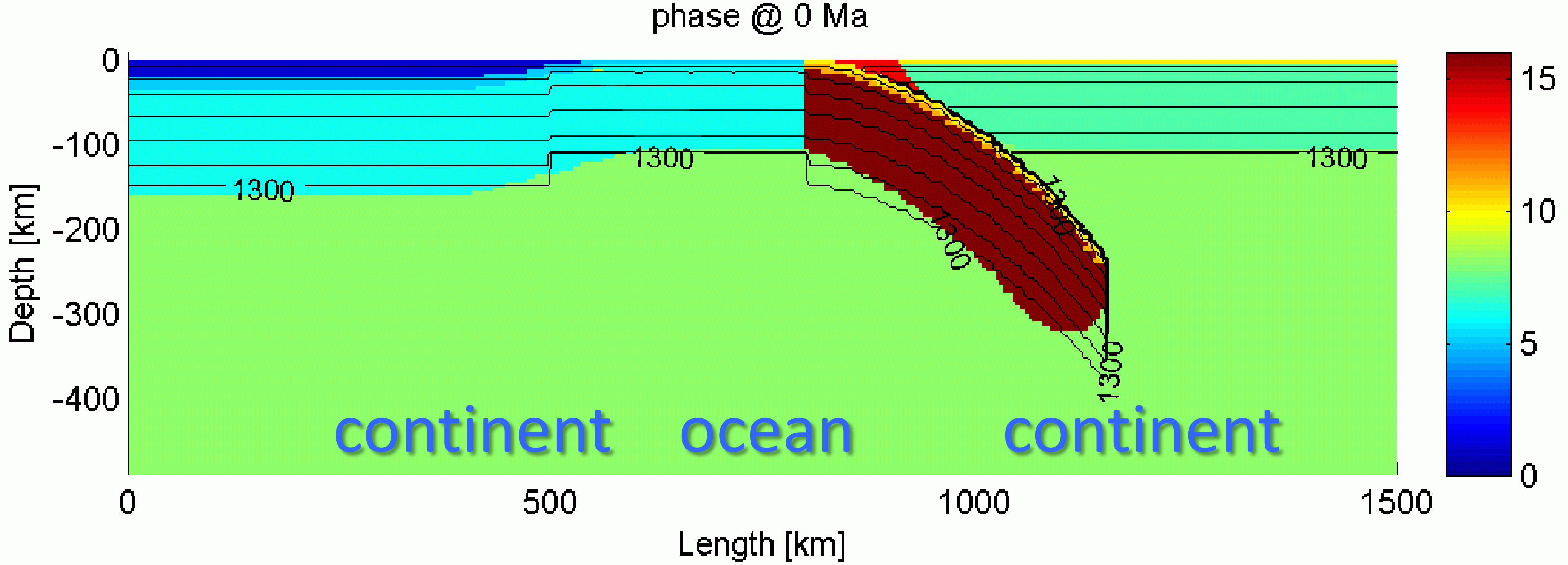

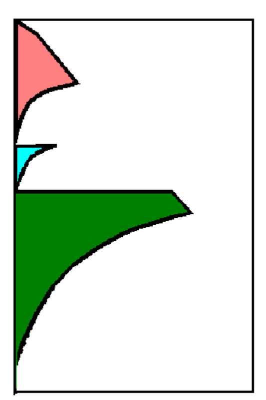

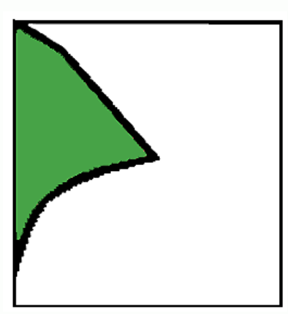

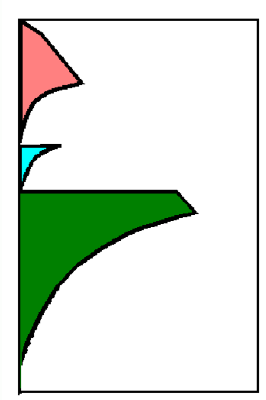

INITIAL MODEL

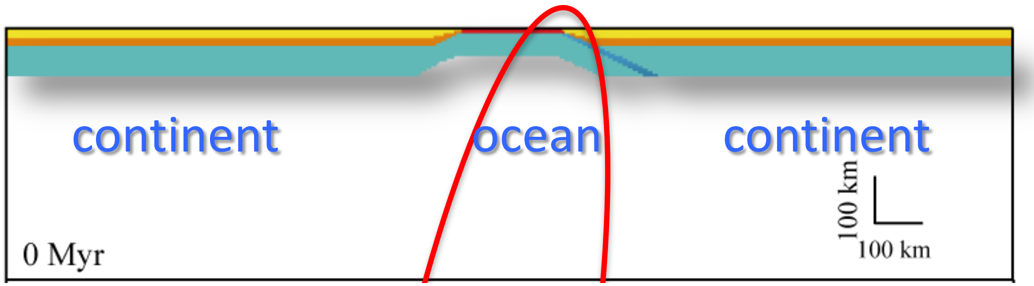

- Trench migration
- growth of the peripheral uprise
- widening of the uplift zone

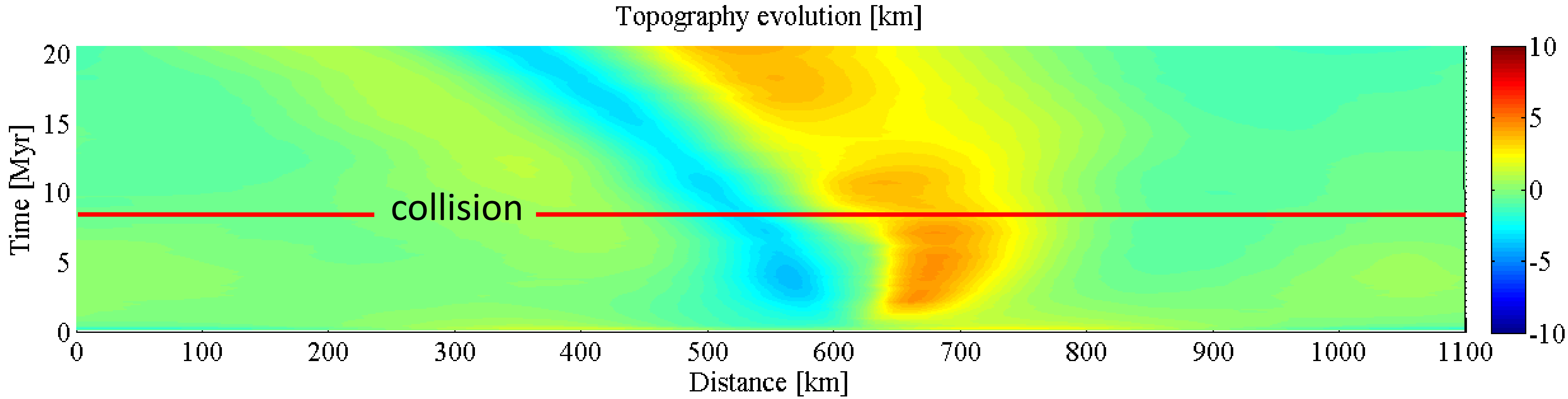

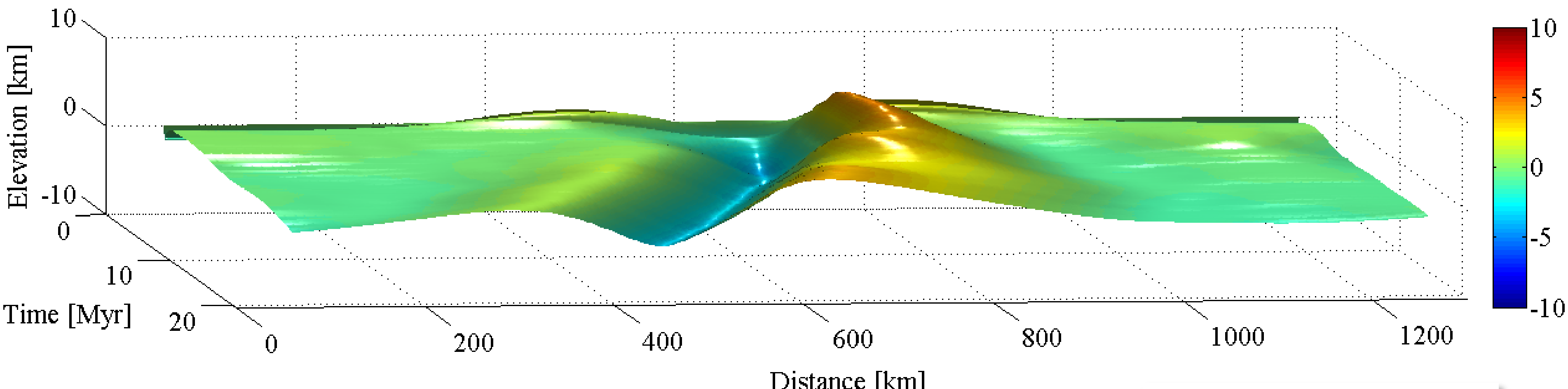

Francois et al., 2010

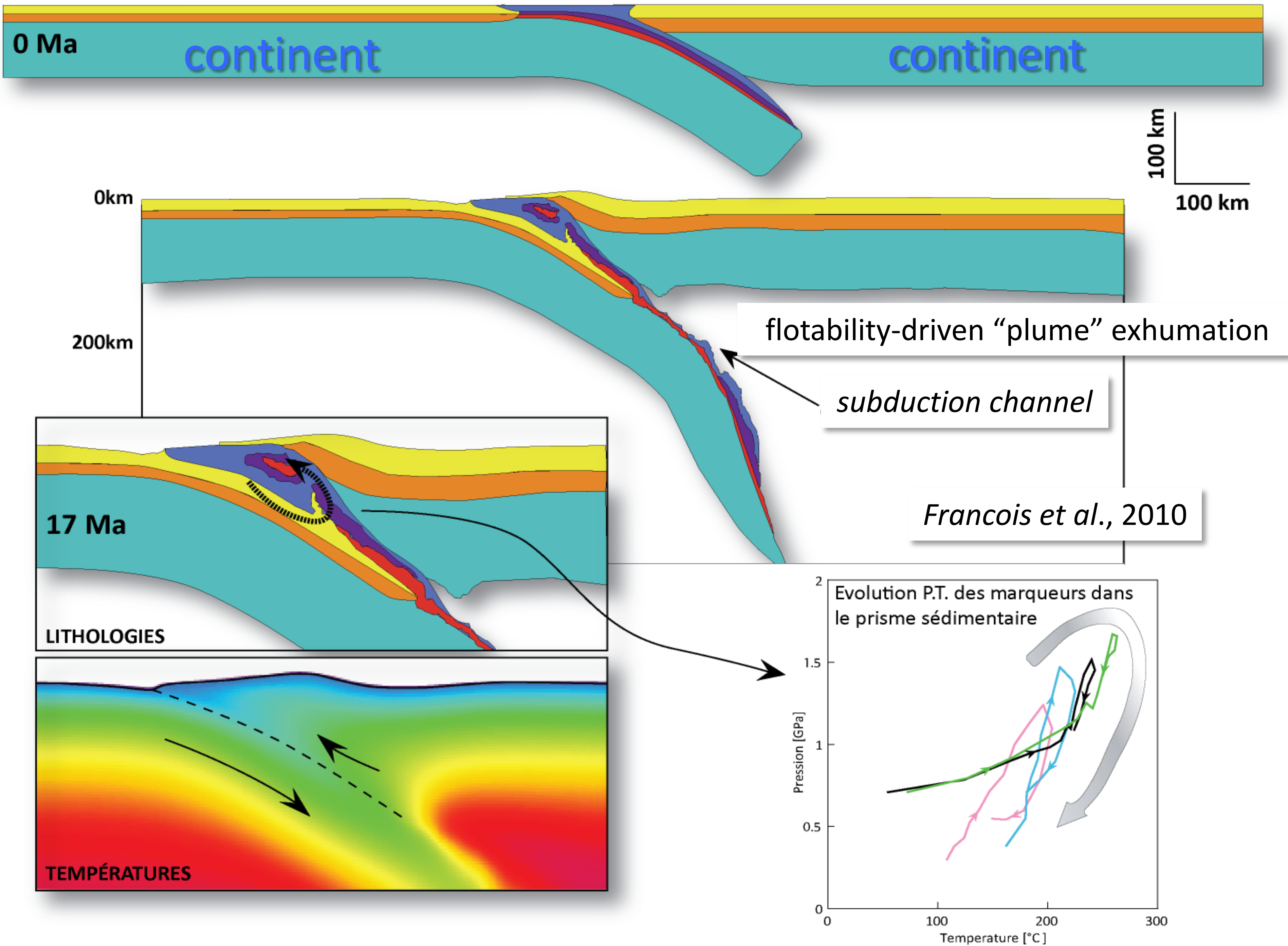

0 Ma
continent
continent
100 km
100 km
0km
200km
flotability-driven "plume" exhumation
subduction channel
Francois et al., 2010
17 Ma
LITHOLOGIES
TEMPÉRATURES
Evolution P.T. des marqueurs dans le prisme sédimentaire
Pression [GPa]
Temperature [°C]
0
0.5
1
1.5
2
0
100
200
300

Zagros-type collision: continental phase, 3 cm/y

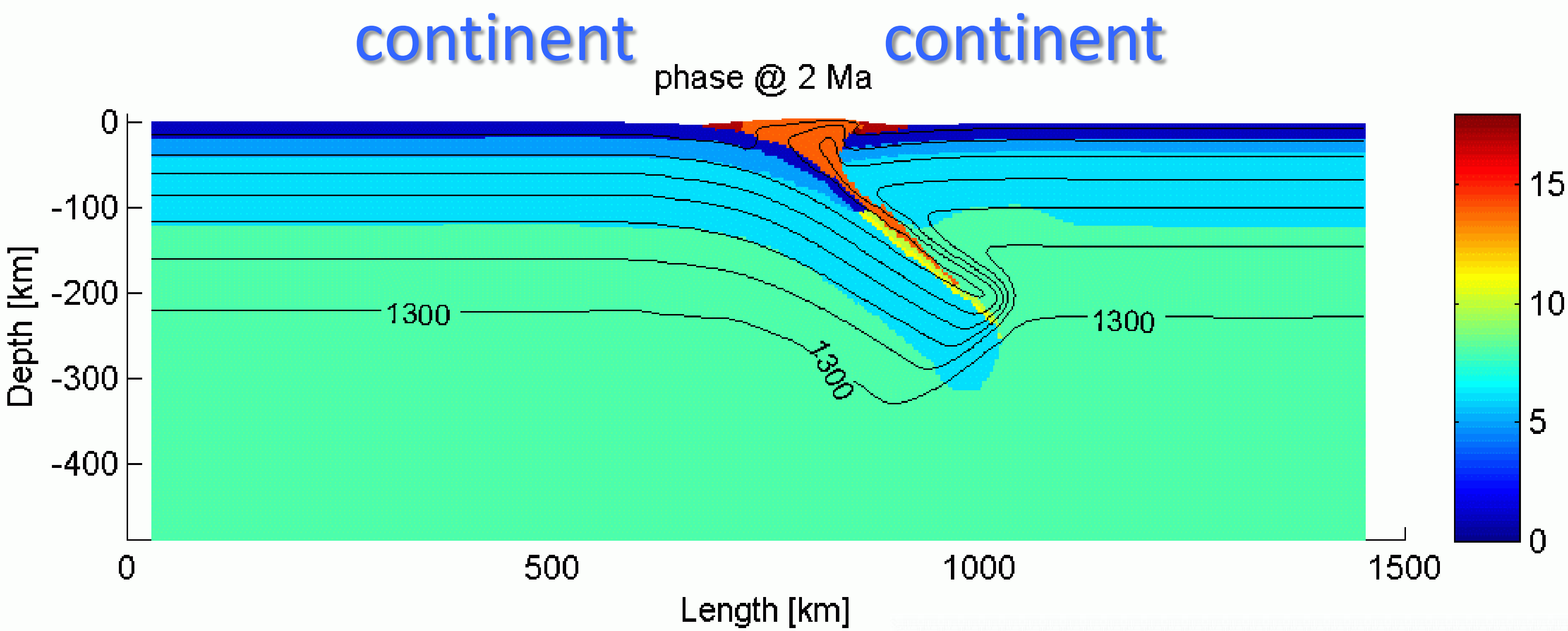

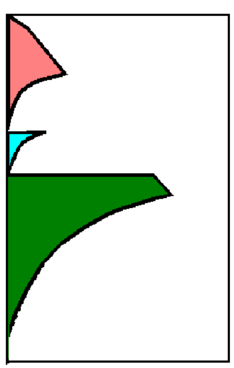

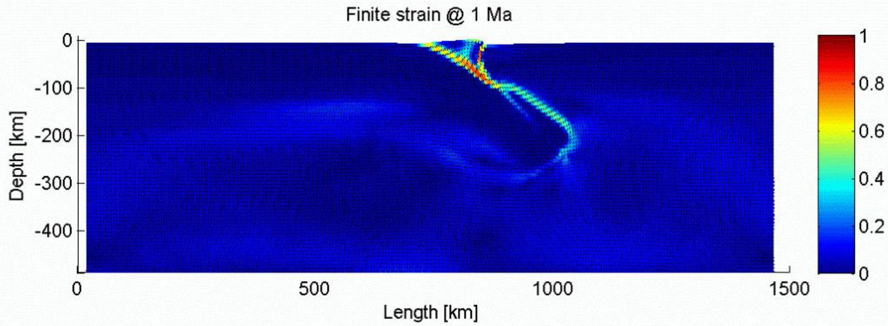

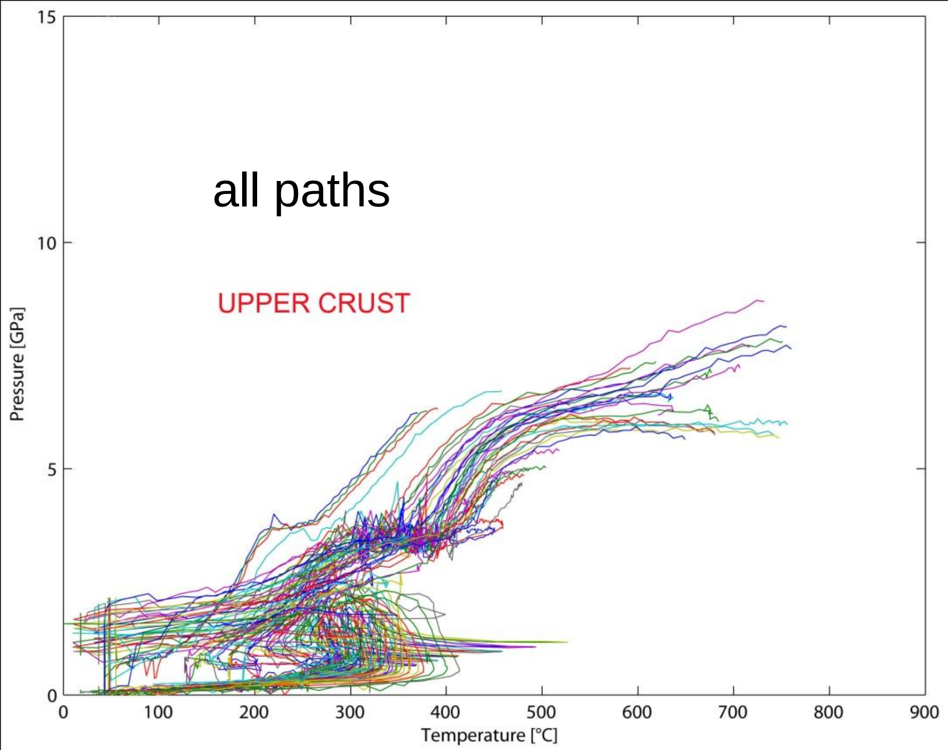
all paths
UPPER CRUST
Pressure [GPa]
Temperature [°C]
0
5
10
15
0
100
200
300
400
500
600
700
800
900

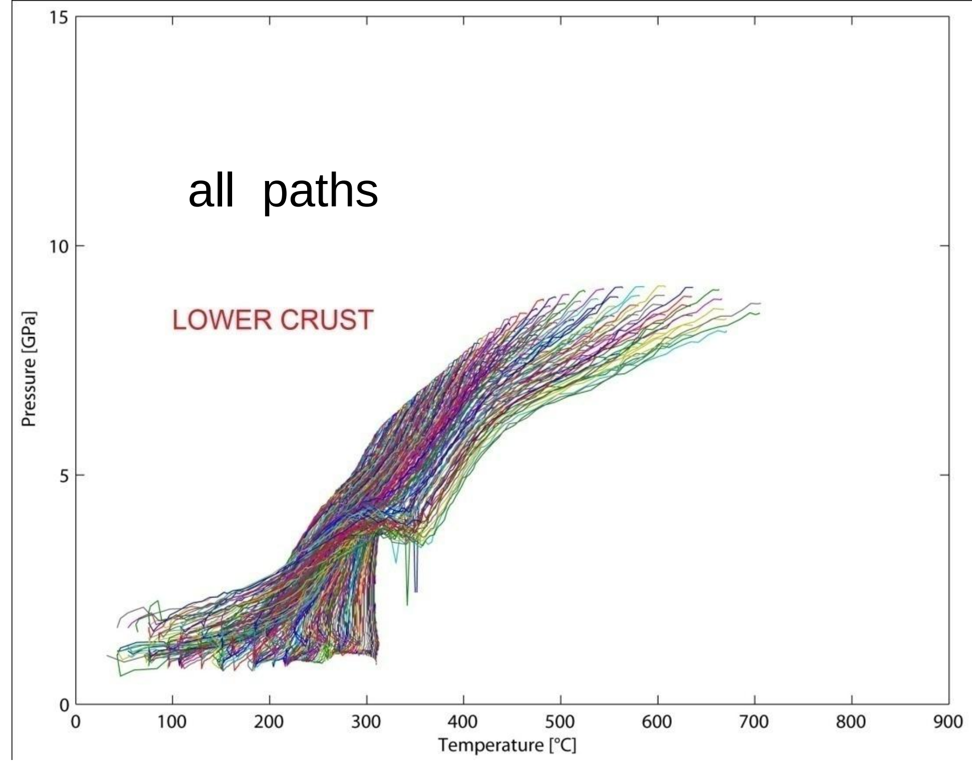
all paths
LOWER CRUST
Pressure [GPa]
Temperature [°C]
0
5
10
15
0
100
200
300
400
500
600
700
800
900

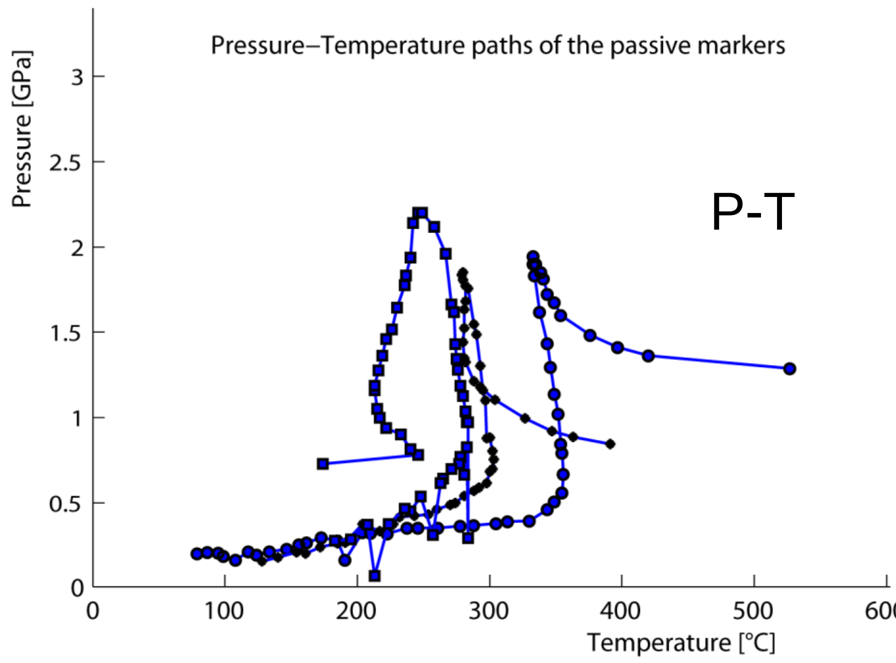
Pressure–Temperature paths of the passive markers
P-T
Pressure [GPa]
Temperature [°C]
0
0.5
1
1.5
2
2.5
3
0
100
200
300
400
500
600

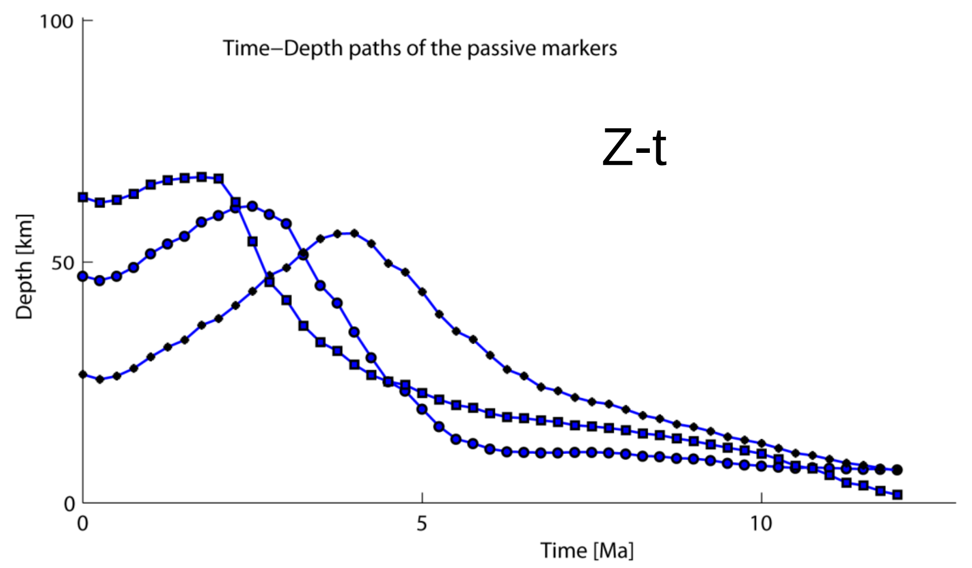
Time–Depth paths of the passive markers
Z-t
Depth [km]
Time [Ma]
0
50
100
0
5
10

continent continent

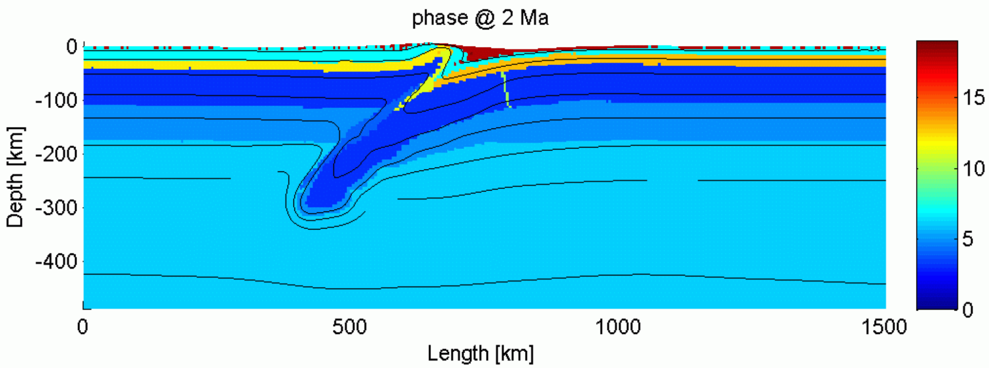

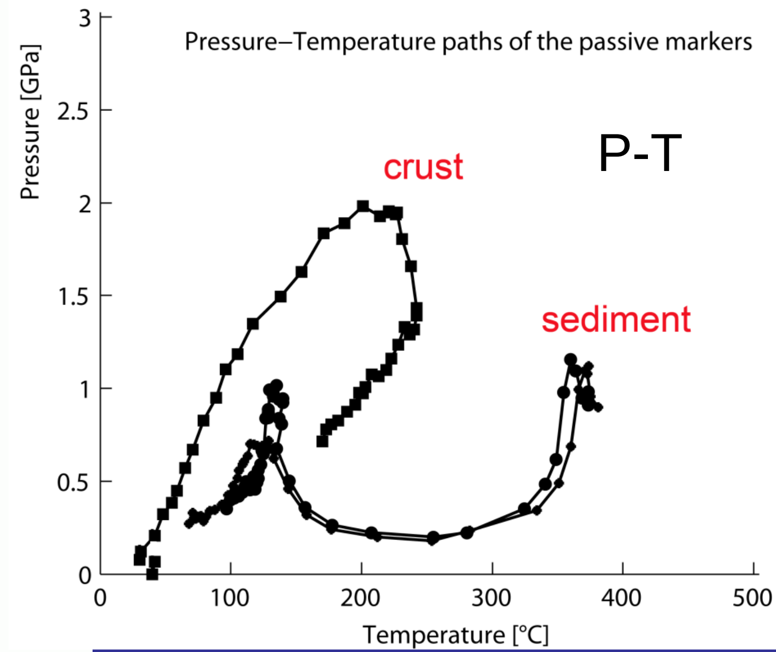

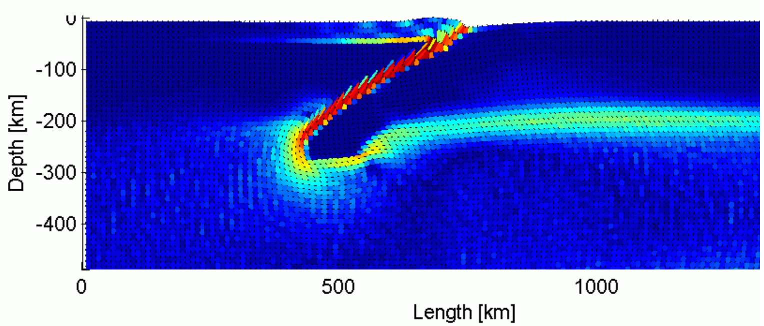

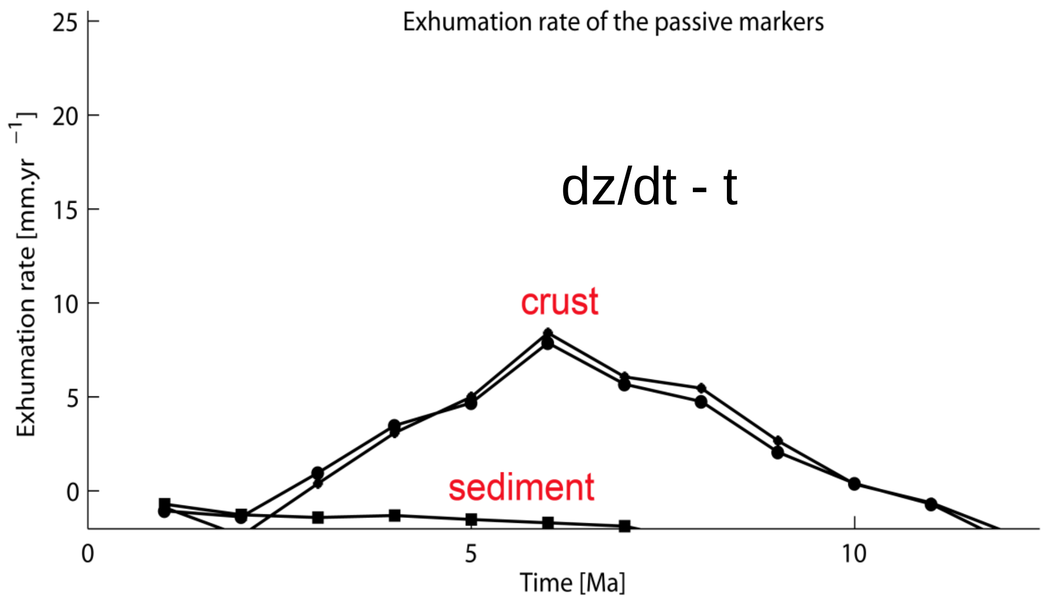

Strong lithosphere (Te > 60 km), « India-Asia » collision

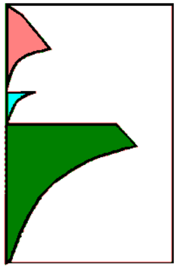

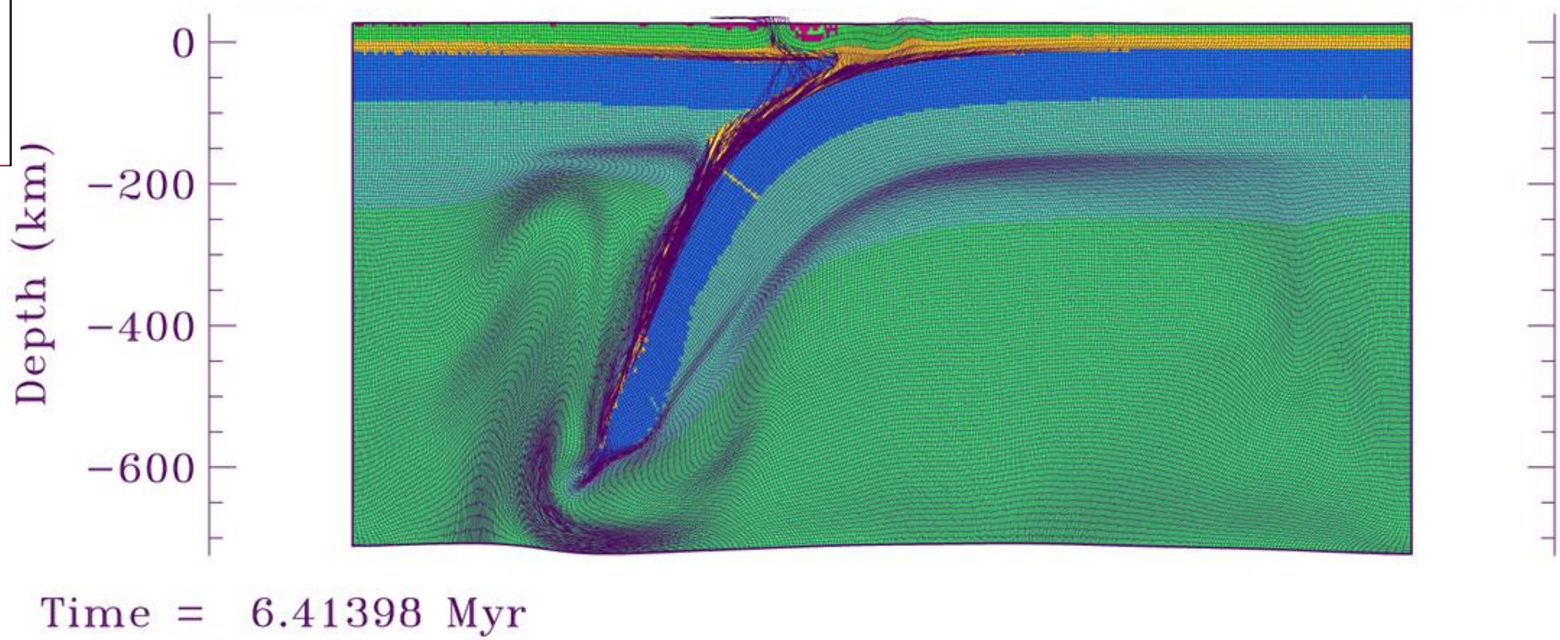

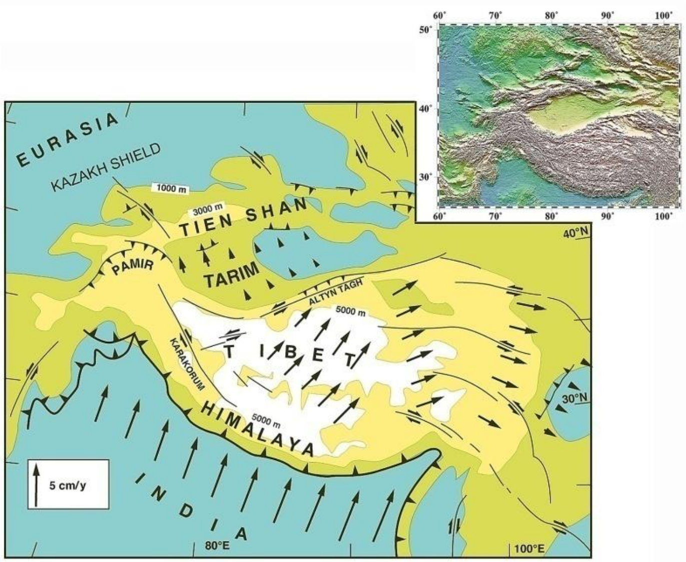

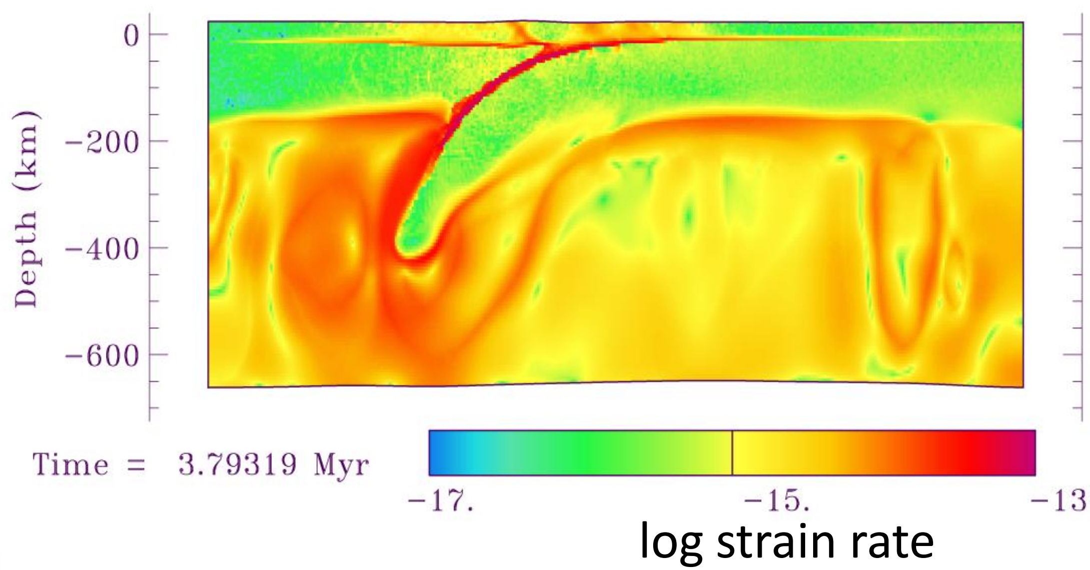

India-Asia collision , thermo-dynamically consistent density, 6 cm/y

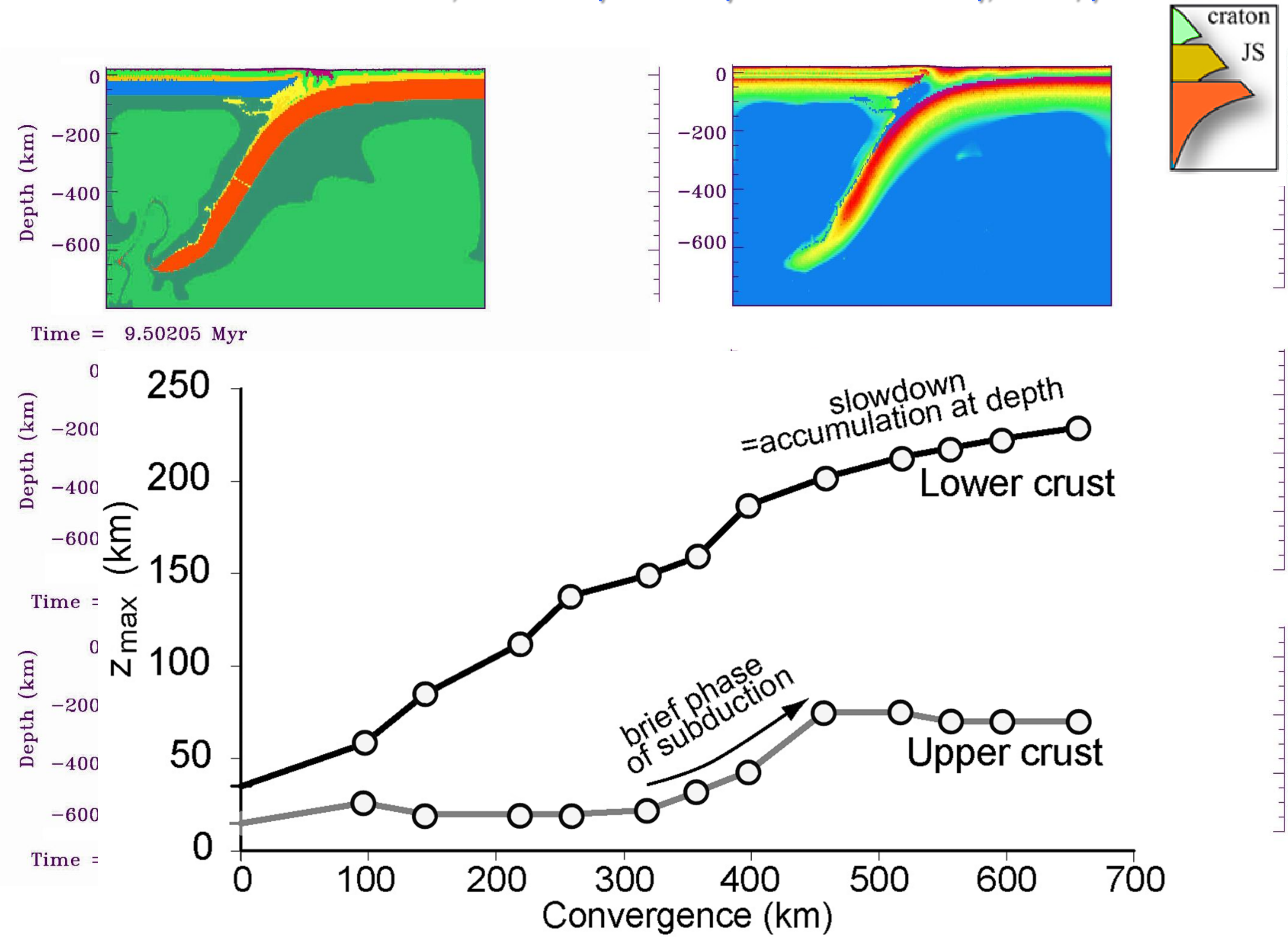

India-Asia collision , thermo-dynamically consistent density, 6 cm/y

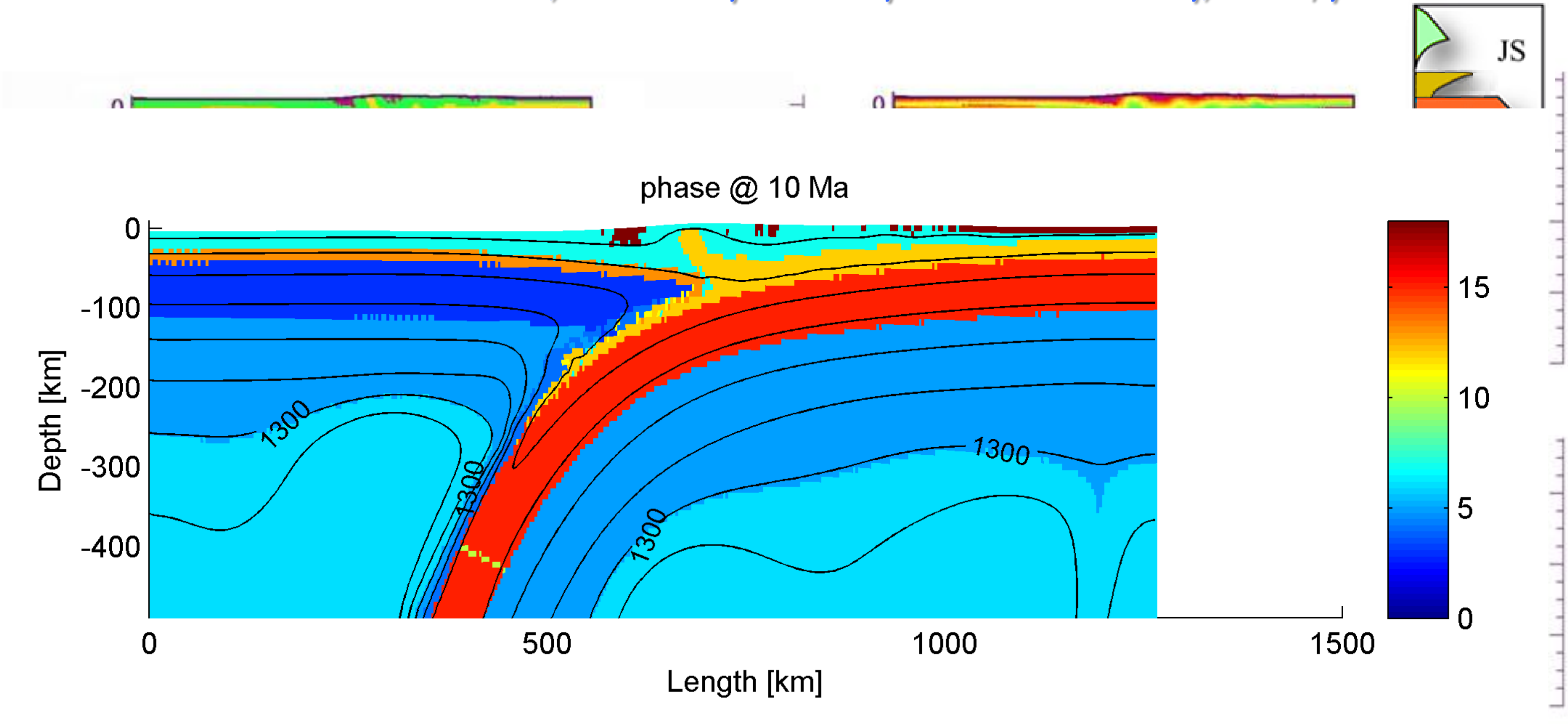

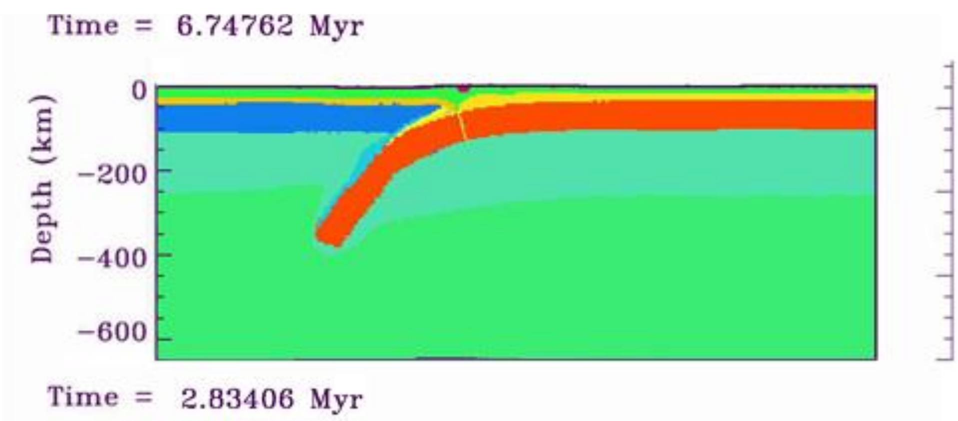

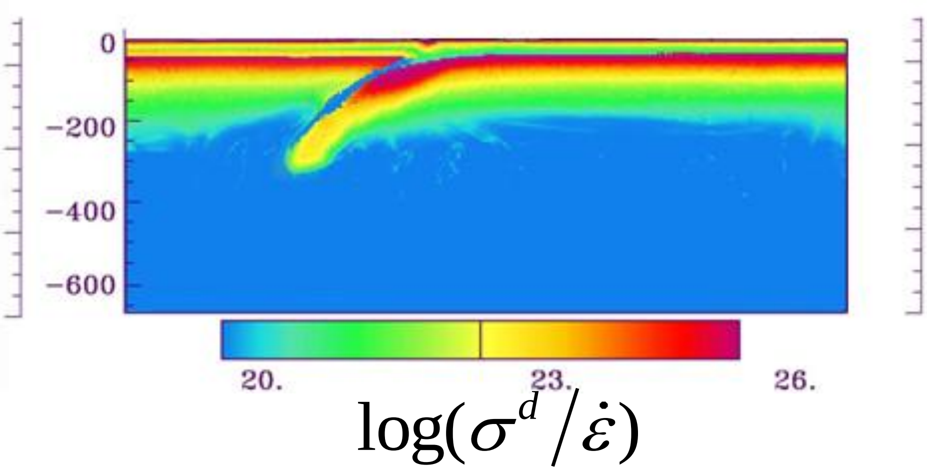

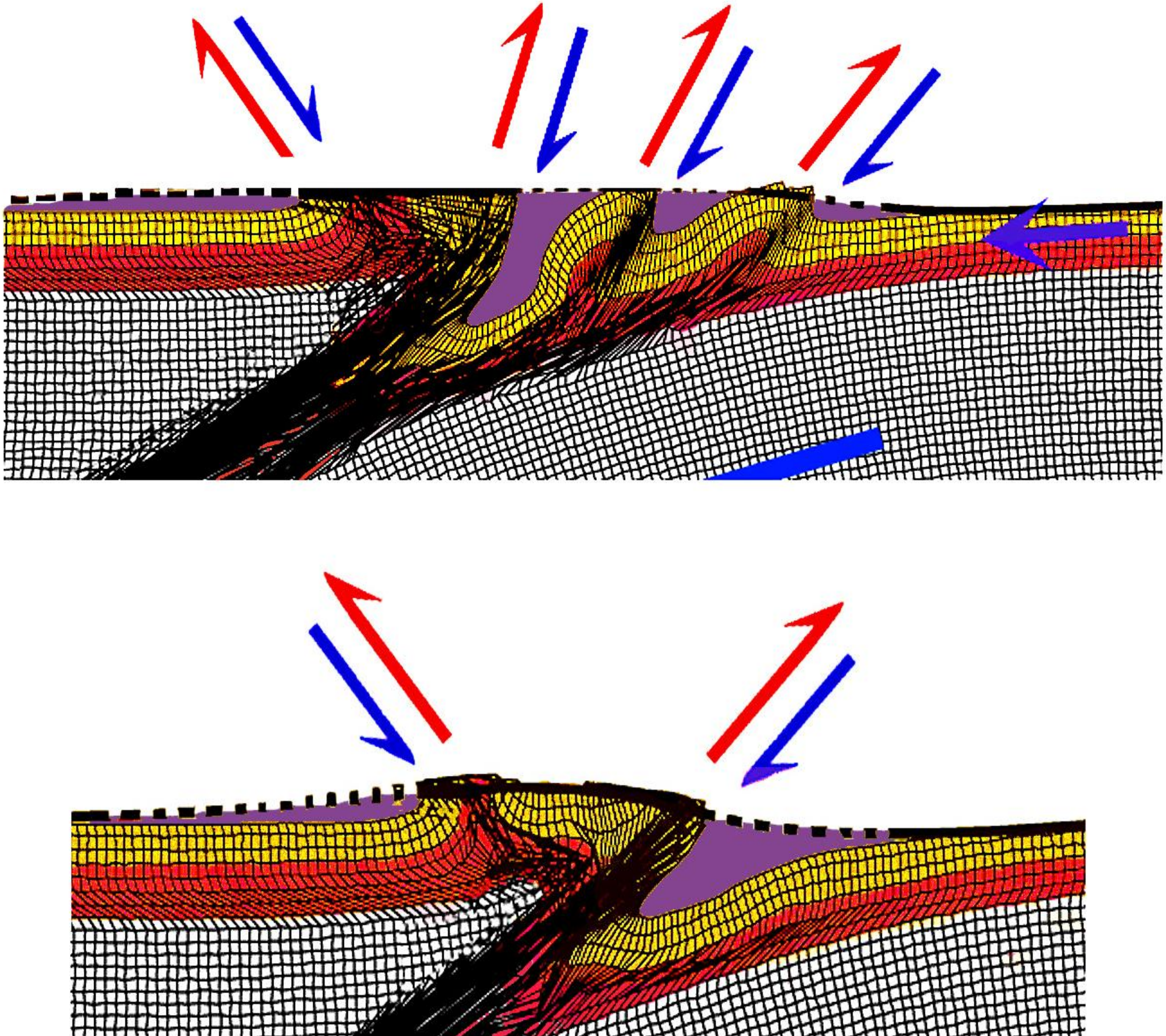

3. Importance of coupling with surface processes

Steady State

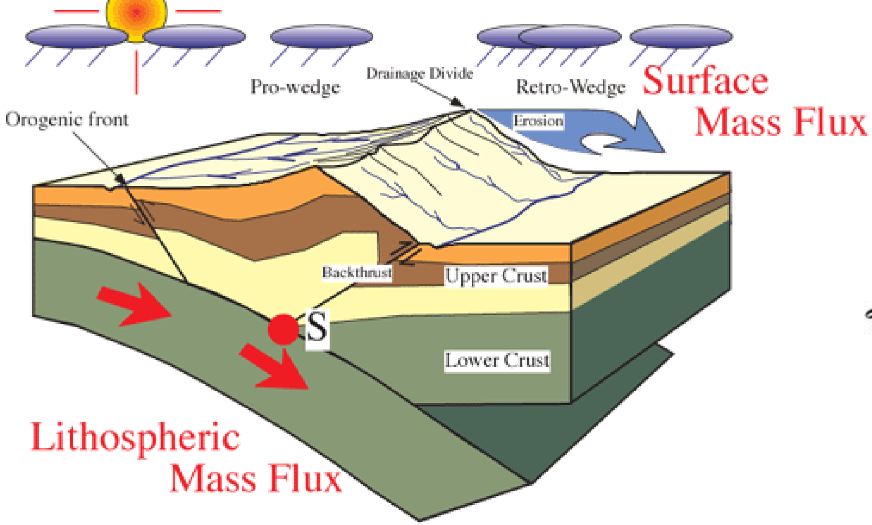

I. Equations of diffusional erosion:

$$dh/dt = k^*(x,h,(\nabla h)^n)\ \Delta h$$

II. The long range transport processes

$$q_{fe} = -K_r q_r dh/dl$$

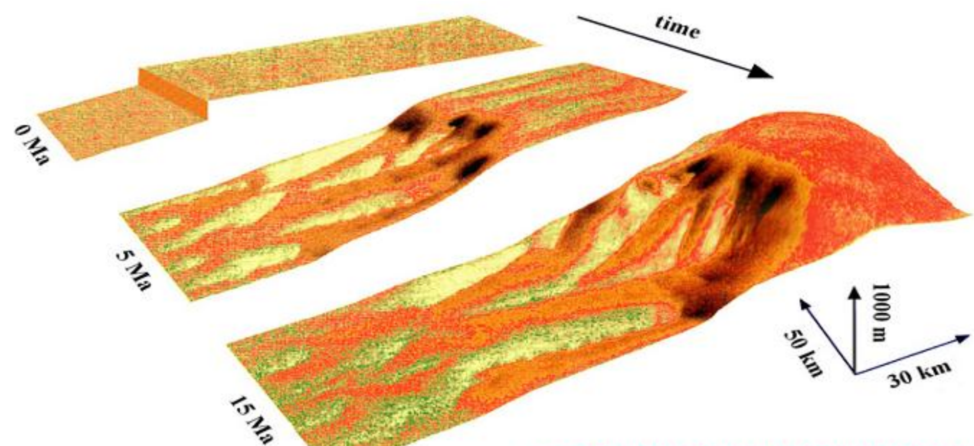

model predicted topographies

Constructive Growth

1. ***topography uplift rates (dh) < 0.01 cmly***
2. ***erosion rates (de) = 0.05 to 0.1 cmly (!)***
3. ***tectonic uplift rates du = dh - de = 0.05 to 0.1 cmly***

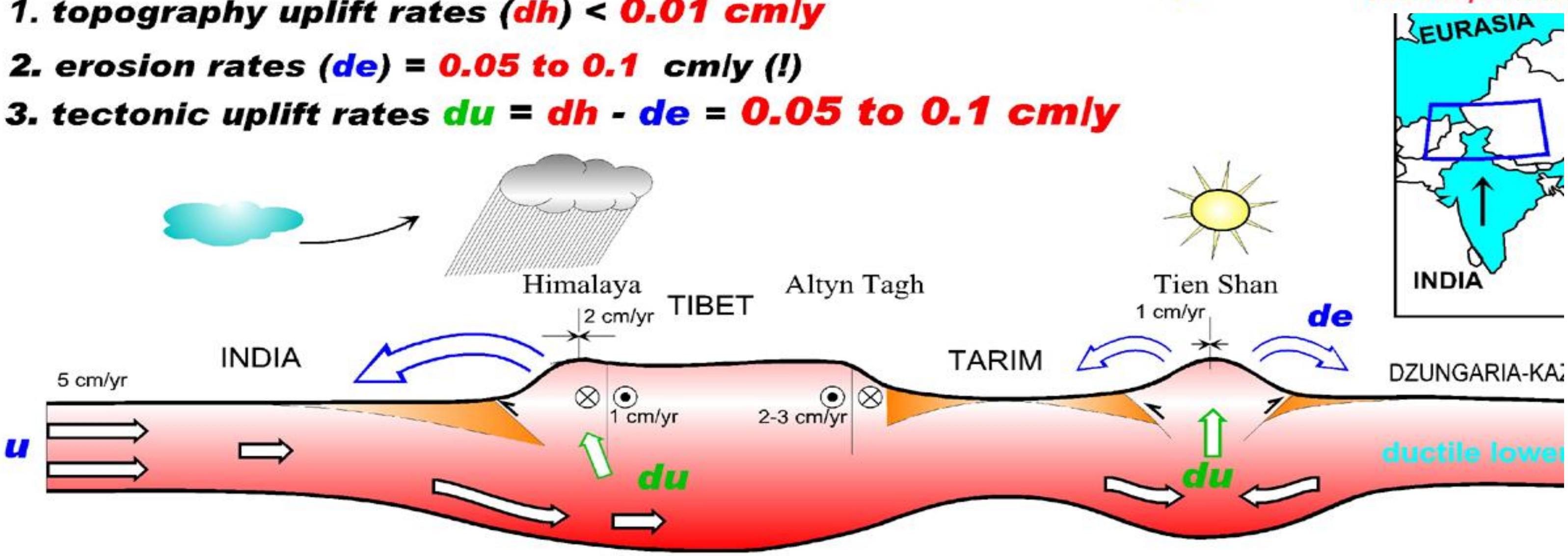

EROSION – TECTONICS FEEDBACK
SEMI-ANALYTICAL PURE SHEAR MODEL

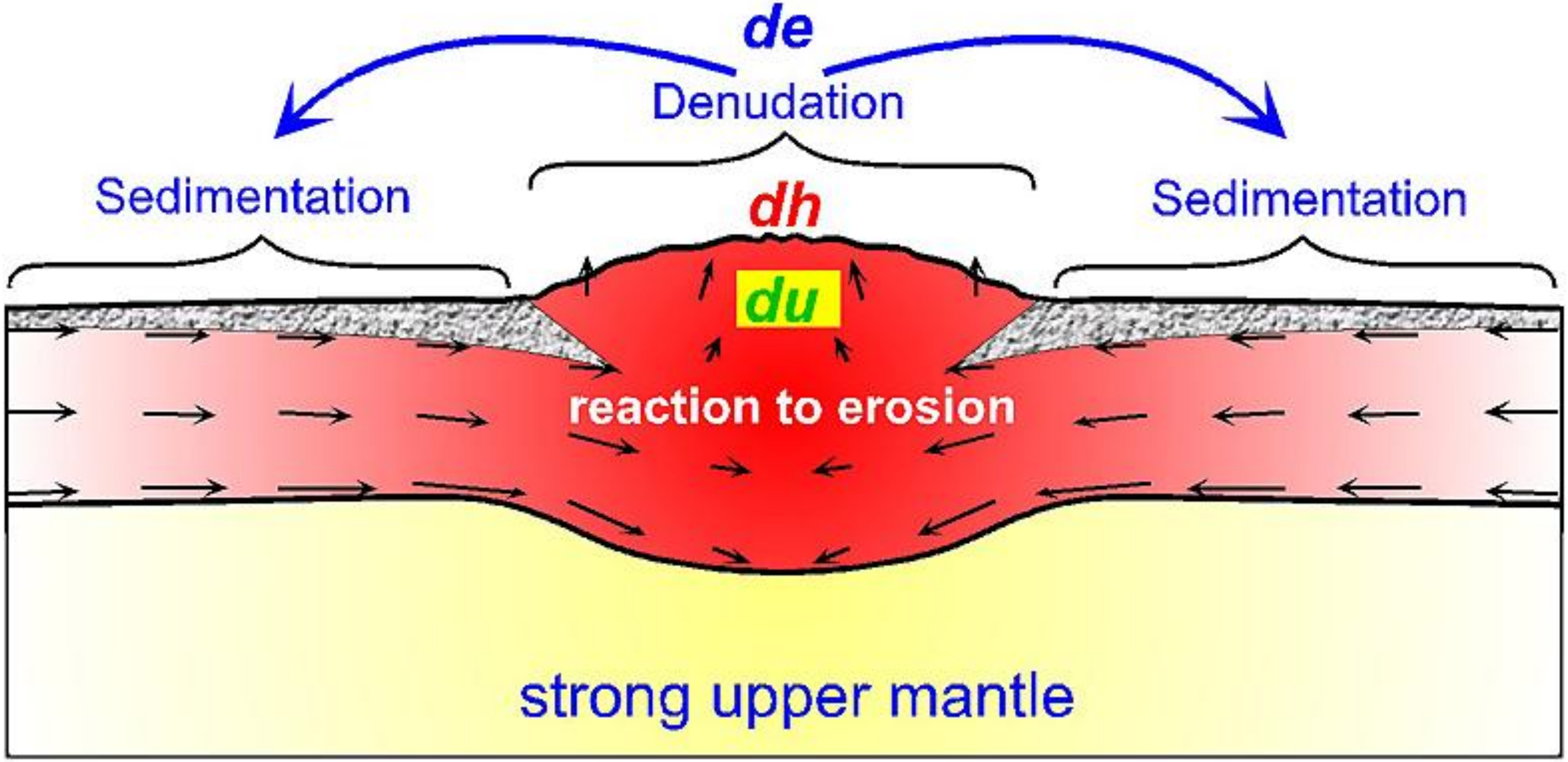

Avouac and Burov, 1996

INSUFFICIENT EROSION

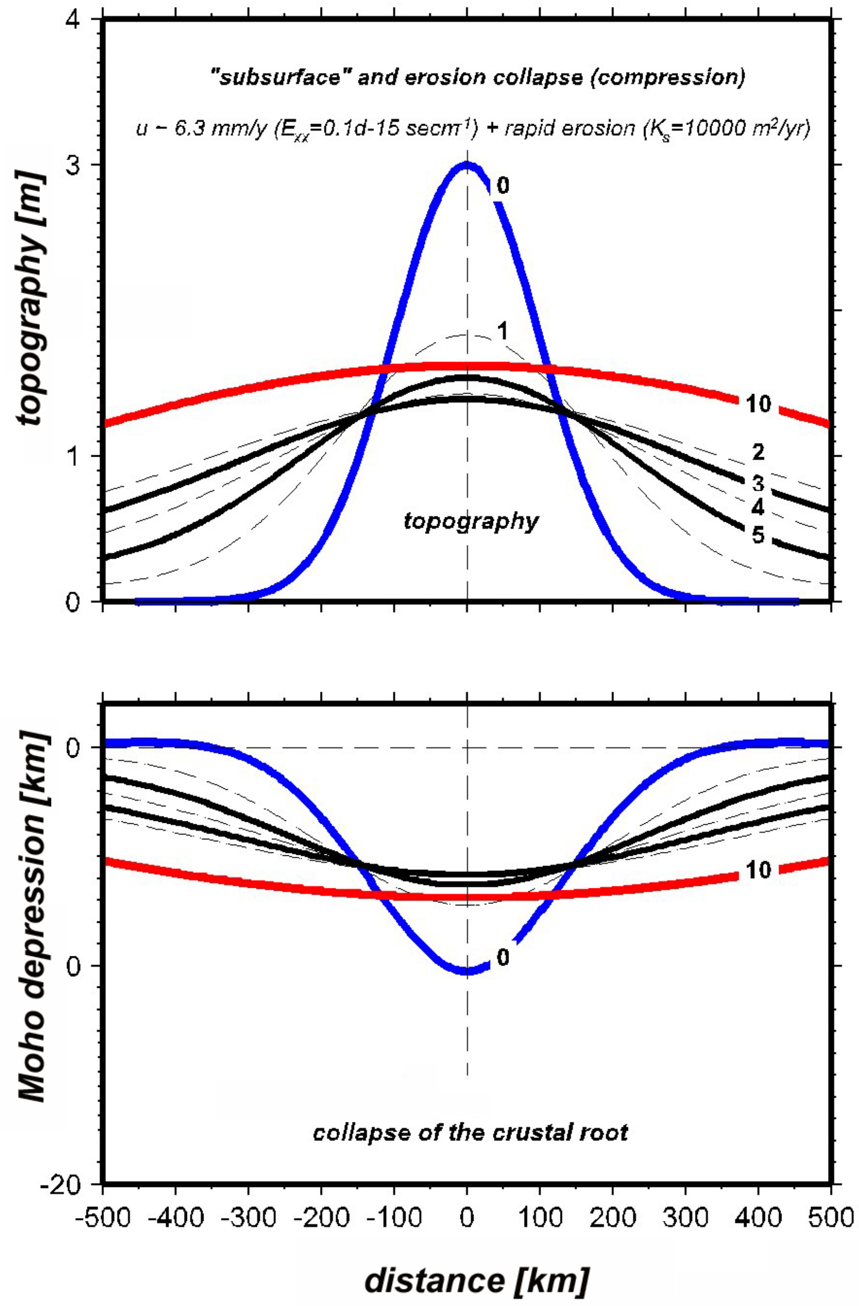

EROSION-TECTONIC BALANCE

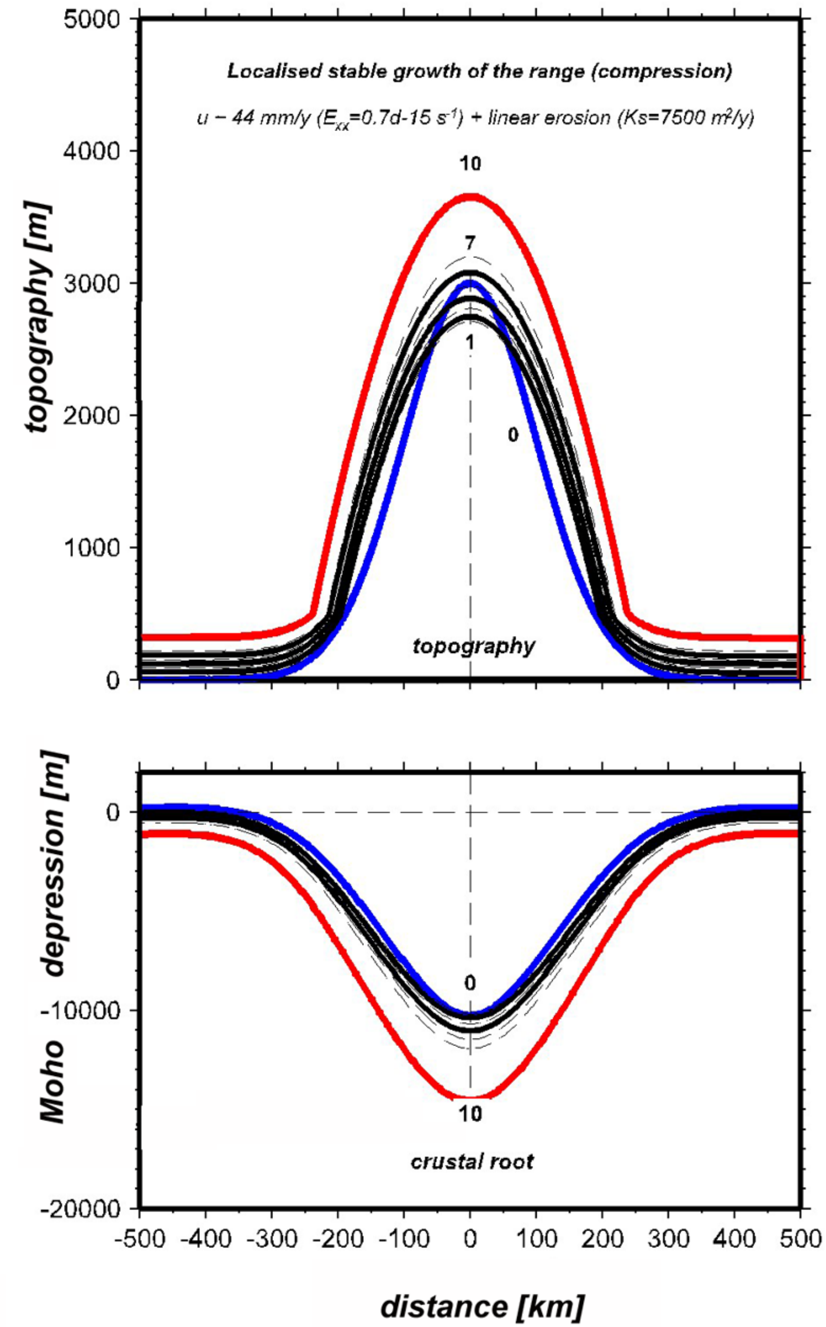

3 MAJOR MODES OF OROGENIC EVOLUTION (PURE SHEAR)

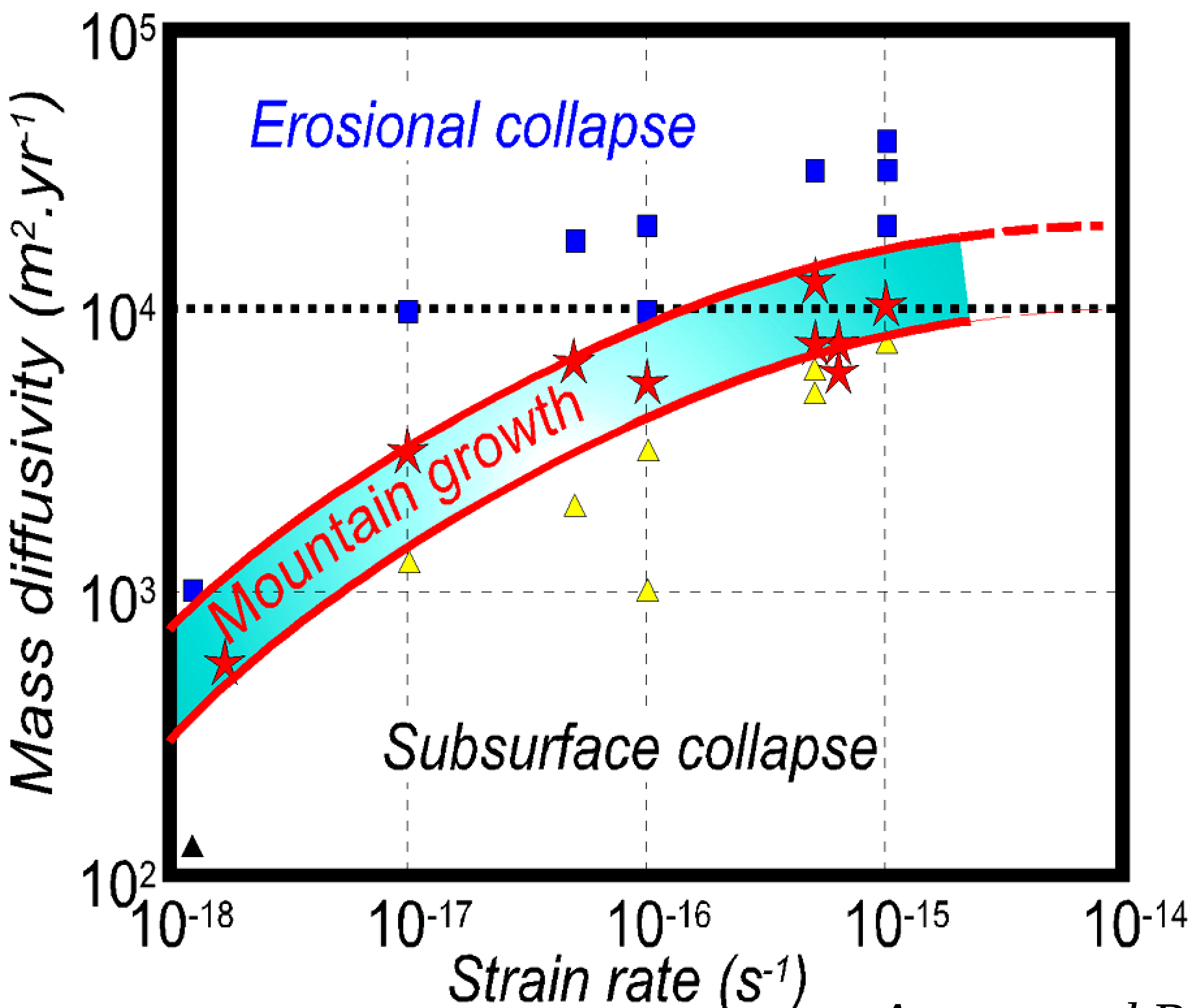

Avouac and Burov, 1996

3 MAJOR MODES OF OROGENIC EVOLUTION (PURE SHEAR)

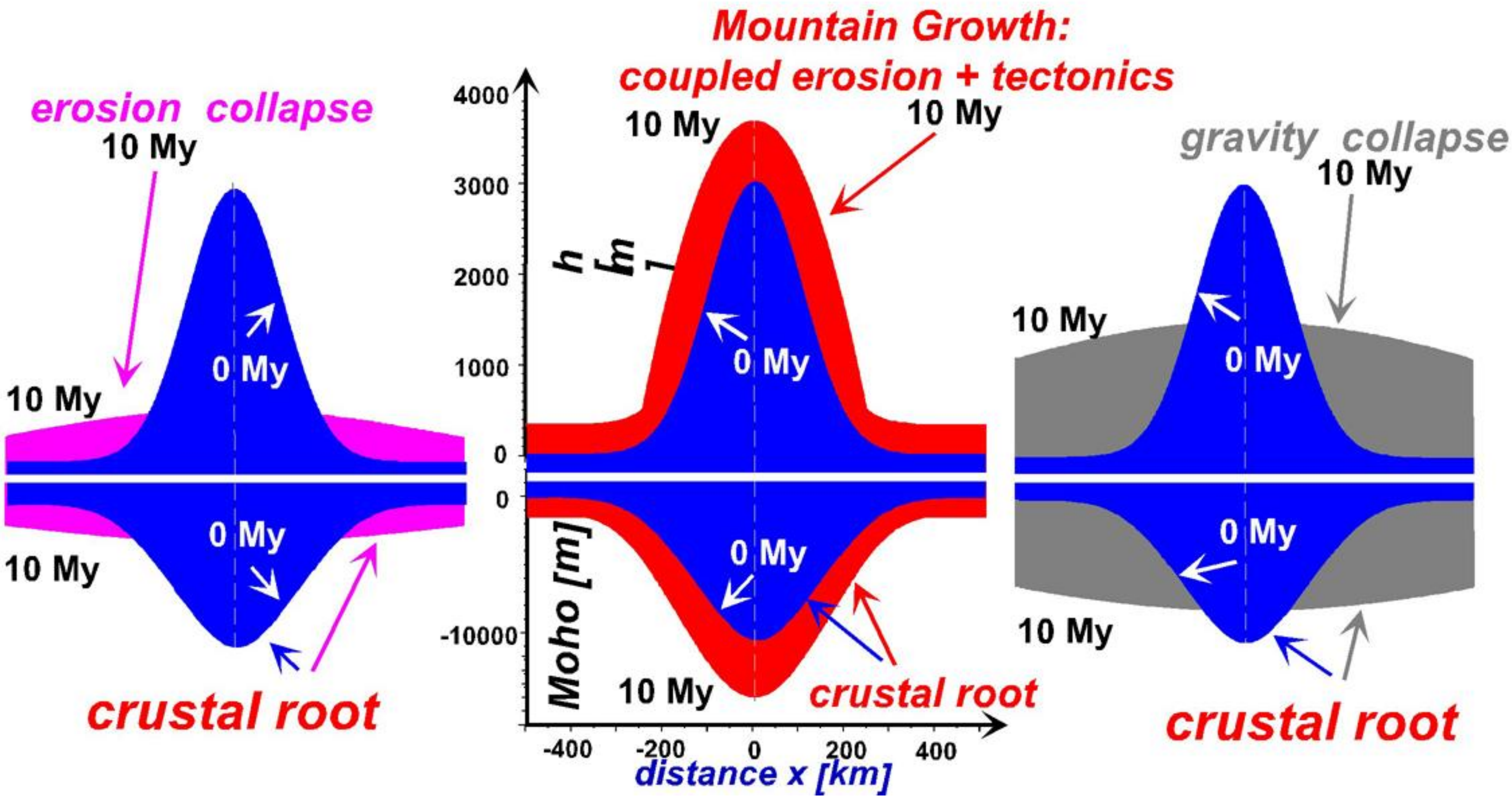

Avouac and Burov, 1996

Final stages of subduction-collision, as function of convergence and erosion rate

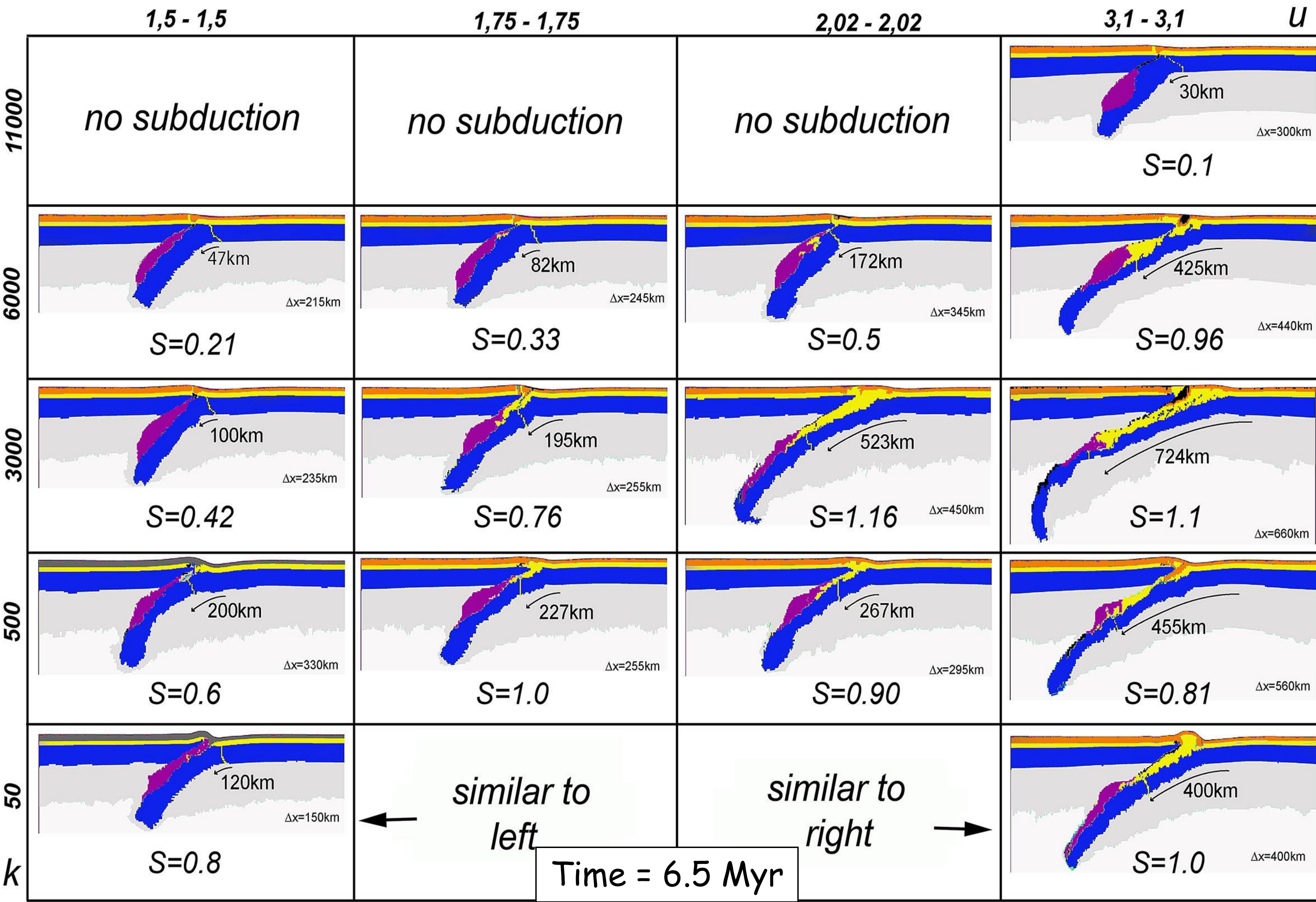

Dependence on efficiency of surface erosion rate (k)

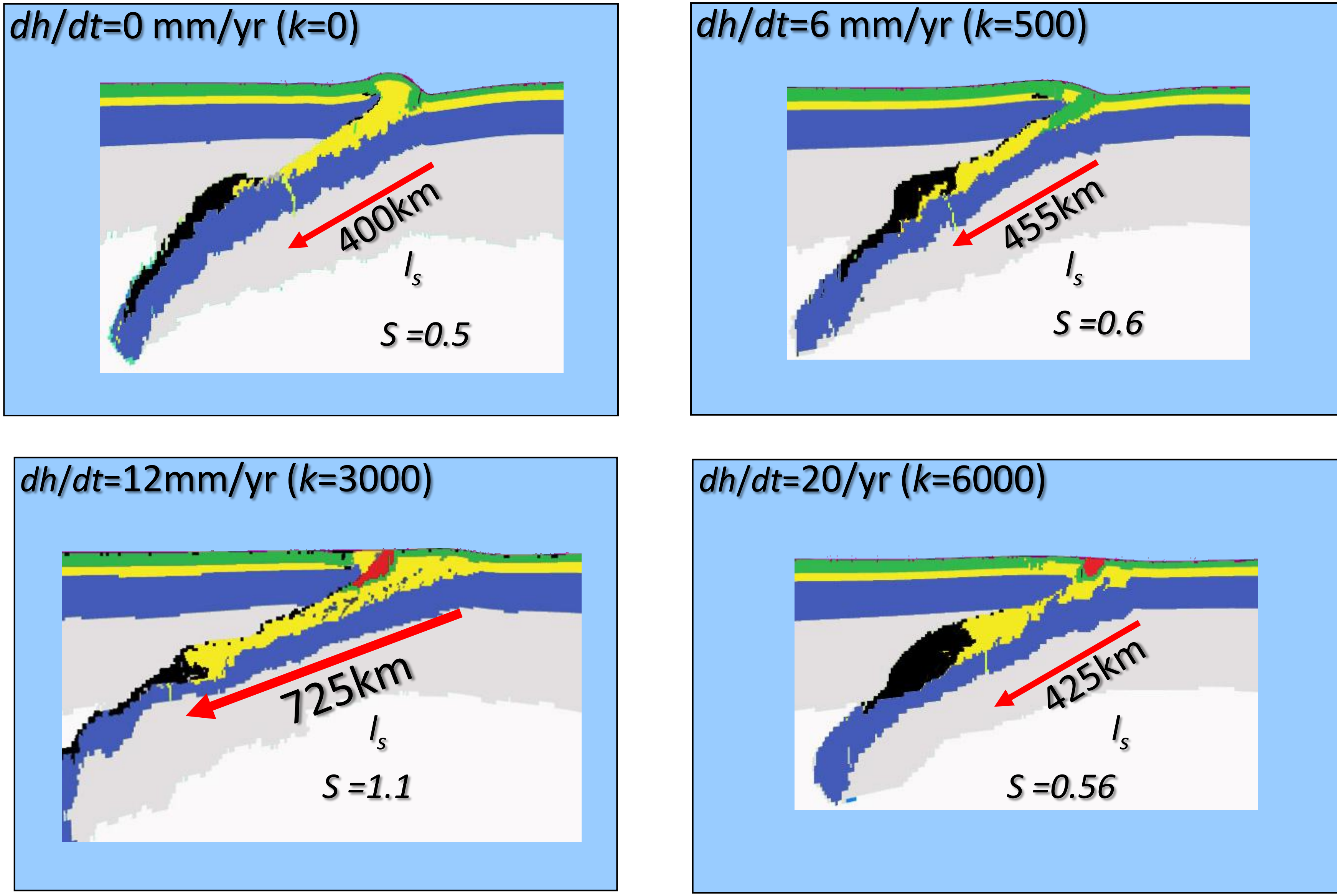

Maximal erosion rate and subduction length as function of k, convergence rate 60 mm/yr

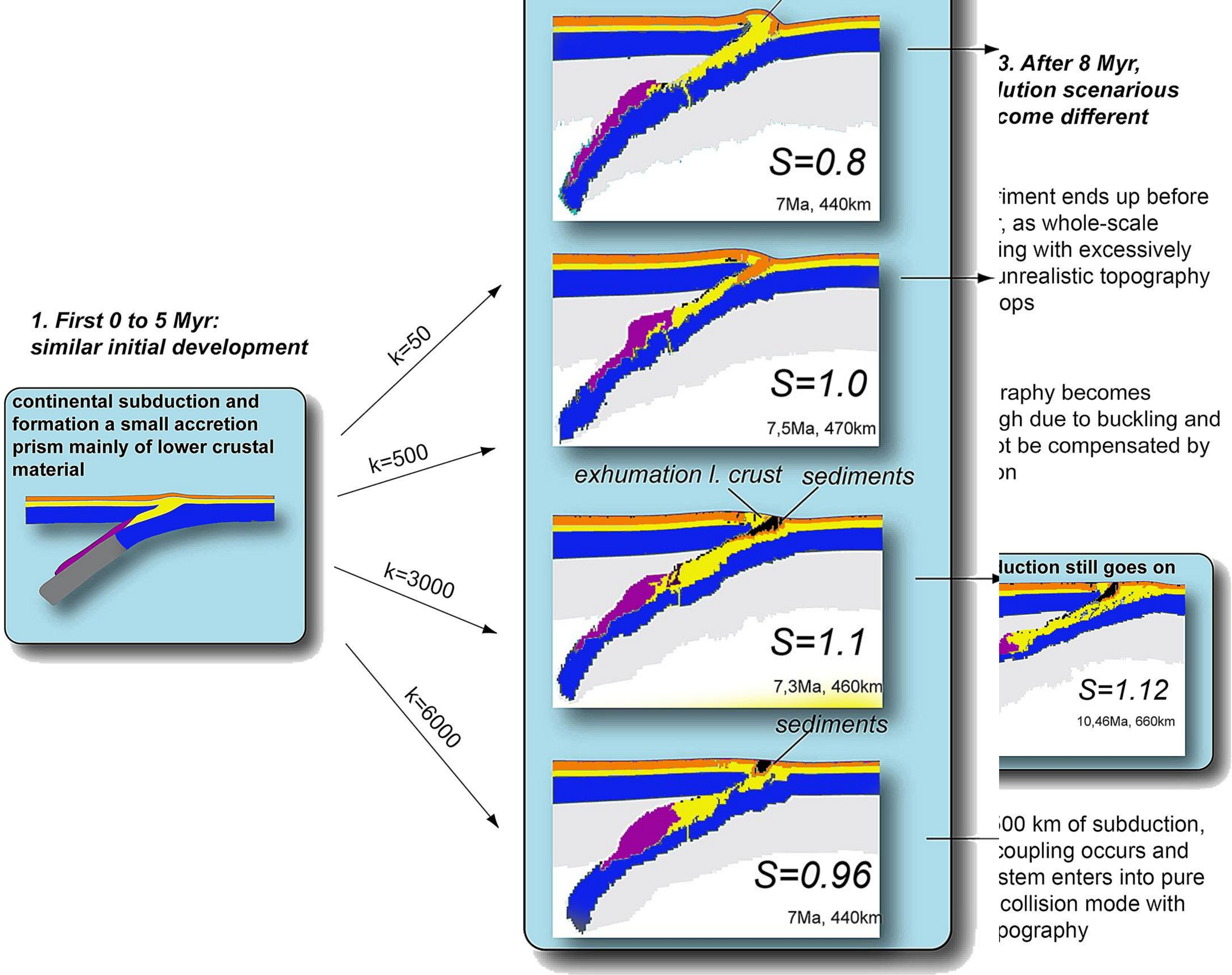

1. First 0 to 5 Myr:
similar initial development
continental subduction and formation a small accretion prism mainly of lower crustal material
k=50
k=500
k=3000
k=6000
S=0.8
7Ma, 440km
S=1.0
7,5Ma, 470km
exhumation l. crust
sediments
S=1.1
7,3Ma, 460km
sediments
S=0.96
7Ma, 440km
3. After 8 Myr,
lution scenarious
come different
iment ends up before
, as whole-scale
ing with excessively
unrealistic topography
ops
raphy becomes
gh due to buckling and
t be compensated by
on
luction still goes on
S=1.12
10,46Ma, 660km
00 km of subduction,
coupling occurs and
stem enters into pure
collision mode with
pography

Topography evolution

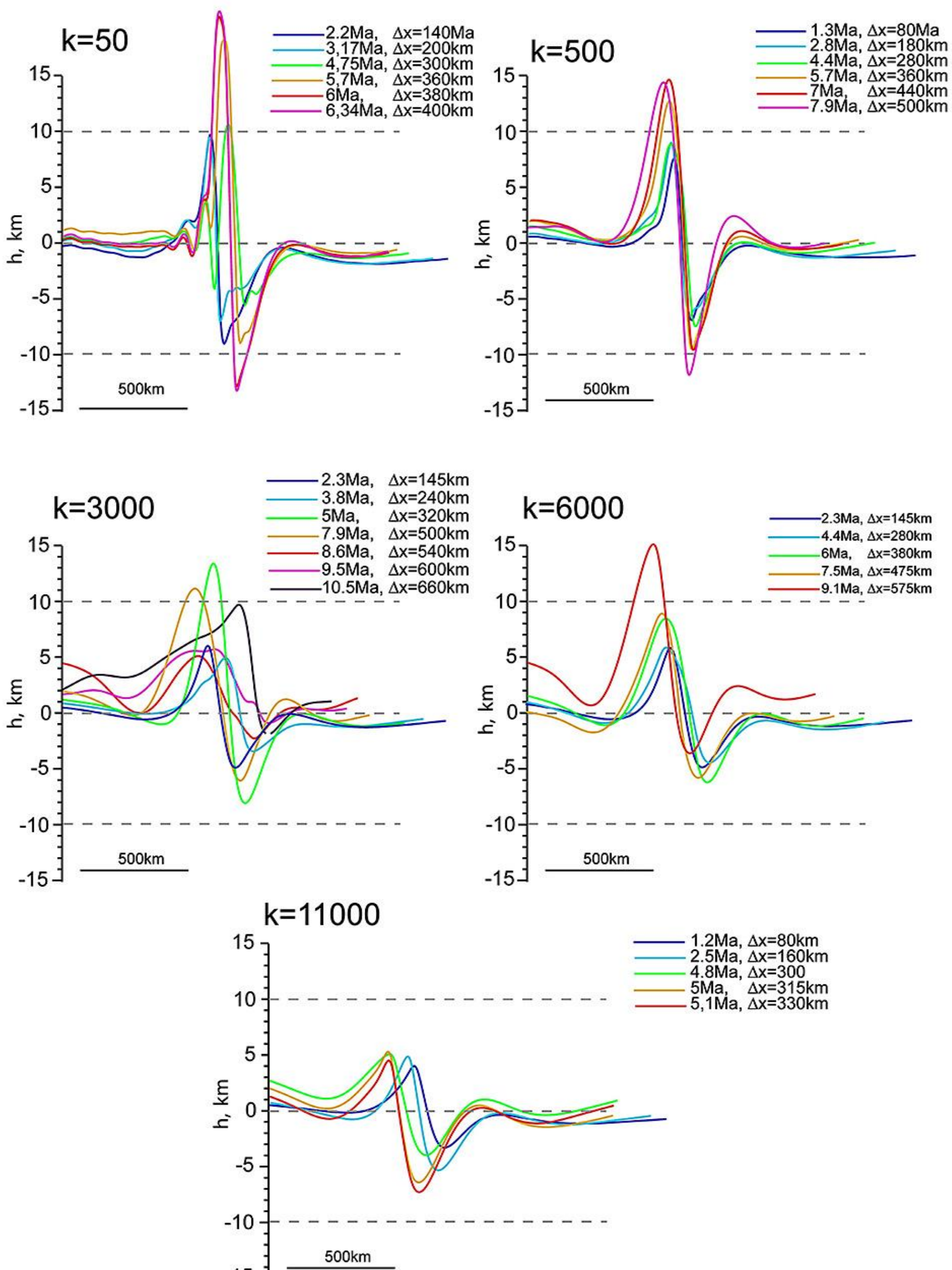

Amount of subduction, *S*, versus surface erosion coefficient, *k*.

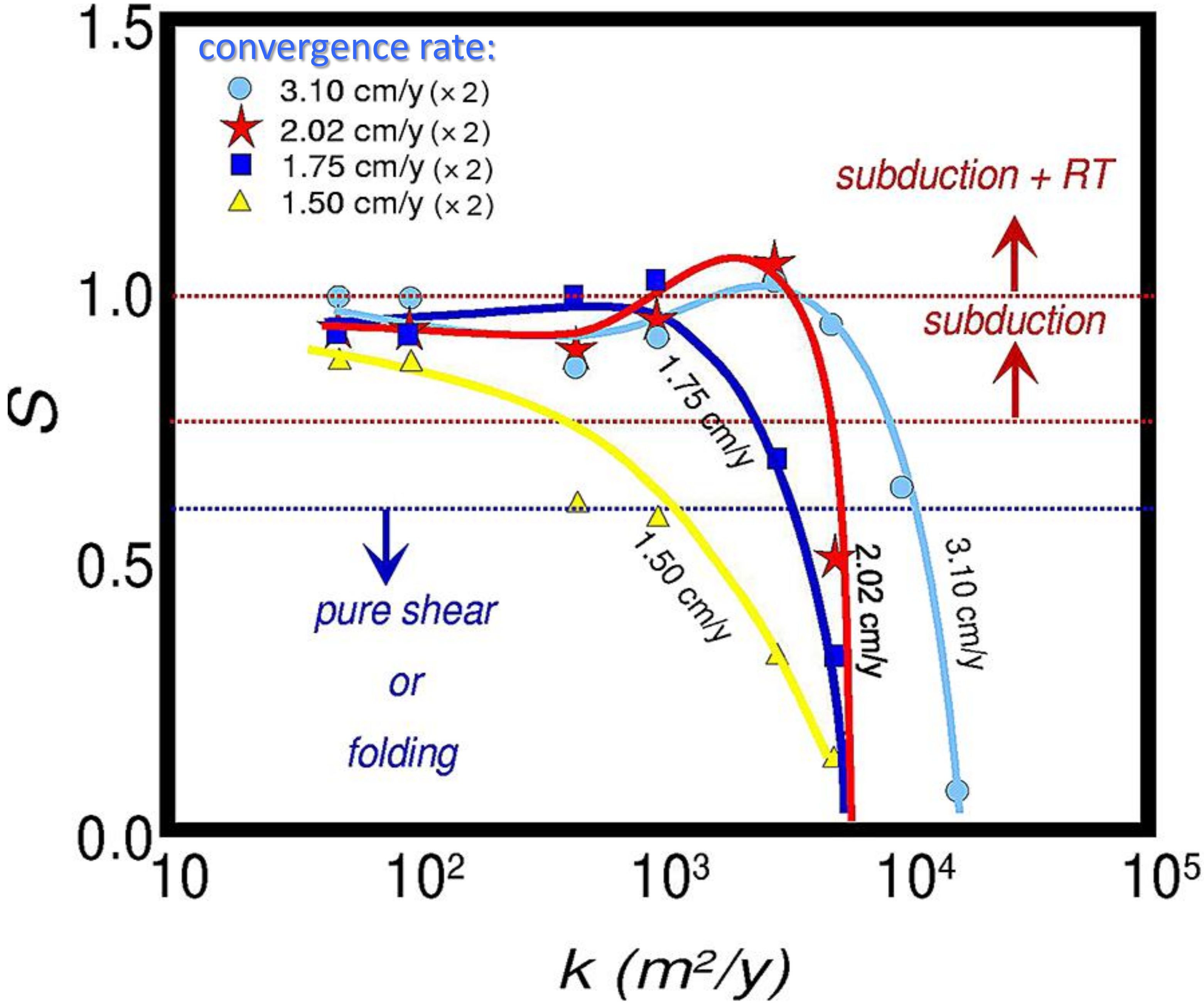

4. End-member case:

Fast convergence

(India-Eurasia Collision)

A simulation compatible with Indian–Asian collision

Geotherm 450 Ma (T_{Moho} = 400°C)

High initial convergence rate (6cm/y)

About 700km of subduction

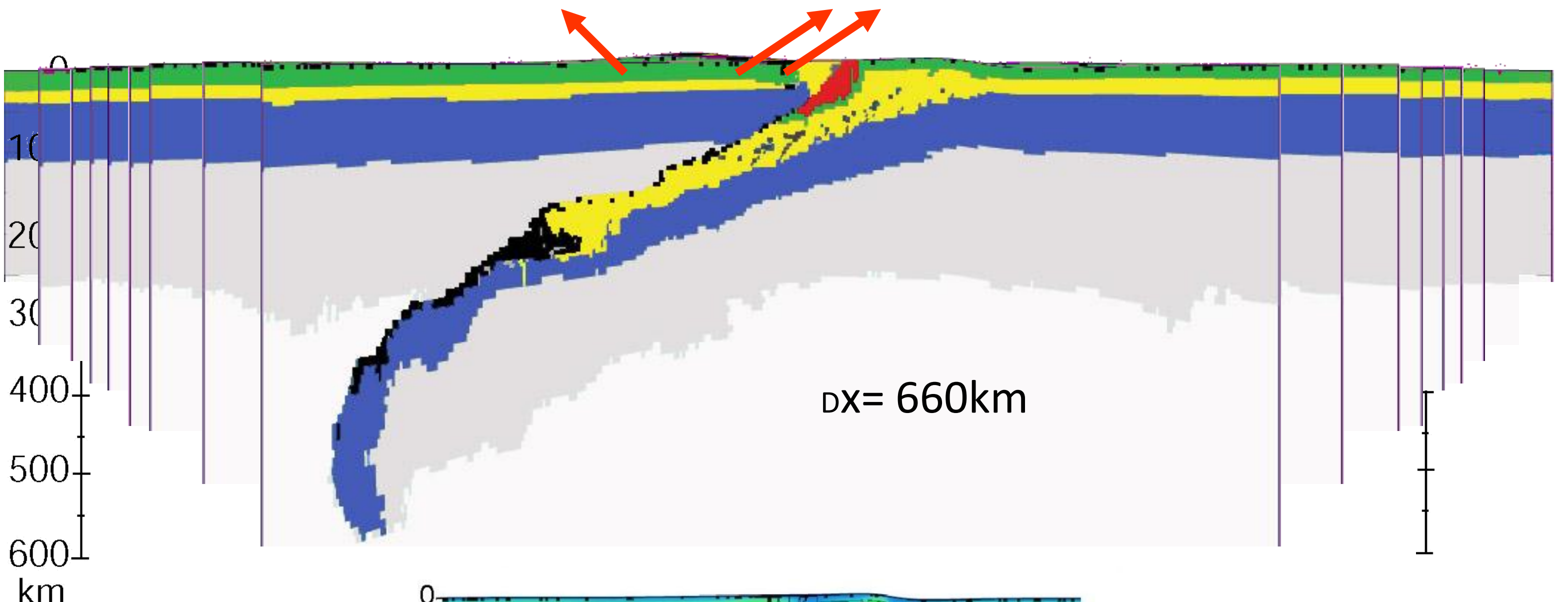

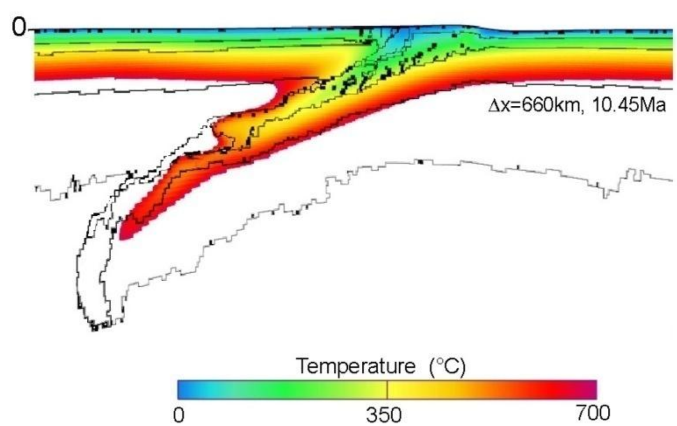

Toussaint, Burov, Avouac, 2004

wait …

Plastic strain

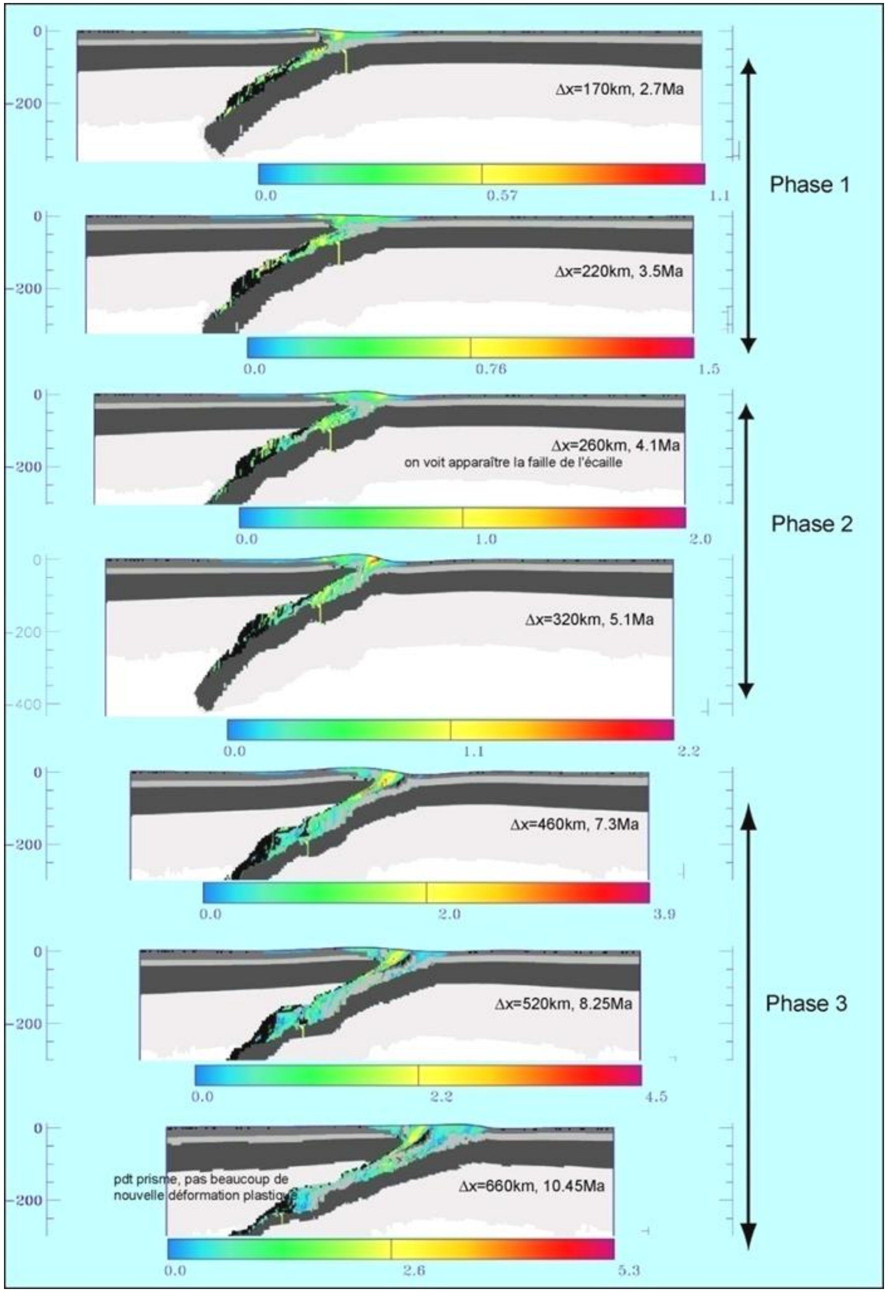

Temperature

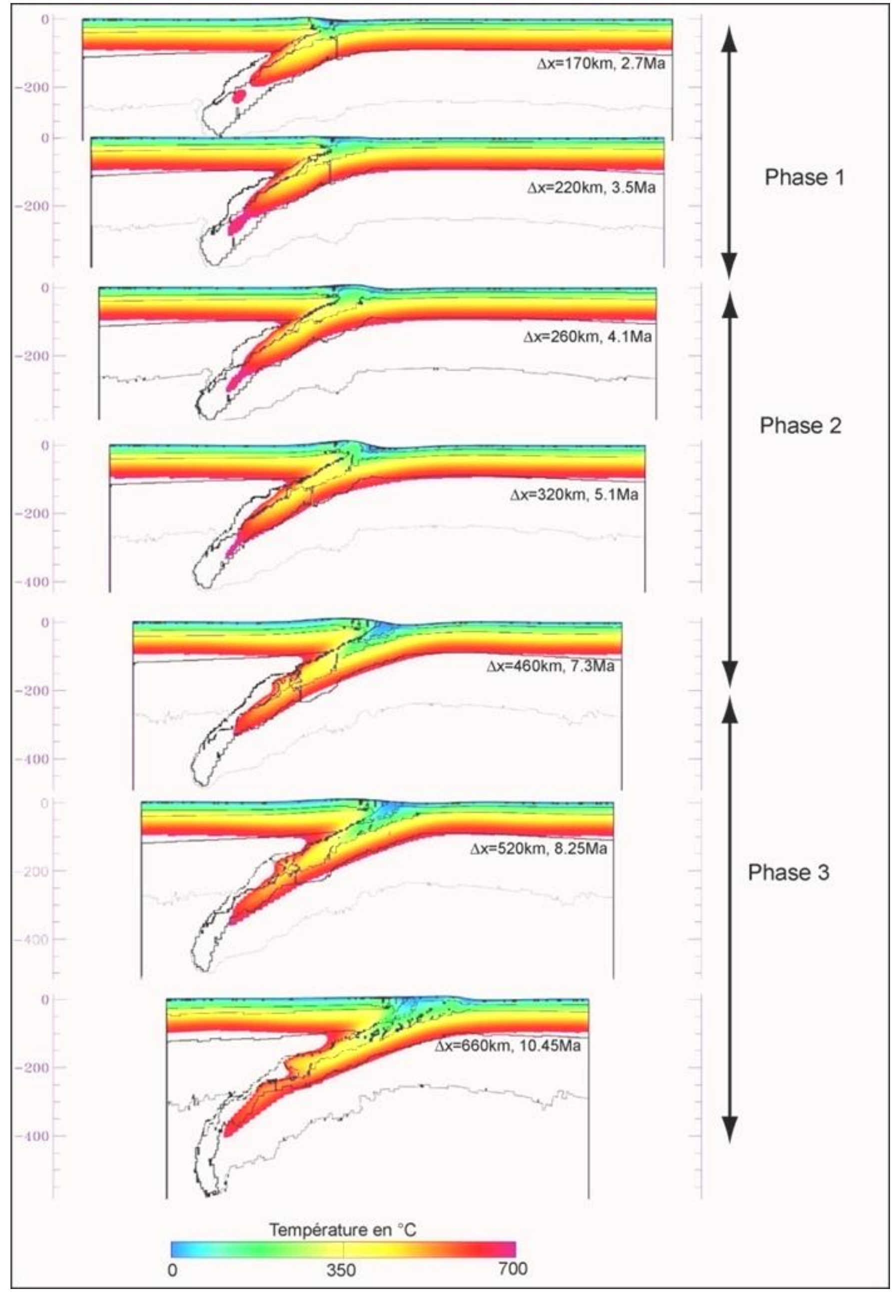

Phase 1 (dx= 0-220km): deformation at suture

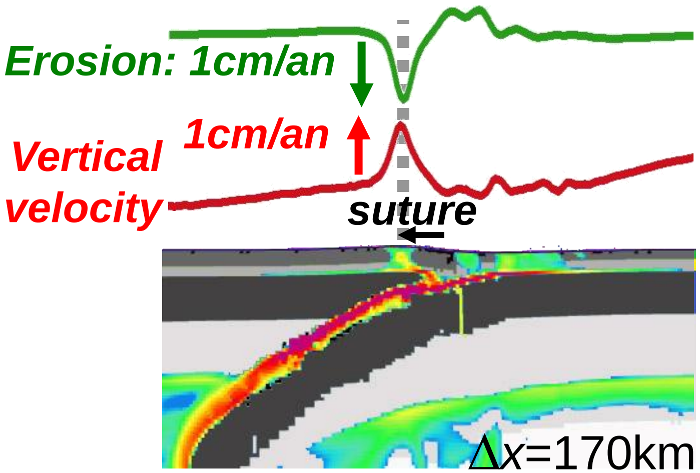

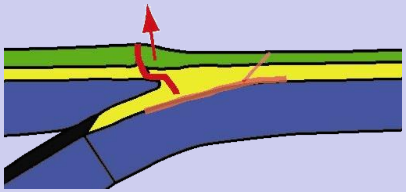

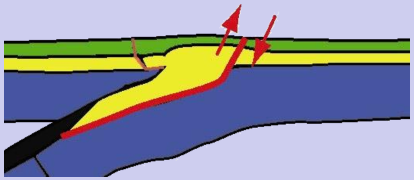

Lower crustal prism

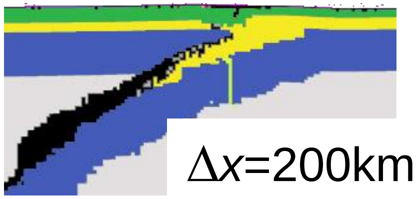

Transitory regime…

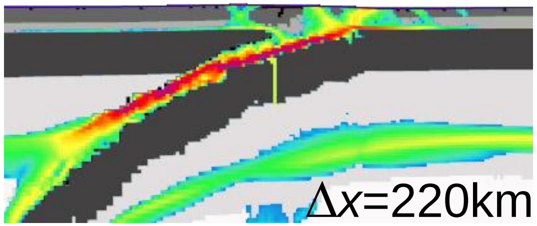

Phase 2: Majour thrust fault activity

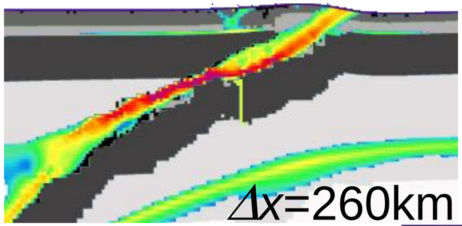

All deformation is concentrated on a single thrust during 250km of shortening

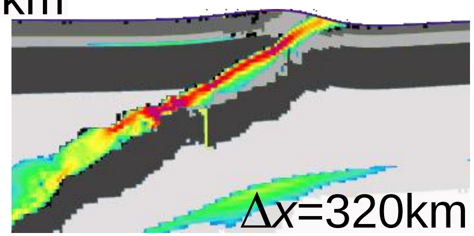

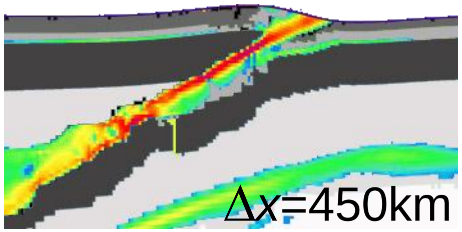

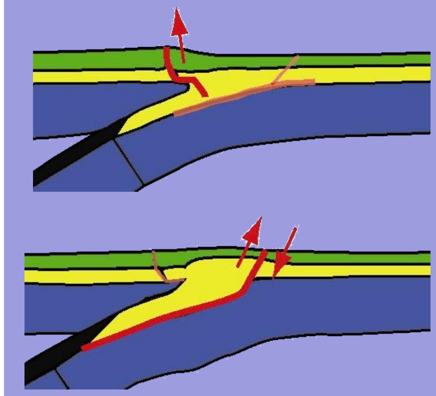

erosion

vertical vel.

horizontal vel.

topography

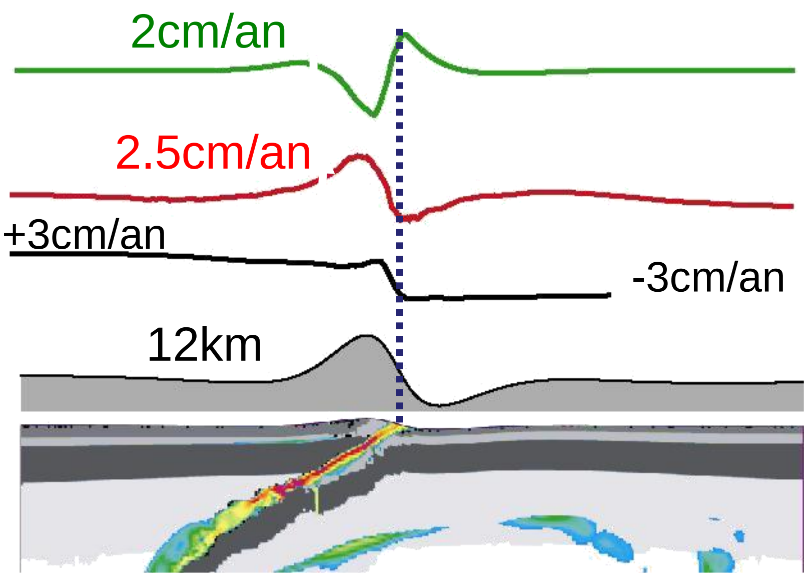

It controlls all surface deformation

Phase 3: accretion of a large crustal prism

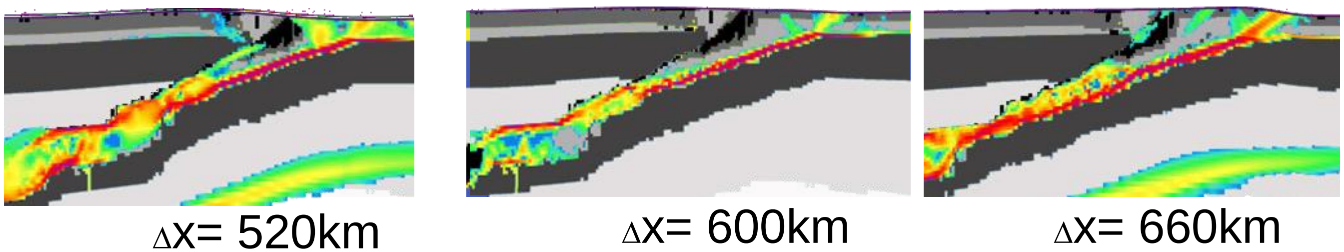

Successions of frontal thrusts towards South

→ Formation of an assymetric chain above the prism

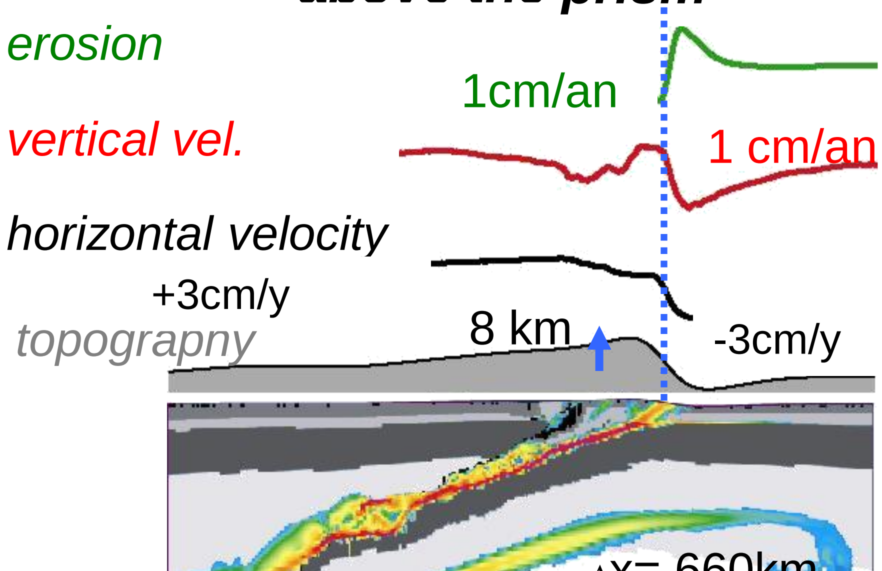

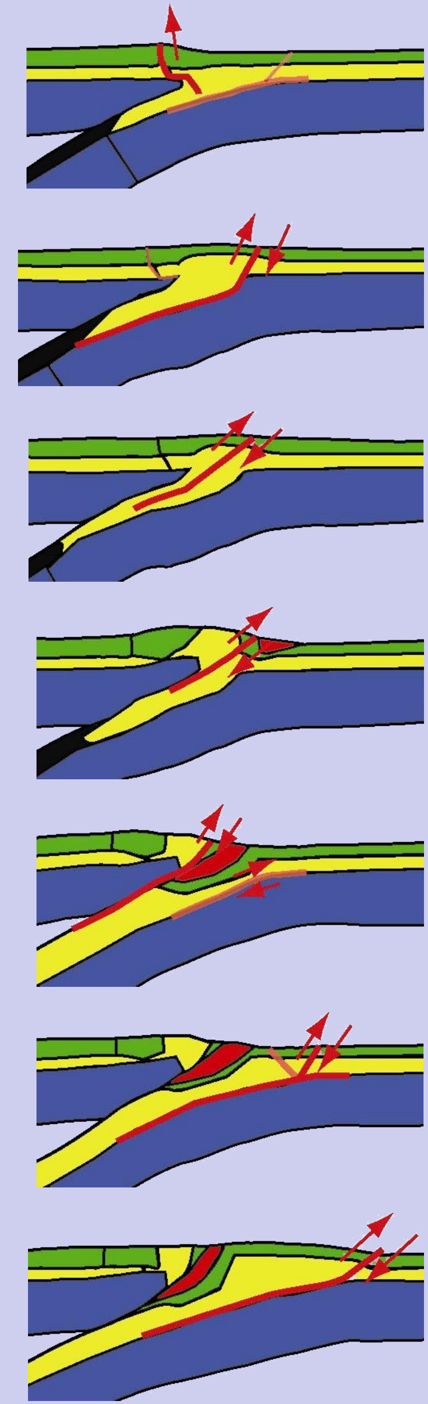

Δx from 220 to

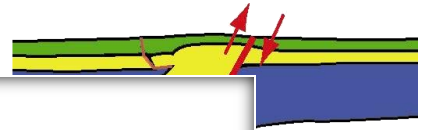

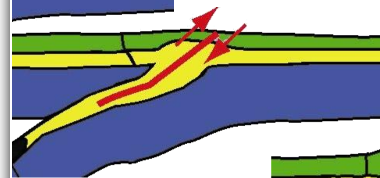

from Δx = 0 to 220km = Himalaya between 50 and 30Ma?

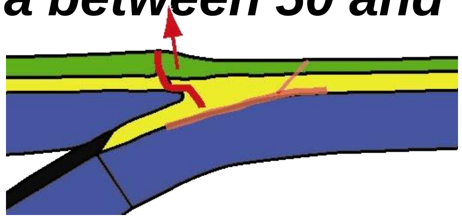

•Deformation (backthrusting at suture)

Major Thrust = MCT ?

lower crustal exhumation

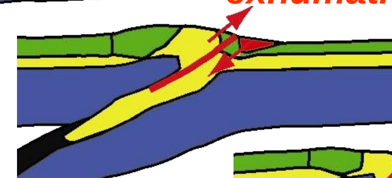

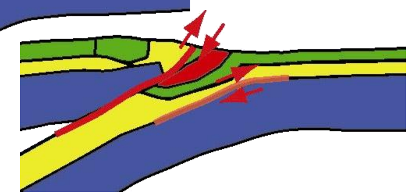

e North of

e Southern

ement STD ?

Δx=660km = Actual Himalaya ?

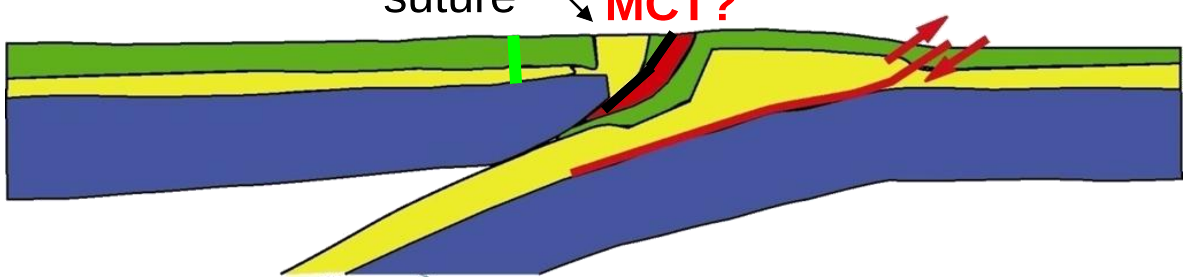

- ***large prism developped at South of suture***
- ***comparable size of the crustal prism***
- ***deformation localized along the Frontal Thrust***

5. End-member case:

Slow convergence (Alpes)

Slow Alpine Collision:

Oceanic phase

PhD thesis of Ph. Yamato;
Yamato et al., 2007

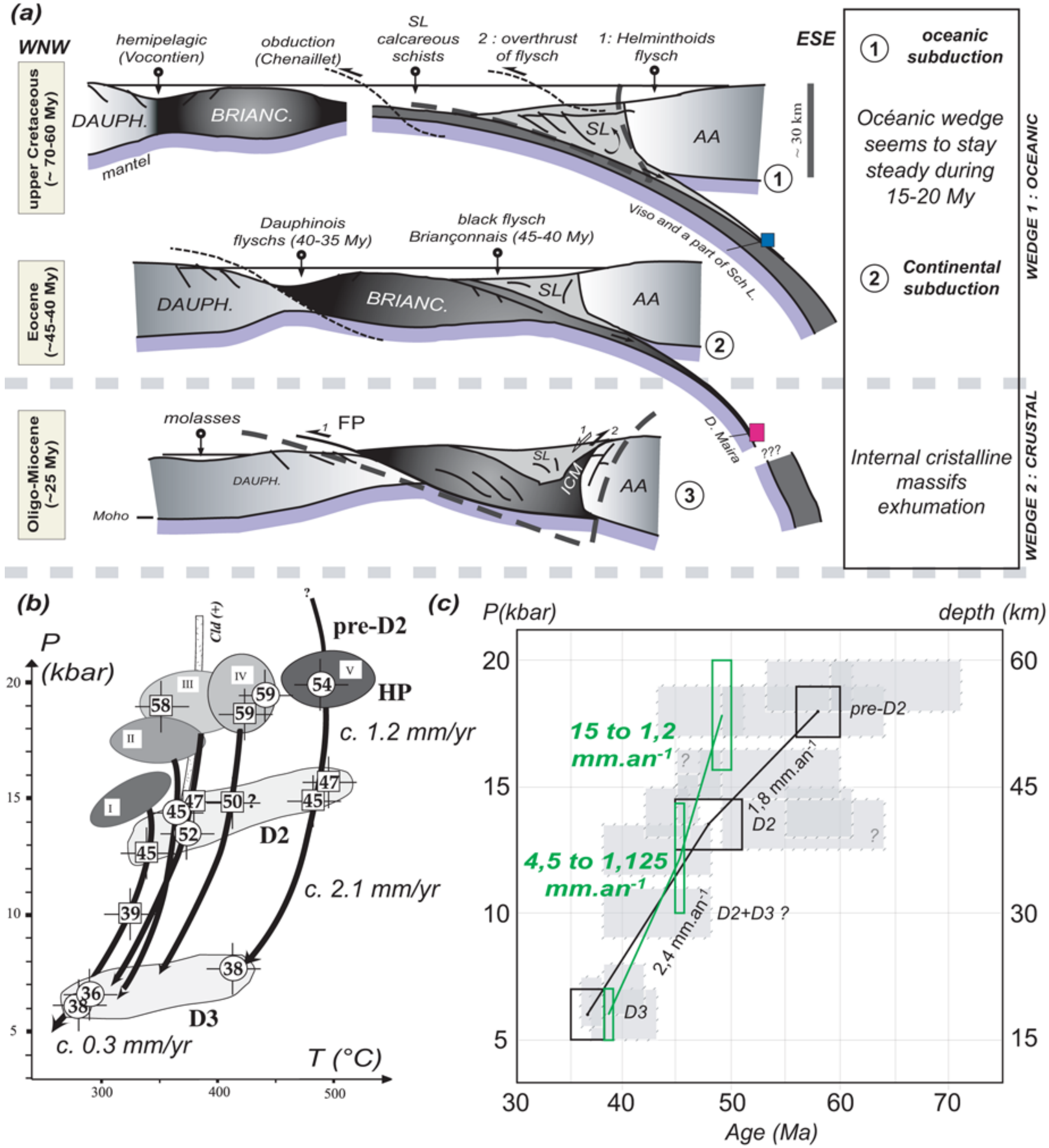

(a)
WNW
ESE
hemipelagic (Vocontien)
obduction (Chenaillet)
SL calcareous schists
2 : overthrust of flysch
1: Helminthoids flysch
upper Cretaceous (~ 70-60 My)
DAUPH.
BRIANC.
mantel
SL
AA
~ 30 km
Viso and a part of Sch L.
Dauphinois flyschs (40-35 My)
black flysch Briançonnais (45-40 My)
Eocene (~45-40 My)
Oligo-Miocene (~25 My)
molasses
FP
ICM
Moho
D. Maira
???
oceanic subduction
Océanic wedge seems to stay steady during 15-20 My
Continental subduction
Internal cristalline massifs exhumation
WEDGE 1 : OCEANIC
WEDGE 2 : CRUSTAL
(b)
P (kbar)
T (°C)
Cld (+)
pre-D2
HP
c. 1.2 mm/yr
D2
c. 2.1 mm/yr
D3
c. 0.3 mm/yr
(c)
P(kbar)
depth (km)
Age (Ma)
pre-D2
D2
D2+D3 ?
D3
15 to 1,2 mm.an-1
4,5 to 1,125 mm.an-1
1,8 mm.an-1
2,4 mm.an-1

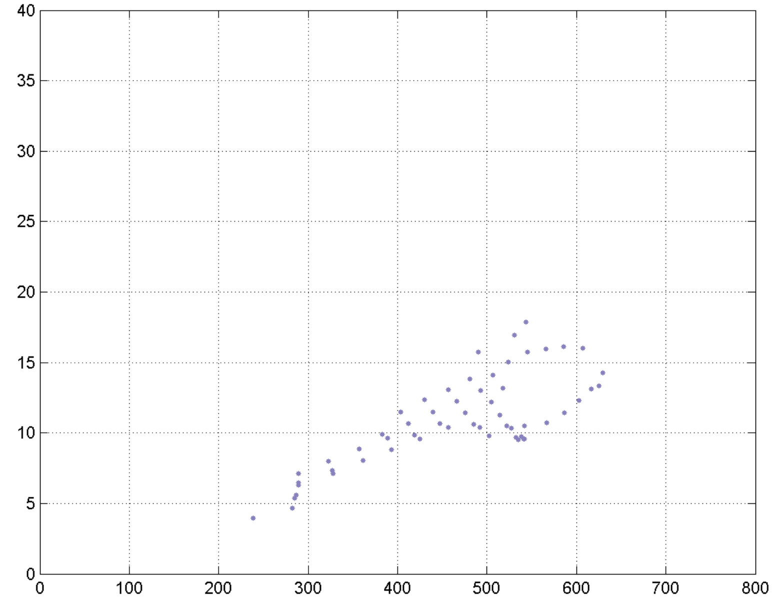

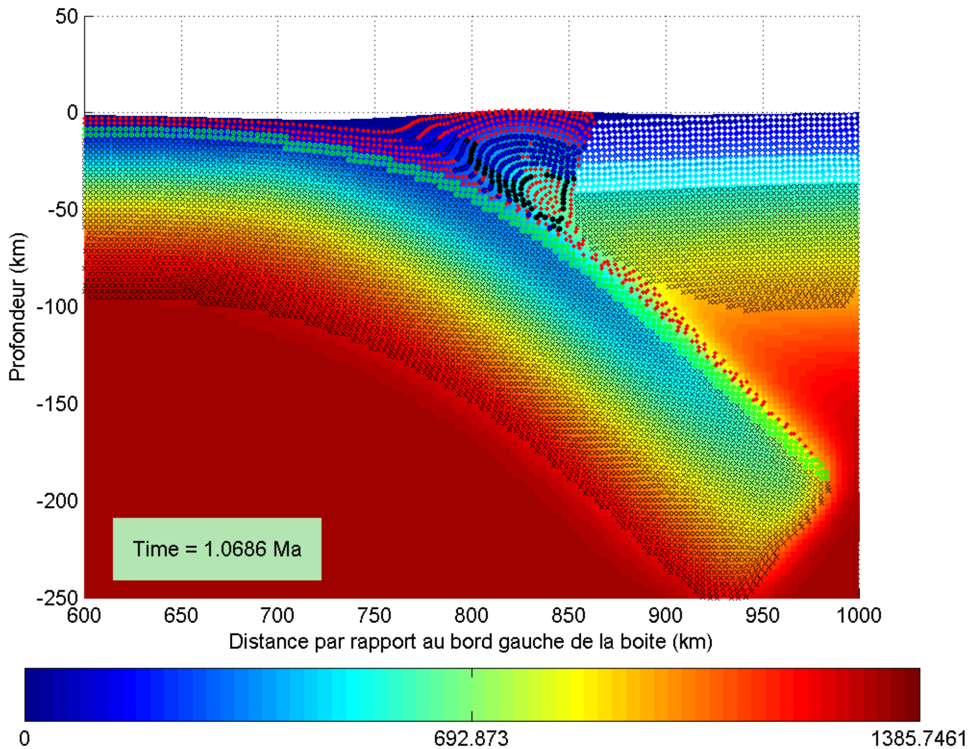

wait …

PhD thesis of Ph. Yamato;
Yamato et al., 2007
Burov and Yamato, 2007

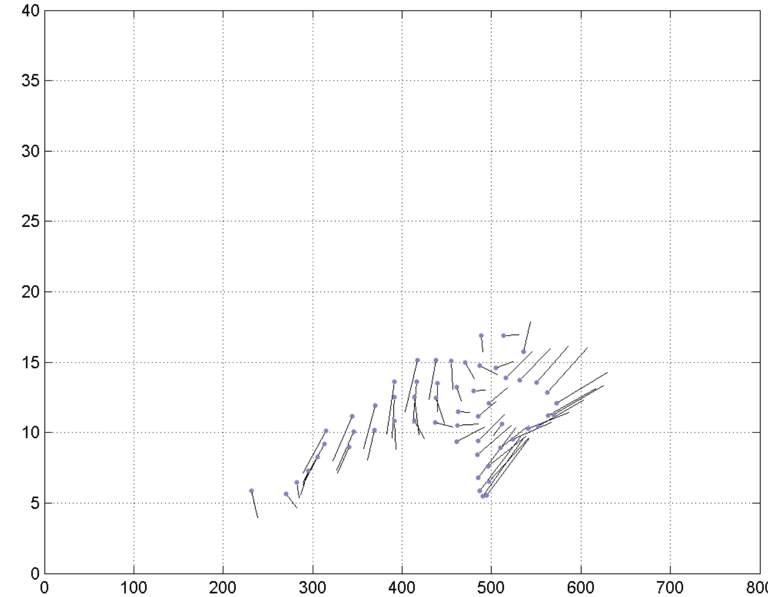

40
35
30
25
20
15
10
5
0
0
100
200
300
400
500
600
700
800

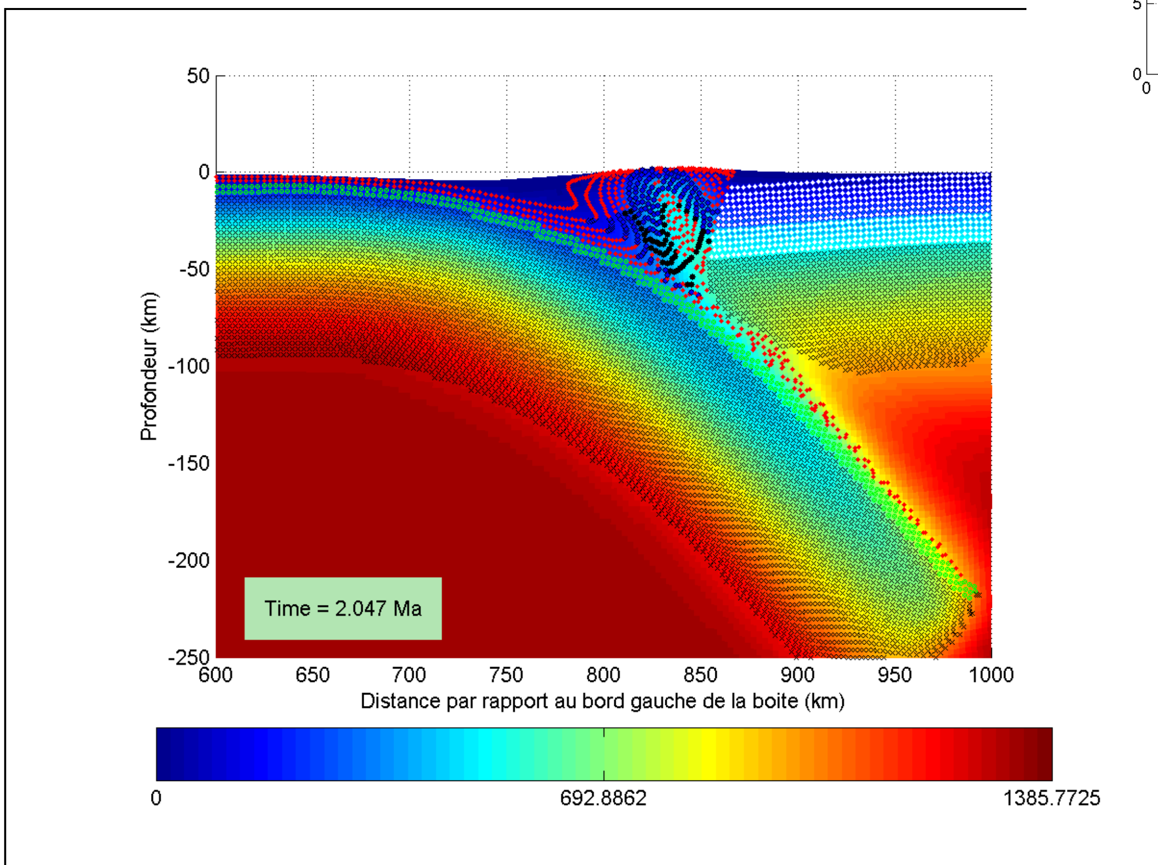

50
0
-50
-100
-150
-200
-250
Profondeur (km)
600
650
700
750
800
850
900
950
1000
Distance par rapport au bord gauche de la boite (km)
Time = 2.047 Ma
0
692.8862
1385.7725

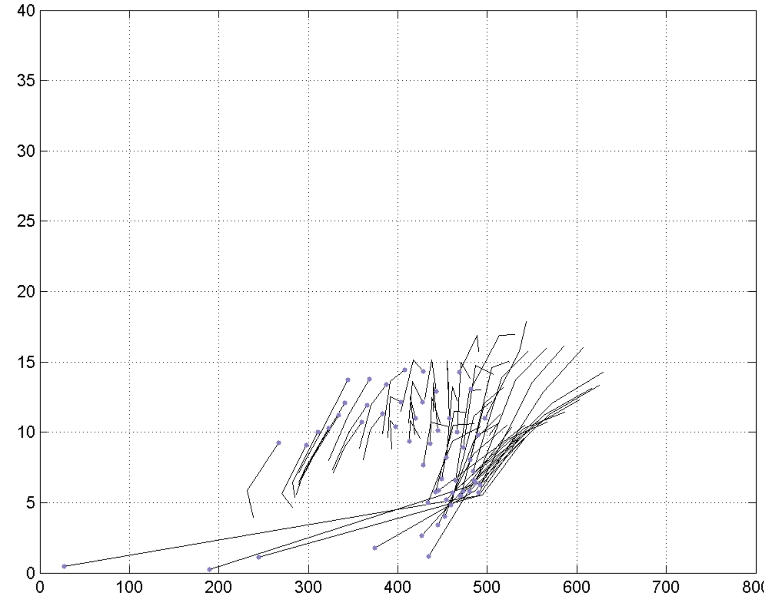
40
35
30
25
20
15
10
5
0
0
100
200
300
400
500
600
700
800

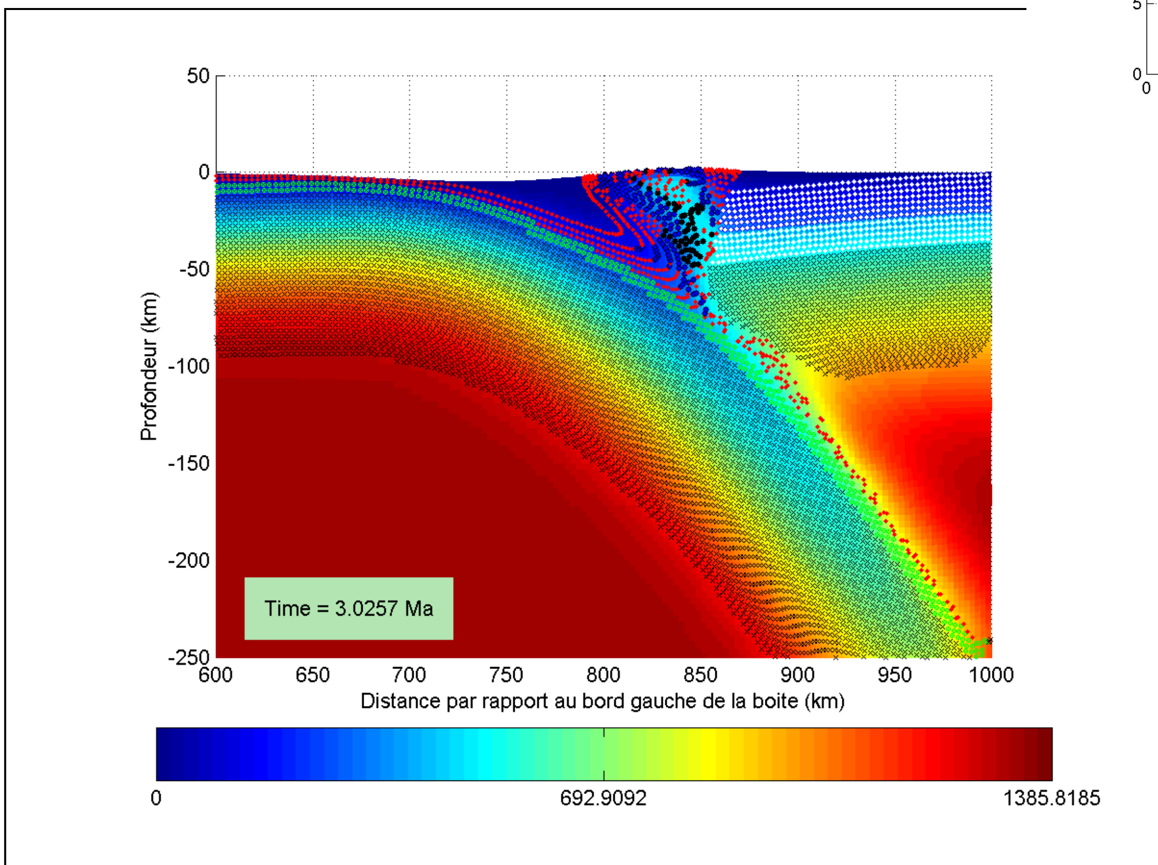
50
0
-50
-100
-150
-200
-250
Profondeur (km)
600
650
700
750
800
850
900
950
1000
Distance par rapport au bord gauche de la boite (km)
Time = 3.0257 Ma
0
692.9092
1385.8185

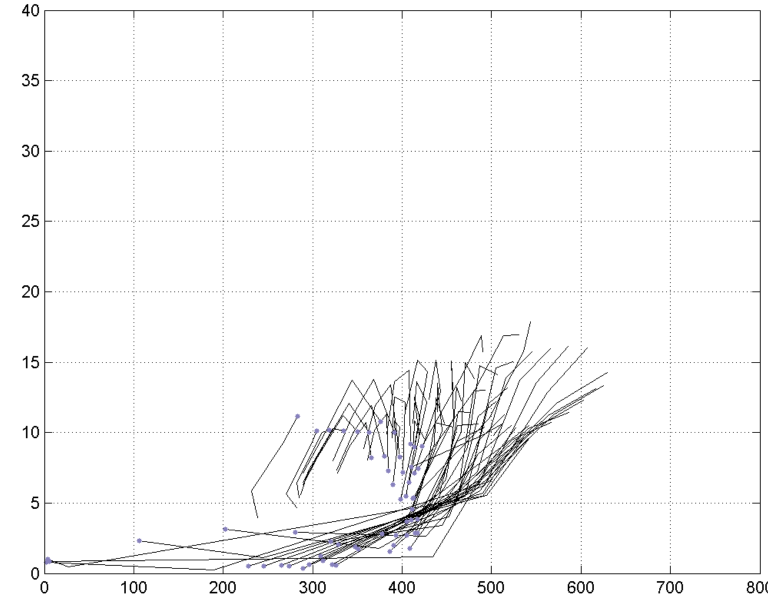
0
5
10
15
20
25
30
35
40
0
100
200
300
400
500
600
700
800

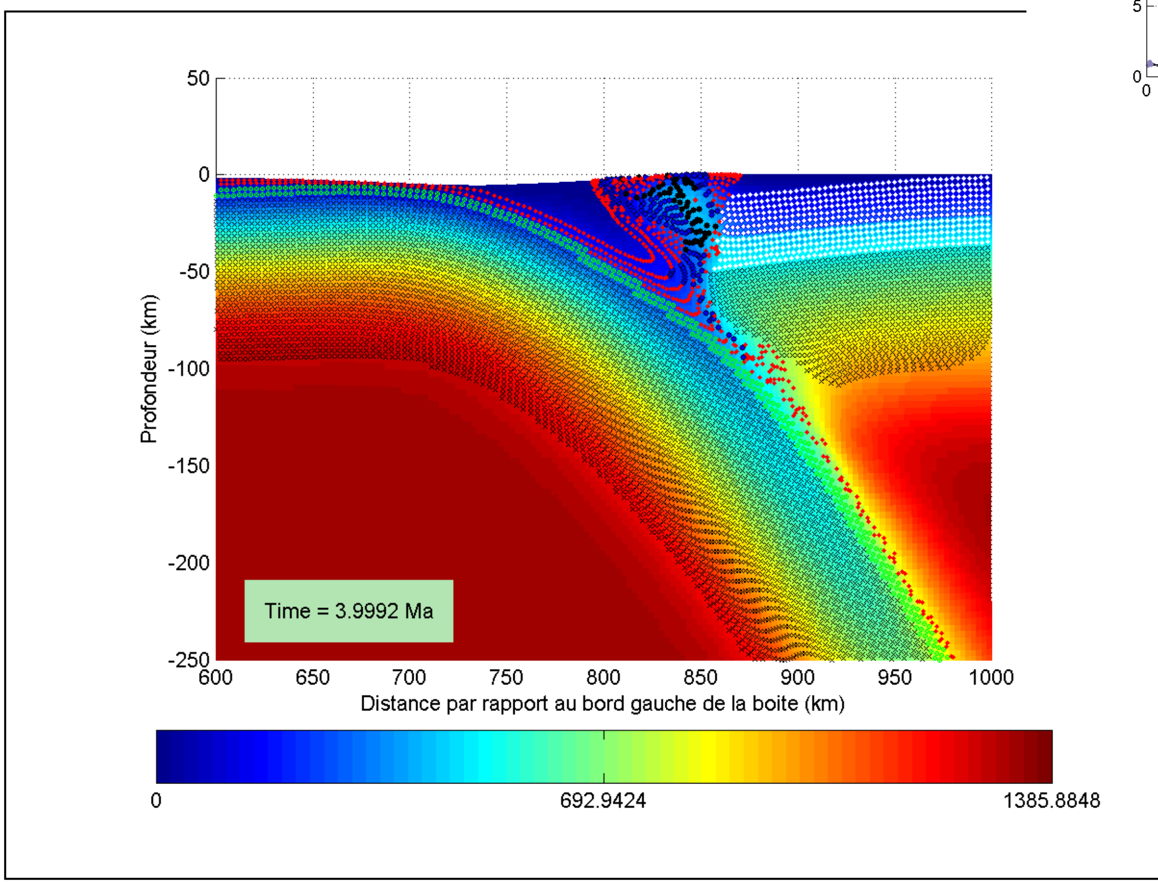
50
0
-50
-100
-150
-200
-250
Profondeur (km)
Time = 3.9992 Ma
600
650
700
750
800
850
900
950
1000
Distance par rapport au bord gauche de la boite (km)
0
692.9424
1385.8848

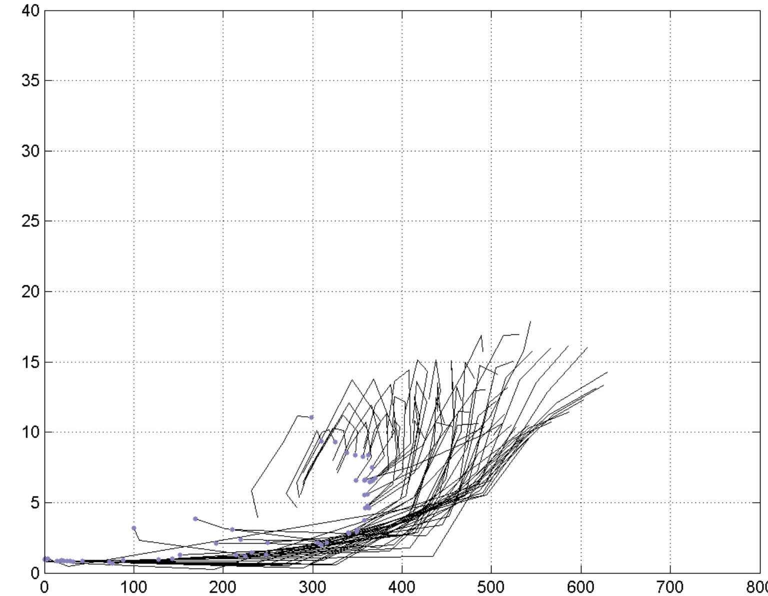

40
35
30
25
20
15
10
5
0
0
100
200
300
400
500
600
700
800

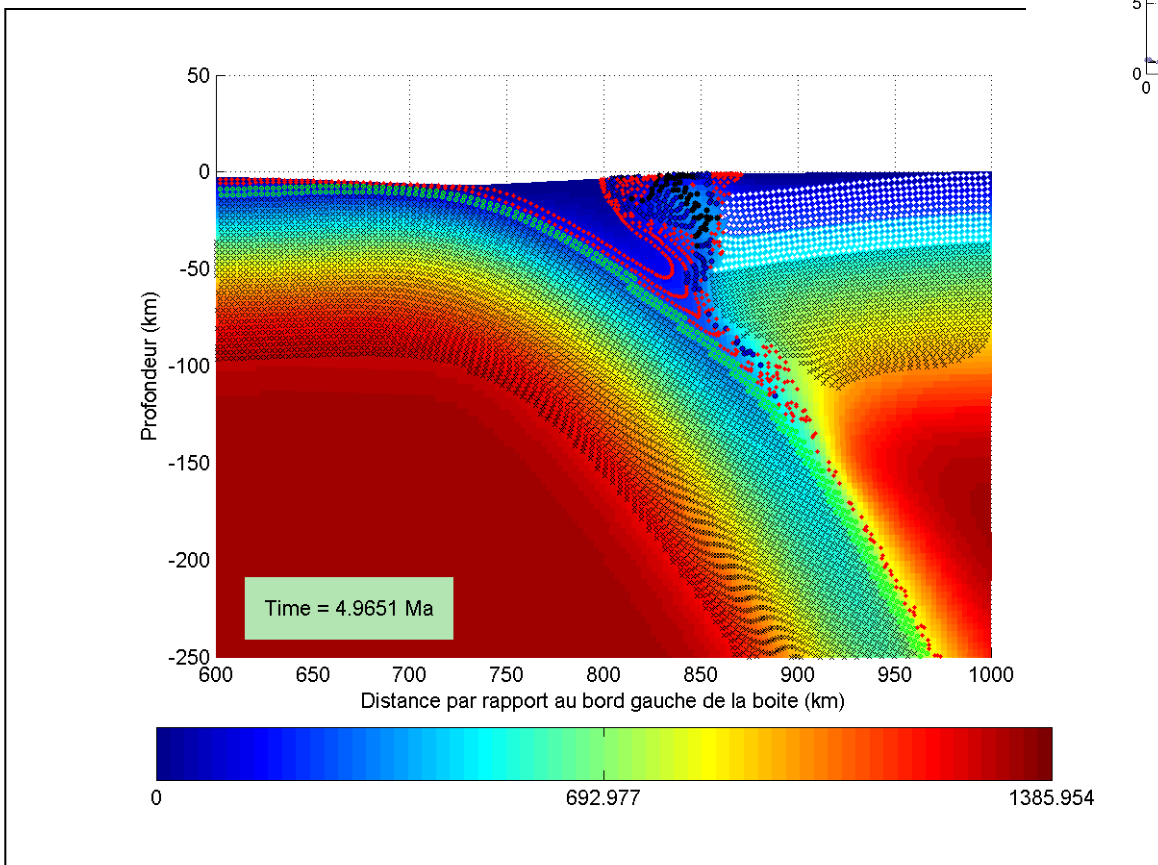

Profondeur (km)
50
0
-50
-100
-150
-200
-250
600
650
700
750
800
850
900
950
1000
Distance par rapport au bord gauche de la boite (km)
Time = 4.9651 Ma
0
692.977
1385.954

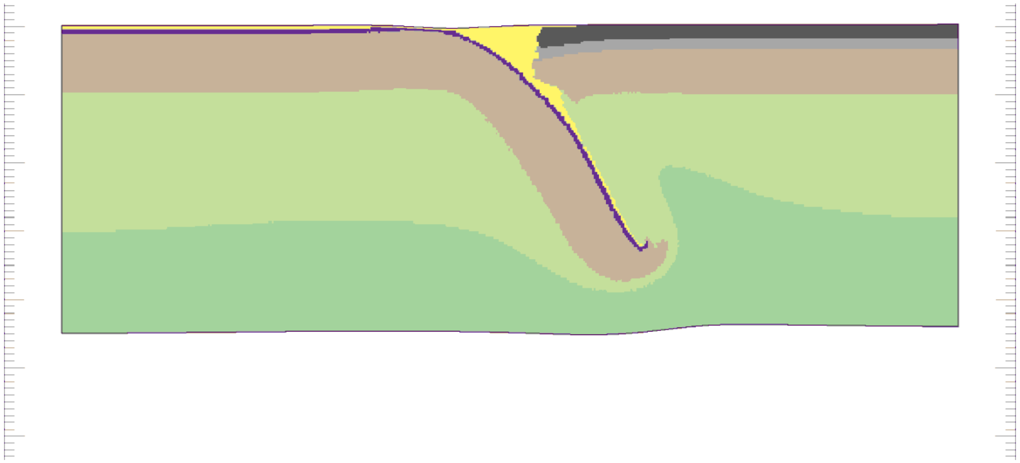

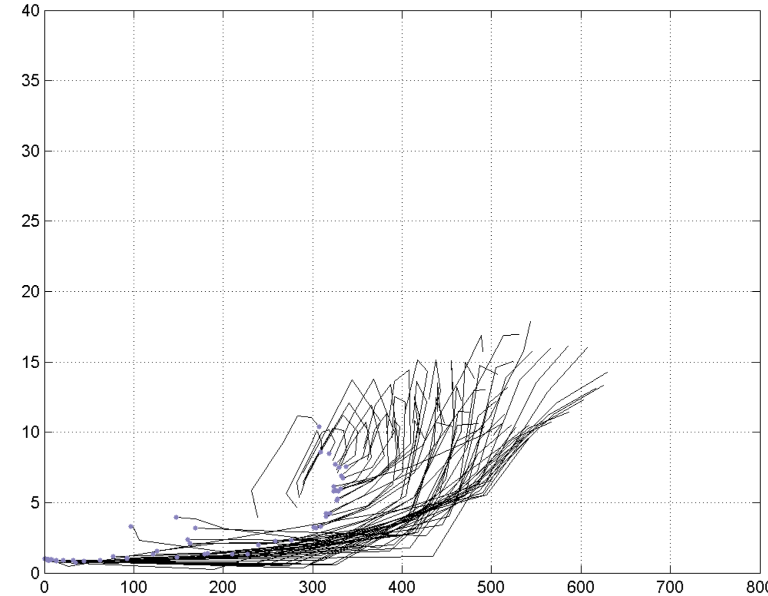

0
5
10
15
20
25
30
35
40
0 100 200 300 400 500 600 700 800

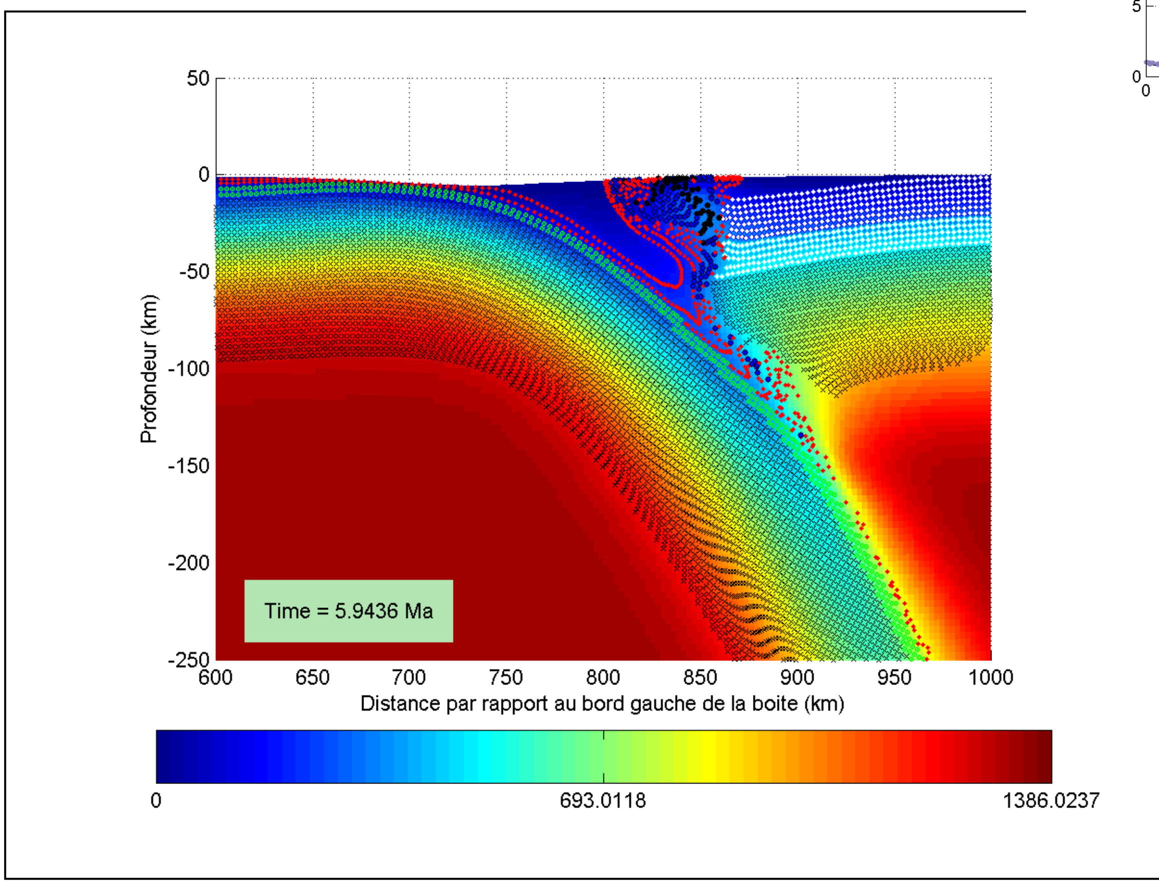

Profondeur (km)
50
0
-50
-100
-150
-200
-250
600 650 700 750 800 850 900 950 1000
Distance par rapport au bord gauche de la boite (km)
Time = 5.9436 Ma
0
693.0118
1386.0237

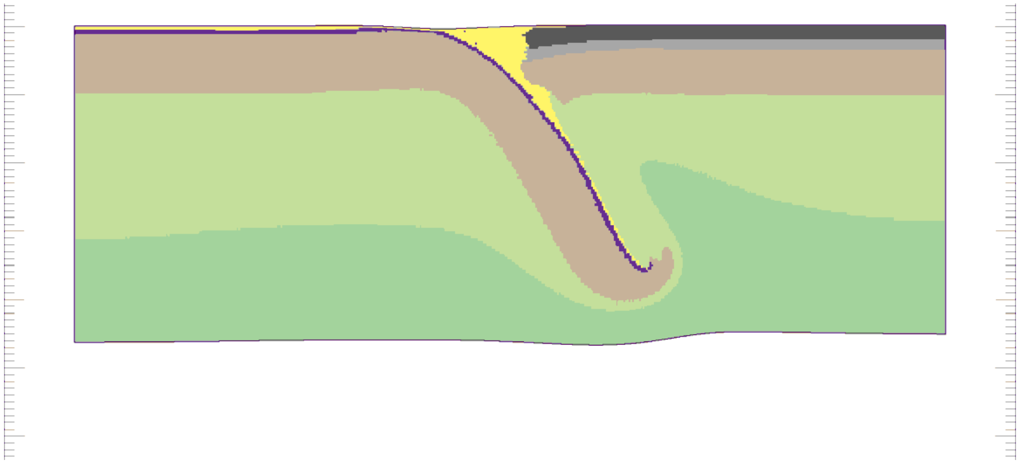

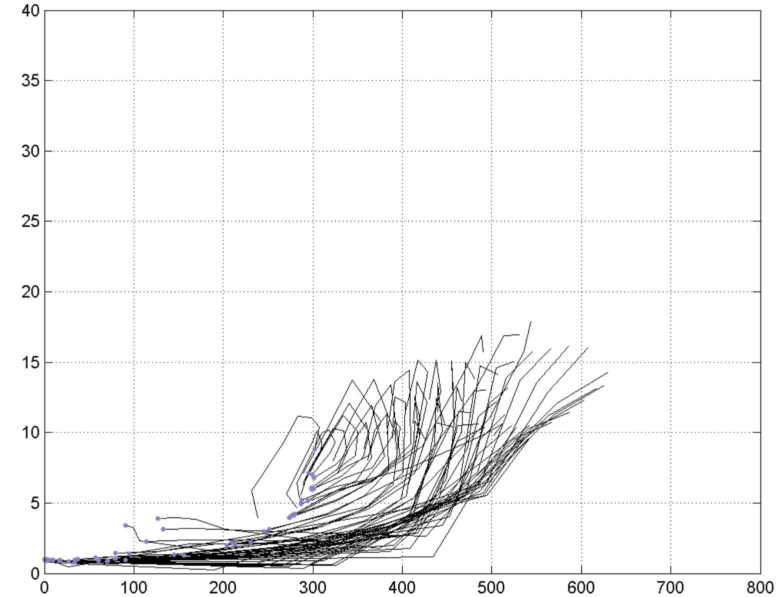

40
35
30
25
20
15
10
5
0
0
100
200
300
400
500
600
700
800

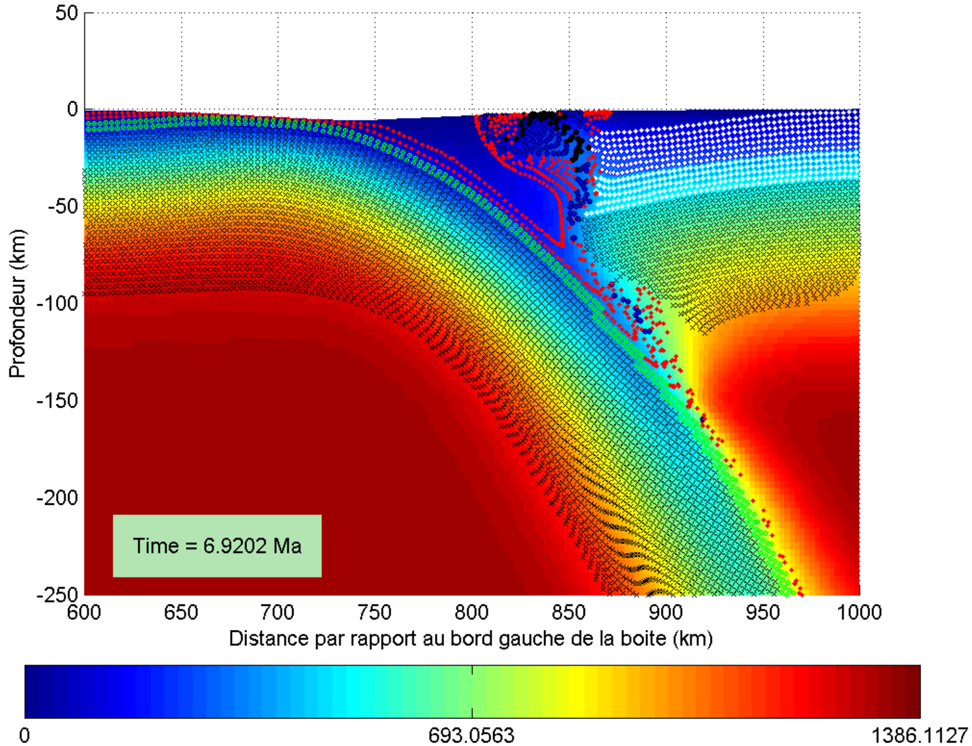

50
0
-50
-100
-150
-200
-250
Profondeur (km)
Time = 6.9202 Ma
600
650
700
750
800
850
900
950
1000
Distance par rapport au bord gauche de la boite (km)
0
693.0563
1386.1127

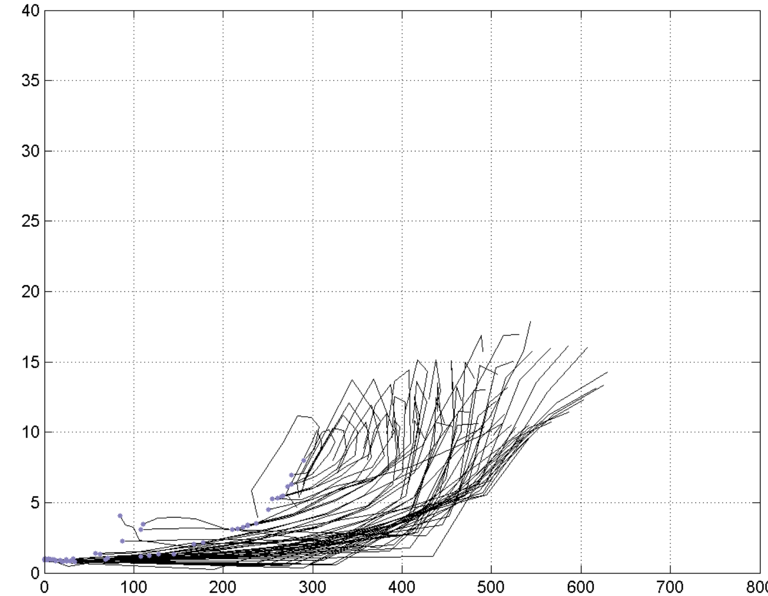

40
35
30
25
20
15
10
5
0
0
100
200
300
400
500
600
700
800

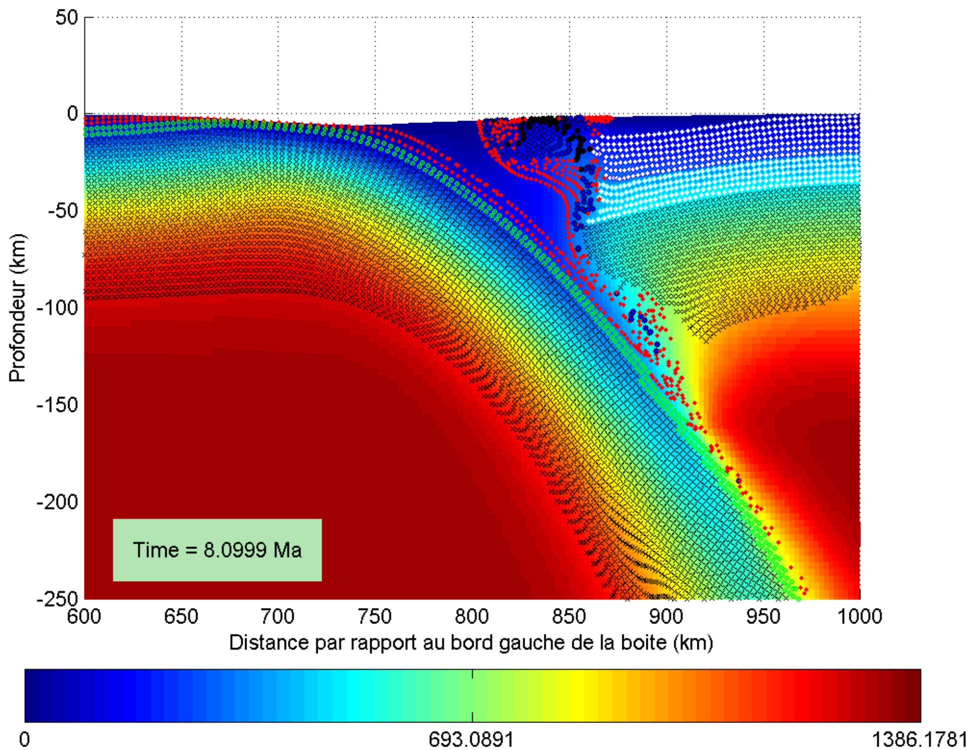

Profondeur (km)
50
0
-50
-100
-150
-200
-250
600
650
700
750
800
850
900
950
1000
Distance par rapport au bord gauche de la boite (km)
Time = 8.0999 Ma
0
693.0891
1386.1781

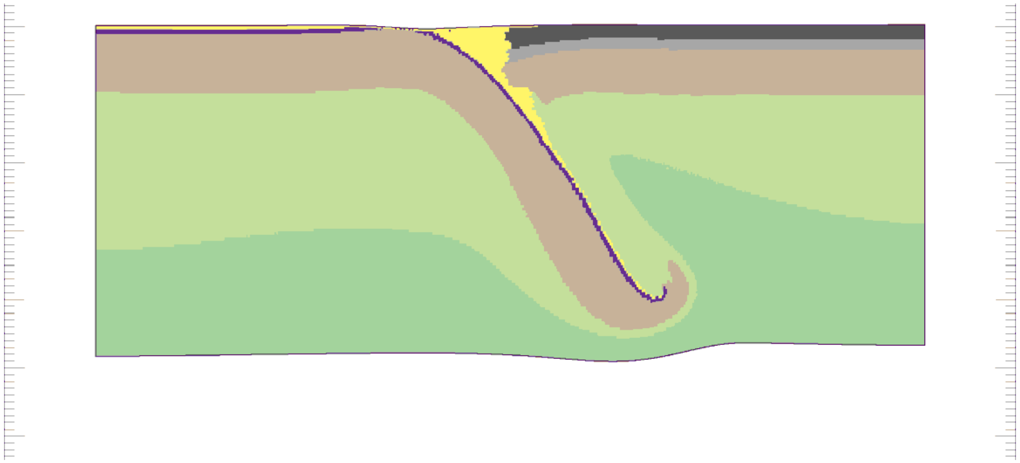

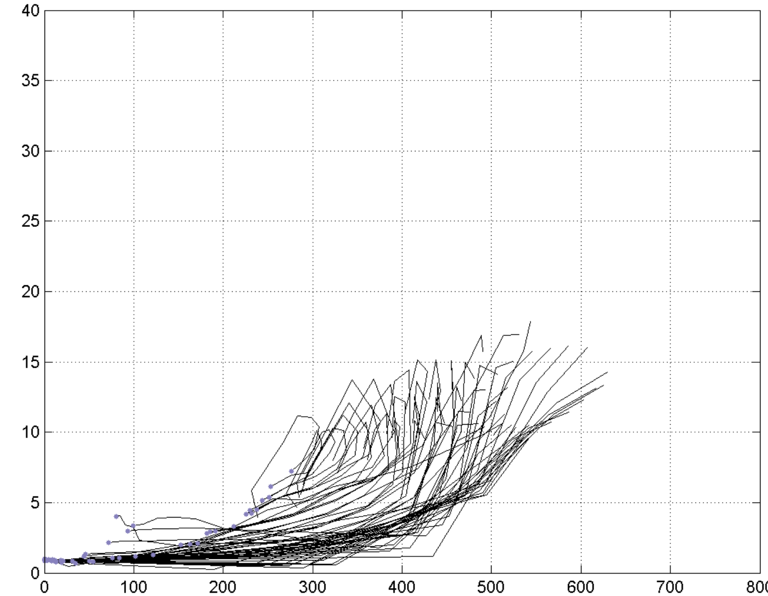

40
35
30
25
20
15
10
5
0
0
100
200
300
400
500
600
700
800

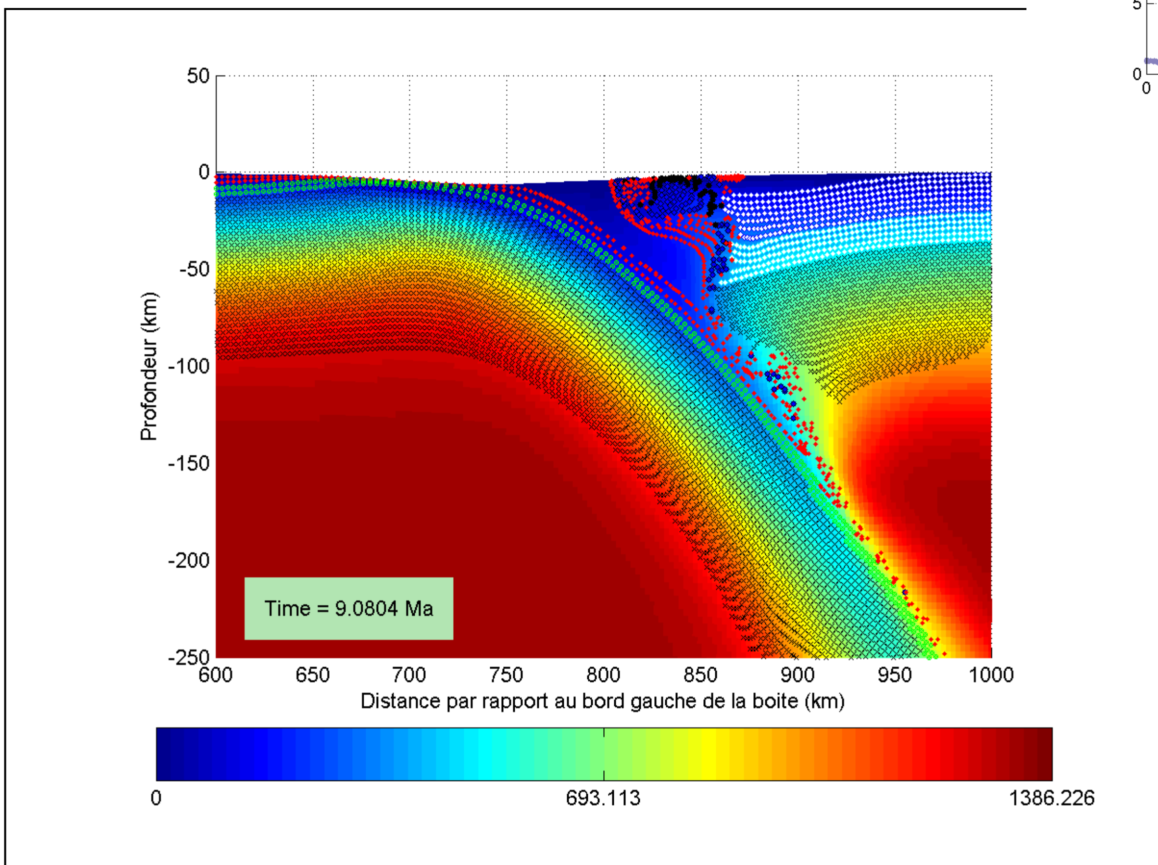

50
0
-50
-100
-150
-200
-250
Profondeur (km)
600
650
700
750
800
850
900
950
1000
Distance par rapport au bord gauche de la boite (km)
Time = 9.0804 Ma
0
693.113
1386.226

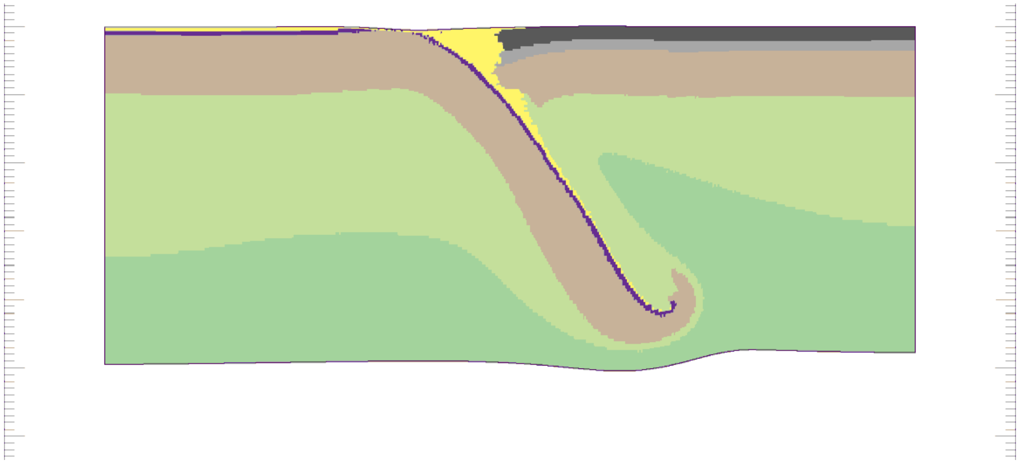

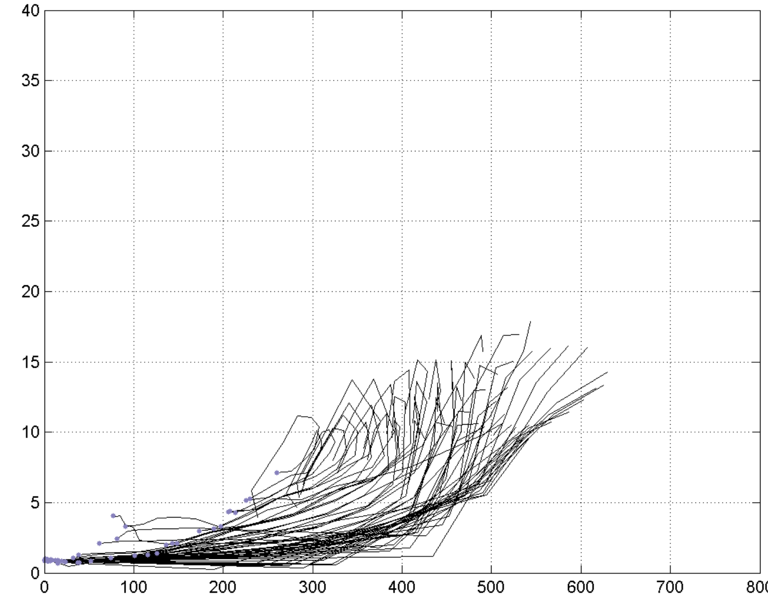

0
5
10
15
20
25
30
35
40
0 100 200 300 400 500 600 700 800

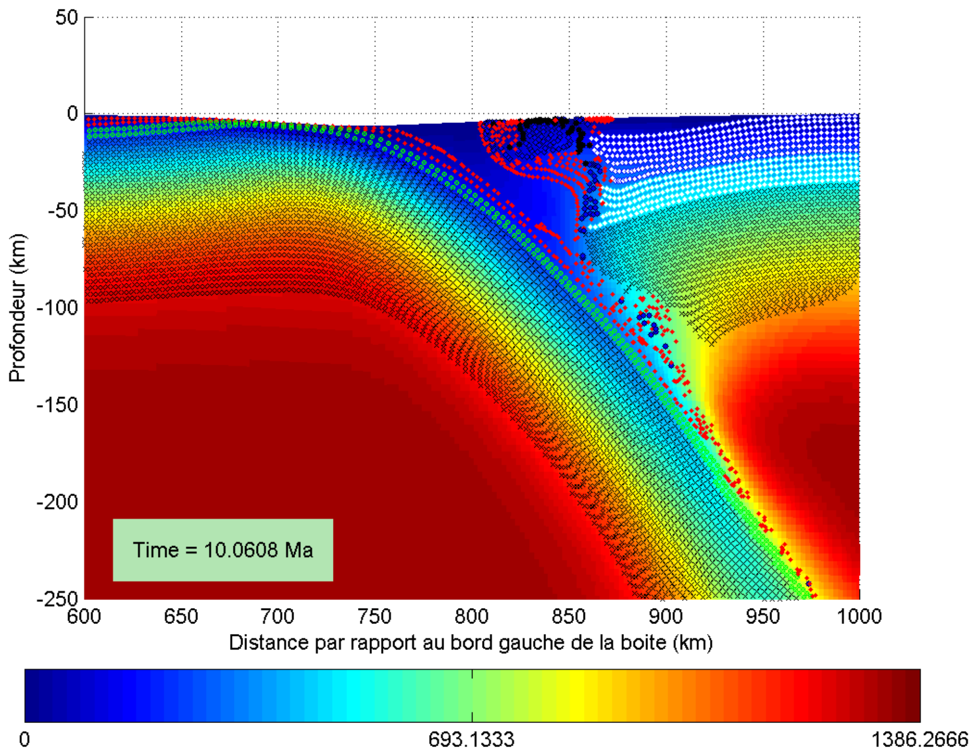

Profondeur (km)
50
0
-50
-100
-150
-200
-250
600 650 700 750 800 850 900 950 1000
Distance par rapport au bord gauche de la boite (km)
Time = 10.0608 Ma
0
693.1333
1386.2666

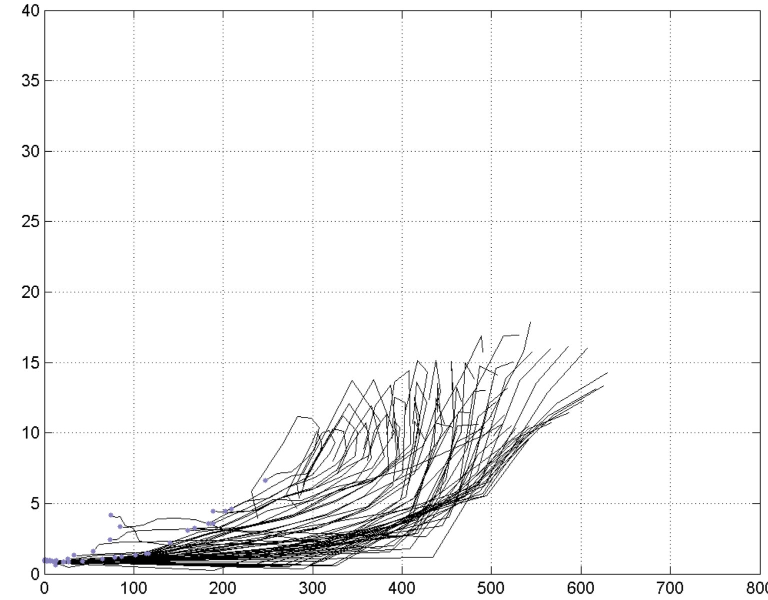

40
35
30
25
20
15
10
5
0
0
100
200
300
400
500
600
700
800

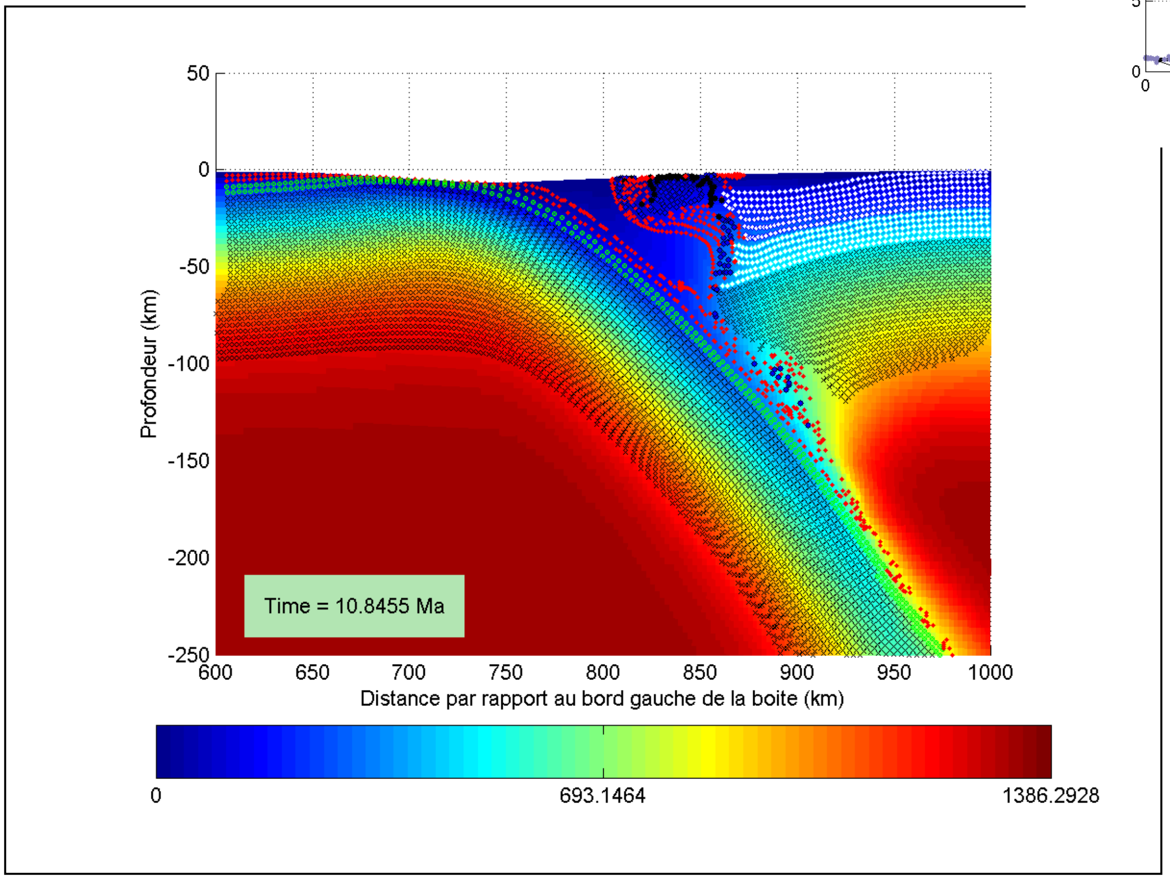

Profondeur (km)
50
0
-50
-100
-150
-200
-250
600
650
700
750
800
850
900
950
1000
Distance par rapport au bord gauche de la boite (km)
Time = 10.8455 Ma
0
693.1464
1386.2928

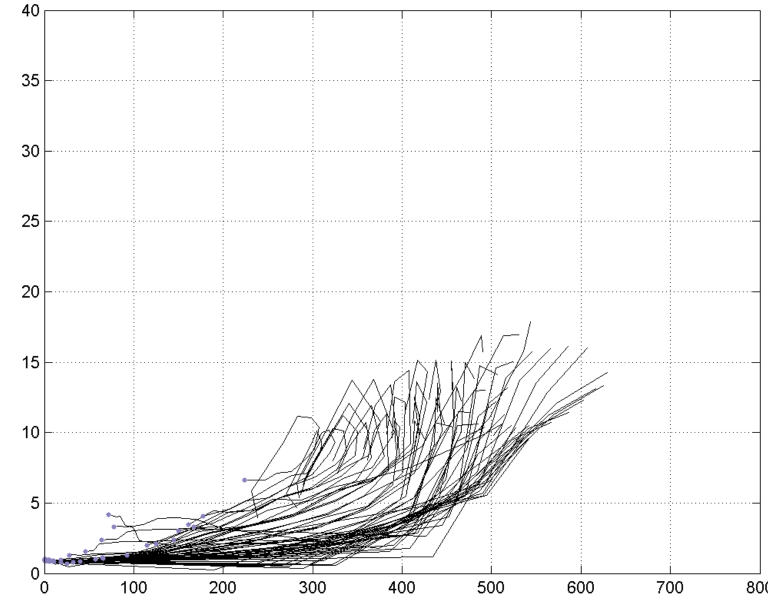

40
35
30
25
20
15
10
5
0
0
100
200
300
400
500
600
700
800

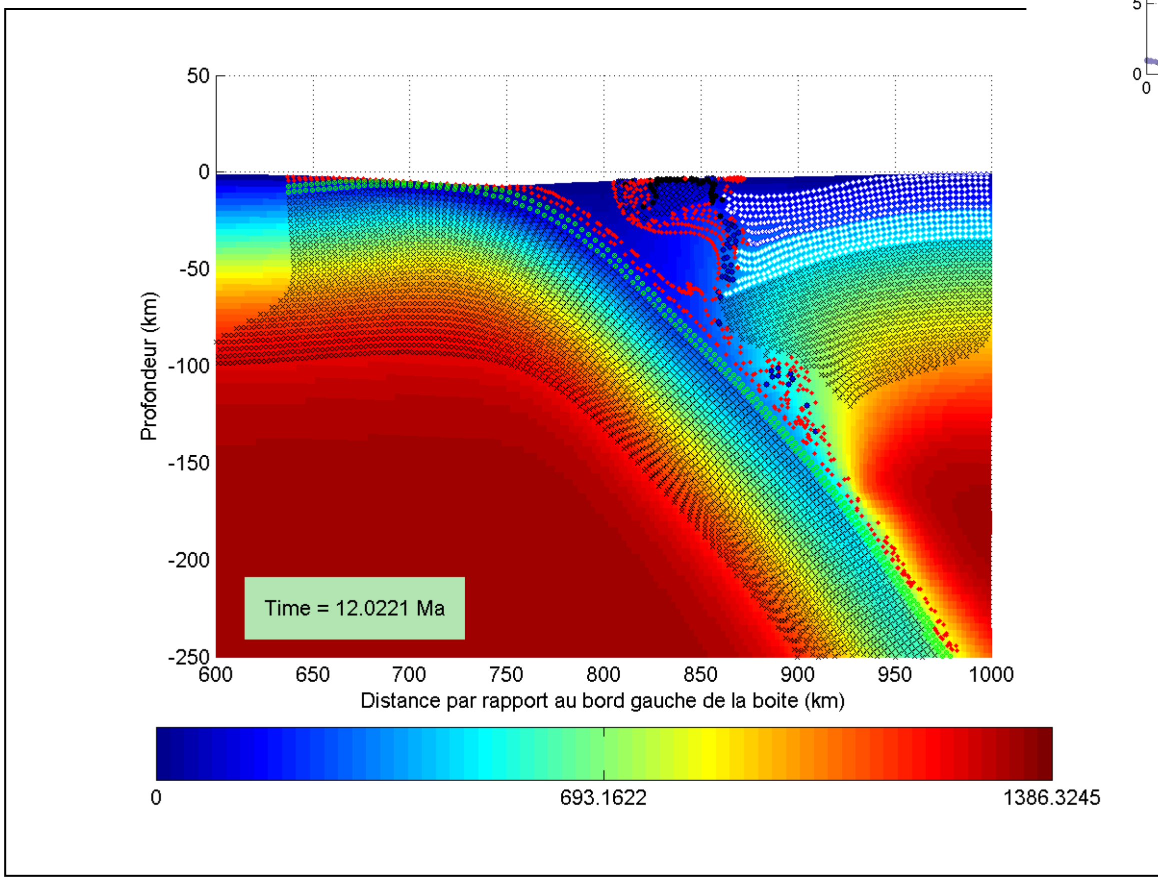

50
0
-50
-100
-150
-200
-250
Profondeur (km)
Time = 12.0221 Ma
600
650
700
750
800
850
900
950
1000
Distance par rapport au bord gauche de la boite (km)
0
693.1622
1386.3245

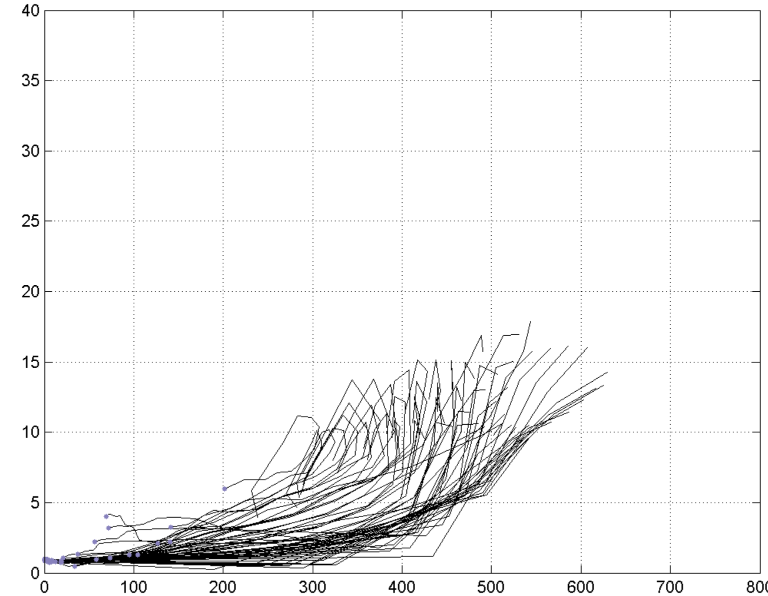

40
35
30
25
20
15
10
5
0
0
100
200
300
400
500
600
700
800

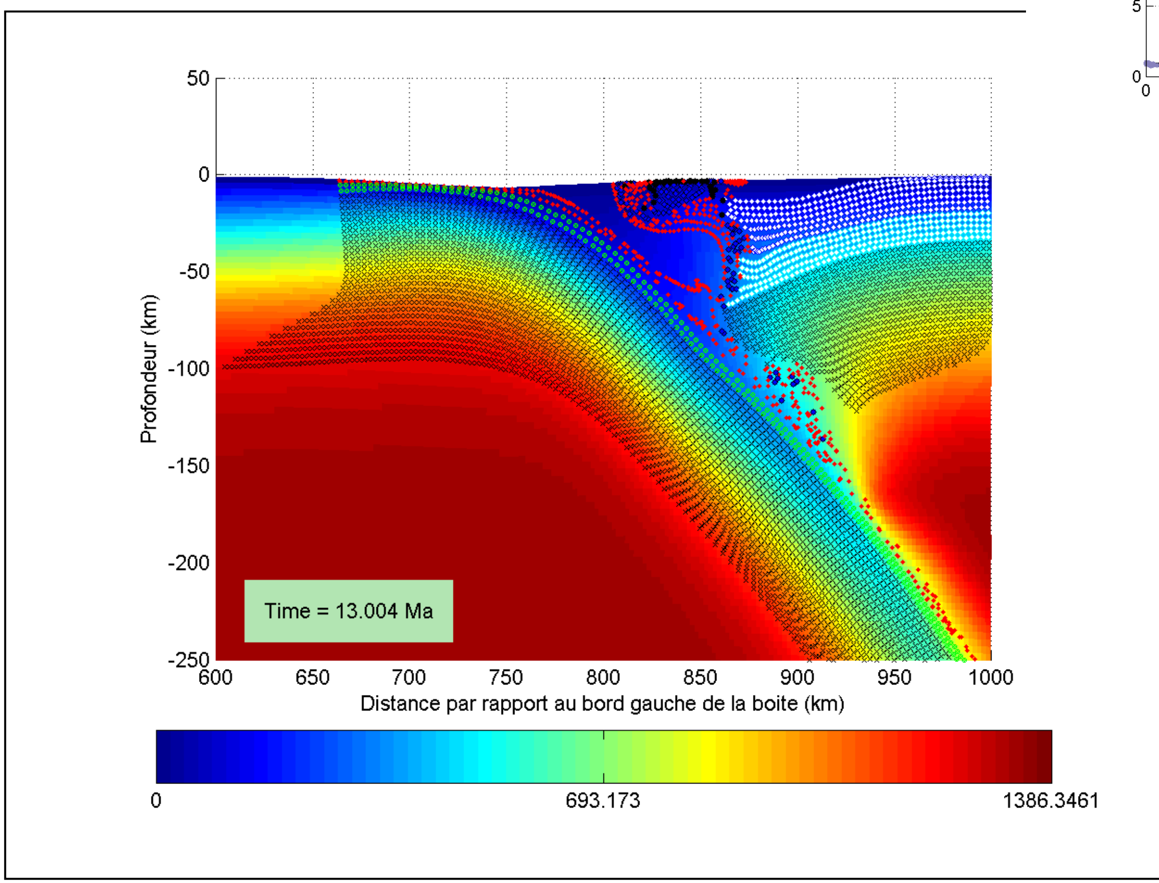

50
0
-50
-100
-150
-200
-250
Profondeur (km)
Time = 13.004 Ma
600
650
700
750
800
850
900
950
1000
Distance par rapport au bord gauche de la boite (km)
0
693.173
1386.3461

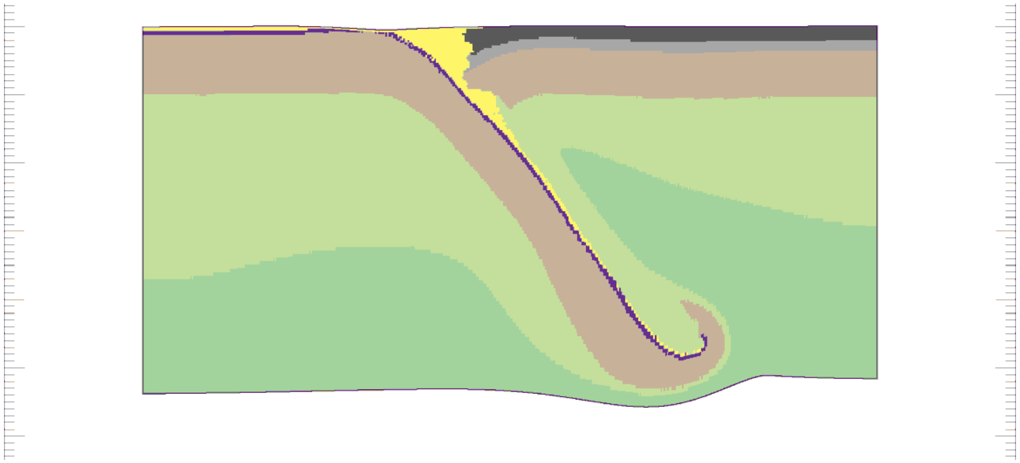

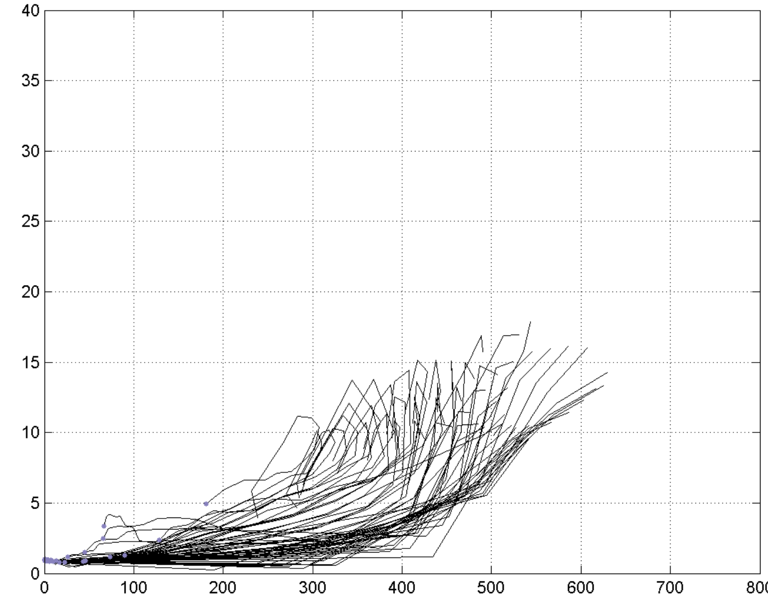

40
35
30
25
20
15
10
5
0
0
100
200
300
400
500
600
700
800

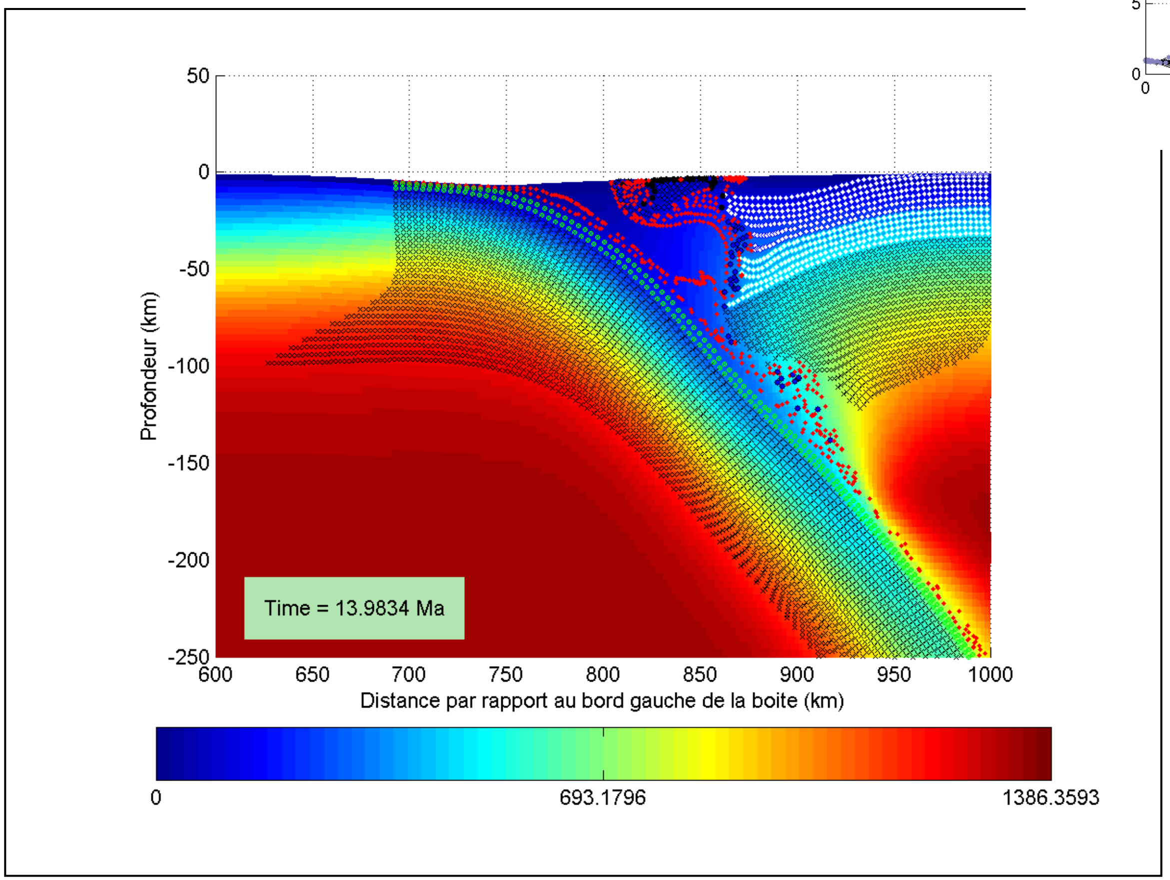

50
0
-50
-100
-150
-200
-250
Profondeur (km)
600
650
700
750
800
850
900
950
1000
Distance par rapport au bord gauche de la boite (km)
Time = 13.9834 Ma
0
693.1796
1386.3593

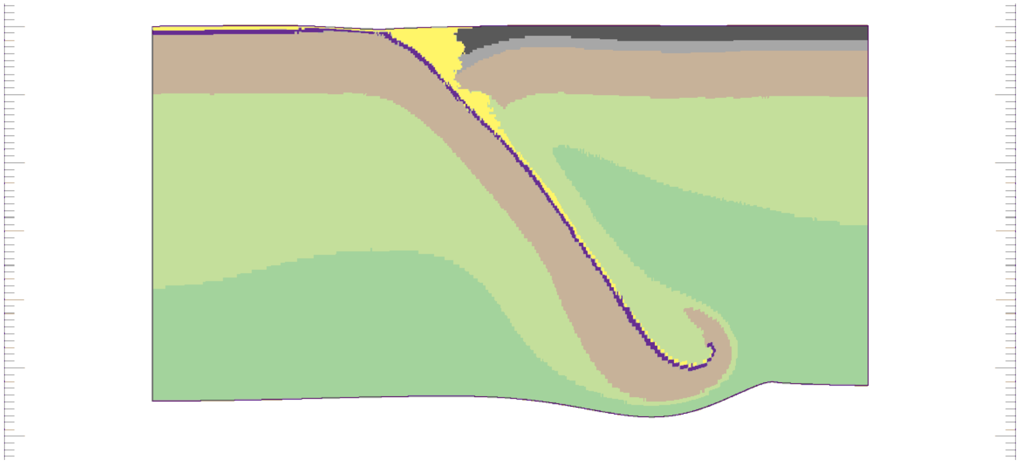

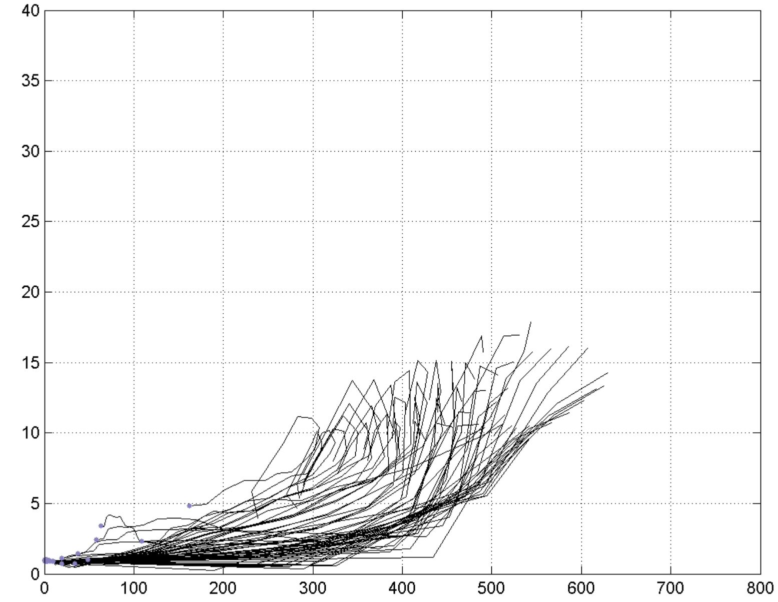

40
35
30
25
20
15
10
5
0
0 100 200 300 400 500 600 700 800

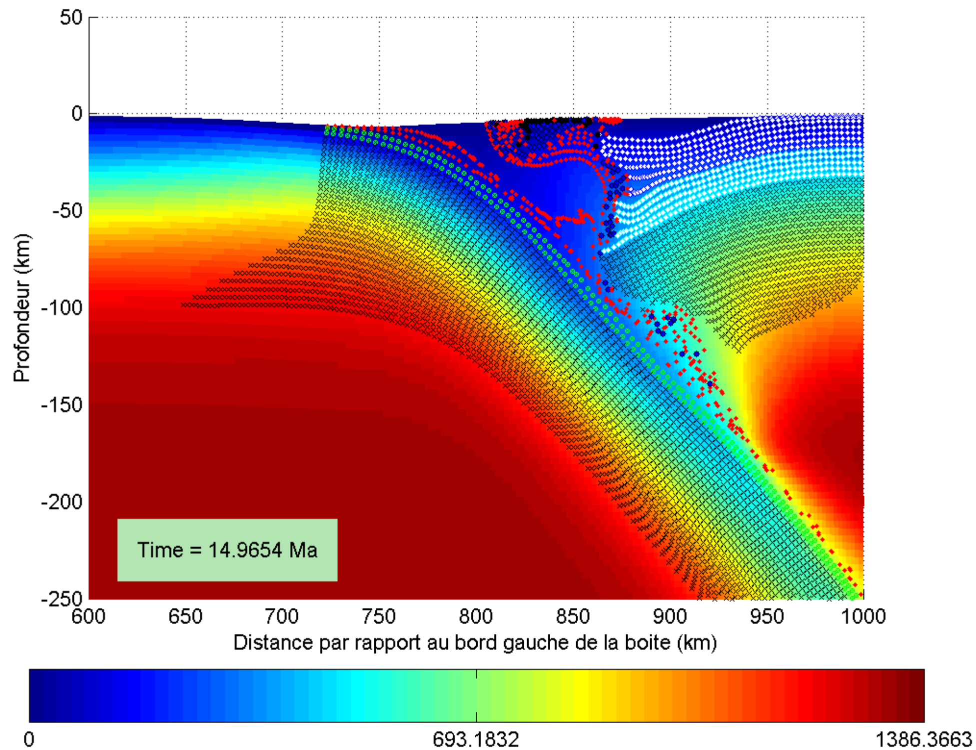

Profondeur (km)
50
0
-50
-100
-150
-200
-250
Time = 14.9654 Ma
600 650 700 750 800 850 900 950 1000
Distance par rapport au bord gauche de la boite (km)
0
693.1832
1386.3663

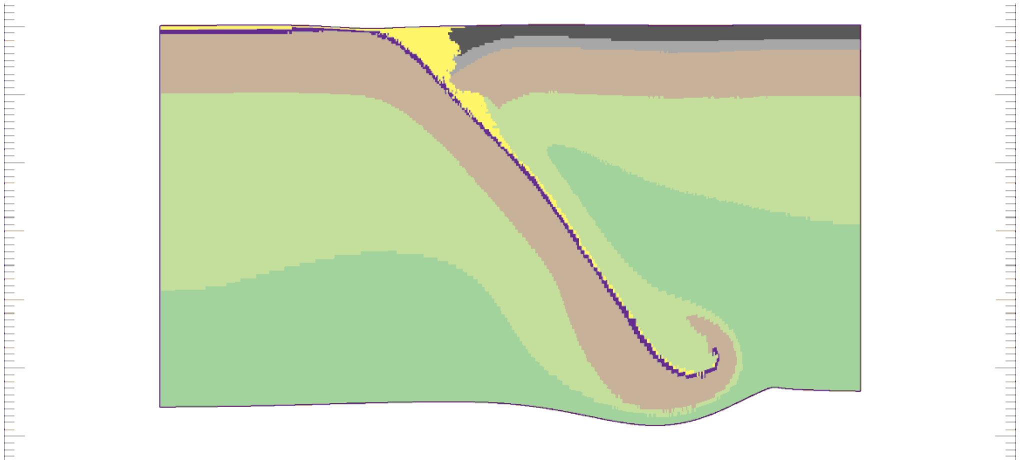

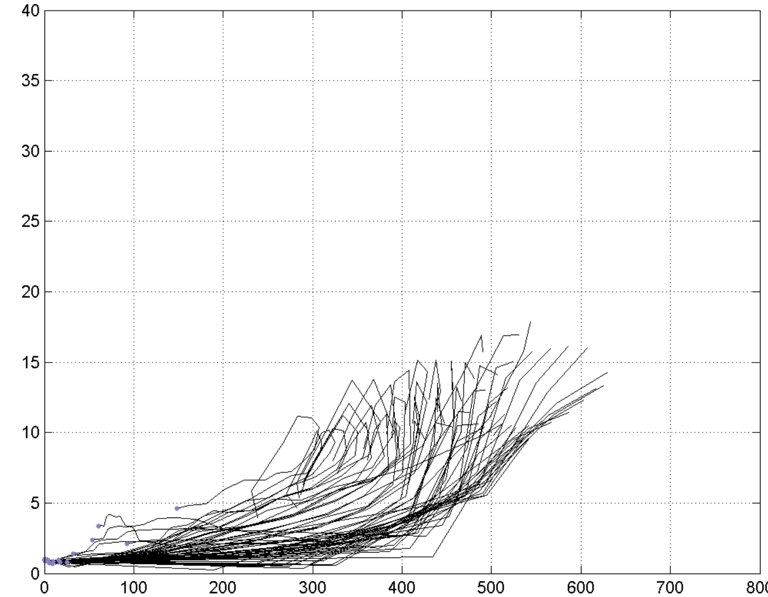

40
35
30
25
20
15
10
5
0
0
100
200
300
400
500
600
700
800

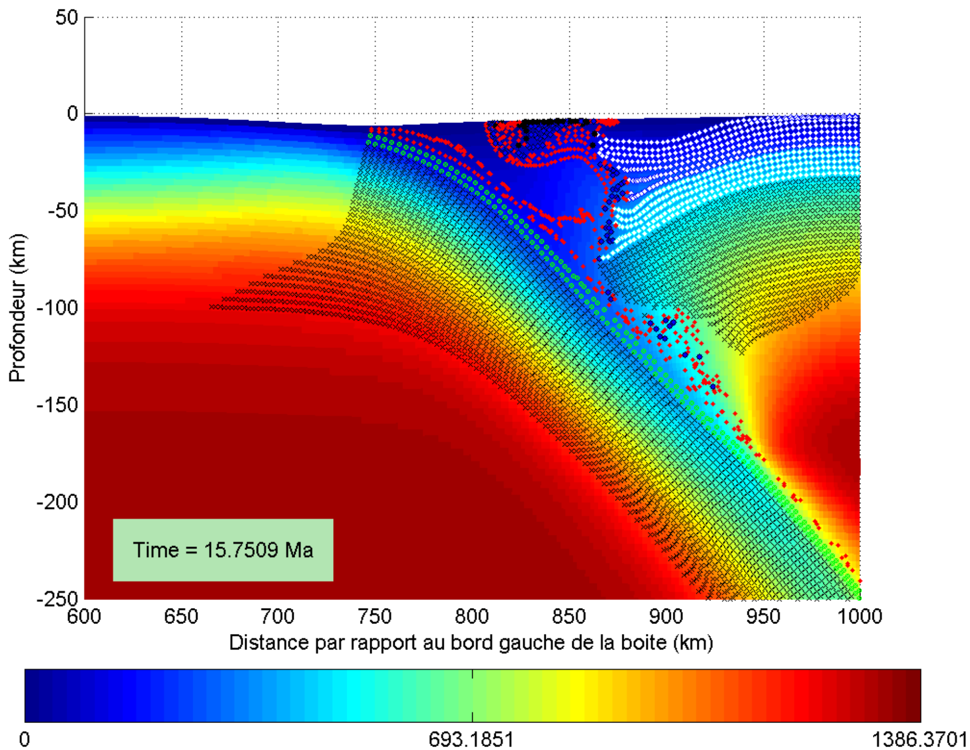

50
0
-50
-100
-150
-200
-250
Profondeur (km)
600
650
700
750
800
850
900
950
1000
Distance par rapport au bord gauche de la boite (km)
Time = 15.7509 Ma
0
693.1851
1386.3701

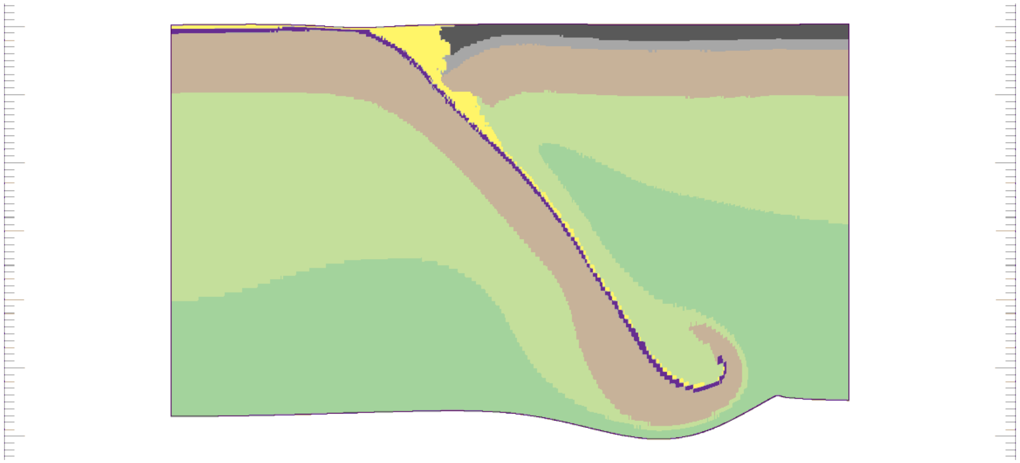

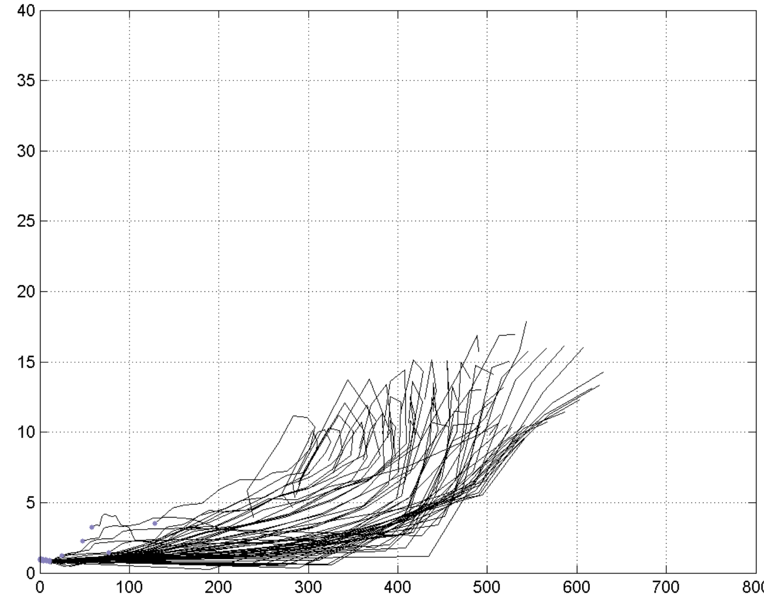

0
5
10
15
20
25
30
35
40
0
100
200
300
400
500
600
700
800

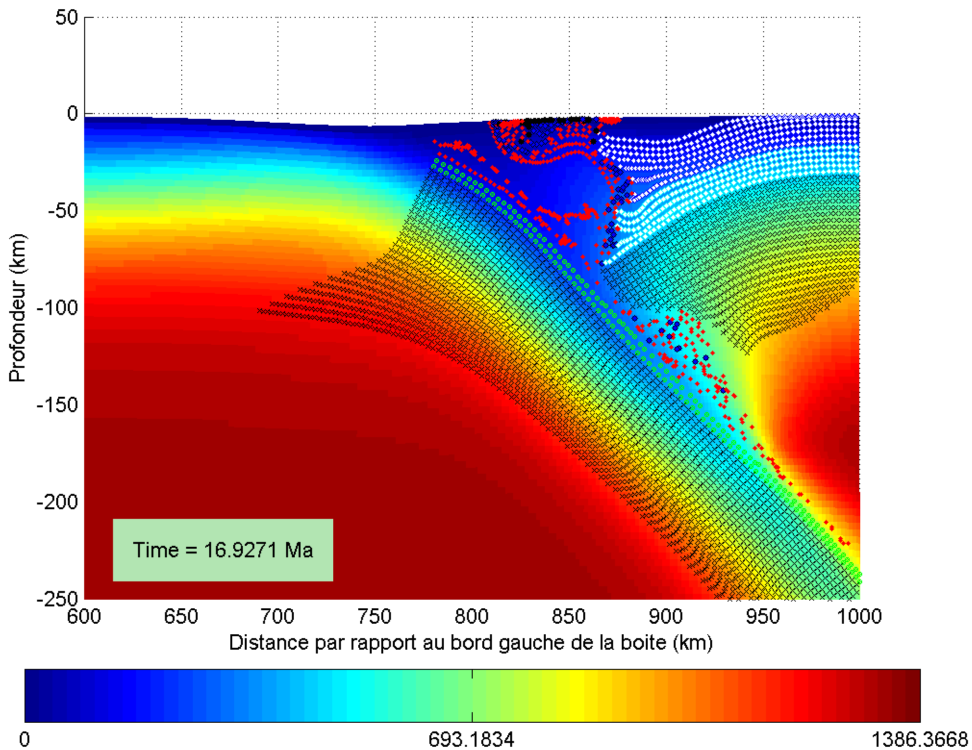

50
0
-50
-100
-150
-200
-250
Profondeur (km)
600
650
700
750
800
850
900
950
1000
Distance par rapport au bord gauche de la boite (km)
Time = 16.9271 Ma
0
693.1834
1386.3668

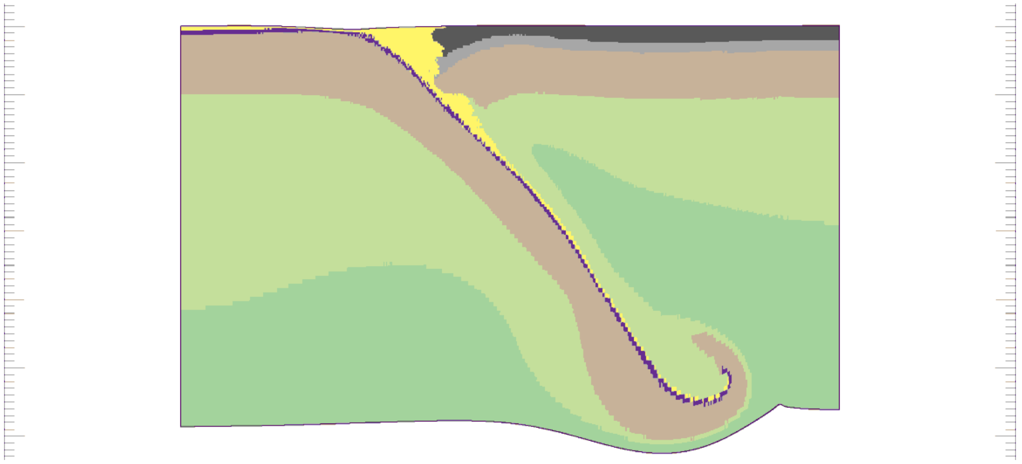

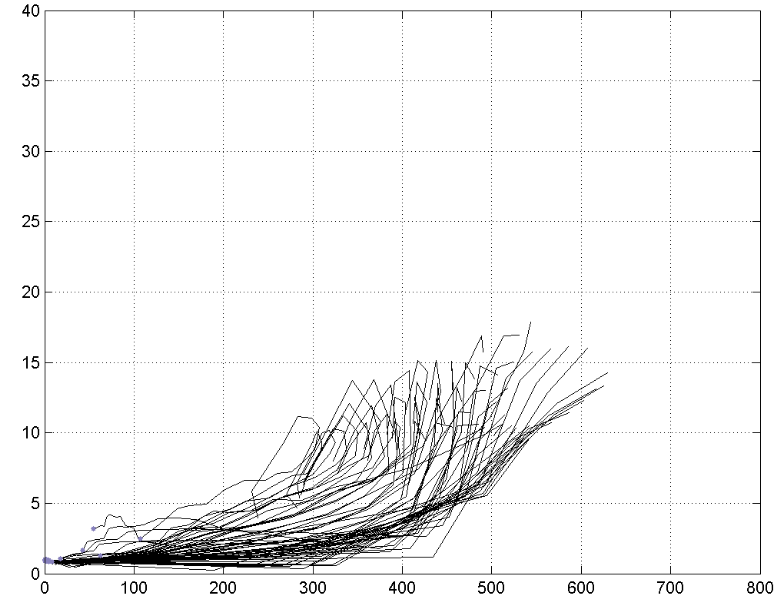
0
5
10
15
20
25
30
35
40
0
100
200
300
400
500
600
700
800

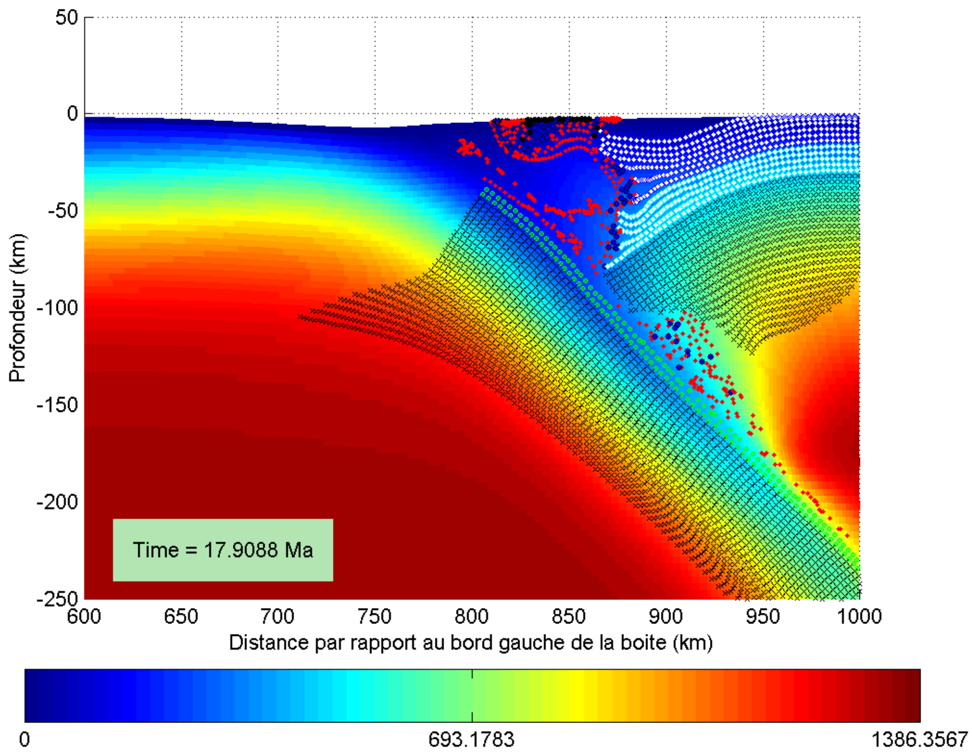
50
0
-50
-100
-150
-200
-250
Profondeur (km)
600
650
700
750
800
850
900
950
1000
Distance par rapport au bord gauche de la boite (km)
Time = 17.9088 Ma
0
693.1783
1386.3567

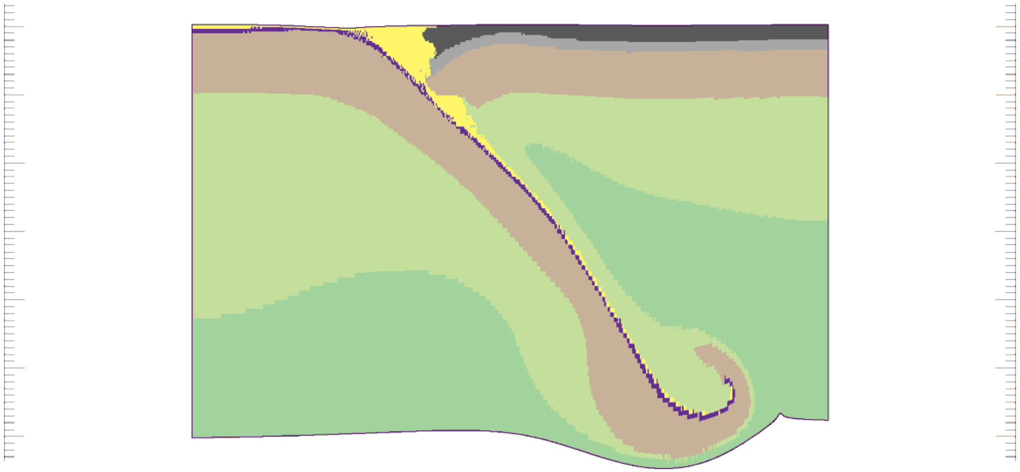

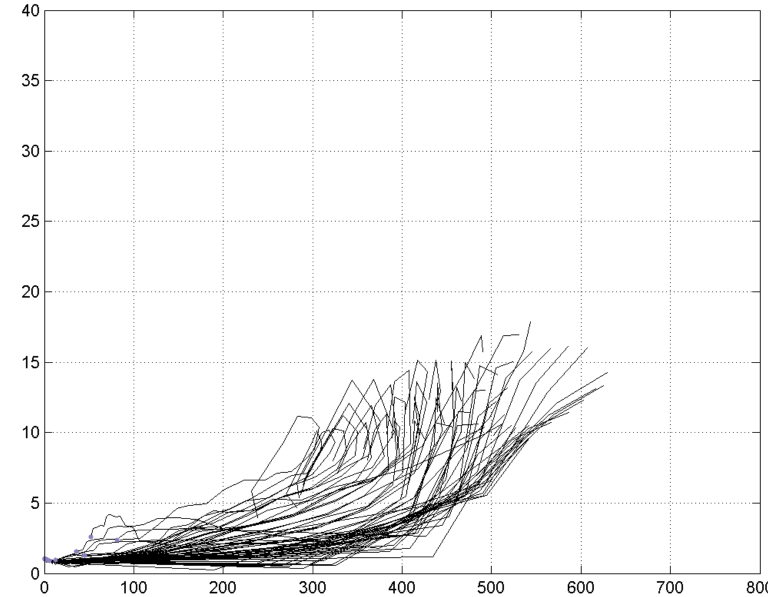
40
35
30
25
20
15
10
5
0
0
100
200
300
400
500
600
700
800

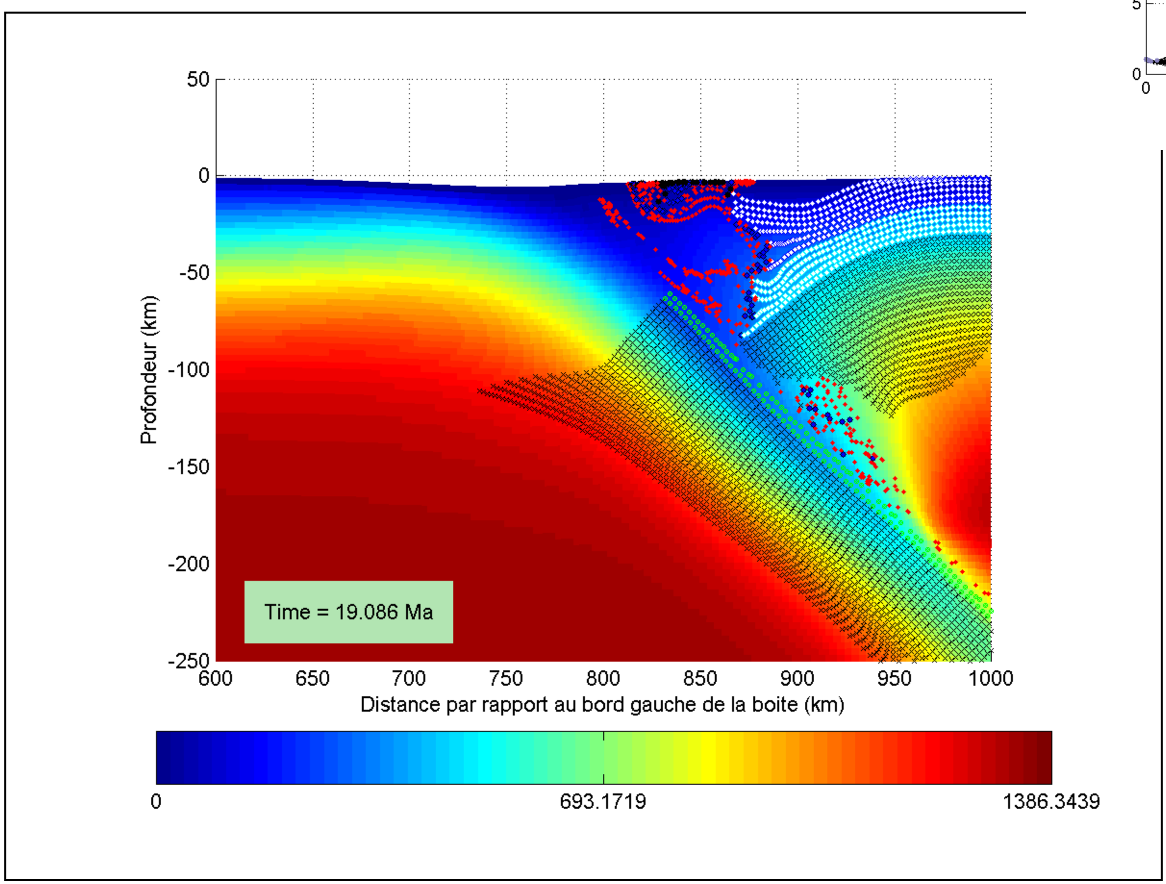
50
0
-50
-100
-150
-200
-250
600
650
700
750
800
850
900
950
1000
Profondeur (km)
Distance par rapport au bord gauche de la boite (km)
Time = 19.086 Ma
0
693.1719
1386.3439

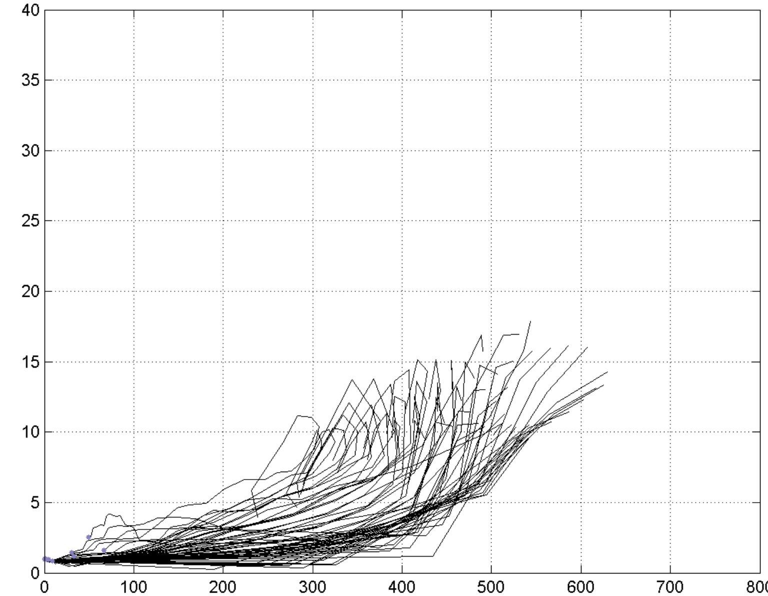

40
35
30
25
20
15
10
5
0
0
100
200
300
400
500
600
700
800

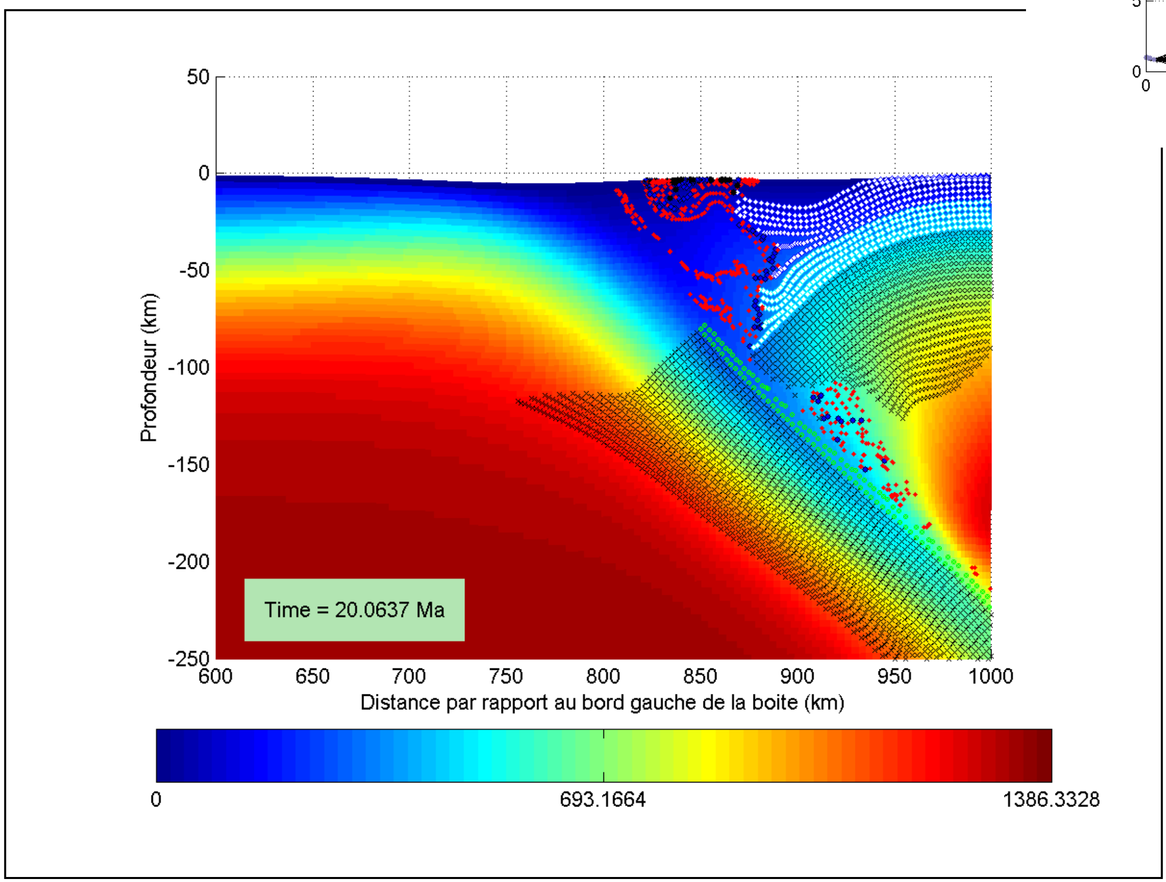

50
0
-50
-100
-150
-200
-250
Profondeur (km)
Time = 20.0637 Ma
600
650
700
750
800
850
900
950
1000
Distance par rapport au bord gauche de la boite (km)
0
693.1664
1386.3328

Evolution of an accretion prism

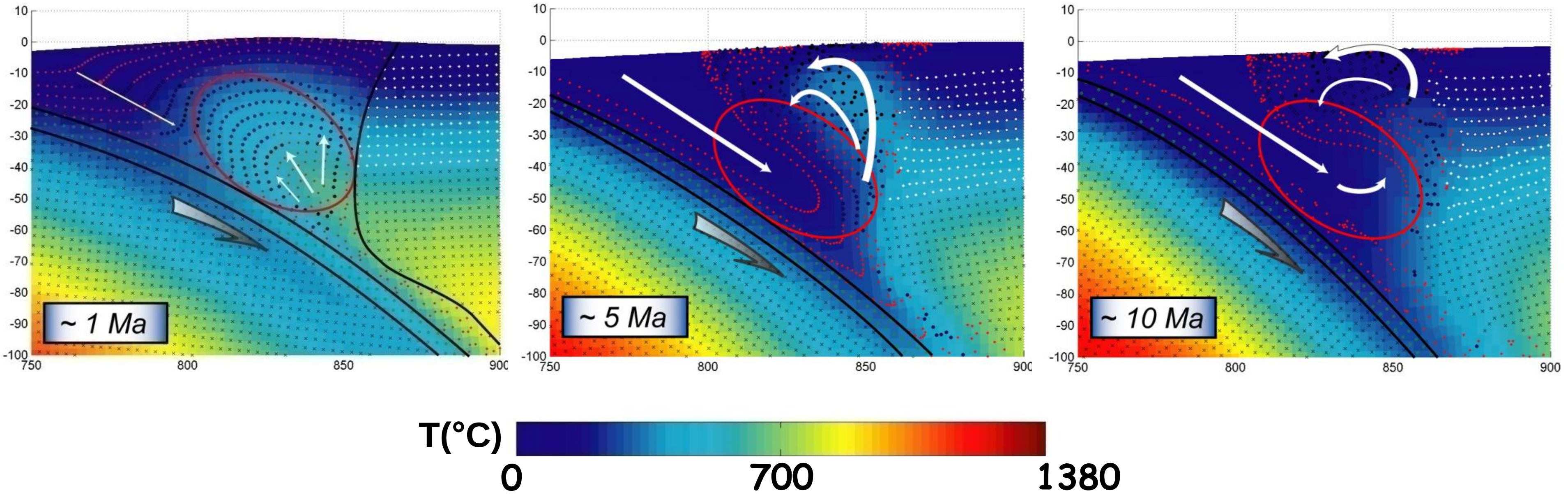

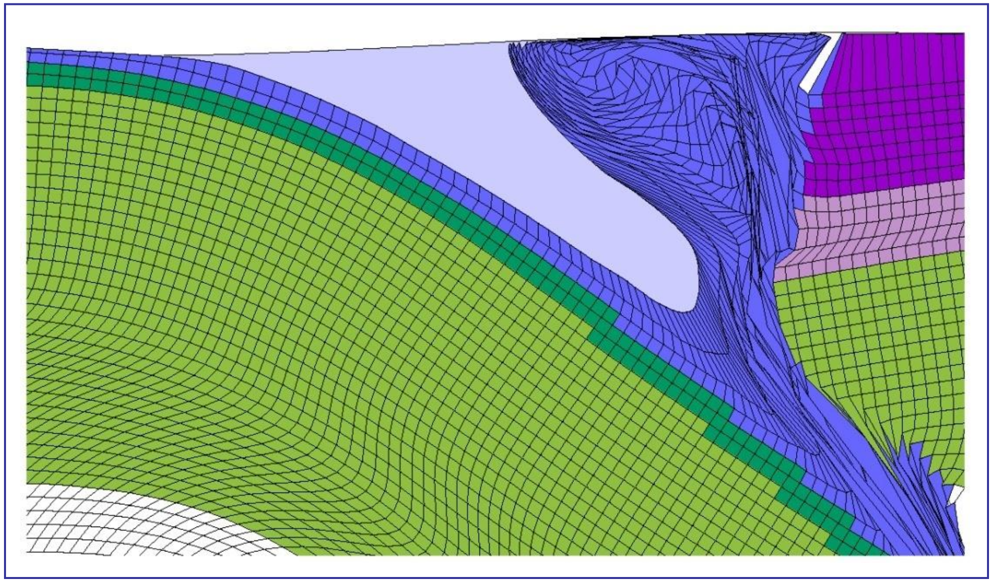

The Results

➪ Observed versus predicted P-T-t paths

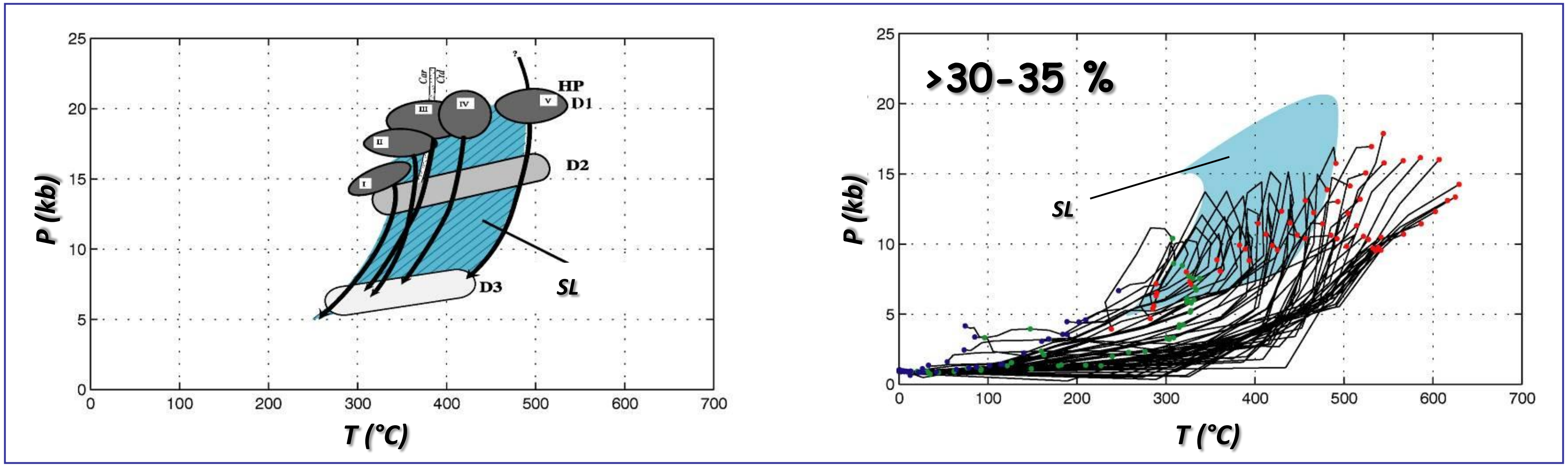

➪ **Exhumation rates of sediments in the accretion prism**

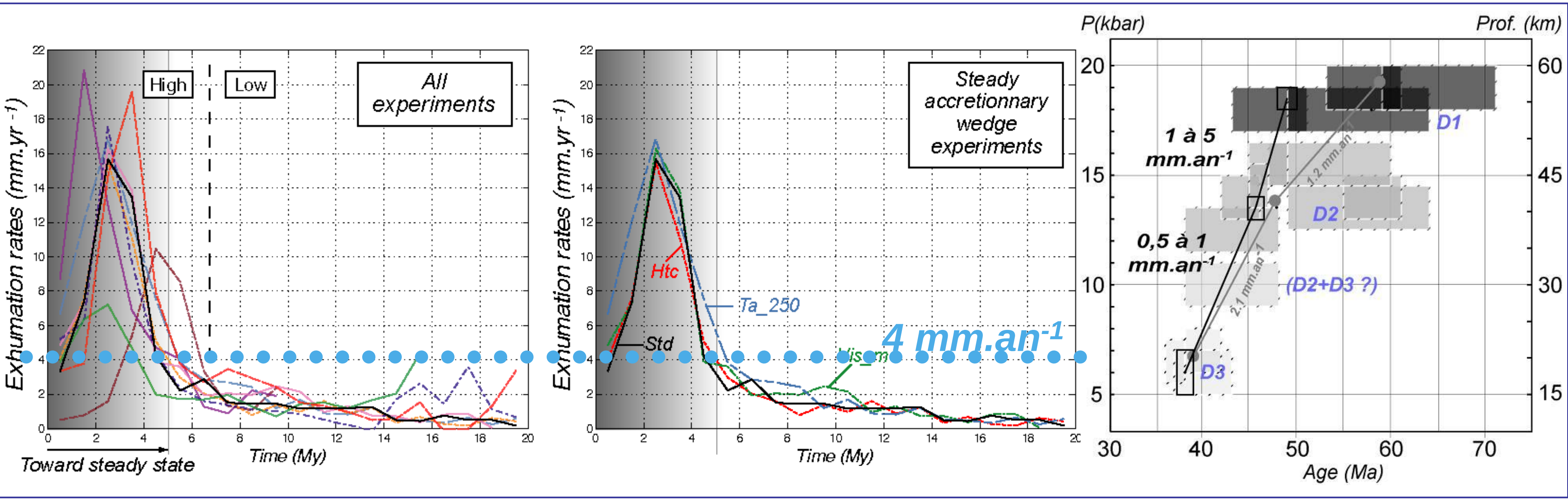

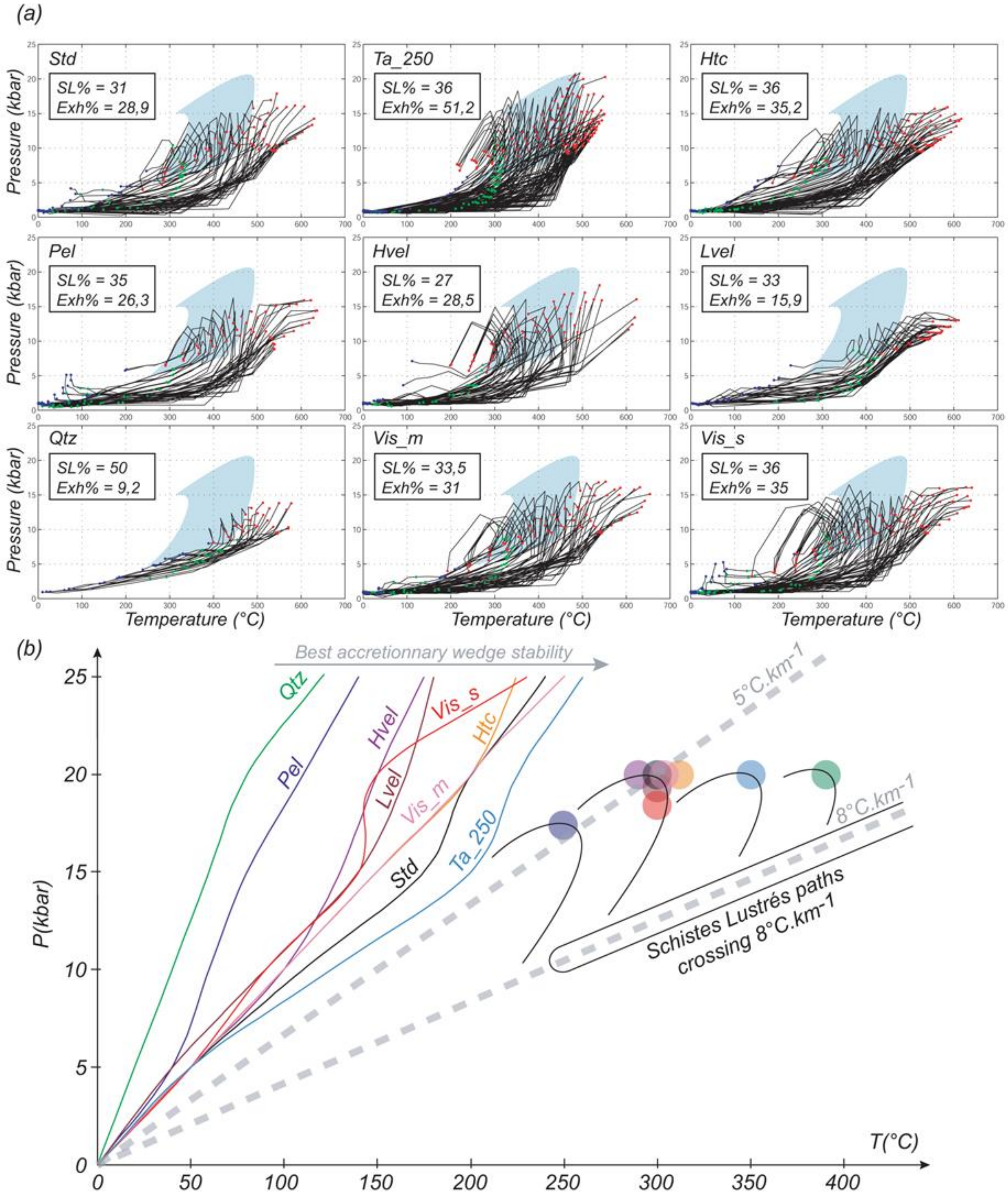
(a)
Std
SL% = 31
Exh% = 28,9
Ta_250
SL% = 36
Exh% = 51,2
Htc
SL% = 36
Exh% = 35,2
Pel
SL% = 35
Exh% = 26,3
Hvel
SL% = 27
Exh% = 28,5
Lvel
SL% = 33
Exh% = 15,9
Qtz
SL% = 50
Exh% = 9,2
Vis_m
SL% = 33,5
Exh% = 31
Vis_s
SL% = 36
Exh% = 35
Pressure (kbar)
Temperature (°C)
(b)
Best accretionnary wedge stability
Qtz
Pel
Hvel
Lvel
Vis_s
Htc
Vis_m
Std
Ta_250
5°C.km-1
8°C.km-1
Schistes Lustrés paths crossing 8°C.km-1
P(kbar)
T(°C)

Serpentinite layer (light, weak) below the oceanic crust: : important impact on oceanic subduction

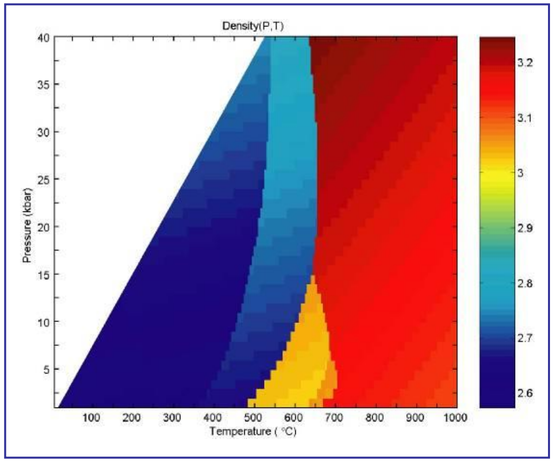

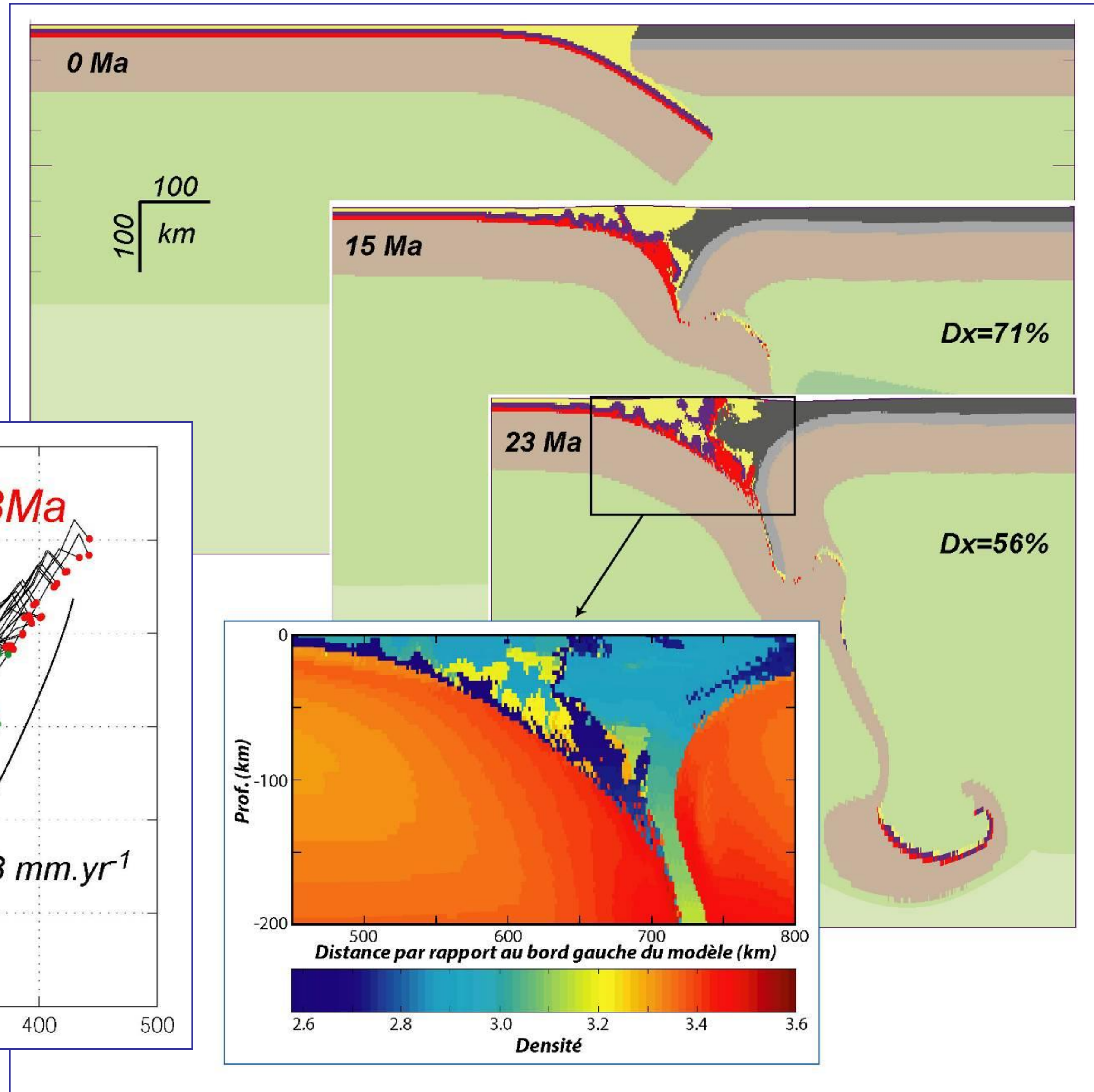

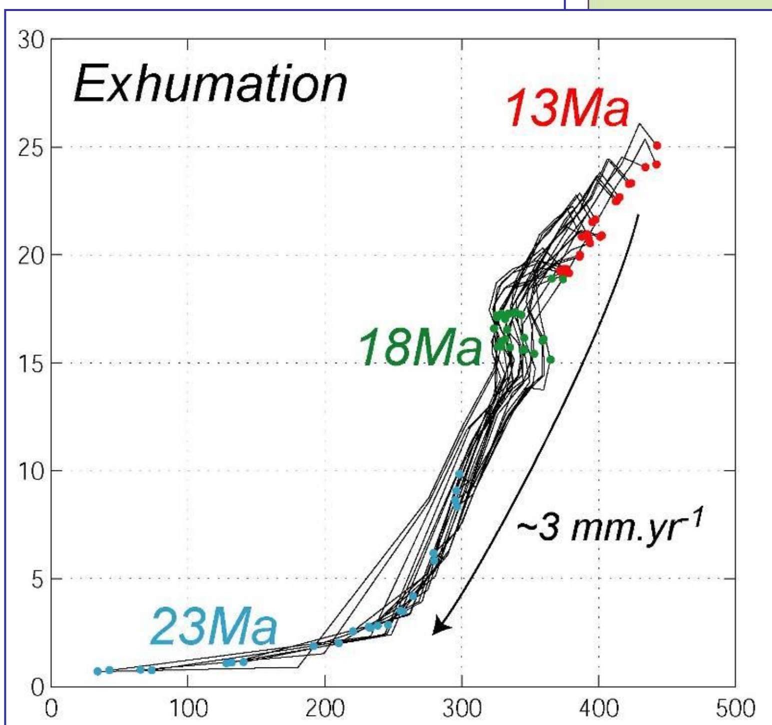

Slow Alpine Collision II:

continental phase

PhD thesis of Ph. Yamato;
Yamato et al., 2007, 2008, Burov and Yamato, 2008

Alpine lithosphere-asthenosphere system

(*Courtesy of E. Kissling*)

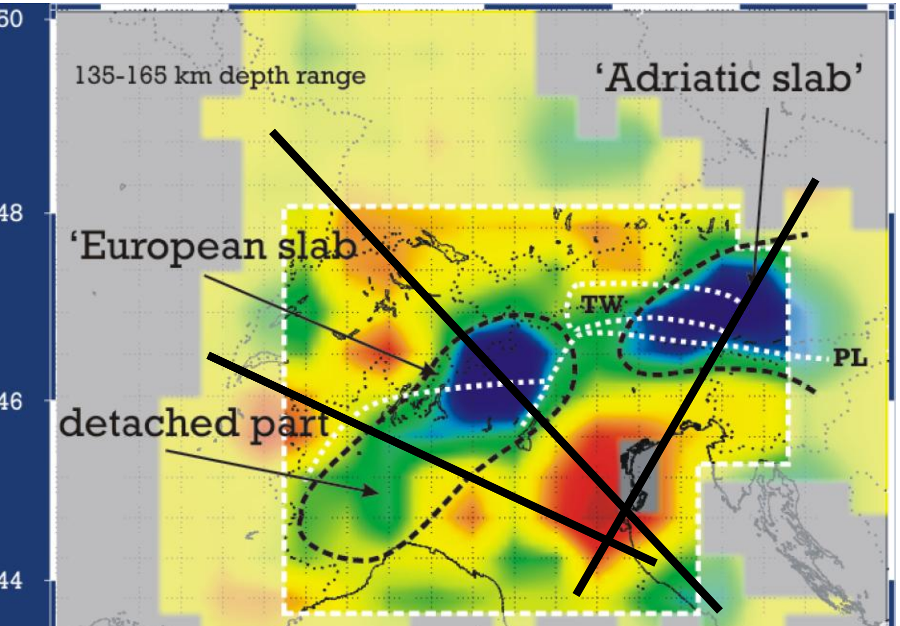

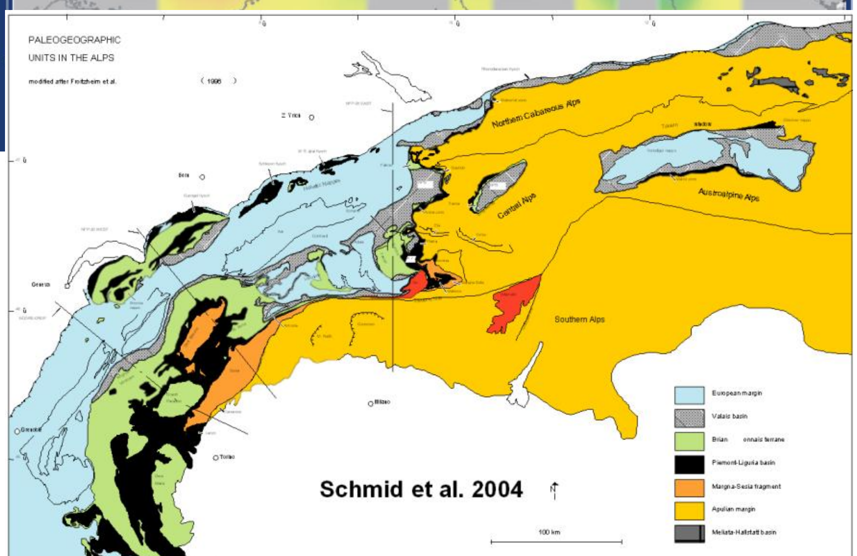

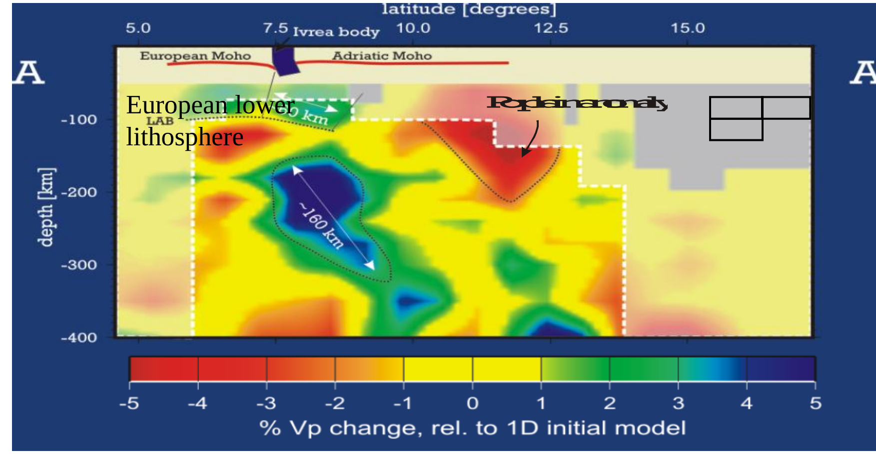

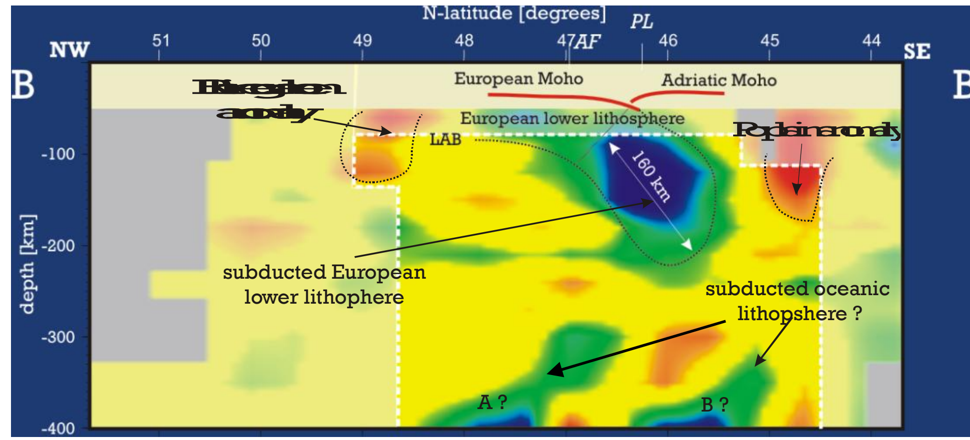

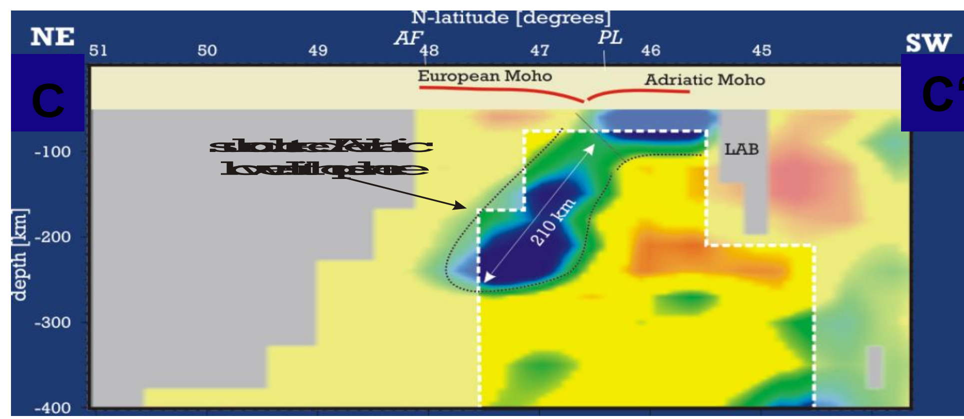

***Lippitsch et al*. 2003, JGR**

SLOW collision, WEAK (Te<30 km) lithosphere

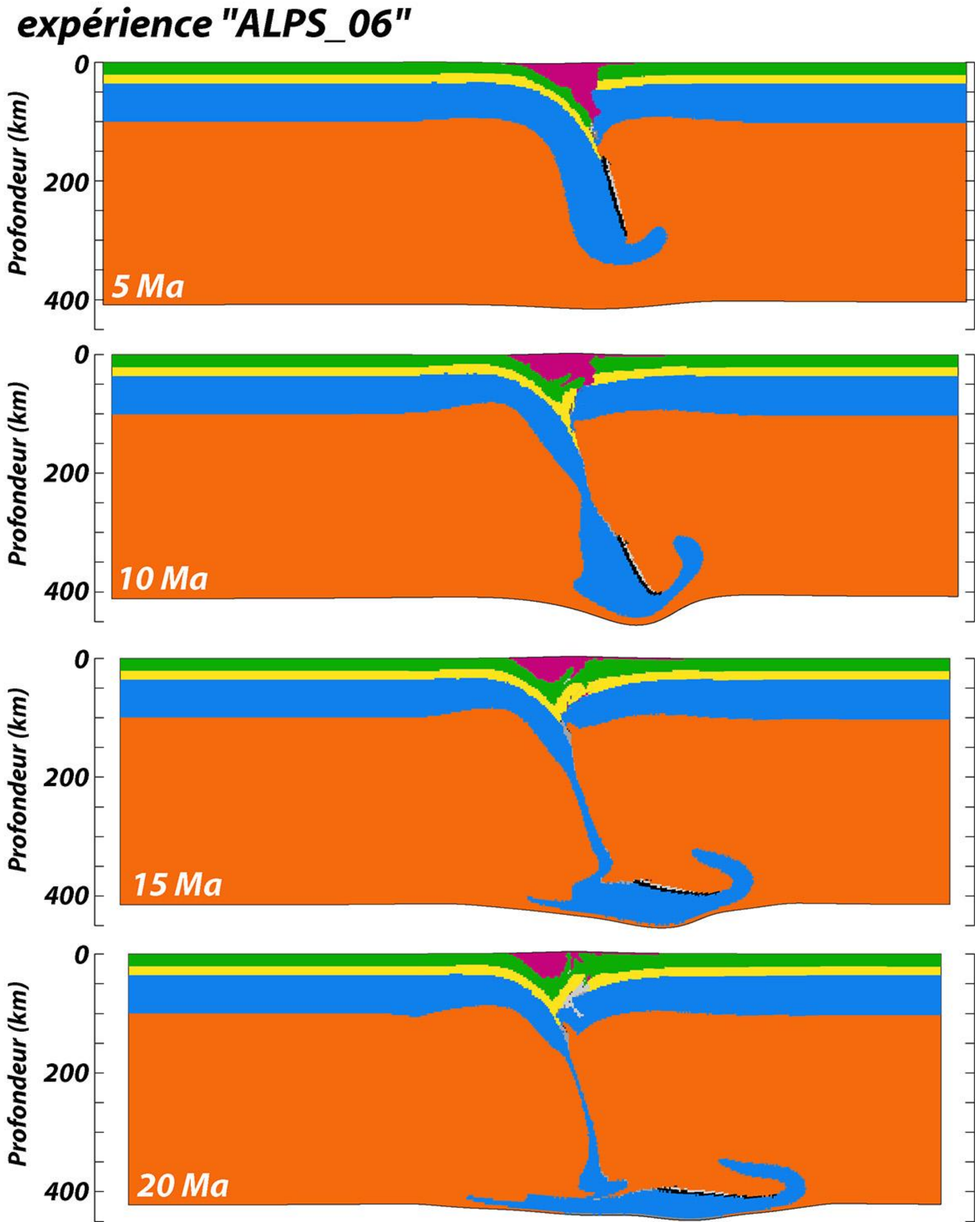

Influence of the crustal rheology

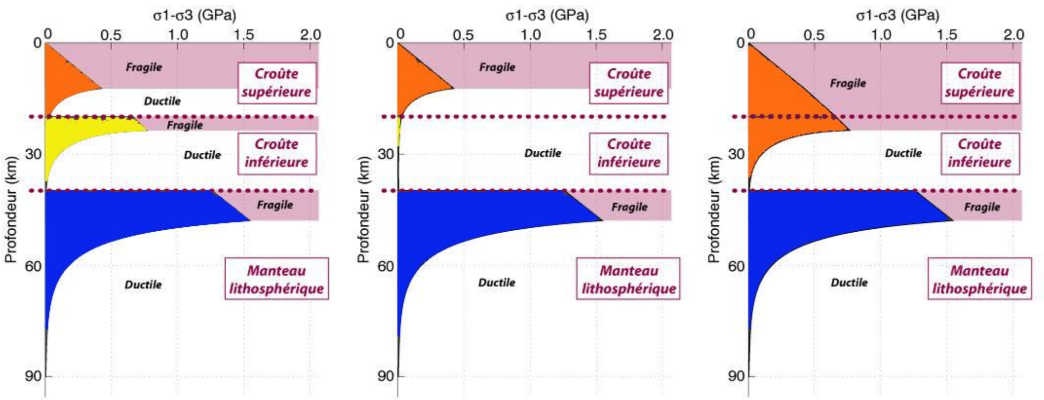

Croûte QD = Quartz - Diabase

Croûte QQ = Quartz - Quartz

Croûte DD = Diabase - Diabase

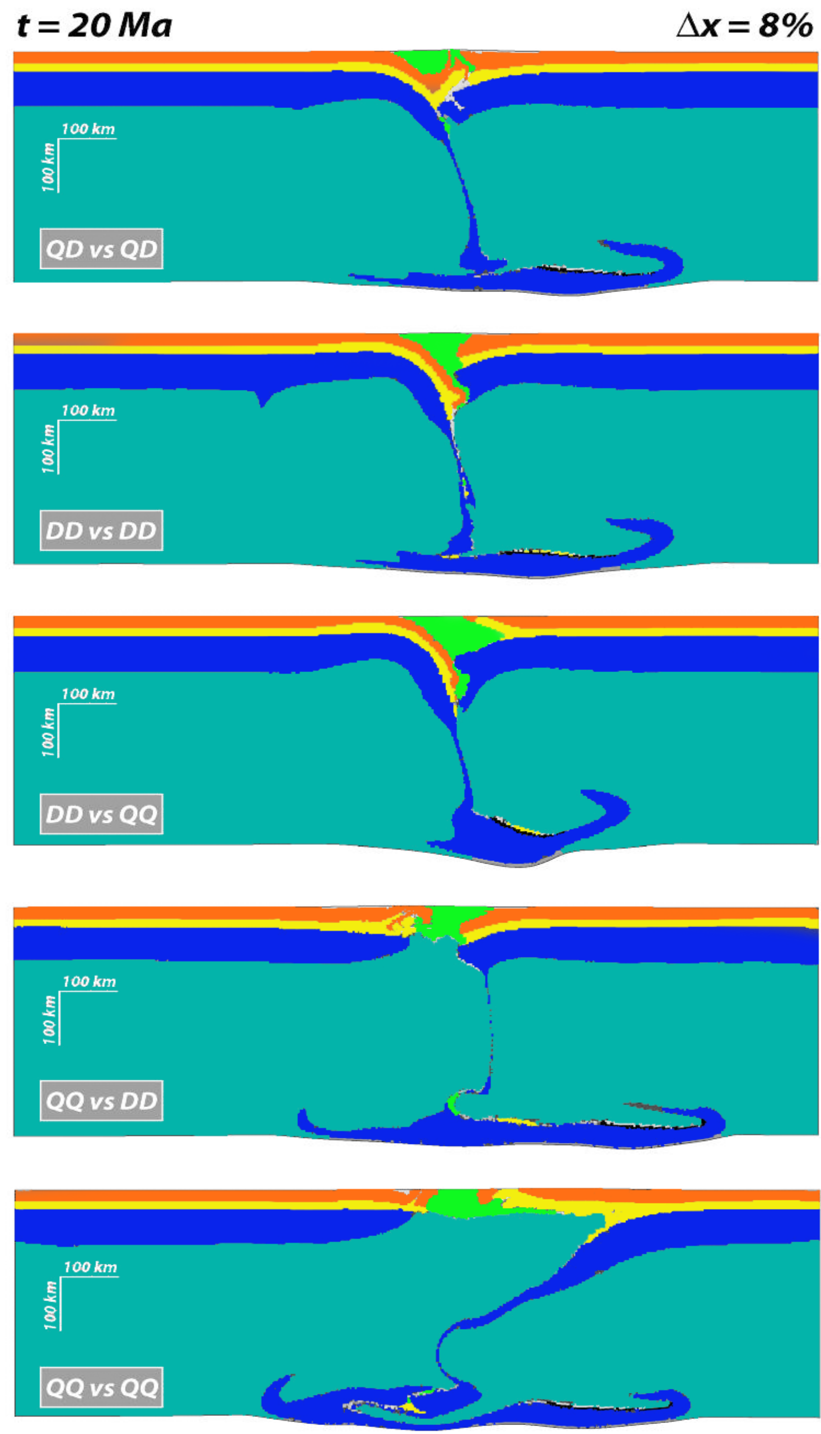

PhD Thesis
Yamato, 2007

Influence of convergence rate

at $\Delta x = 5\%$ ***at $t = 20$ Myr***

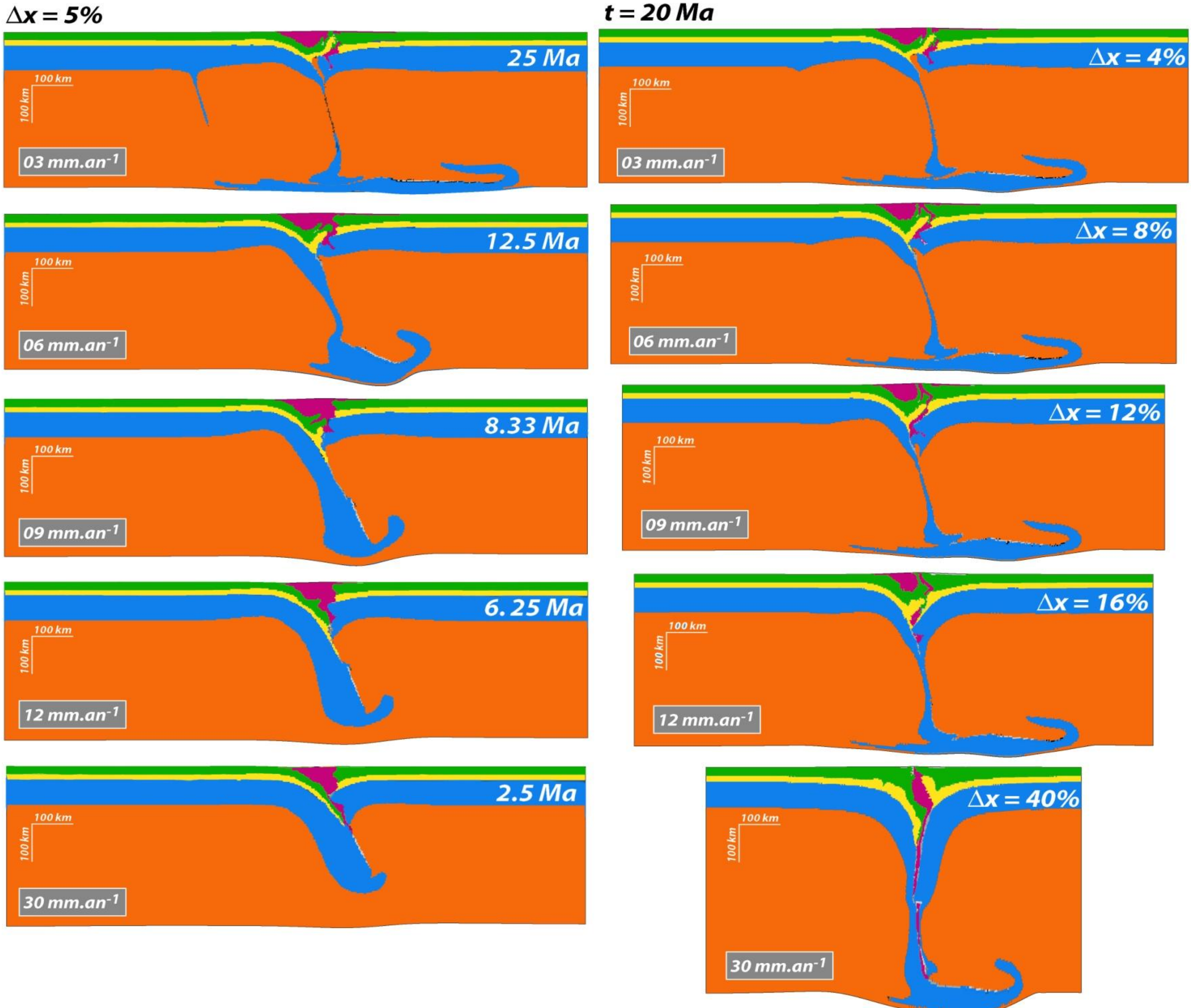

Influence of erosion (k) on collision mode

$t = 20$ Ma, $\Delta x = 8\%$, Vtot = 6 mm.an^{-1}

$k = 3000 m^2 y^{-1}$

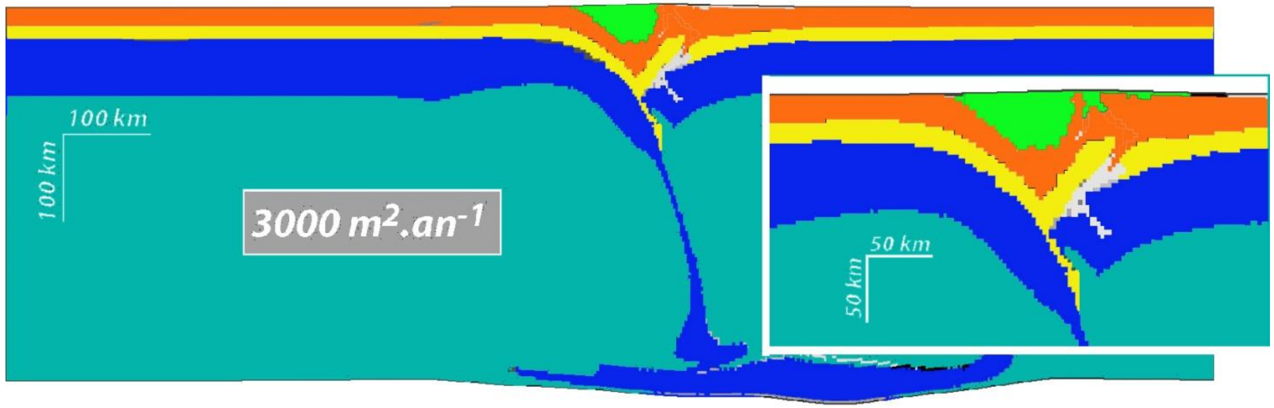

$k = 1500 m^2 y^{-1}$

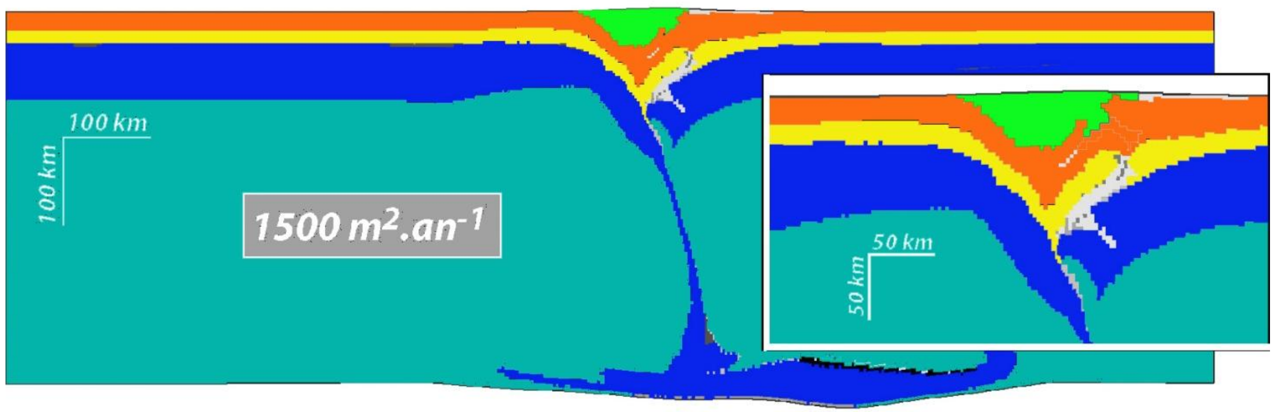

$k = 500 m^2 y^{-1}$

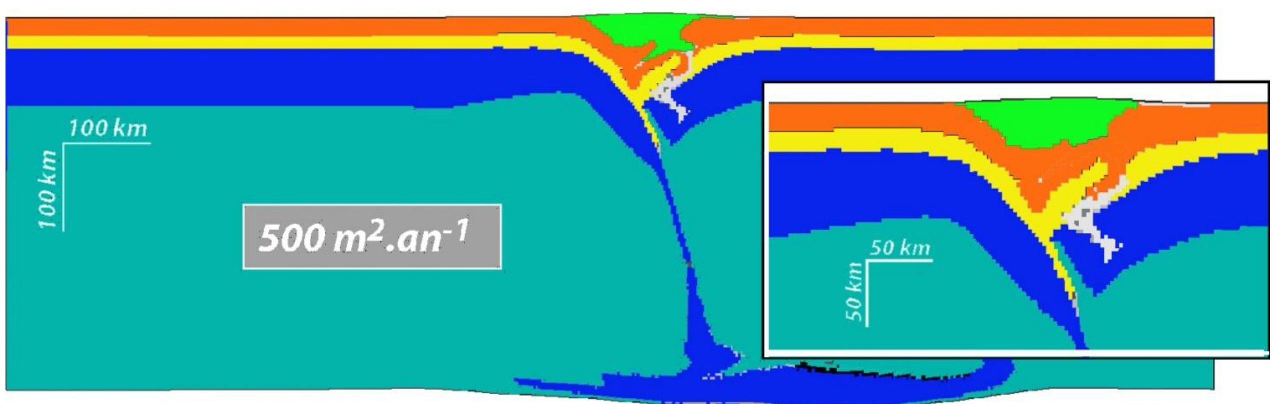

Reference case: evolution details

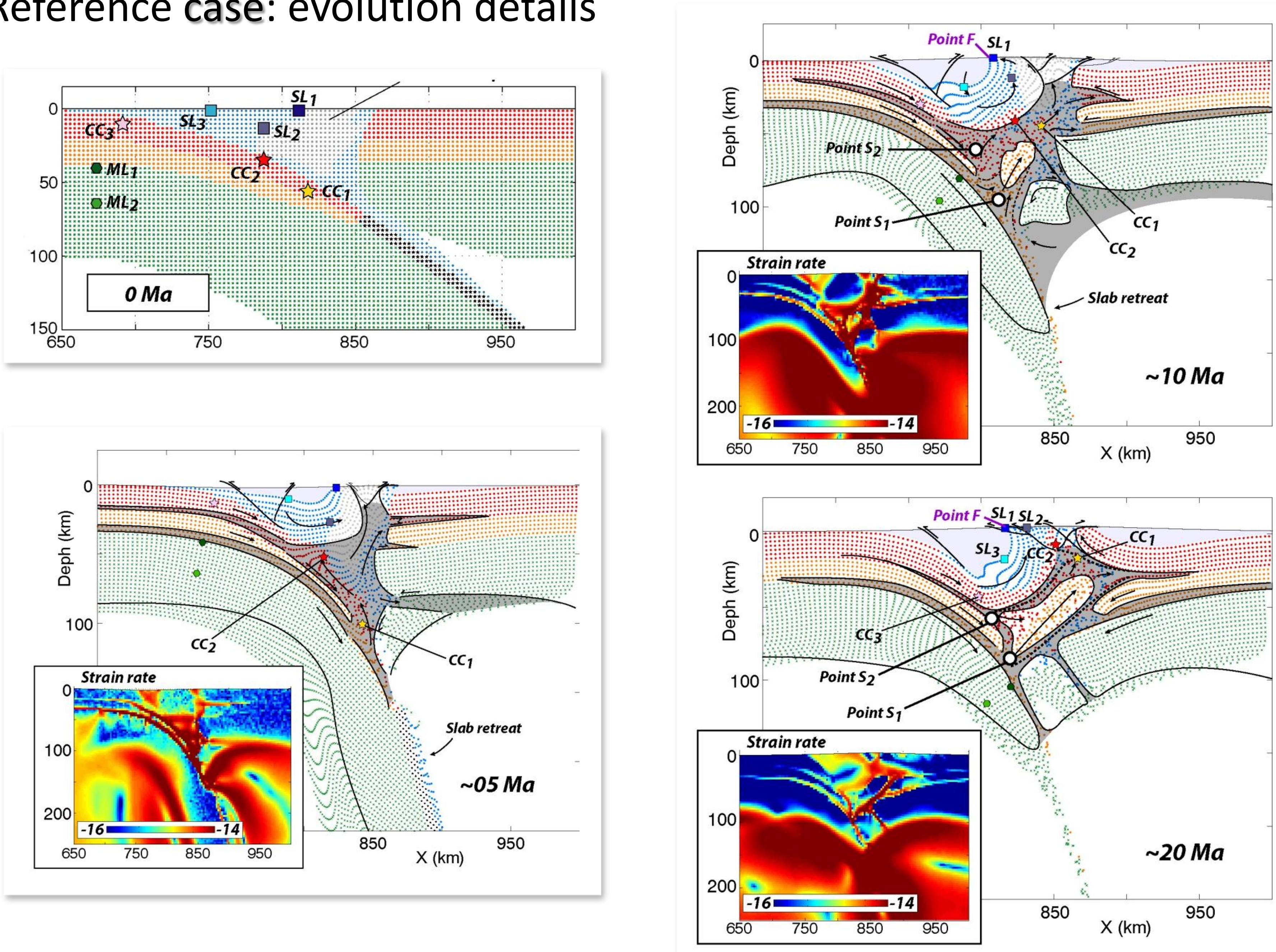

Reference case: predicted P-T-t paths

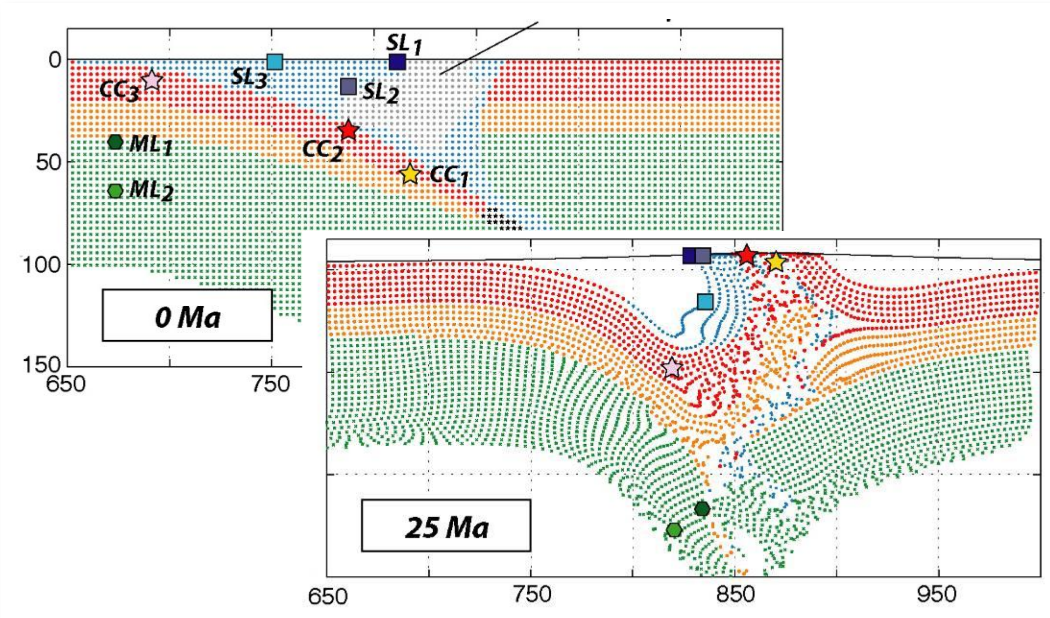

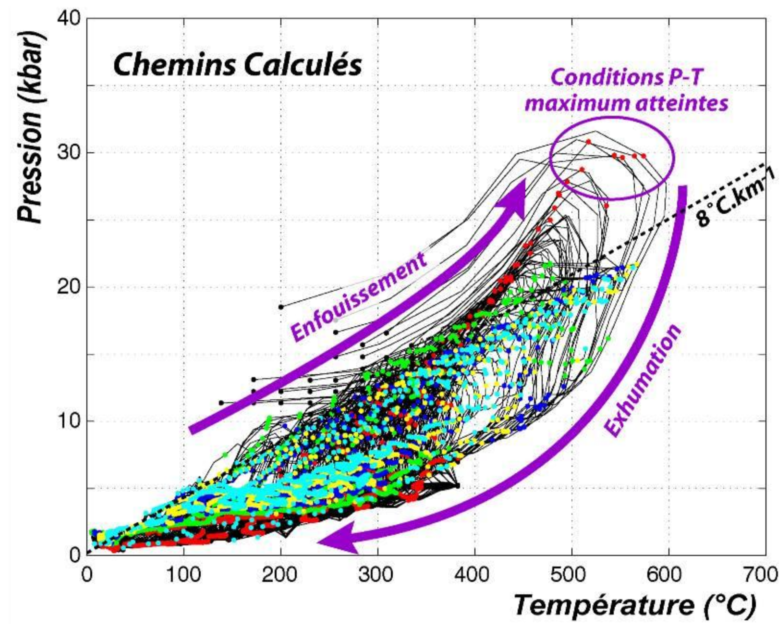

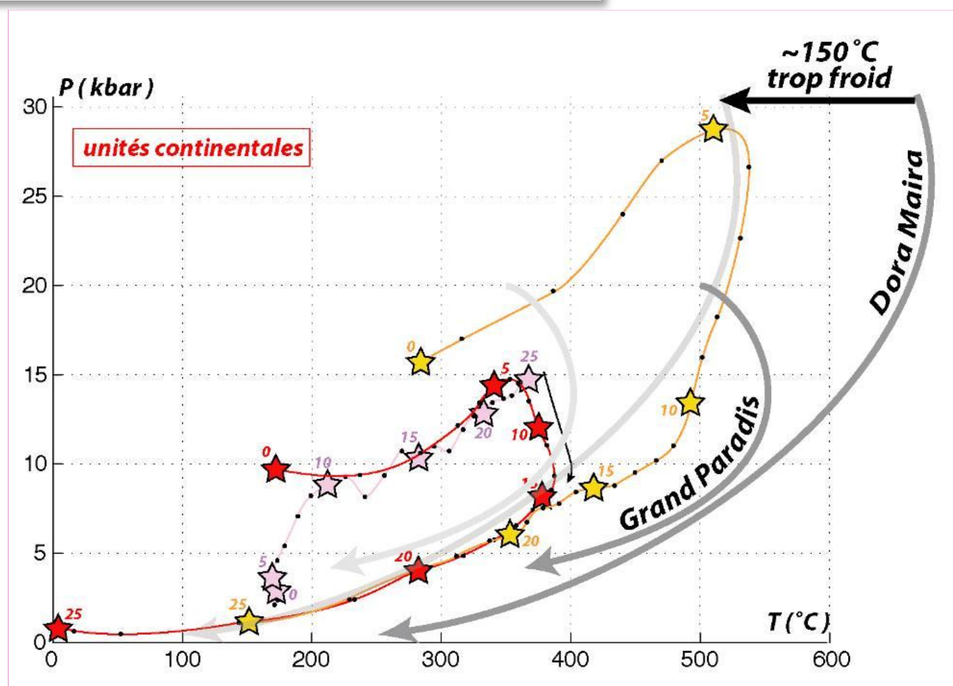

P-T-t Path

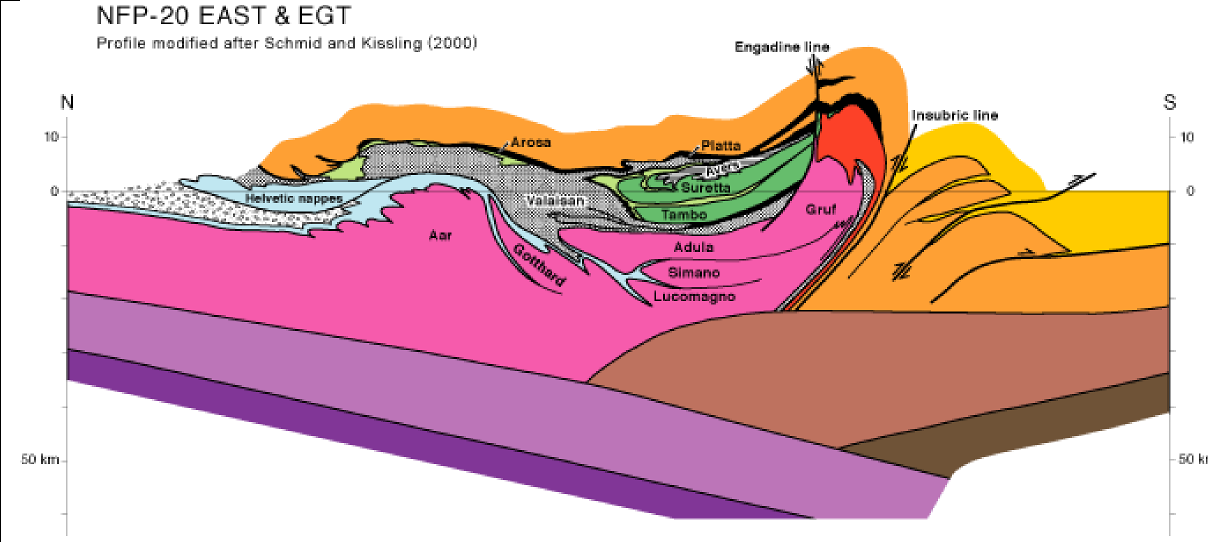

Epicenters and Hypocenters 1975 - 1999

Swiss Seismological Service

ETH Zürich

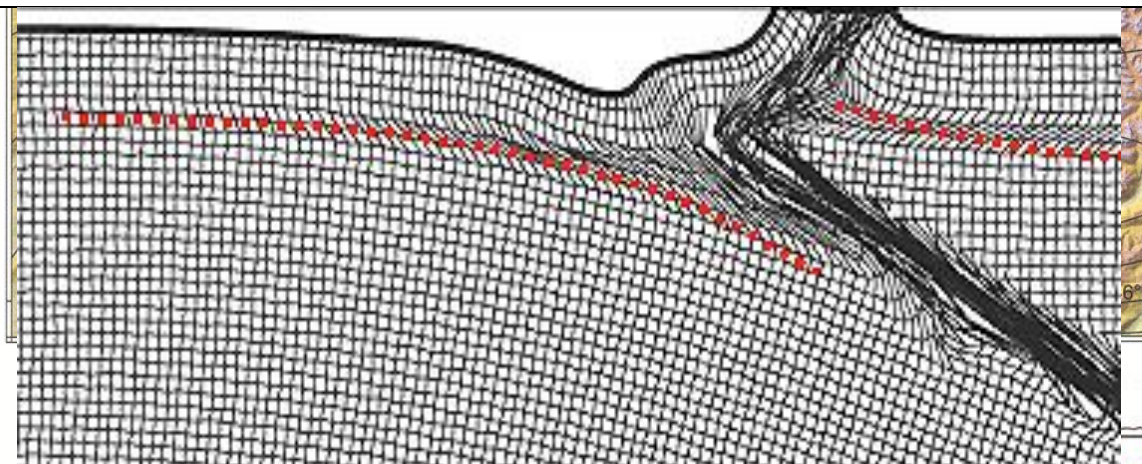

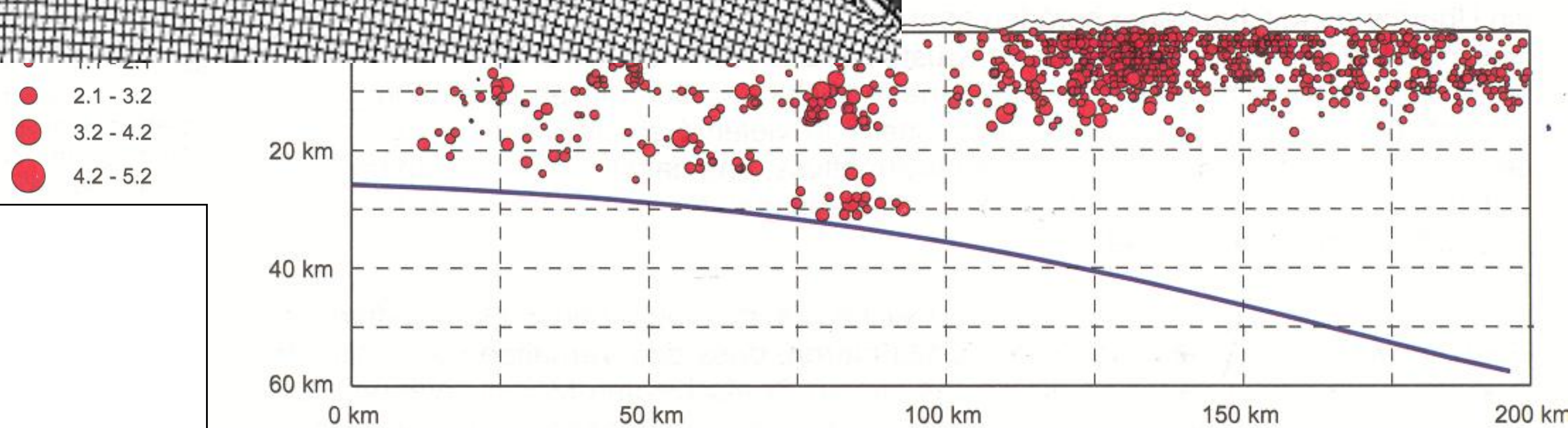

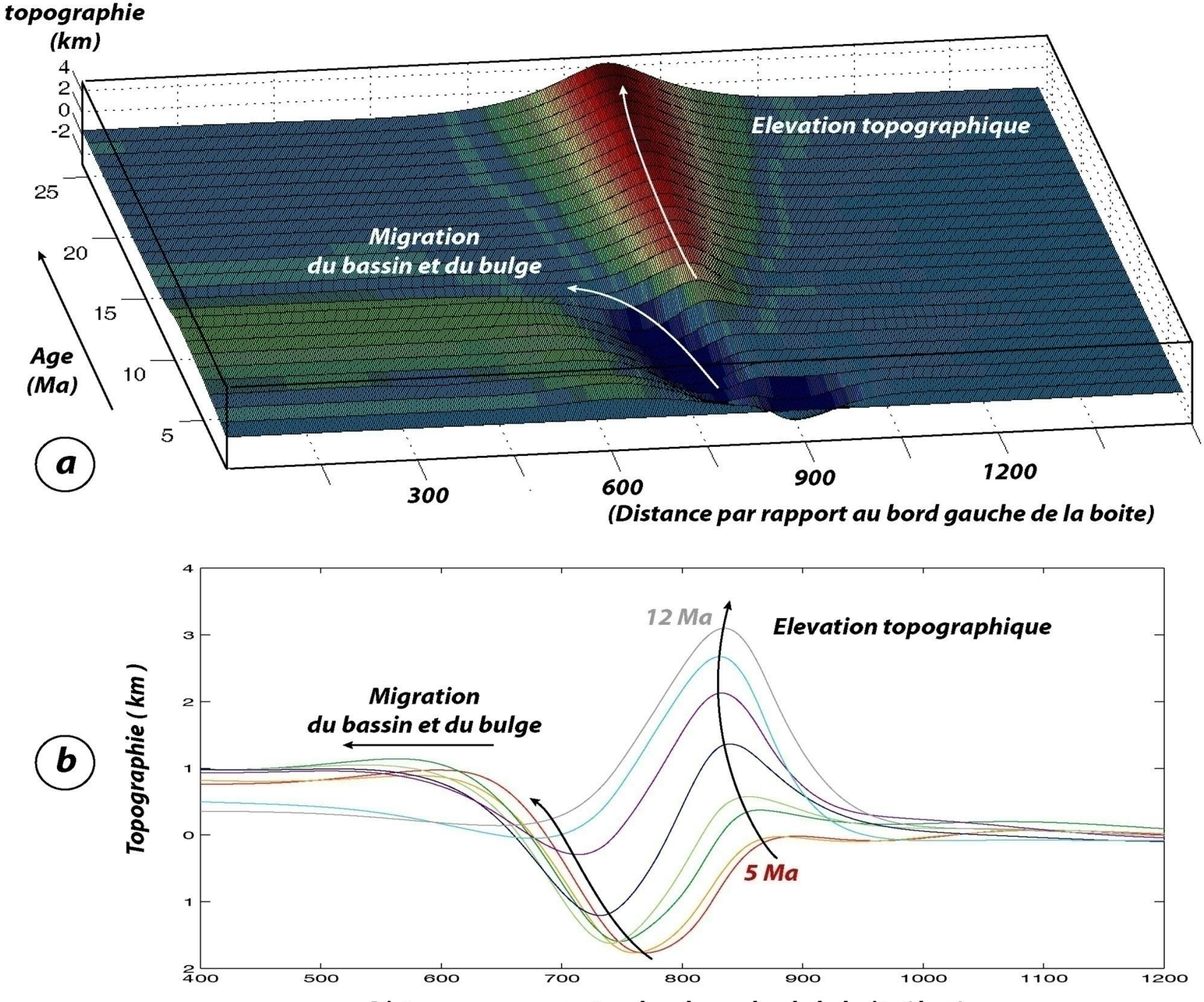

topographie (km)
4
2
0
-2
25
20
15
10
5
Age (Ma)
Elevation topographique
Migration du bassin et du bulge
a
300
600
900
1200
(Distance par rapport au bord gauche de la boite)
b
Topographie (km)
12 Ma
Elevation topographique
Migration du bassin et du bulge
5 Ma
4
3
2
1
0
1
2
400
500
600
700
800
900
1000
1100
1200

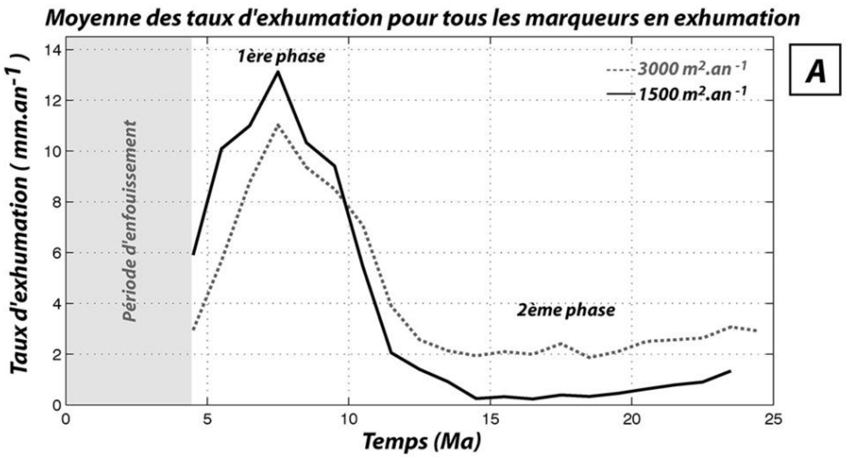

Exhumation rates as function of the erosion rate (first 20 Myr)

Top: markers that have achieved 20-40 kbar and 300-700°C

Bottom: markers that have achieved 10 kbar.

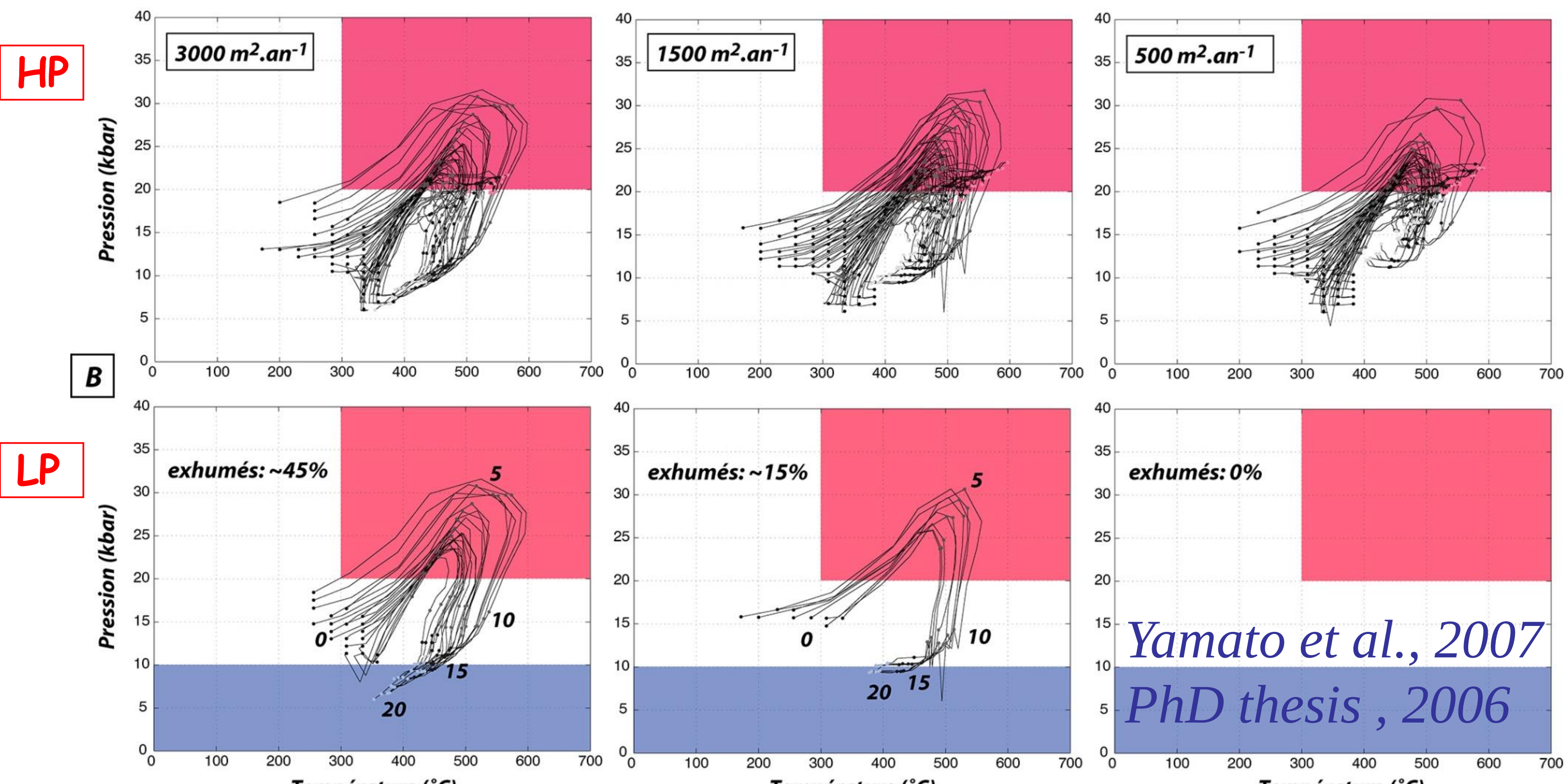

Alpes: Oceanic versus Continental subduction

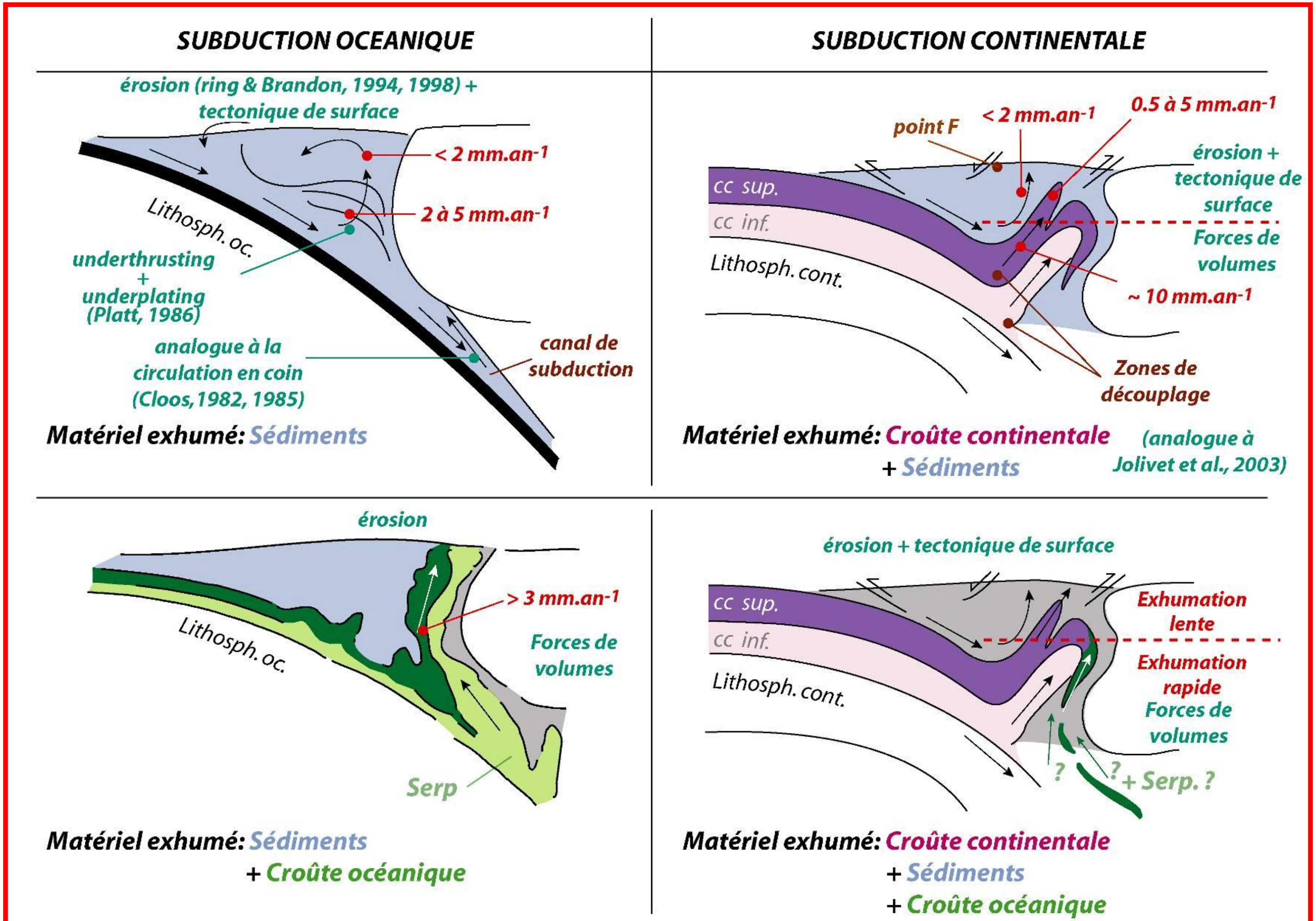

Burov et al., 2001

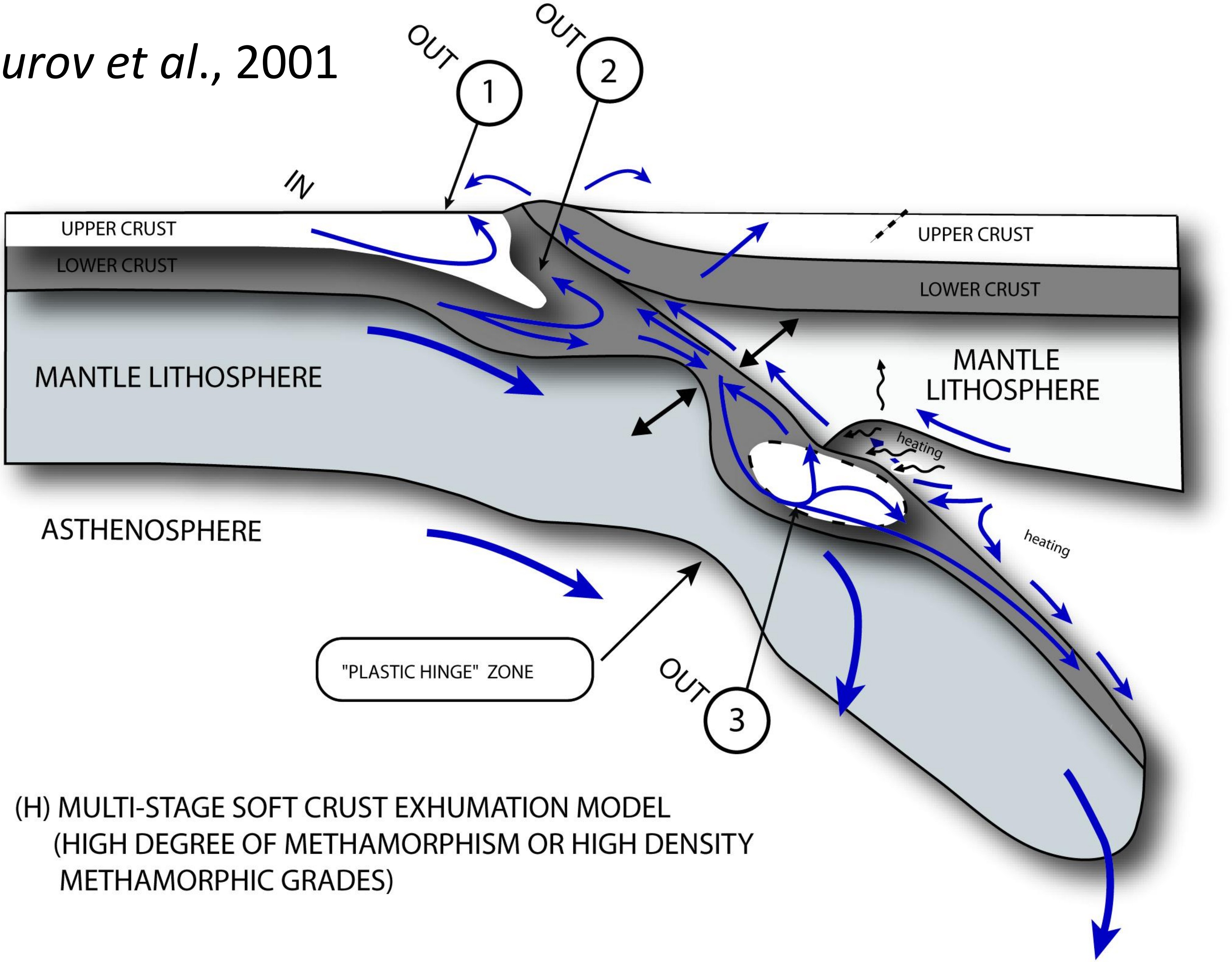

(H) MULTI-STAGE SOFT CRUST EXHUMATION MODEL
(HIGH DEGREE OF METHAMORPHISM OR HIGH DENSITY
METHAMORPHIC GRADES)

6. Collision, Roll-Back and Exhumation

(Aegean Sea)

Aegean Sea accretion history

Tirel et al., 2010,2011

Map of the Mediterranean bathymetry (m)

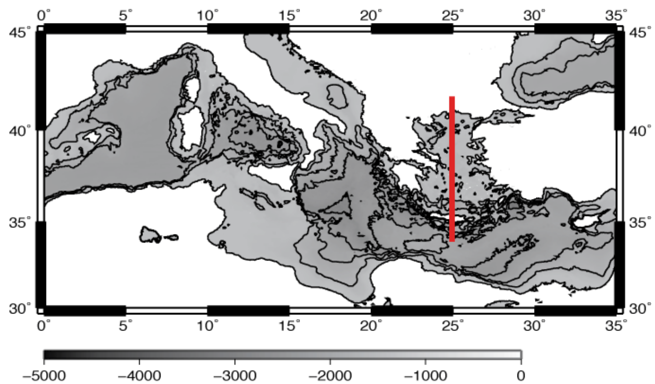

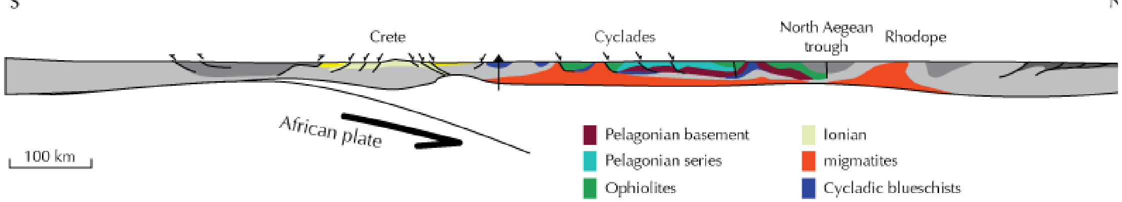

Aegean PTt paths

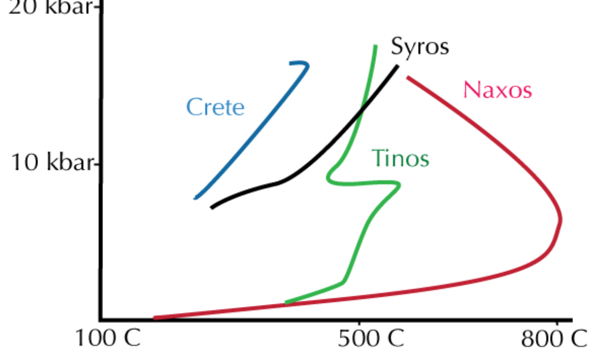

Accretion history

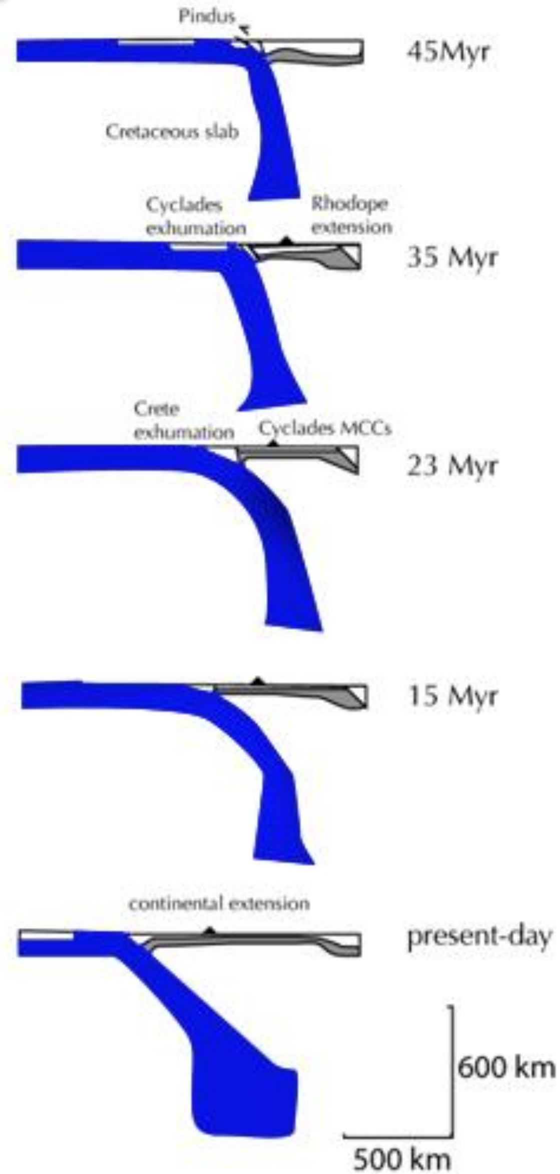

Schematic cross-sections and PTt paths derived from Jolivet & Brun (2008), Brun & Faccenna (2008)

- Major events:
  - Subduction, consumption of oceanic domains and accretion of several continental terranes
  - Several episodes of continental extension due to the African slab retreat

Geological map of Greece

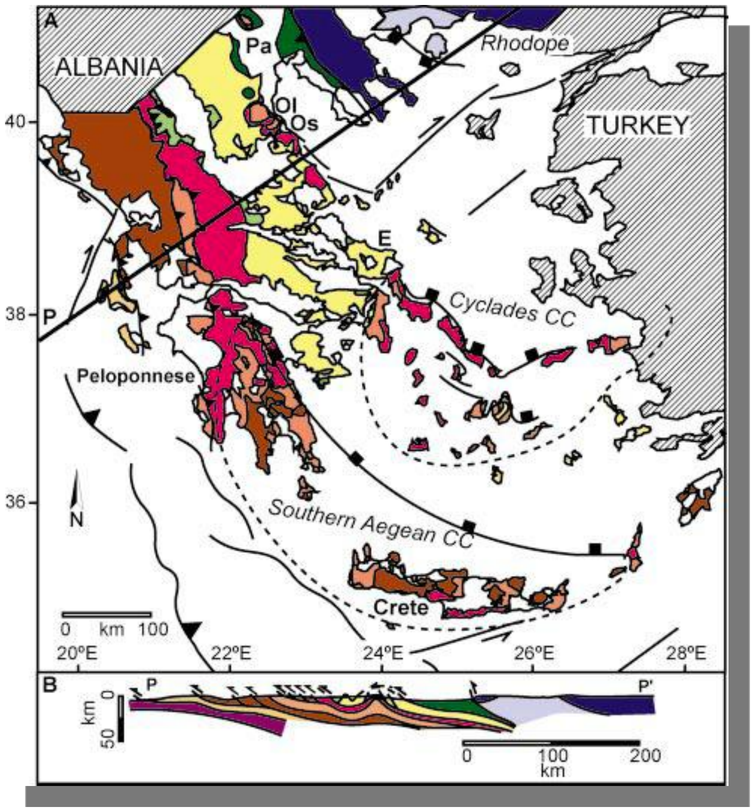

Van Hinsbergen et al., 2005

History of the terranes accretion

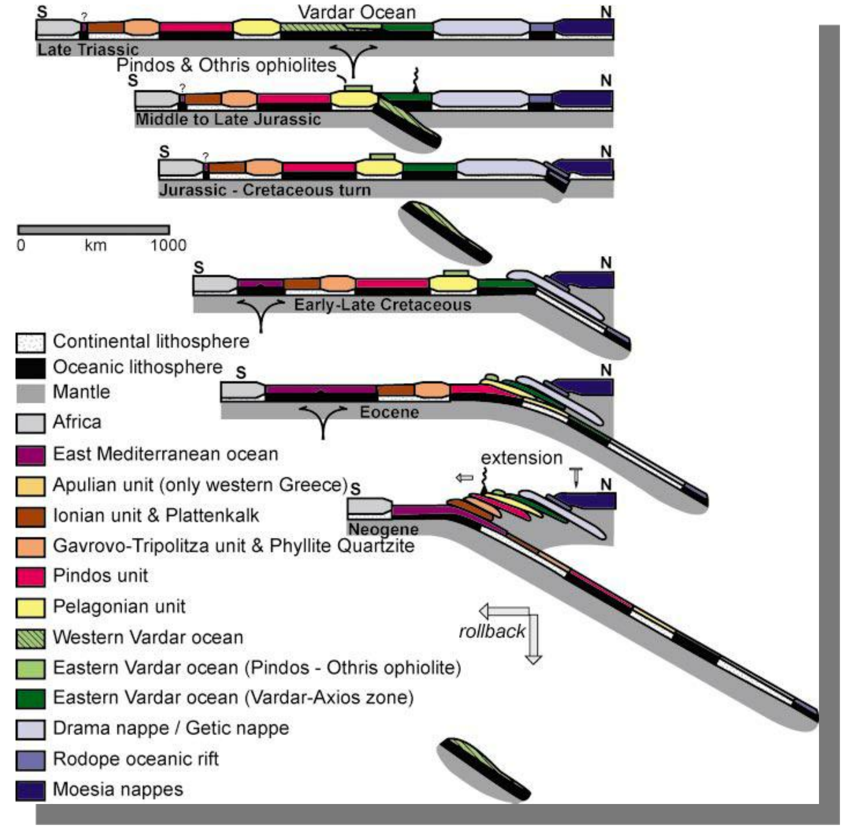

Tirel et al., 2010,2011

setup

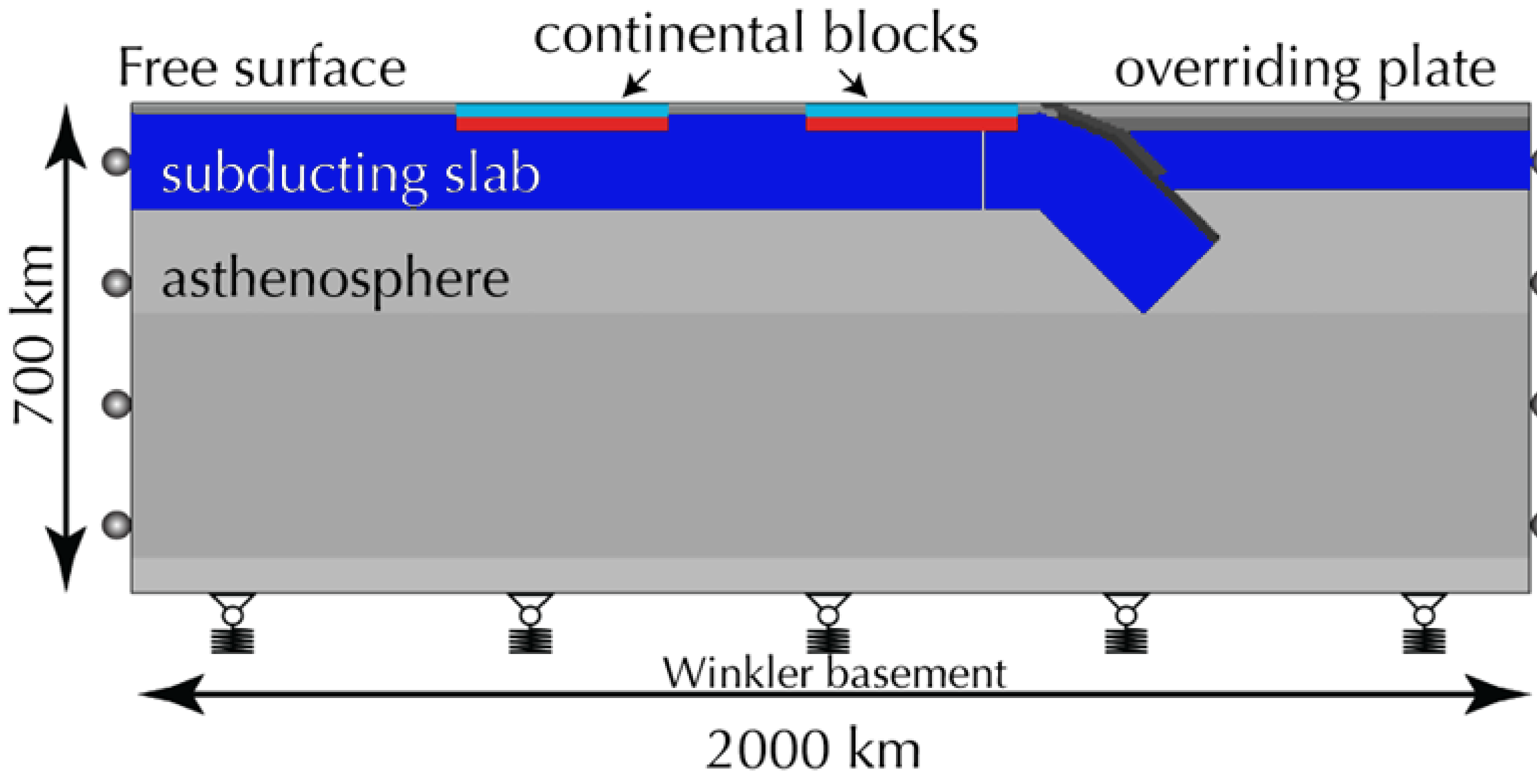

Tirel et al., 2010,2011

1 nappe terrain

Tirel et al., 2010,2011

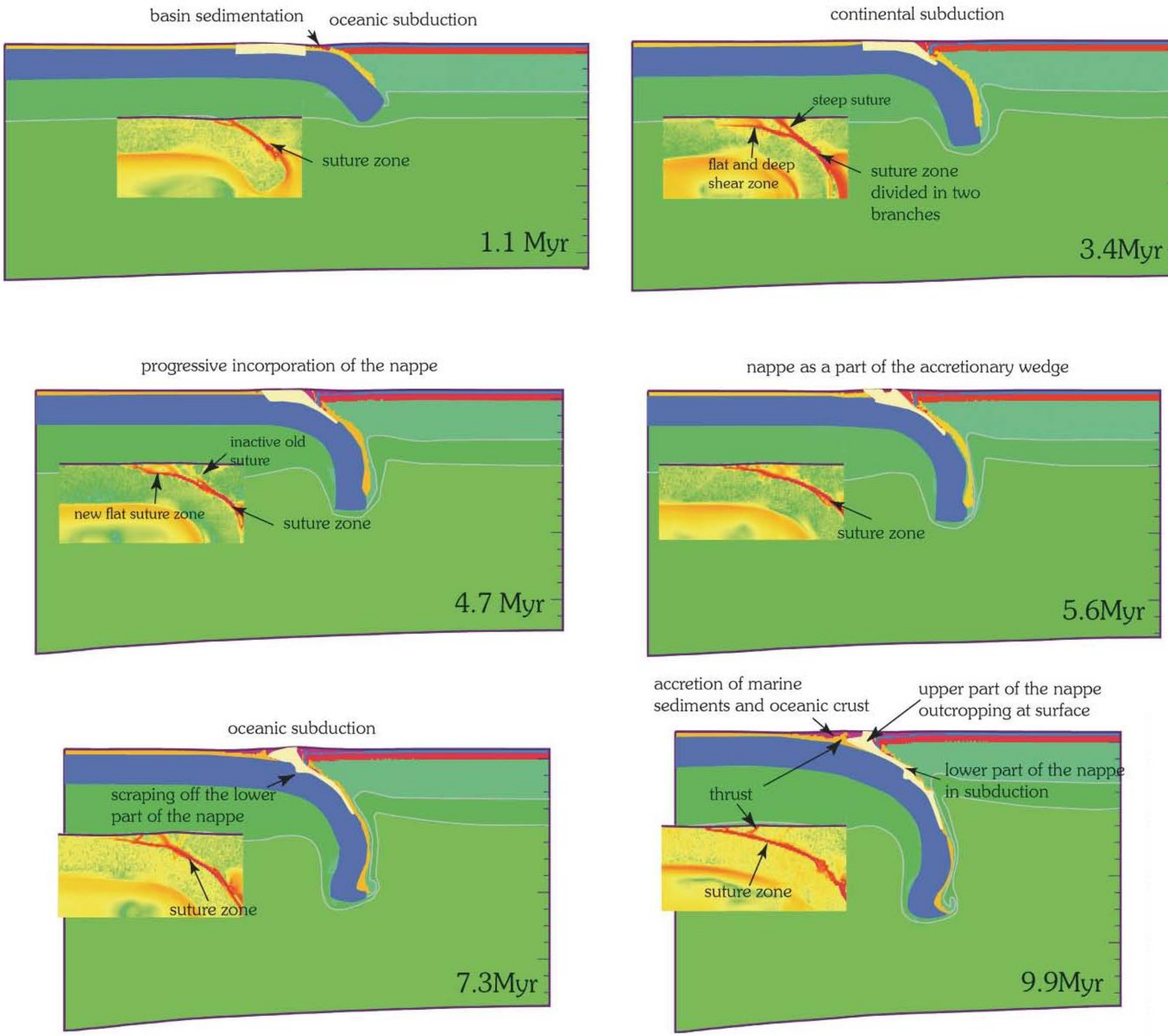

Roll-back extension 1 nappe terrain

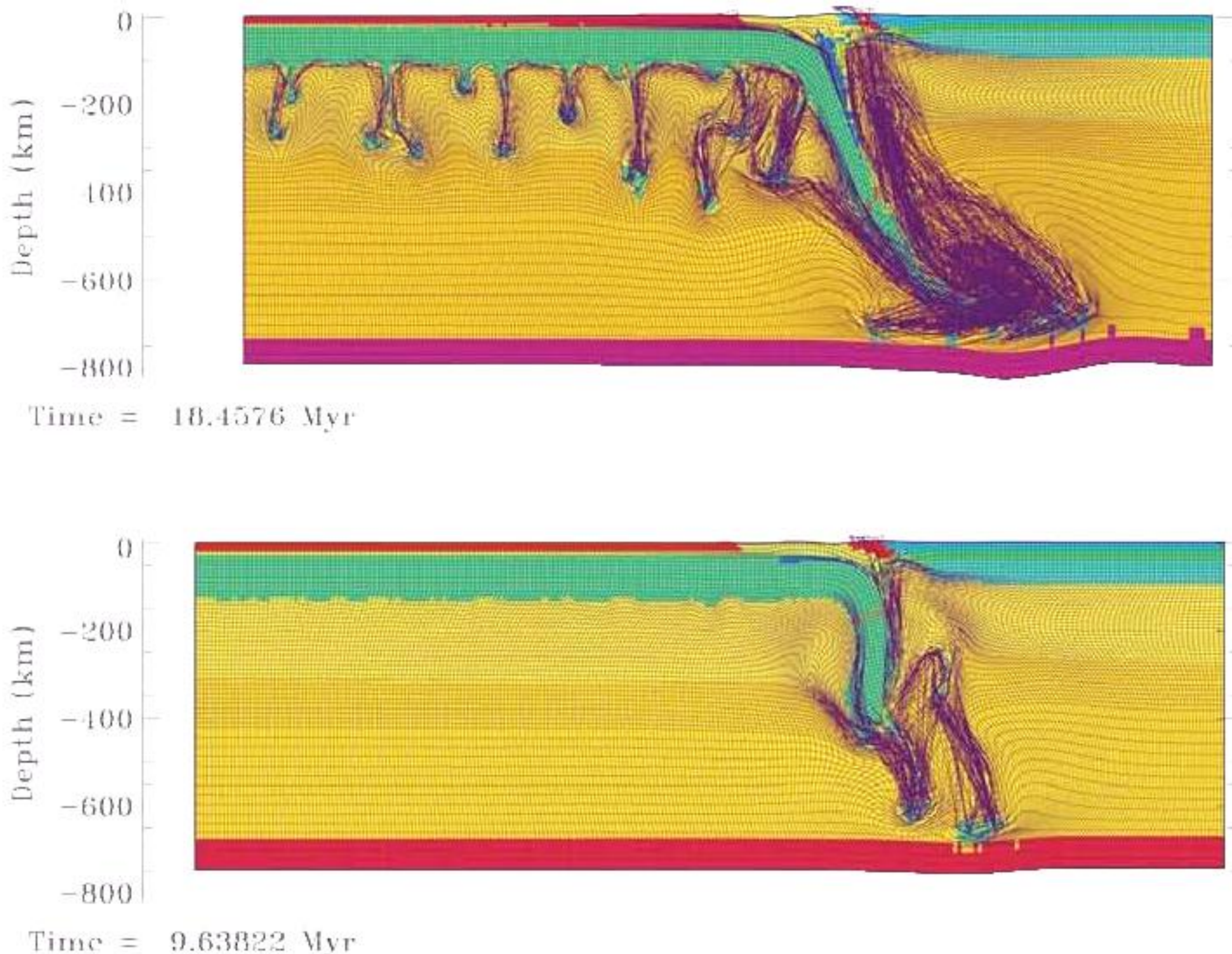

Tirel et al., 2010,2011

Processes of subduction-accretion-exhumation

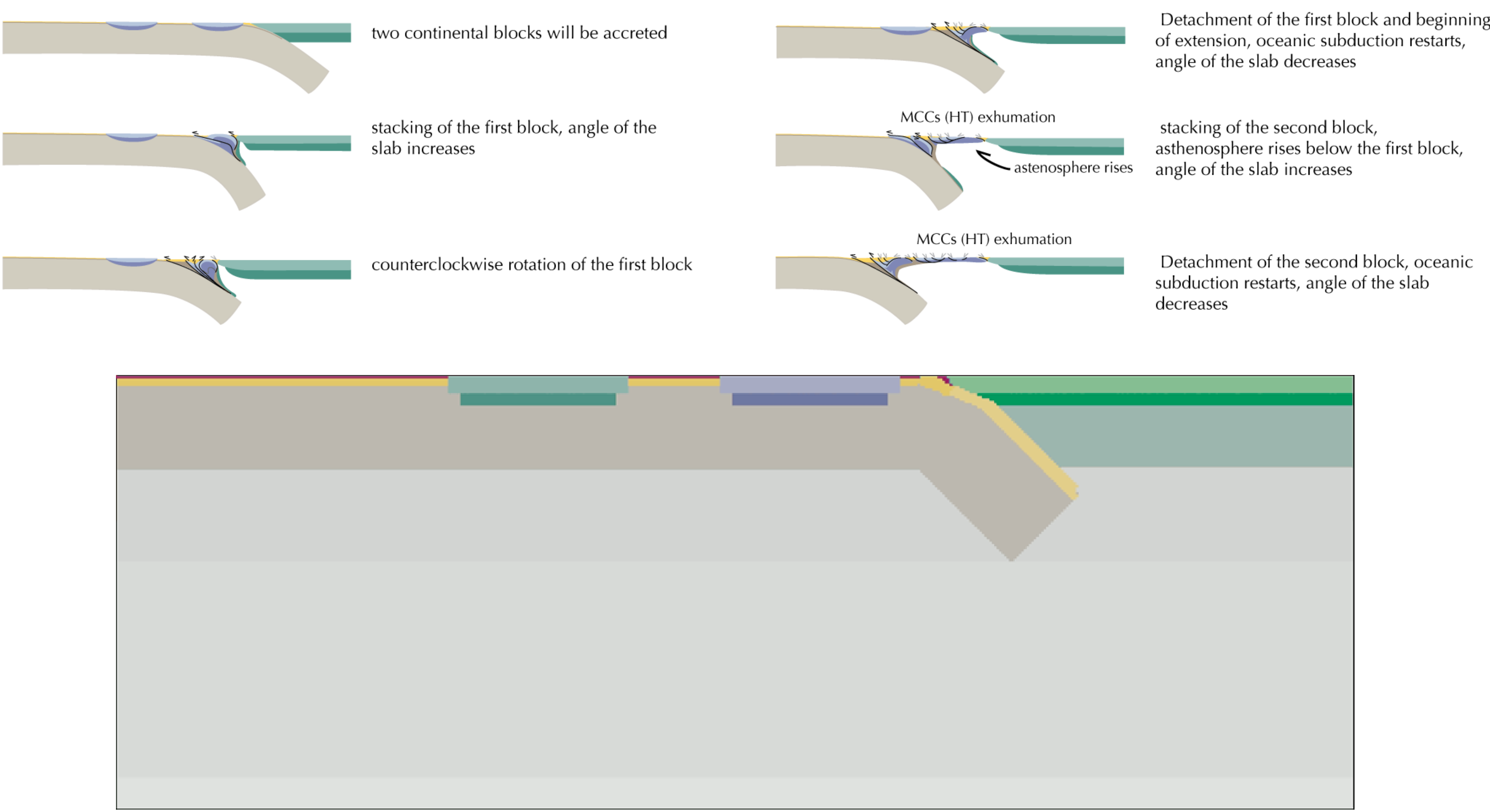

Tirel et al., 2010,2011

2 nappe terrains

2 nappes

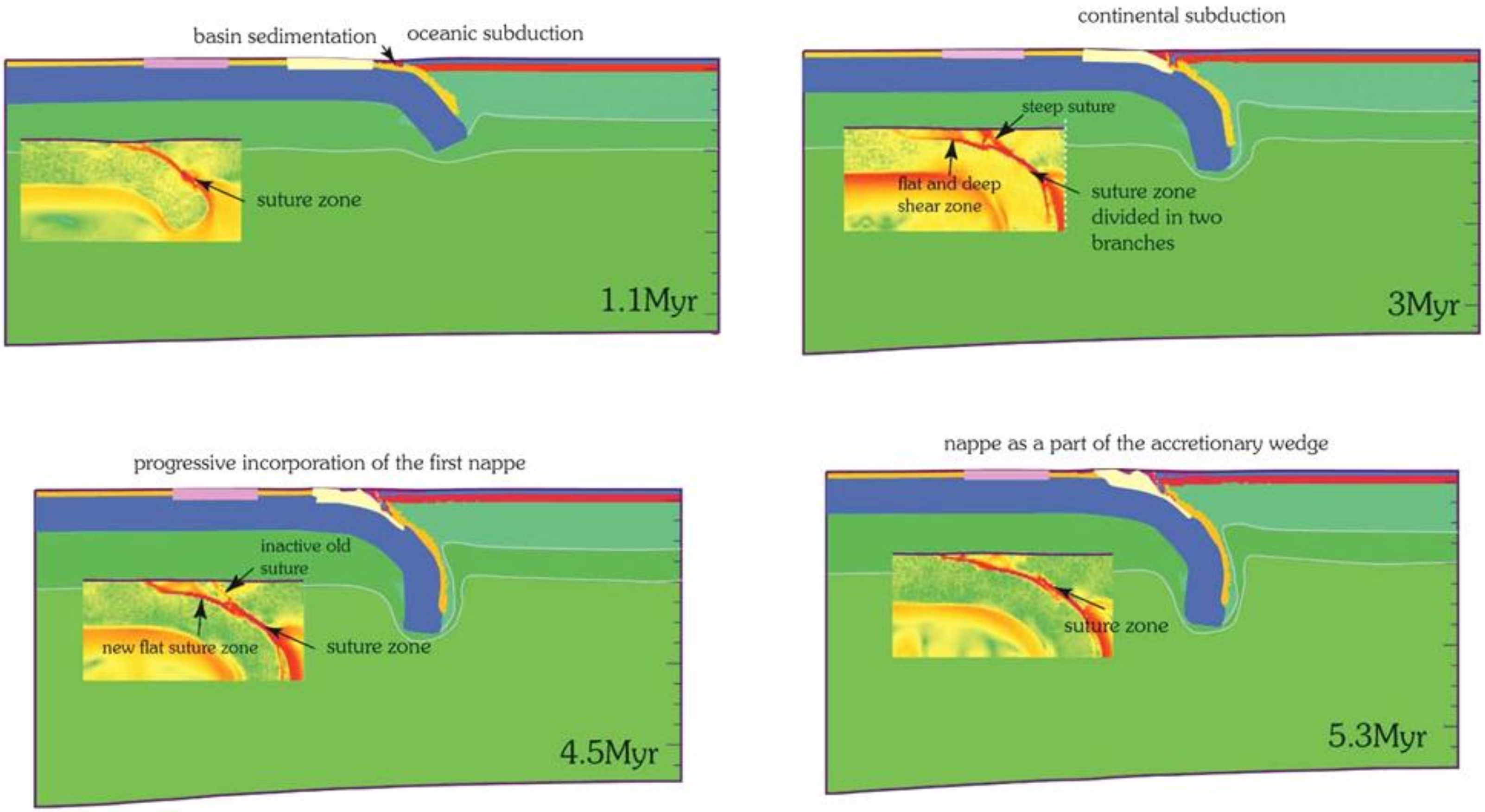

Tirel et al., 2010,2011

2 nappe terrains

2 nappes

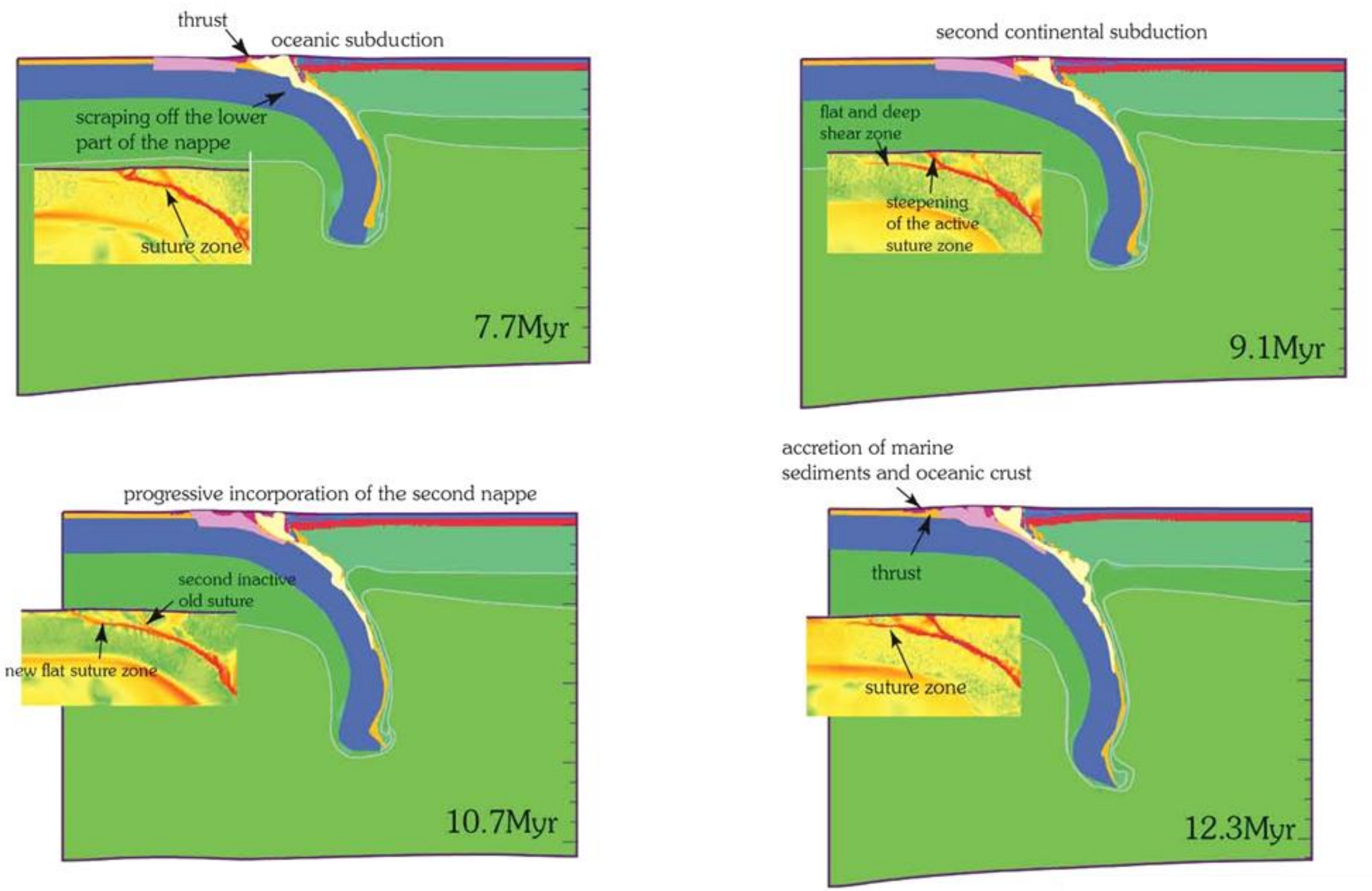

Tirel et al., 2010,2011

2 nappe terrains A roll-back extension

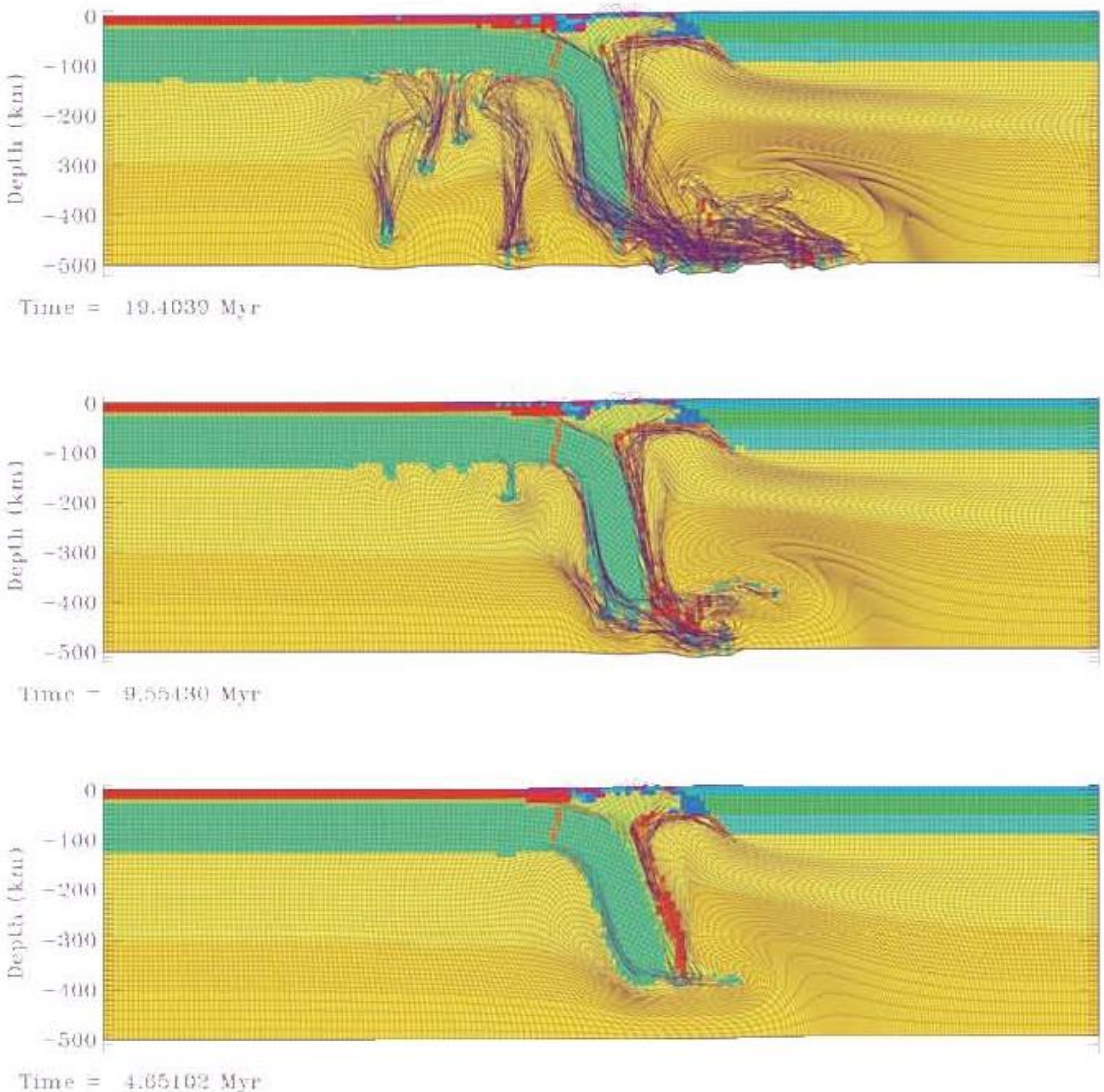

Tirel et al., 2010,2011

2 nappe terrains B roll-back extension

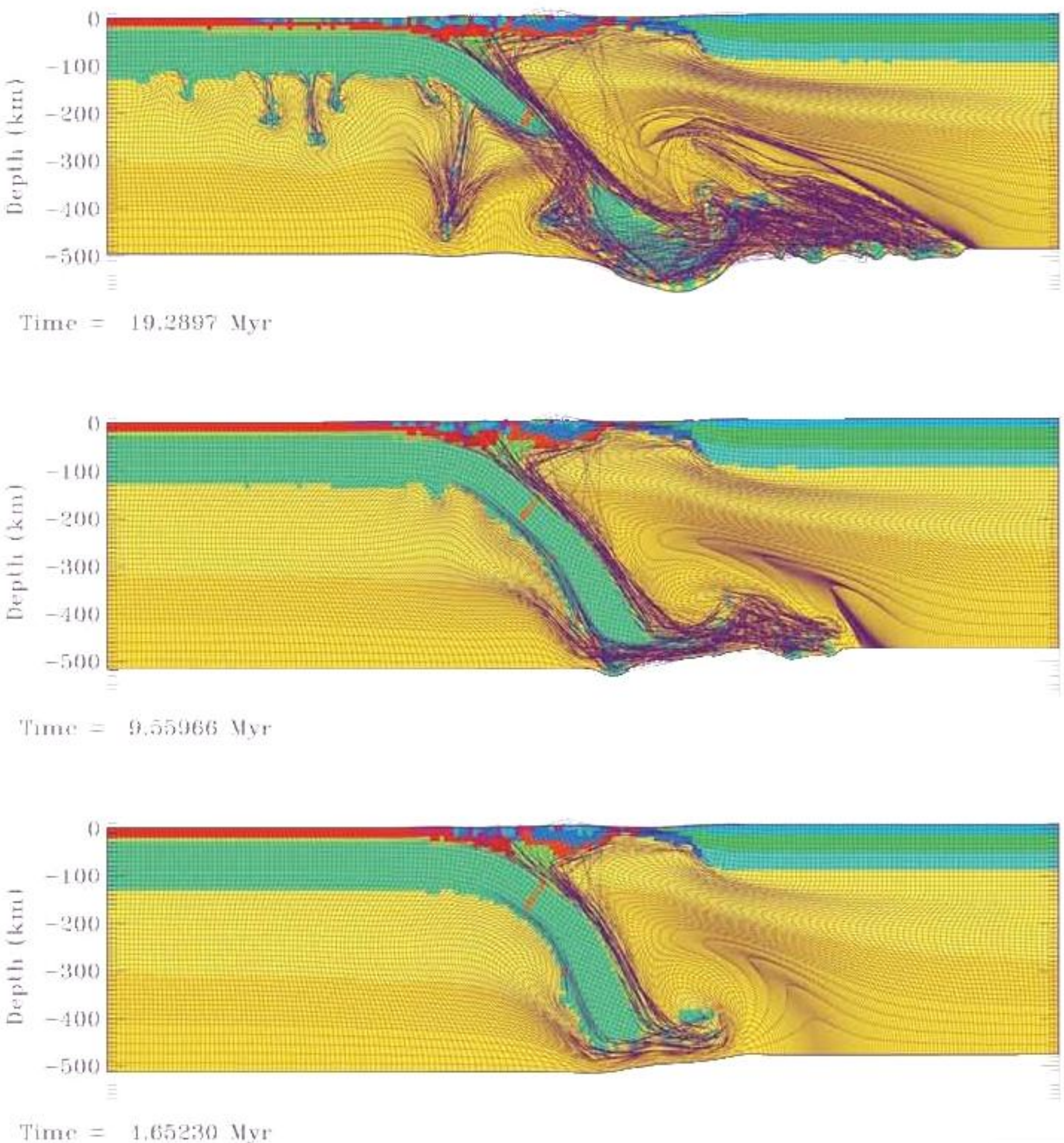

Tirel et al., 2010,2011

2 nappe terrains C roll-back extension

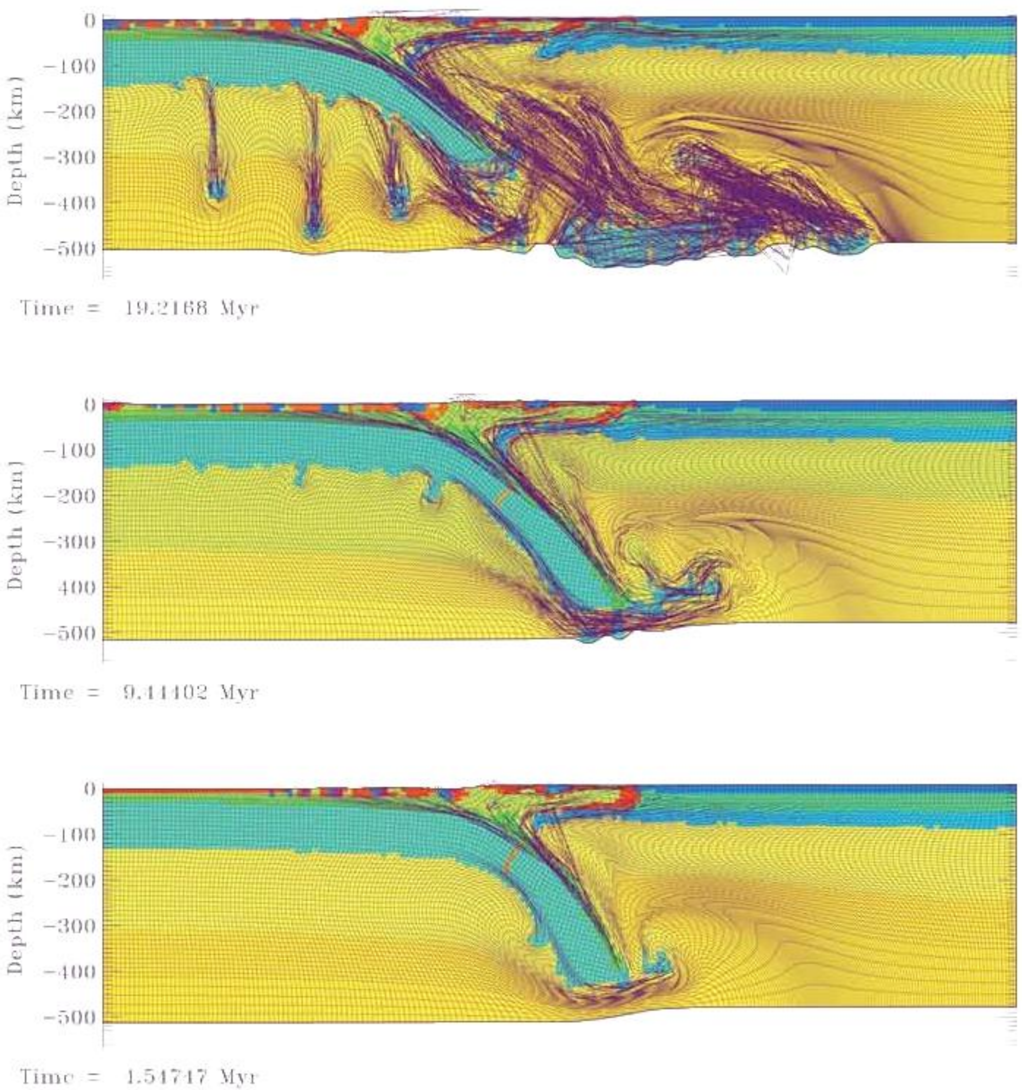

Tirel et al., 2010,2011

Comparisons with the Aegean Sea

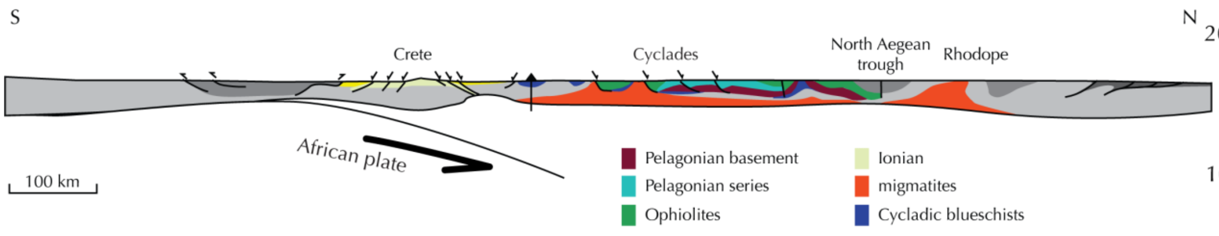

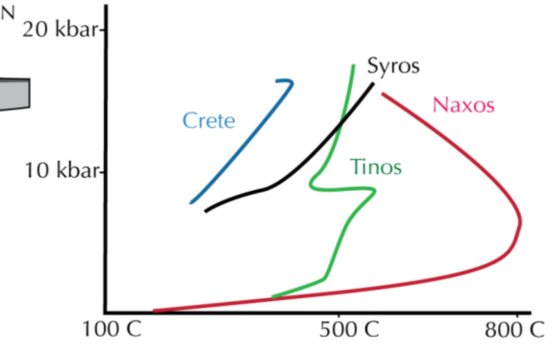

Modified after Jolivet & Brun, 2008

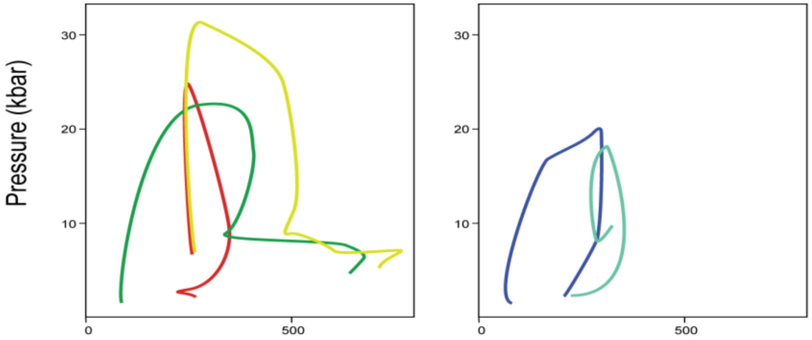

Exhumation of UHP-HP rocks, followed by an increase of temperature in the first block

Tirel et al., 2010,2011

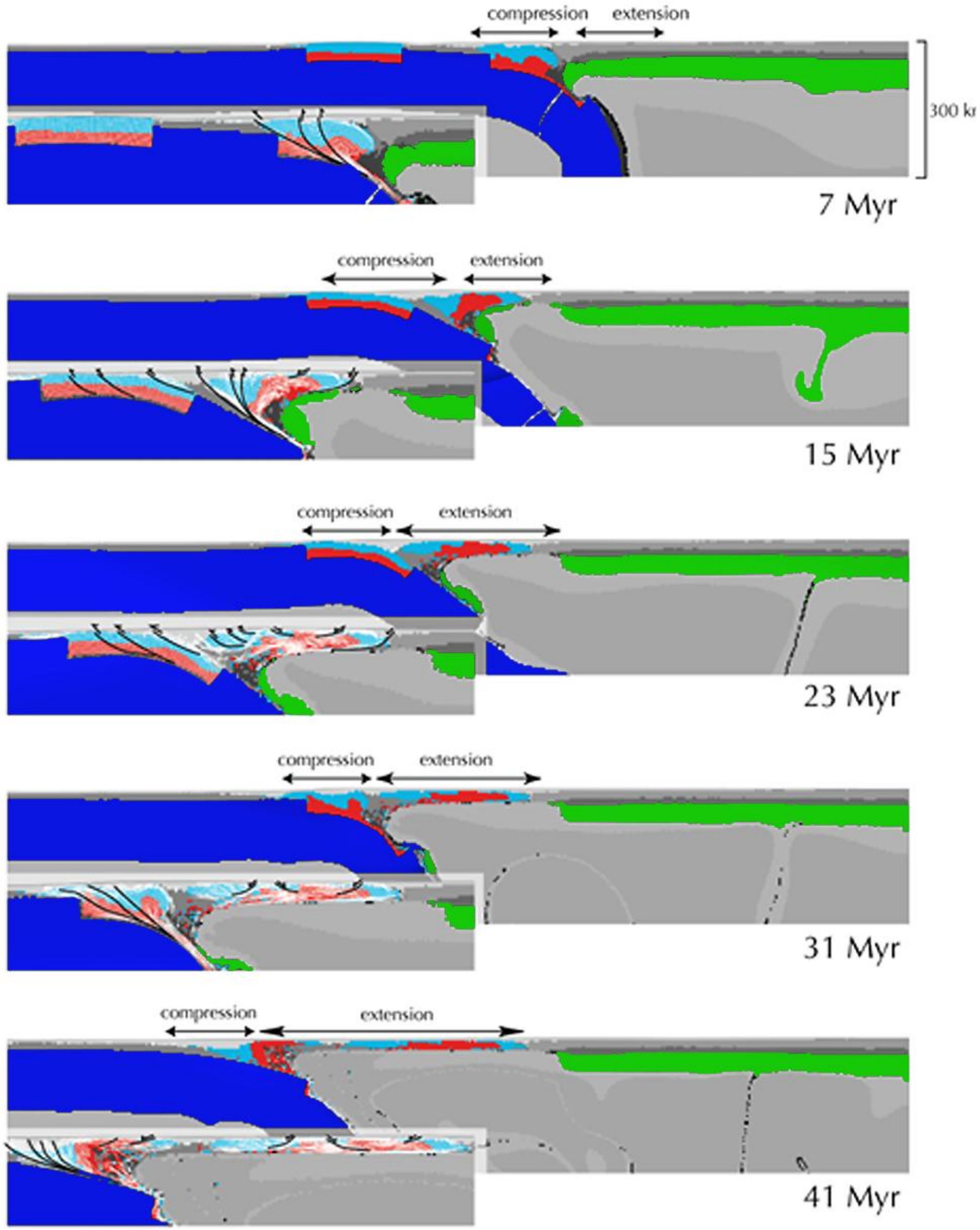

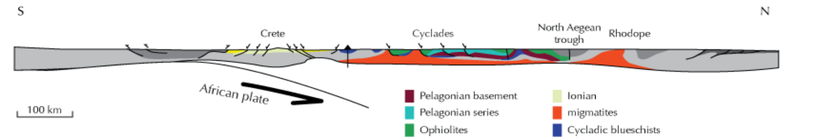

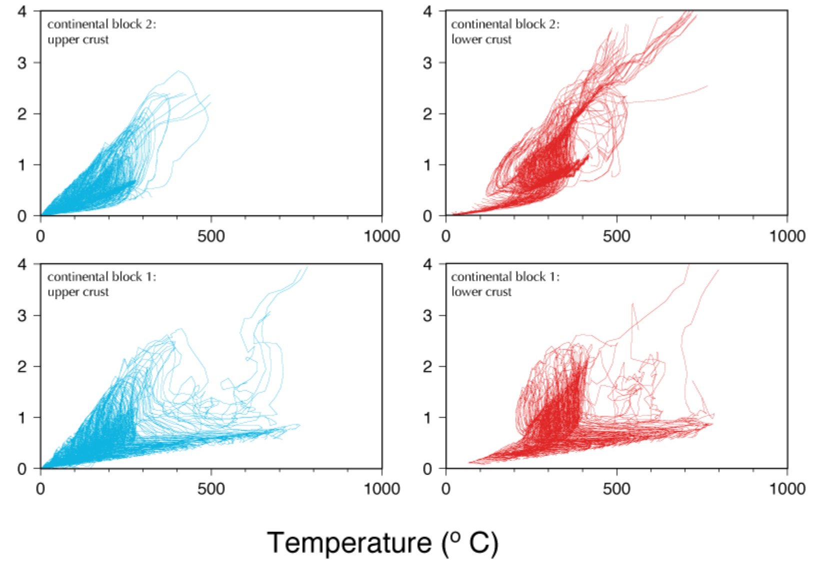

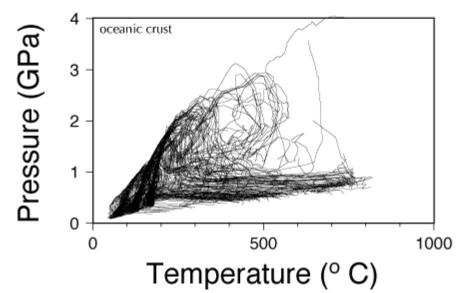

Tirel et al., 2010,2011

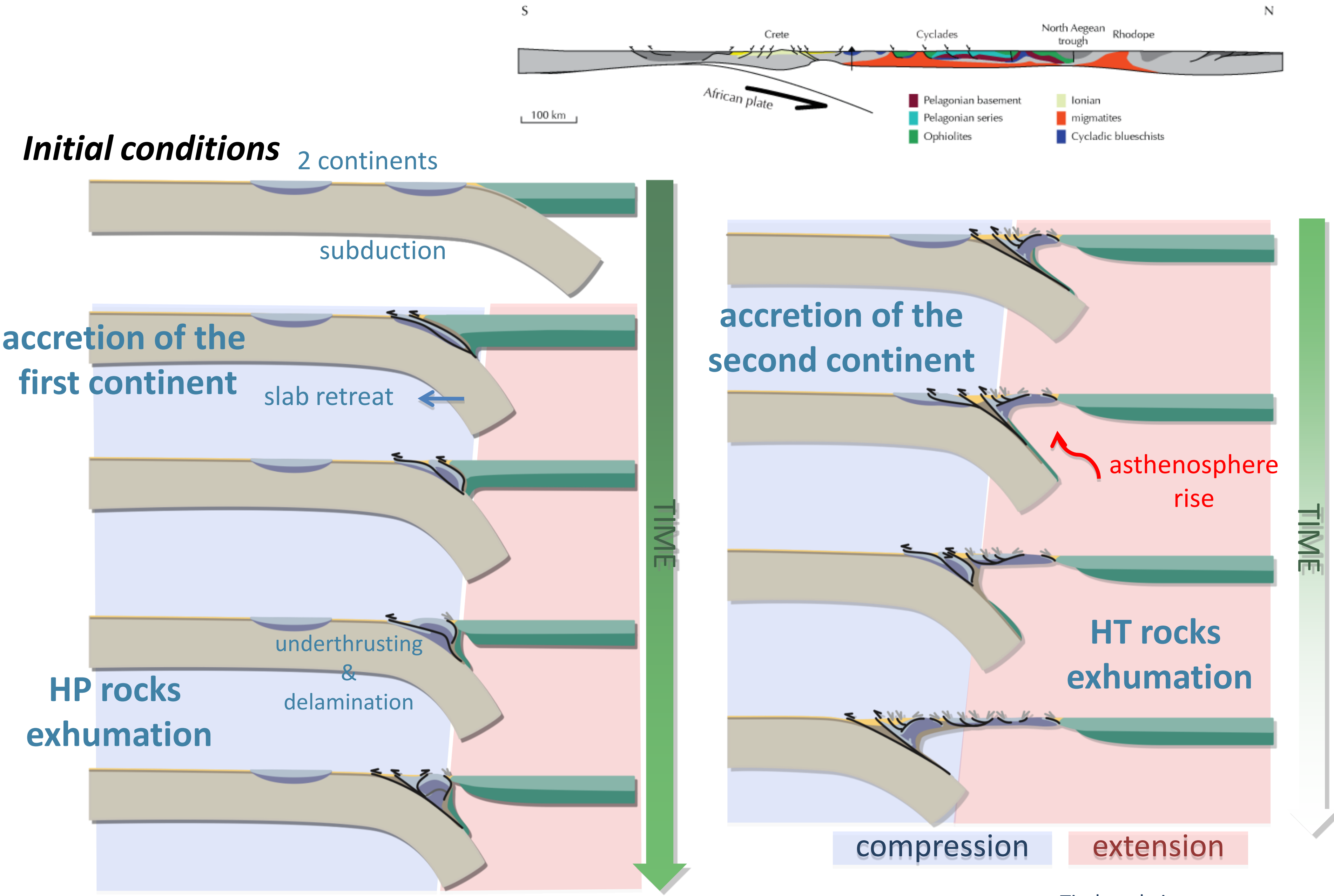

Tirel et al., in progress

SUBDUCTION-ACCRETION-EXHUMATION

(SOME) CONCLUSIONS

- Rheologically strong mantle and subduction rate > 1.5 cm/y is a primary condition for continental subduction.

- The HP-UHP exhumation mechanisms are different for different convergence styles and rates, as well as during different phases of collision. P-T-t data here represent a important constraint on the dynamics of collision zones.

- Slow convergence rates (e.g., Alpine) favour UHT/UHP exhumation through *a* multi-level exhumation mechanism with QD crust rheology

- Fast convergence rates (e.g., Himalaya) favour polyphase evolution with *several episodes of crustal prism evolution and exhumation*.

- In real life, slow-down of the convergence rate during collision should play a primary role for exhumation and futher evolution of collision

- Surface but also subsurface evolution strongly depends on dynamic interplays between subsurface and surface processes

- Tectonic heritage can have a major impact on subduction and exhumation style